Decellularised natural biomaterials for reconstructive bioengineering of the lower urinary tract

Debora Morgante MD

PhD

The University of Hull and The University of York

Hull York Medical School

Biomedical Sciences

June 2024

Abstract

Surgical reconstruction is required for congenital and acquired diseases affecting the lower urinary tract in adult and paediatric patients. In conditions such as small-contracted urinary bladders linked to infections, incontinence and renal damage, and hypospadias where baby boys' external urethral orifice is abnormally positioned, the lack of tissue availability and quality can compromise reconstructive outcomes, making the case for biomaterials with tissue-integrative properties.

Natural biomaterials comprise extracellular matrix proteins that are conserved among different species. Such biological tissues possess the strength of the tissues from which they have been derived and can serve as scaffolds for tissue regeneration, providing a natural microenvironment for cell attachment, migration, and proliferation.

A non-cross-linked porcine acellular matrix (PABM) has been previously developed by the decellularisation of full-thickness porcine bladders through a series of hypotonic buffers, detergents and enzymes to remove soluble cell and DNA content. The biomatrix retains the major structural components and physical characteristics, in terms of compliance and strength, of the originating organ tissue, and resulted biocompatible and with potential for use in urological surgery and tissue-engineering applications.

The need for a scalable manufacturing process that allows for the transfer of the porcine biomatrix production from the benchtop to an industrial scale was identified.

The overall aim of the present research was to investigate the PABM's biomaterial integration properties and tissue regeneration characteristics when applied in homologous surgical settings. It was hypothesised that this acellular biomatrix would promote an adequate initial mechanical support and favourite a biological environment able to promote tissue regeneration as an implant in in vivo models.

PABM was therefore prepared testing different decellularisation techniques for full-thickness porcine urinary bladders and the suitability for scaling up the decellularisation process was investigated.

Biological response parameters for this non-cross-linked natural material were determined and compared to a commercially available cross-linked biomatrix following in vivo surgical application.

PABM integration properties and tissue regeneration characteristics were examined in a homologous surgical setting where the PABM was implanted in a large animal model of urinary bladder reconstruction.

This study contributed to demonstrate the feasibility of a commercial manufacturing production for decellularised full-thickness porcine bladder tissue, and it produced evidence that PABM provides an anti-inflammatory, pro-regenerative tissue-integrative environment in in vivo settings. Based on its specific characteristics, PABM was here shown to be a candidate biomaterial for surgical applications in urinary tract reconstruction and beyond, with potential to contribute to ameliorating quality of life in paediatric patients worldwide.

List of contents

List of tables

List of figures

Acknowledgements

I firstly express my gratitude to my academic supervisor, Prof Jenny Southgate, for her invaluable feedback and guidance. I also thank my clinical supervisor, Prof Ram Subramaniam, who generously provided his invaluable surgical expertise for this project.

I would like to express my deepest appreciation to Prof Eileen Ingham, the remaining members of my TAP (Thesis advisory panel), Mr Nick Smith, and especially to the Chair, Dr Bob Phillips, who generously provided knowledge and guidance.

Additionally, this journey would not have been possible without the Grow MedTech program that generously supported this research (IKC (Innovation and Knowledge Centre) POC045 and POF000012).

Special thanks go to each member of the JBU, fellows, researchers, technicians and students for their friendship and technical knowledge. This journey would not have been the same without any of you.

I would like to extend my thanks to Dr Khawar Abbas for his excellent veterinary support and to the whole technical team at the Central Biomedical Services at the University of Leeds. Thanks, should also go to the HYMS Postgraduate office, to the staff of the Technology Facility, the IT services, and especially the DISC team at the University of York for their patience and assistance.

I am so grateful to every one of my friends who impacted, inspired and always supported me.

Last but foremost, I'd like to mention my whole family, especially my husband and our son. Their love, emotional support and belief in me has kept my motivation and spirits high during this journey.

Author’s declaration

I confirm that this work is original and that if any passage(s) or diagram(s) have been copied from academic papers, books, the internet or any other sources these are clearly identified by the use of quotation marks and the reference(s) is fully cited. I certify that, other than where indicated, this is my own work and does not breach the regulations of HYMS, the University of Hull or the University of York regarding plagiarism or academic conduct in examinations. I have read the HYMS Code of Practice on Academic Misconduct, and state that this piece of work is my own and does not contain any unacknowledged work from any other sources.

Chapter 1
Introduction

The present chapter introduces the urinary bladder and illustrates the clinical need for bladder reconstruction alongside current reconstructive strategies.

The pathologic condition of hypospadias, which affects the male urethra, is presented in Chapter 4, alongside the need for alternative surgical repair options.

1.1 The urinary bladder: structure and function

The urinary bladder is a complex, highly compliant organ with two primary functions, to store variable volumes of urine under relatively low and stable pressure and to expel urine cyclically in a process called micturition (Chang et al., 1998; Lewis, 2000; Farhat et al., 2003). By retaining urine at safe, physiological pressures, the bladder protects the kidneys from organ damage and failure (Thomas, 1997). The bladder capacity and compliance depend on the structural composition, biomechanical and biological properties of the bladder wall and the highly specialised urothelium.

The urinary bladder consists of four anatomical parts (apex or dome, the body, the base or fundus and the neck) and is in contiguity with the ureters (above) and the urethra (below).

In mammals, the bladder wall is composed of four main distinct layers: an outer serous layer or adventitia surrounding the muscular layer (detrusor muscle), which is made up of loosely arranged layers of smooth muscle, the lamina propria that is a viscoelastic collagenous connective tissue supporting a variety of cellular structures, including blood vessels, sensory and motor neurons. A basal lamina separates the lamina propria from the urothelium, a transitional epithelium with specificities between stratified squamous and simple non-stratified epithelia (Skandalakis, 2004).

Major extracellular components include collagen, elastin, laminin, fibronectin, proteoglycans. These macromolecules are organised in a dynamic tri-dimensional network called extracellular matrix (ECM) able to provide support and signalling to the bladder cells (Chang et al., 1998; Aitken and Bägli, 2009b; Kaya et al., 2016).

The primary function of the detrusor muscle is allowing the bladder to contract or relax during micturition. This facilitates excretion of urine into the urethra or holding and storage of urine in the bladder (Sam, Nassereddin and LaGrange, 2024). The basal tone of the smooth detrusor muscle is

primarily responsible for the active mechanical tension in the bladder wall, while the proteins that make up the extracellular matrix (ECM) regulate the bladder's elasticity (Morgante and Southgate, 2022).

The bladder wall stretches in different directions in a not homogeneous way, with some areas subjected at a higher stress. A correlation of the organ histoarchitecture with its biomechanical characteristics helps explaining such intrinsic heterogenicity. The region of the trigone is characterised by an increased network of collagen fibres and thicker muscular layers and appears to have less compliance with more resistance to deformation along the longitudinal direction. A more elastin-based network characterises the dorsal and ventral regions, which appear to be more compliant as more affected by distension along the apex-to-base direction (Gabella and Uvelius, 1990; Gloeckner et al., 1999, 2002; Korossis et al., 2009).

The urothelium

The urothelium luminally lines the urinary tract from the renal pelvis to the ureters, the bladder, and the proximal urethra. It has two different embryological derivations: endodermally derived from the urogenital sinus in the bladder and mesodermally (Wolffian duct) derived in the ureters (Tanaka et al., 2010; Hustler et al., 2018).

Histologically, the urothelium is stratified and organised into basal and terminally differentiated superficial, often binucleated, flattened 'umbrella' cells (or 'facet cells'), interposed by three to seven layers of intermediate cells that vary according to the degree of distension of the bladder (Baker and Southgate, 2011; Horsley et al., 2018; Dalghi et al., 2020). Urothelium, specifically the superficial cells, are highly specialised and provide the primary urinary barrier maintained during the filling-voiding bladder cycles, characteristically limiting permeability to water and solutes via transcellular and paracellular barrier functions (Smith et al., 2015). The urothelium is recognised as the tightest of all body epithelia (Acharya et al., 2004; Slobodov et al., 2004), and this is mainly due to the presence of ion channels and membrane pumps, tight junctions (TJ) and plaques of the asymmetric unit membrane (AUM).

Ion channels and membrane pumps are in the apical and basolateral membrane compartments and control transcellular ion transport.

TJ are located at the superior aspect of the intercellular junctional complex, control paracellular diffusion and are composed of zonular occludens (ZO) proteins, occludin, junctional adhesion molecule (JAM), claudins (Tsukita and Furuse, 2002; González-Mariscal et al., 2003; Schneeberger and Lynch, 2004; Varley et al., 2006; Smith et al., 2015).

Varley et al. (2006) identified that differentiation is accompanied by changes in transcription, protein expression and localisation of TJ proteins, suggesting a role in a coordinated, integrated differentiation programme essential for urinary barrier function. Understanding how TJ proteins are regulated and how this is integrated into developing a fully differentiated, functional urothelium is essential, as in several bladder diseases, the urothelium fails to form a functional urinary barrier.

The thickened plaques of AUM are uniquely embedded in the external aspect of the apical membrane of the superficial cells (Hicks, 1965), consisting of thousands of regularly arrayed particles approximately 16.5 nm across formed by the interaction of four mannosylated transmembrane glycoproteins urothelium-restricted called uroplakin (UP = 'urothelium-plaque') proteins (Hu et al., 2002; Khandelwal, Abraham and Apodaca, 2009; Wu et al., 2009; Horsley et al., 2018) providing mainly transcellular barrier function.

AUM plaques, a unique feature of the urothelium, are formed in the Golgi apparatus and are then transported as fusiform vesicles to the apical membrane (Tu, Sun and Kreibich, 2002). Thus, they provide a source of membrane for accommodating changes in surface area and maintaining a low-pressure environment during bladder filling (Wu et al., 1990; Yu et al., 1994; Olsburgh et al., 2003). The relationship between urothelial structure and function implies that the loss of one component of the AUM can have devastating effects on the urothelial structure and transcellular barrier properties (Hu et al., 2000, 2002). Thus, urothelial differentiation antigens provide objective markers of urothelial cytodifferentiation and may also be regarded as surrogate markers of urinary barrier function by their role in the urothelium.

Epithelial barrier/tightness is commonly assessed by transepithelial electrical resistance (TER), with TER measurements above 500 Ω.cm2 considered 'tight' (Frömter and Diamond, 1972; Cross et al., 2005; Smith et al., 2015).

Alongside the UP family, urothelium also elaborates a mucopolysaccharide-rich layer of glycosaminoglycans or GAG, which is believed to protect the bladder from infections and irritants (Baker, Shabir and Southgate, 2014). Among others, chondroitin sulphate, heparan sulphate, hyaluronic acid, dermatan sulphate and keratin sulphate have been reported as the most studied, with chondroitin sulphate believed to have an essential role in urothelial barrier function and shown to have luminal and basal expression in human and porcine bladders while heparan sulphate has been reported detected in the luminal portion of calf bladders, suggesting a reasonable doubt re differences between species (Rübben et al., 1983; Janssen et al., 2013; Cervigni et al., 2017; Horsley et al., 2018).

The urothelium lining not only serves as a urinary barrier but also has mechanosensory functions (Evren et al., 2010; Birder and Wyndaele, 2013) and plays a vital role in maintaining normal homeostasis (Farhat et al., 2003), highlighting the bladder's self-regulatory function.

The urothelium is usually mitotically quiescent or 'stable', with a slow cell turnover of around 200 days (Hicks, 1975) but has a high ability to regenerate in response to damage and acute injury (Peyton et al., 2012). This makes it one of the fastest-regenerating mammalian tissues (Varley et al., 2005; Khandelwal, Abraham and Apodaca, 2009). It has been found that urothelial damage in rats repairs within 72 hours, with intermediate cells maturing rapidly to form differentiated umbrella cells (Lavelle et al., 2002). This regenerative property, critical for maintaining the bladder's barrier function and urine-proofing properties makes it an ideal target for tissue engineering and regenerative strategies (Baker and Southgate, 2011).

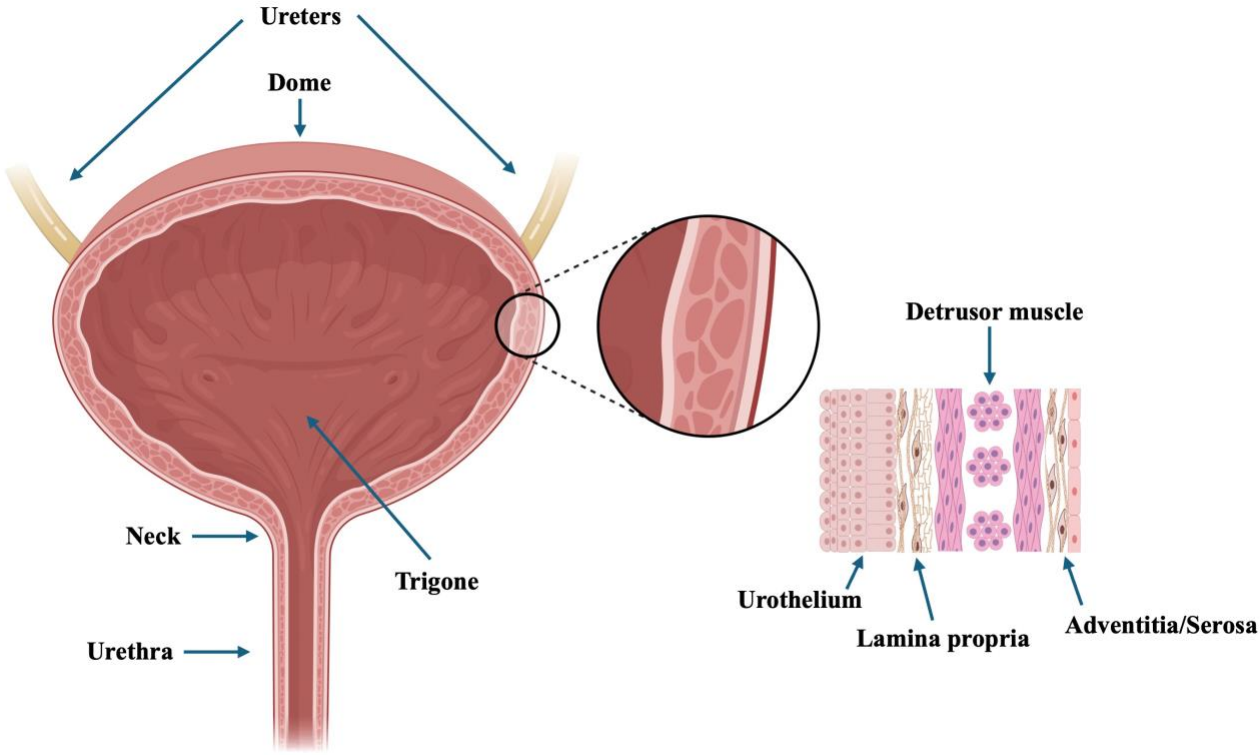

Figure 1.1 Bladder structure anatomy and histological characteristics.

1.2 The clinical need for urinary bladder reconstruction

A wide variety of benign and malignant clinical conditions, including congenital abnormalities, cancer, trauma, infection, chronic inflammation, and iatrogenic injuries, among others, can cause damage or loss of function in the urinary bladder (poor compliance or reduced capacity) requiring surgical reconstruction either by augmentation or substitution (Khoury et al., 1992; Atala, 2001; Pokrywczynska et al., 2015).

Incontinence is one of the debilitating consequences, affecting approximately 400 million people worldwide (Buckley, Lapitan and Epidemiology Committee of the Fourth International Consultation on Incontinence, Paris, 2008, 2010; Tran and Puckett, 2024). In most cases, smooth muscle cell hypertrophy and increased connective tissue deposition cause the thickening of the bladder wall and, consequently, a reduced compliance (Chang et al., 1999). It has been proposed that this may happen secondarily to an increased distension of the bladder wall, as in cases of bladder outlet obstruction, and such distension may provoke hypertrophy and hyperplasia (Korossis et al., 2009).

With more than 573000 new cases in 2020, bladder cancer is the tenth most common cancer diagnosis worldwide, being the sixth most commonly occurring cancer in men and the 17th most commonly occurring cancer in women (Jubber et al., 2023; Zhang et al.). Those patients undergoing partial or radical cystectomy (partial or complete removal of the bladder) represent the largest group requiring surgical reconstruction of the lower urinary tract. Current approaches for urinary diversions and neobladder replacement following cystectomy commonly involve reconfiguring the bowel in the form of orthotopic ileal neobladders, ileal conduit stomas or continent pouches (Studer, Varol and Danuser, 2004; Stein and Skinner, 2006).

Furthermore, benign congenital or acquired diseases or surgical procedures can induce severe changes in the neural control of the bladder, causing alterations in bladder function. Such changes can interfere with the structure, thickness and biomechanics of the bladder wall. Consequently, the bladder can become unstable under high pressure, or develop reduced capacity or compliance (German et al., 1994; Kruse, Bray and de Groat, 1995; Watanabe, Rivas and Chancellor, 1996; Korossis et al., 2009). Resulting clinical problems can vary from chronic urinary incontinence to kidney damage secondary to the bladder forced to work at abnormally high pressures, damaging the upper tract and ultimately leading to renal failure requiring organ transplantation. Examples include neuropathic bladder (e.g. secondary to myelomeningocele, myelodysplasia, spina bifida, multiple sclerosis or spinal cord injury), bladder exstrophy, posterior urethral valves, severe detrusor instability and end-stage interstitial cystitis.

There have been attempts to medically manage neurogenic bladders using antimuscarinics, alpha-blockers, imipramine, combination therapy of alpha-blockers with antimuscarinics, and desmopressin (Cameron, 2016). Intradetrusor injection of Botulinum Toxin-A (Fowler et al., 2012; Utomo, Groen and Blok, 2014; Leitner et al., 2016) and sacral neuromodulation/neurostimulation have also been applied in selected cases.

However, bladder augmentation remains currently the surgical solution for those patients who develop a thickened-walled, small-capacity, poorly compliant urinary bladder, where intractable incontinence or pain destroys the quality of life or where severe kidney damage is imminent (Cain and Rink, 2010; Biers, Venn and Greenwell, 2012). As discussed below (section 1.3.1), the bowel is most commonly used for bladder augmentation (enterocystoplasty). To date, the surgical augmentation of the bladder using bowel segments is still considered the 'gold standard' treatment for end-stage bladder disease. However, it is associated with several minor and major risks and short- and long-term clinical complications, including mucus production, recurrent infections, stones, spontaneous perforation, metabolic disturbances and malignancy (Khoury et al., 1992; Shekarriz et al., 2000a; Greenwell, Venn and Mundy, 2001; Kispal et al., 2011), that are driving researchers to find alternative approaches involving tissue engineering and regenerative medicine.

1.2.1 Urinary bladder auto-augmentation

In 1989, auto-augmentation was first tested in a canine model and subsequently in a clinical setting (Cartwright and Snow, 1989b, 1989a). In their experience, Cartwright and Snow excised the detrusor muscle (detrusorectomy) over the bladder dome, creating a large diverticulum by leaving the underlying urothelial mucosa intact. In this way, they obtained a reduction in intravesical pressure without utilising any intestinal segment. In 1994, a Canadian group tested the concept of auto-augmentation via detrusorotomy (no muscle excision) in an animal model. They reported successfully applying the technique in a clinical setting by performing auto-augmentation/detrusorotomy in 12 children with neurogenic bladder (Johnson et al., 1994; Stothers et al., 1994). Despite those initial encouraging results, further studies highlighted the need to optimise the patients' selection (pre-end-staged bladder disease) (Marte et al., 2002; MacNeily et al., 2003) and described complications such as poor mechanical support provided by the bulging mucosa, shrinkage, fibrosis (Perovic et al., 2002; MacNeily et al., 2003; Gurocak et al., 2007; Lee et al., 2017) alongside spontaneous perforation of the auto-augmented bladder (Rivas et al., 1996; Ehdaie et al., 2013). Undoubtedly, an advantage of urinary bladder auto-augmentation (detrusorotomy) resides in the lack of those side effects described when utilising a GI segment in a bladder augmentation procedure (enterocystoplasty).

1.3 Concepts for bladder reconstruction and tissue engineering

1.3.1 Strategies

During filling-emptying cycles, the urinary bladder faces considerable volume changes and bears inhomogeneous mechanical stretching/stress. As compliance is essential to store urine at a low pressure to protect the upper urinary tract and preserve kidney function, it is clear how bladder reconstruction and regeneration aim to increase capacity and compliance in diseased bladders. Several authors described the ideal and most favourable material for urinary bladder reconstruction as biocompatible, biodegradable with mechanical properties proper of the urinary bladder like strength, compliance and elasticity (Dahms et al., 1998; Pokrywczynska et al., 2015). The development of sensory self-voiding function does not seem to be part of current objectives achievable with bladder reconstruction. It is anticipated that voluntary emptying will be aided by clean intermittent self-catheterisation (CISC) via the urethra, an ileal conduit stoma, or a vesicostomy, as described by Mitrofanoff (1980).

The term “tissue engineering” (TE) was introduced in 1988 and defined as “an interdisciplinary field that applies the principles and methods of engineering and life sciences toward the fundamental understanding of structure-function relationship in normal and pathological mammalian tissue and the development of biological substitutes to restore, maintain, or improve tissue function or a whole organ”. Currently, the term TE is joint to the term “regenerative medicine” (RM; TERM), with the primary aim to regenerate structurally and functionally normal body parts (Langer and Vacanti, 1993; Vacanti and Langer, 1999; Badylak, 2005; Orlando, 2024).

Two elements are necessary for the techniques in use in TE: matrix and cells, where the matrix is the scaffold where tissue may organise, and cells are either cells stimulated to regenerate in vivo, aided by implantation of a matrix (guided TE) or cells cultured outside the body (in vitro) and later returned as auto-transplant (Zini et al., 2004; Abuharb et al., 2024). Specifically, TERM may use matrices alone or matrices with cells. When cells are used for TE, donor tissue (autologous, isogeneic, allogeneic, xenogeneic) is dissociated into individual cells, which are implanted directly into the host or expanded in culture, attached or not to a support matrix to provide structure, and reimplanted after expansion. The theoretical advantage of the latter approach is that clinically useful numbers of cells can be produced by propagation in a laboratory setting prior to surgical reimplantation into the host as a nascent or functional tissue.

One of the main limitations and still a major challenge with all approaches in reconstructive surgery in the genito-urinary tract is the lack of autologous tissue due to the underlying pathology. If the

underlying pathology of the donor/host is unresolved, sourcing of properly functional, autologous cells for ex vivo TE approaches and biomaterial integration may result impossible. Subramaniam and co-authors evaluated the suitability of urothelial cells from patients with abnormal bladders for surgical reconstruction using a TE approach that required expansion by propagation of cultured autologous urothelial cells. They found that while normal urothelium was highly regenerative with the derived cells highly proliferative in culture, the urothelium from abnormal paediatric bladders indicated a reduced capacity for proliferation and differentiation in vitro, suggesting the need to identify alternative cell sources for engineered bladder reconstruction (Subramaniam et al., 2011).

Most of the proposed experimental TE animal surgical models have utilised healthy animals. As a result, challenges may arise when promising approaches are applied in a clinically diseased setting.

1.3.2 Biomaterials

Mechanical and physical biomaterial properties need to be considered during bioscaffold selection, and can be summarised as follows:

- to maintain a 3D architecture that permits structural support, access to cells and formation of new tissue,

- to guide the development of new specific tissues with appropriate functions by creating a 'friendly' environment or 'niche', providing nutrients to enable cells to engraft, interact and survive,

- to facilitate localisation and delivery of tissue-specific cells to achieve specific tissue development and differentiation,

- to be biocompatible, without causing any local and systemic harmful tissue reaction.

Biocompatibility is a proper requirement for biomaterials used as biomedical devices. This property involves the ability of the biomaterial to not harm, to achieve its desired functions stimulating a host response from the contact tissues in a definite purpose without causing any adverse local or systemic effects but instead promoting a positive, beneficial cellular or tissue response after implantation.

Alongside the above, some structural features, such as pore structure, degradation rate, and surface chemistry, are required for tissue regeneration (Abbott and Kaplan, 2016).

It has been recognised that biomechanical properties modulating cell-matrix interactions may influence cell phenotype and tissue function (Nerem and Sambanis, 1995; Li and Xie, 2005; Rizvi and Wong, 2005; Engler et al., 2006; Rohman et al., 2007; Baker et al., 2009; Engelhardt et al., 2010). This reflects the fact that the tissue structure results from an active and dynamic development process.

To date, several bioscaffolds have been described for soft tissue applications and can be grouped into three big categories:

- Natural decellularised matrices, derived from organs such as the small intestine, skin, liver, respiratory tract, urinary bladder, pericardium, heart valves, and nerve, among others, from several different species (Crapo, Gilbert and Badylak, 2011; Keane, Swinehart and Badylak, 2015).

- Matrices produced from natural polymers like, for example, alginate (Rowley, Madlambayan and Mooney, 1999), hyaluronan (Arimura et al., 2005), collagen (Gilbert et al., 2008) and chitosan (Drewa et al., 2008).

- Synthetic polymers including poly(ethylene glycol) (PEG) (Adelöw et al., 2008), poly(lactic-co-glycolic acid) (PLGA), polyglycolic acid (PGA) and poly(ε-caprolactone) (PCL) (Aitken and Bägli, 2009b; Baker et al., 2009, 2011; Wiesmann and Lammers, 2009).

Biomaterials derived via the decellularisation of mammalian tissue can promote and facilitate remodelling processes to form functional tissue. Exploiting such properties, several methods of tissue and organ decellularisation have been used for the preparation of biological scaffolds, including physical methods (e.g. temperature, direct application of force and pressure, immersion and agitation, supercritical fluid), chemical methods (e.g. acids and bases, hypotonic and hypertonic solutions, ionic, non-ionic and zwitterionic detergents, solvents) and biologic agents (e.g. enzymatic agents, chelators and toxins) (Crapo, Gilbert and Badylak, 2011; Keane, Swinehart and Badylak, 2015).

Complete decellularisation of the originating tissue is critical. Failure to effectively decellularise tissues results in retained cell remnants, including residual nuclear material that could cause cytocompatibility problems in vitro and an intense inflammatory reaction in vivo, which can partially or entirely interfere with the reconstructive remodelling process (Brown et al., 2009; Nagata, Hanayama and Kawane, 2010; Zhang et al., 2010; Keane et al., 2012; Keane, Swinehart and Badylak, 2015). For example, residual phospholipids have been associated with valve and conduit calcification (Kim, 1976; Jorge-Herrero et al., 1994; Levy et al., 2003; Crapo, Gilbert and Badylak, 2011).

Stephen Badylak's group from Pittsburgh proposed a three-part minimal criterion for a satisfactory decellularisation:

- no visible nuclei upon histologic evaluation via Haematoxylin and eosin (H&E) or 4',6-diamidino-2-phenoylindole (DAPI) stainings,

- the double-stranded DNA (dsDNA) content should result in less than 200 base pair fragment length,

- the amount of dsDNA should be less than 50 ng per mg of the dry weight of the material (Crapo, Gilbert and Badylak, 2011; Keane et al., 2012; Keane, Swinehart and Badylak, 2015).

A particular advantage of animal-derived natural matrices is that following decellularisation, they retain tissue-specific architectures and extracellular matrix (ECM) proteins (Bolland et al., 2007) providing a wide range of biological and physical material properties specific to the originating tissue (Gilbert, Sellaro and Badylak, 2006; Davis et al., 2010). As mentioned above, the high degree of conservation of ECM proteins (e.g. collagens, laminins, fibronectins) between species implies that such matrices tend to be non-immunogenic and represent natural substrates to facilitate cellular migration and tissue integration (Marçal et al., 2012).

1.4 Past and current approaches in bladder reconstruction

Delivering successful (i.e. safe and functional) engineering of partial or whole bladder organ constructs requires fit-to-purpose biomaterials and a comprehensive understanding of bladder structure, cell/tissue biology and physiology. The most favourable material for urinary bladder reconstruction must possess good biocompatibility, biodegradation profile, and mechanical properties, especially strength and elasticity (Pokrywczynska et al., 2015). Given that until recently, the urinary bladder was considered to be a passive urine storage organ, it is unsurprising that past attempts to reconstruct it with unsuitable materials have failed.

1.4.1 Vascularised tissue grafts

The practice of using vascularised or pedicled host tissue grafts to obtain bladder augmentation during surgical reconstruction has a long history. For end-stage diseased bladders, the most common procedure to replace or augment the bladder involves using a vascularised segment of the patient's gastrointestinal tract (GI) to create a more compliant bladder to store urine at low pressure. As detailed above, this procedure (enterocystoplasty) entails the isolation of a segment of the GI tract with its vascular pedicle, detubularising it along the antimesenteric border and integrating it into the bivalved bladder (augmentation cystoplasty) as a conduit or orthotopic neobladder after radical cystectomy (Beier-Holgersen, Kirkeby and Nordling, 1994; Greenwell, Venn and Mundy, 2001; Nimeh and Elliott, 2018).

Augmentation cystoplasty was first performed and reported in 1889 by Rutkowski and von Mikulicz in a patient with bladder exstrophy, a year after the technique was described in a canine model (Tizzoni and Foggi, 1888; Mikulicz, 1899; Rutkowski, 1899). However, only after the 1950s, it became popular and routinely performed when Couvelaire applied it to treat small, contracted tuberculous bladders. Since its advent, many different tissue sources have been used as the

reconstructing segments. Stomach (gastrocystoplasty) was first described for urinary diversion in a dog model (Sinaiko, 1956) before being clinically applied a couple of decades later (Leong and Ong, 1972, 1975). Ileum (ileocystoplasty), cecum and sigmoid colon (colocystoplasty) have also been performed, with the ileocystoplasty the most commonly used in the UK (Thomas, 1997).

In recent decades, technological innovations in minimally invasive surgery (MIS) have increased the feasibility and demand for the MIS approach for such reconstructions (Nimeh and Elliott, 2018). In 2002, the first pure laparoscopic enterocystoplasty was reported (Elliott et al., 2002). Cases with the procedure performed robotically have been more recently reported (Murthy et al., 2015; Nimeh and Elliott, 2018), as it has been suggested that the minimally invasive robotic approach could decrease the surgical morbidity of open surgery, allowing such reconstruction to be performed with minimal collateral trauma (Gundeti, Acharya and Zagaja, 2009; Chowdhary et al., 2014; Murthy et al., 2015; Wiestma et al., 2016).

Contraindications to perform the procedure of enterocystoplasty include conditions where it is not possible to safely use GI segments, such as congenital bowel anomalies, inflammatory bowel diseases, radiation enteritis, and short gut syndrome (Budzyn et al., 2019). Despite a reasonable success rate of bladder augmentation in terms of increase in bladder capacity, reduced intravesical pressure and improved incontinence, enterocystoplasty is associated with the potential for several complications:

-bowel obstruction

-bladder calculi

-bladder perforation

-excessive mucous production

-metabolic acidosis and metabolic deterioration

-malignant transformation

(Thomas, 1997; Shekarriz et al., 2000b; Greenwell, Venn and Mundy, 2001; Budzyn et al., 2019; Langer et al., 2019). A main problem is that the bowel mucosa is structurally and physiologically not created to be exposed to urine. Therefore, given that some of the side effects of enterocystoplasty are caused by the long-term contact of the bowel mucosa with the urine, the logical progression would be to remove the bowel epithelium and leave the muscle surface facing the lumen (seromuscular enterocystoplasty using demucosalised intestinal tissue). Since the 1980s, experimental application

of the latter approach in rats, rabbit, canine, porcine and bovine surgical models resulted in graft contraction, fibrosis, shrinkage, diverticulation and metaplasia, most probably due to a severe inflammation secondary to urinary exposure and infection of the graft and to ischemia or damage to the bowel segment during surgical dissection (Oesch, 1988; Motley et al., 1990; Salle et al., 1990; Niku et al., 1995; Clementson Kockum, Willén and Malmfors, 1999; Aktuğ et al., 2001; Fraser et al., 2004; Hafez et al., 2005). This could be related to side of the bowel wall that faces the lumen. Severe fibrosis was also observed when a non-seeded vascularised capsule-flap of the abdominal wall or gracilis muscle was incorporated into a rat bladder (Schoeller et al., 2004). However, in a series of 129 human bladder augmentations using demucosalised intestine, Lima and colleagues suggested that fibrosis and shrinkage were prevented using a silicon balloon left in place in the bladder for two weeks post-augmentation (Lima, Araújo and Vilar, 2004). Pedicled omental flaps to repair or augment the bladder (omentocystoplasty) have been also applied clinically and in animal models, mainly when used to close defects associated with vesicovaginal fistula (Kiricuta and Goldstein, 1972).

Although demucosalisation of the bowel prior to incorporation into the bladder has resulted in graft fibrosis and shrinkage, when urothelium has been allowed to cover the augmenting graft, shrinkage occurred minimally or not at all (Aktuğ et al., 2001; Schoeller et al., 2004; Hafez et al., 2005). Shaefer and colleagues transferred urothelial cells to gastric and colon grafts in an in vitro setting (Schaefer et al., 1998) and Blanco's group reported no increase in capacity in rats following intestinal grafts seeded with urothelium and observed a high mortality rate in their series (Blanco Bruned et al., 2001).

An aerosol transfer technique was developed and applied in a porcine model using urothelial and bladder smooth muscle cell suspensions in fibrin glue (Hafez et al., 2003, 2005). The authors described isolating autologous urothelial cells at the time of the hemicystectomy. Urothelial cells, with or without smooth muscle cells, were sprayed onto the demucosalised colon and then incorporated into the remaining bladder. After six weeks, this led to the development of a multilayered, stratified differentiated (uroplakin-positive) urothelium covering a bladder or colonic smooth muscle submucosa, respectively, with no evidence of inflammation. In their experience, the technique did not involve the propagation of urothelial cells in culture. However, it could do so, leaving the open question of whether cells generated in vitro would remain able to develop into morphologically differentiated urothelium after being transplanted back into an in vivo setting. This has been more recently exploited, with results showing the effectiveness of such a technique in terms of epithelial coverage, in a Yucatan miniature swine model (Hidas et al., 2015). However, no information on results with neuropathic bladder cells has been reported (Langer et al., 2019).

A cell-engineering technique has been applied in a porcine surgical model of enterocystoplasty. Autologous urothelial cells were propagated in vitro, and the cell sheets were implanted onto a vascularised, de-epithelialised host smooth muscle segment utilised for bladder augmentation (Fraser et al., 2004). A Vicryl™ mesh was used as a carrier to transfer urothelium tissue from cell culture to the surgical site. This proposed 'composite cystoplasty' technique implies that the in vitro steps of the procedure involve only the propagation of a single cell type (urothelial cells) that is then used with a smooth muscle host tissue segment surgically prepared, maintaining its innervation and vascularisation.

In a surgical series (Turner et al., 2011), the technique of extra-luminal dissection described by Hafez and colleagues (2005) was adapted to produce a de-epithelialised segment of the bowel that was combined with an autologous differentiated, functional urothelium generated in vitro (Turner et al., 2008) at the time of the composite cystoplasty reconstruction. Seven pigs underwent bladder augmentation using this technique, and when sacrificed at three months, the bladder augments were found to be viable with no evidence of fibrosis or contraction. When examined histologically, all the augmented segments were covered entirely with urothelium. The authors reported no evidence of colonic mucosal or crypt regrowth, and unlike the initial study (Fraser et al., 2004), only minimal inflammatory changes were observed (Turner et al., 2011).

1.4.2 Free tissue grafts

The evolution of bladder augmentation has more than 100 years of history. After the first colocystoplasty using the sigmoid reported by Lemoine (Lamoine, 1913), several alternatives were proposed, and attempts were made to incorporate free biological tissue into the bladder. In 1917, Neuhof performed bladder augmentation in dogs using a free fascia graft, with no current availability of details of the outcome (Neuhof, 1917). In 1955, Marucci and Shoemaker described the characteristics of the ideal segment for bladder augmentation (Shoemaker, 1955; Shoemaker and Marucci, 1955). Since then, several experimental animal studies have been performed using, for example, muscle-backed peritoneum (myoperitoneocystoplasty) (Weingarten, Cromie and Paty, 1990), rectus abdominis muscle flaps in rats (Manzoni et al., 2001) with adverse effects of bladder stones and chronic inflammation. Split skin grafts, placenta, peritoneum, dura mater, placenta, and pericardium have been used as patches, with an overall lack of urothelium regeneration and significant fibrosis observed (Draper, Stark and Lau, 1952; Goldstein and Dearden, 1966; Kelâmi et al., 1970; Kelâmi, 1971; Novick et al., 1977; Hutschenreiter et al., 1978; Fishman et al., 1987; Kambic et al., 1992; Dewan et al., 1994; Jelly, 2010; Jednak, 2014; Barski et al., 2017; Langer et al., 2019).

The appeal of using free biological tissue persisted. Stenzl (2000) performed detrusor myectomy using latissimus dorsi (LD) grafts in four dogs. This approach was based on Carpentier's LD cardiac wrap for patients with severe cardiomyopathy, the first reported case of substituting non-skeletal muscle with skeletal muscle (Carpentier and Chachques, 1985). The detrusor myoplasty has been transferred to the clinical setting, although it is still considered experimental (Gakis et al., 2011).

De-epithelised bladder wall grafts (Yamataka et al., 2003; Thangappan et al., 2012), ureterocystaugmentation (from megaureters) (Ikeguchi, Stifelman and Hensle, 1998), hysterocystolpasty (Dapena et al., 2012, 2013; Kotecha and Toledo-Pereyra, 2012) have also been attempted in animal studies with several adverse effects reported.

1.4.3 Acellular matrices

Conceptually, the ideal tissue/material for bladder reconstruction should retain the originating tissue architecture, allow recellularisation by the recipient's cells, and be biocompatible without causing any immune- or inflammatory adverse reaction. The decellularisation of an autologous, allogeneic or xenogeneic tissue can potentially provide a bio-compatible and tissue-compatible polymeric scaffold or matrix that maintains essential extracellular matrix components such as collagen, fibronectin, laminin, glycosaminoglycans, and growth factors that can allow cell migration, growth, and differentiation and stimulate the regeneration of smooth muscle and urothelial cells (Jednak, 2014). Decellularised matrices retain the tissue-specific architecture with the potential for tissue-specific cell-matrix interaction and differentiation-specific functions. They also carry the potential risk for contamination by xenogenic factors and immunological reactions in incomplete decellularisation (Stanasel, Mirzazadeh and Smith, 2010). Other potential problems include the availability of the source and its inherent biological variability, in terms of age, sex, health state of donors, as well as the natural intraspecies population heterogeneity.

The two natural products to have generated the most enthusiasm are the most common acellular matrices described for potential use in bladder reconstruction: the porcine small intestinal submucosa (SIS) (Kropp et al., 1995, 2004; Zhang et al., 2000) and the bladder acellular matrix (BAM) (Dahms et al., 1998; Piechota et al., 1999).

Due to their biocompatibility, these biomaterials have been used in preclinical animal trials (Kropp et al., 1996b; Piechota et al., 1999; Brown et al., 2002) and clinical studies (Caione et al., 2012; Schaefer et al., 2013) with different outcomes (Ajalloueian et al., 2018). In their natural tissue state, these tissues are diffusely cell populated. Therefore, they must undergo extensive decellularisation to remove all potentially immunogenic material.

Non-cross-linked natural tissue matrices play a role in bladder reconstruction. They act as slow-release vehicles of naturally occurring growth factors. Once implanted, they slowly degrade, serving as a scaffold for new ECM proteins produced by the in-growing cells (Kim, Baez and Atala, 2000; Badylak, 2002). This function is crucial in the regeneration process and underscores the potential of these matrices in bladder reconstruction.

1.4.3.1 SIS

In the 1980s, Badylak and his group first proposed SIS as a collagen-based 0.15-0.25 mm thick bioscaffold for bladder augmentation, prepared from porcine small intestine after mechanical delamination removal of several layers of the bowel wall to leave the collagen- and elastin- rich submucosal layer (Badylak et al., 1989). SIS has been proposed as a reconstructive biomaterial promoting regeneration in skin (Lindberg and Badylak, 2001), ligaments/musculoskeletal (Ledet et al., 2002; Musahl et al., 2004; Liang et al., 2006), vascular structures (Badylak et al., 1989; Robotin-Johnson et al., 1998; Shell et al., 2005) and in urological applications (Colvert et al., 2002; Palminteri et al., 2007; Roth et al., 2011). Specifically for bladder augmentation and lower urinary tract reconstruction, SIS has been studied in several animal models such as pigs (Liatsikos et al., 2001; Caione et al., 2006), dogs (Kropp et al., 1996a; Vaught et al., 1996; Kropp et al., 2004; Zhang et al., 2006; Roth et al., 2011) and rodents (Kropp et al., 1995; Ashley et al., 2010; Qin and Dunn, 2011). In published studies on bladder reconstruction/regeneration, SIS has been used in different forms: matrix alone (Kropp et al., 1996b, 1996a, 2004; Caione et al., 2006, 2012), seeded with cells (Lakshmanan et al., 2005; Lu et al., 2005; Zhang et al., 2006; Qin and Dunn, 2011), or in combination with synthetic or natural biomaterials (Roth et al., 2011; Chung et al., 2014; Zhao et al., 2015). Differences between distal versus proximal porcine SIS grafts were also investigated in a rat bladder augmentation model, showing that proximal SIS is inferior, suggesting that the origin of SIS is relevant to regenerative outcomes (Ashley et al., 2010). Such a broad application of SIS showed inconsistent results (Ajalloueian et al., 2018). Ajalloueian and colleagues suggested how not only the location of the origin of the SIS but also its source could explain the reported inconsistencies between studies. Furthermore, results from two clinical studies published by Caione and his group and Schaefer and colleagues reported unsatisfactory results regarding bladder capacity, compliance, muscle regeneration and continence (Caione et al., 2012; Schaefer et al., 2013). Urodynamic studies/strain testing have been reported performed in 18 studies of bladder regeneration using SIS in dogs, pigs, in vitro, rats, baboons, murines, humans and rabbits, again with inconsistent results (Ajalloueian et al., 2018). Interestingly, however, most studies that used SIS as a cell graft seeded or unseeded for bladder reconstruction were performed in normal bladders. When studies were performed in a model of the diseased urinary bladder (where most of the detrusor muscle was removed), results showed

limited bladder regeneration, with inflammatory cells and fibrosis, poor vascularisation, adhesions, shrinkage, bone formation and calcification at the graft site (Zhang et al., 2006).

1.4.3.2 BAM

The preparation of the bladder acellular matrix (BAM) was first described in 1975 (Meezan et al., 1975) and involved physical, chemical and enzymatic decellularisation methods following mechanical separation of bladder wall layers. The isolation of the bladder submucosa by dissection has also been described (Chen, Yoo and Atala, 1999). More commonly, the split or full-thickness bladder is decellularised (Sutherland et al., 1996; Probst et al., 1997, 2000; Dahms et al., 1998; Piechota et al., 1998; Merguerian et al., 2000; Reddy et al., 2000; Brown et al., 2002; Bolland et al., 2007; Marçal et al., 2012).

BAM prepared from rat bladder was then used in vivo in a homologous model to augment normal rat bladders following hemicystectomy. Animals were sacrificed at different time points, and authors observed ingrowth of bladder wall components, with no signs of rejection and a normal bladder capacity preserved in all animals (Probst et al., 1997). BAM has also been reported to be prepared from dogs, rabbits, and hamsters. When xenotransplanted as a graft into rats, BAM showed similar results with functional and morphological bladder regeneration (Piechota et al., 1998). Less favourable results were found when the technique was transferred to a larger animal model using pigs. Macroscopic contracture was observed with no evidence of recellularisation in the central parts of the implanted graft (Reddy et al., 2000; Brown et al., 2002). This could be related to several causes, including the size of the augmented area and, consequently, of the implanted patch, lack of vascularisation and tissue oxygenation, and the presence of a pro-inflammatory environment rather than a pro-regenerative one. Such observations need to be taken into consideration in the design and optimisation of future large animal surgical studies in terms of biochemical and biomechanical characteristics, implant size, and surgical techniques before translation to humans.

In 1998, the potential use of BAM as an acellular collagen graft for bladder augmentation was evaluated in a canine model (Yoo et al., 1998). The authors used seeded (with urothelial cells on one side and smooth muscle cells (SMCs) on the other) and unseeded allogeneic bladder submucosa. They showed better outcomes in the seeded group, leading to the first initial pilot human clinical study (Atala et al., 2006). However, most patients showed deterioration in bladder capacity, compliance and leak point pressure.

Stem cells from different sources have been used to promote urinary bladder regeneration post-reconstruction. In a further study, BAM was used seeded (with marrow-derived mesenchymal stem

cells (MSCs) and unseeded, and authors found similar results (Coutu et al., 2014). Bone marrow mesenchymal cells seeded onto BAM were also used in a rat model of urinary bladder reconstruction/regeneration by Pokrywczynska and colleagues, who found that MSCs promoted smooth muscle regeneration by upregulating the expression of anti-inflammatory cytokines (Pokrywczynska et al., 2013). Interestingly, opposite results were found by Zhang and colleagues, who reported limited regeneration, shrinkage and adhesions when using seeded SIS grafts. The latter group reported similar results using unseeded SIS grafts. The pioneering work of Baskin and colleagues is of underlying relevance to the tissue engineering approach using seeded biomatrices. They first showed that bladder smooth muscle development from the foetal mesenchyme depended on paracrine interactions with the urothelium (Baskin et al., 1996; DiSandro et al., 1998). The potential for reciprocal interactions between urothelial and smooth muscle compartments during bladder tissue engineering has also been investigated in vitro (Fujiyama, Masaki and Sugihara, 1995; Zhang et al., 2000; Ram-Liebig et al., 2004, 2006; Brown et al., 2005). Heterotypic cell-cell interactions are likely to play a critical role in developing functional tissue-engineered bladders. However, practical and technical limits need to be considered before the clinical use of seeded bioscaffolds for organ reconstruction. Such limits would include the need for more than one operation if autologous cells are used, a possible de-differentiation of urothelial cells and SMCs during in vitro cultivation, and the risk of pathogen acquisition before implantation (Chamley-Campbell, Campbell and Ross, 1979; Bolin, Matthews and Ridpath, 1991; Atala et al., 2006; Flieger et al., 2008; Ajalloueian et al., 2018).

Emptying/filling (contraction/relaxation) cycles have been described in urinary bladders reconstructed using BAM but, similarly to SIS, at a reduced magnitude relative to normal bladders. A functional difference between BAM and SIS is the compliance of the biomaterial prior to implantation, with the SIS reported 30 times less compliant than the native bladder or regenerated SIS (Kropp et al., 1996a). Non-regenerated split-thickness and full-thickness BAM showed similar biomechanical properties to the native bladder (Dahms et al., 1998).

Decellularised bioscaffolds may retain biological activity, and this may encourage cell ingrowth and tissue regeneration. Furthermore, as the structure and composition of the ECM are characteristic and exclusive to specific tissues, there may be advantages in a homologous use of biomatrices (e.g. biomatrix derived from full-thickness urinary bladder to be used in urinary bladder reconstruction in the same animal species). For example, BAM may be predicted to contain more appropriate growth factors for bladder regeneration and tissue engineering than SIS (Badylak, 2004; Bolland et al., 2007; Marçal et al., 2012). BAM was shown to be capable of sustained release of exogenous basic fibroblast growth factor and was demonstrated in a dose-dependent manner to reduce graft shrinkage in a rat

bladder augmentation model (Kanematsu et al., 2003). Potentially, infiltration and organisation of smooth muscle bundles in SIS and BAM grafts may be enhanced by incorporating growth factors and other bioactive substances (Chen, Zhang and Wu, 2010). Using different techniques, several groups incorporated growth factors in BAM in animal models of urinary bladder regeneration (Kanematsu et al., 2003; Youssif et al., 2005; Kikuno et al., 2009; Loai et al., 2010). These attempts revealed inconsistent results.

Potential problems associated with applying decellularised matrices include stone formation, graft shrinkage and limited, incomplete and disorganised infiltration of smooth muscle cells. Graft shrinkage has been shown to increase with time, with up to a 48% reduction in the graft size (Brown et al., 2002). Although regenerated smooth muscle tissue at the graft size is often minimal and not organised in bundles in animal models, the speed and extent of cell ingrowth are dependent on the size of the graft. In rat models, for example, graft size is small (ca 0.5 cm2). In contrast, it is much more significant in large animals (e.g. 4 x 4 cm2 acellular dermal biomatrix patches incorporated into pig bladders (Akbal et al., 2006)). Therefore, as mentioned above, it is not surprising that smooth muscle bundles have been reported to be scanty at the centres of large grafts (Piechota et al., 1998; Brown et al., 2002). It needs to be considered that the surface area of bladder augmentation in humans is an order of magnitude greater than many described experimentally in vivo. This still represents a limitation to the translating much reconstructive bladder research, mainly where rodents and small animals have been used.

Lithogenesis is also a particular problem reported in animal studies of bladder augmentation with SIS and BAM, with up to respectively 75% and 80% of animals (rats) found to have bladder stones (Vaught et al., 1996; Piechota et al., 1998). Reddy and colleagues discovered microcalcifications in the suburothelial zone of implanted BAM and, therefore, treated pigs with an inhibitor of osteoclasts (alendronate) to reduce urinary calcium concentration (Reddy et al., 2000). Such a treatment does not allow for an accurate determination of the risks involved.

Porcine BAM mechanical properties were studied following different decellularisation and manufacturing techniques, with reported evidence of a direct impact on BAM mechanical properties, such as ball-burst strength (biaxial load), maximum load and elongation, maximum tangential stiffness, energy absorbed, suture retention strength (Freytes et al., 2004, 2008). Following decellularisation, BAM tensile modulus seams to increase, stretchability decreases and scaffold resistance to deformation increases. Such alterations in the biomechanical properties of the bladder tissue could be secondary to the delamination process. These changes in the decellularised tissue compared to the originating tissue need considering when designing a pre-clinical or clinical model.

Based on structure and properties of the BAM used for urinary bladder regeneration to date, it is observable that BAM possesses suitable composition and morphology to enhance cell ingrowth, proliferation, and differentiation. This is due to its physicochemical and mechanical characteristics.

For biomaterials like BAM to be used in in vitro and in vivo experiments, as well as in clinical settings, they are required to be aseptic, with asepsis meaning the absence of any living microorganism (Xue, 2008). However, disinfection and sterilisation methods can alter biomaterials physical and chemical characteristics, as well as their biological function (Pekkarinen et al., 2004; Hussein et al., 2013; Burton et al., 2014; Rnjak-Kovacina et al., 2015; Monaco et al., 2017; Gosztyla et al., 2020; Tao et al., 2021).

Sterilisation procedures and their impact on the properties of the BAM have been investigated. Evidence shows that gamma irradiation and electron beam irradiation directly impact the mechanical characteristics of BAM, as they can damage the matrix components by increasing its degradation, causing changes in the tissue strength. They were shown to decrease the uniaxial and biaxial strength, maximum tangential stiffness, and the energy dissipation of the ECM scaffolds. Residual peroxidated lipids produced by these ionising radiations have also been linked to cytotoxicity. (Crapo, Gilbert and Badylak, 2011; Keane, Saldin and Badylak, 2016). Ethylene oxide is considered a suitable sterilisation type to preserve mechanical properties in BAM (Freytes et al., 2004; Pokrywczynska et al., 2015). However, ethylene oxide can cause an unwanted host immune response and is known to be a human carcinogen (Jackson, Windler and Simon, 1990; Jinot et al., 2018).

Natural matrices that undergo chemical or non-chemical processing/cross-linking to enhance the stability of the material are invariably rendered inert and may engender cytotoxic responses, thus ultimately inhibiting cellular incorporation (Badylak, 2002; Kimuli, Eardley and Southgate, 2004; Feil et al., 2006). Although some processed biomaterials have shown preliminary results comparable to SIS and BAM, further development is necessary to investigate better the characteristics and the full potential of processed biomatrices for surgical applications (Nuininga et al., 2004).

1.4.3.3 PABM

A decellularisation process using low-concentration sodium dodecyl sulphate(0.1% (w/v) SDS and proteinase inhibitors has been developed for the production of porcine and human tissue-based scaffolds including cardiac valves (Booth et al., 2002; Vafaee et al., 2018), dermis (Hogg et al., 2015; Helliwell et al., 2017), arteries (Wilshaw et al., 2012) and musculoskeletal tissue (Stapleton et al., 2008a, 2011; Jones et al., 2017). Such processes preserve the biomechanical and biological properties of the originating tissues. This approach has been applied in preclinical (Paniagua Gutierrez et al.,

2015) and clinical studies (Greaves et al., 2013, 2015; Kimmel and Gittleman, 2017). Subsequently, the process has been adapted to create an acellular porcine bladder biomatrix, the Porcine Acellular Bladder Matrix or PABM (Bolland et al., 2007). PABM is a highly compliant non-cross-linked acellular matrix produced by the decellularisation of full thickness porcine bladders by distension through a series of hypotonic buffers, detergents and enzymes to remove soluble cell and DNA content (Bolland et al., 2007; Ward et al., 2021). Following decellularisation, PABM has been shown to retain the underlying histoarchitecture of the originating bladder tissue. The collagen fibers in the lamina propria that are linked to the organ overall strength and compliance are also retained. No statistical difference has been found in the pressure required to burst the entire decellularised bladders in comparison to the fresh ones. Furthermore, no difference has been identified in the ultimate strength and in the ability in retaining sutures of the decellularised tissue compared to fresh bladder tissue (Bolland et al., 2007). PABM has been shown to provide an anti-inflammatory tissue integrative environment in ex vivo organ culture (Bullers et al., 2014). In that ex vivo tissue culture model, surgically excised fresh full-thickness human ureteric tissue was combined with PABM to study the cellular events at the biomaterial-human tissue interface. Findings suggested that PABM was involved in actively recruiting and polarising macrophages from a pro-inflammatory M1 (CD80 positive) to an M2 anti-inflammatory (CD163 positive) phenotype.

1.4.3.4 Natural ECM/Collagen Grafts

The natural material derived from the ECM, collagen, has been used extensively as a xenogeneic and allogenic biomaterial for cells of many types, reflecting its natural evolution as a tissue scaffold. As detailed above, collagen is the most abundant protein within the ECM and the major structural protein in the body. It is also largely responsible for the strength and conformability of natural materials. Collagen has been shown to encourage cell growth, to have minimal immunogenicity and can be readily purified and moulded into the desired form, making it an ideal tool for tissue-engineering applications (Furthmayr and Timpl, 1976; Elbahnasy et al., 1998; Hubbell, 2003; Hattori et al., 2006). The FDA has approved collagen for use in several medical settings, such as dermal wounds and abdominal wall repair (Serrano-Aroca, Vera-Donoso and Moreno-Manzano, 2018). Purified collagen, however, when used for reconstruction in the urinary tract, has been shown to lose its tensile strength and to be susceptible to tearing during suturing (Elbahnasy et al., 1998). Even if natural matrices based on collagen have been applied in preclinical studies of bladder reconstruction, the slow and poor SMC ingrowth has limited its widespread use (Roelofs et al., 2018).

To overcome such problems, attempts have been made to reinforce collagen with synthetic materials and natural tissues, including a pedicled omental flap (Hattori et al., 2006). The latter investigators employed a porcine in vivo model to demonstrate that a collagen sponge became vascularised when

combined with omentum for seven days and that only when thus pre-conditioned could the collagen sponge support passive bladder engineering. This approach has important implications for other natural or synthetic biomaterials, as it provides a strategy for the in vivo preintegration of a scaffold for subsequent use in passive tissue engineering. However, the anatomical characteristics of the animal model in use may result in a substantial limitation for successfully applying this method.

A few materials and technique were compared. In 2010, Parshotam and colleagues compared INTEGRA® collagen matrix, SURGISIS® collagen matrix and demucosalised enterocystoplasty in lambs. The authors reported better results when INTEGRA® was used, with adverse effects such as mucous cysts, bowel obstruction, fibrosis and graft contraction in the enterocystoplasty and the SURGISIS® (Parshotam Kumar et al., 2010). Furthermore, Vardar and colleagues studied a collagen-fibrin scaffold by adding an insulin-like growth factor, reporting satisfactory results in terms of urothelialisation and smooth muscle cell growth, but hypertrophy of the constructed urothelium was found with the potential risk of urinary outlet obstruction (Vardar et al., 2016). More recently, a comparison between unseeded versus seeded collagen grafts was conducted in a cystoplasty model in minipigs. The authors showed inconsistent results in terms of urothelial cells and smooth muscle cells in growth leading to poor contractile function (Leonhäuser et al., 2017). Application of an acellular collagen scaffold enriched with heparin, and combined with vascular endothelial growth factor, fibroblast growth factor 2 and heparin-binding epidermal growth factor was also evaluated. The authors reported the observation of a well-layered neobladder wall, but there was no evidence of improvement in the regeneration quality despite the applied growth factors (Roelofs et al., 2018).

1.4.4 Synthetic grafts

Synthetic scaffolds have been developed as an alternative to natural matrices. The precise reproducibility of their composition is considered a clear advantage. This can result in lower production costs if compared to the production costs of biological matrices and, therefore, can ease production at an industrial scale. However, they lack the inherent biochemical components that naturally direct tissue regeneration and neovascularisation (Jednak, 2014).

The first attempts to replace bladder tissue with synthetic materials were described in the 1950s when patients underwent plastic urinary bladder implantation (Bohne and Urwiller, 1957; Portilla Sanchez et al., 1958). A foreign body reaction was described when polyvinyl sponges were used in a canine bladder augmentation model (Kudish, 1957). Teflon® and Gore-Tex® have also been used in bladder experimental studies in dogs, with no bladder capacity improvement but evidence of fibrosis, incomplete urothelial growth and no SMC ingrowth (Kelâmi et al., 1970; Virseda Chamorro et al., 1994).

The resin-sprayed paper was also reported in the 1970s as a bladder augment in contracted tuberculous bladders, resulting in fibrous pseudo-bladders (Fujita, 1978).

The most used polymers for synthetic scaffolds are poly-α-esters such as poly(L-lactide) or polylactic acid (PLA), polyglycolic acid (PGA), poly(lactide-co-glycolic acid) or copoly(lactic/glycolic) acid (PLGA) (Atala, 1998; Matoka and Cheng, 2009; Petrovic, Stankovic and Stefanovic, 2011). PLA, PGA and PLGA are biodegradable thermoplastics, biocompatible, non-toxic, widely applied in several biomedical applications, and approved for clinical use by the FDA, for example, in surgical suturing (Pillai and Sharma, 2010; Patel and Chakraborty, 2016). Porous scaffolds made with synthetic PGA, PLA and PLGA can be manufactured using several techniques and technologies. It has been proposed that synthetic electrospun scaffolds can create favourable conditions to improve cell adhesion and migration. An electrospinning protocol to create a PLGA scaffold with required porosity to enhance neovascularisation and cell proliferation from the bladder mucosa has been optimised by Ajalloueian and colleagues (2014). In 2017, an electrospinning protocol was successfully applied to create poly(ε-caprolactone)/poly(l-lactic acid) scaffolds for bladder wall replacement in dogs. Such matrices were then seeded with SMCs and showed an in vivo growth of local native cells (Shakhssalim et al., 2017). SMCs have been thought to migrate longitudinally along poly(ε-caprolactone) nanofibers acquiring contractile phenotype, indicating that electrospun nanofibers may be able to provide a sort of guidance or regenerating smooth muscle components.

Hybrid scaffolds have also been introduced as a promising strategy for bladder tissue engineering. In 2013, Ajalloueian and colleagues introduced a scaffold made of plastic-compressed collagen containing a reinforcing knitted fabric of poly(ε-caprolactone) (PCL) seeded with minced bladder mucosa. After six weeks of in vitro incubation, the authors found that cells migrated from the bladder mucosa particles and reorganised on the supporting scaffold. There was evidence of a multilayer (stratified urothelium?). They achieved close contact between the collagen and the knitted fabric after modifying the surface of the PCL fabric with alkaline hydrolysis followed by polyvinyl alcohol (PVA) adsorption treatment. The same authors developed another scaffold containing electrospun PLGA with increased porosity and plastic-compressed collagen seeded with minced bladder mucosa. They found comparable tensile strength but increased stiffness when comparing such a hybrid construct with the characteristics of the human urinary bladder (Ajalloueian et al., 2013, 2018).

Artificial scaffolds for bladder regeneration have been used either cell-seeded and unseeded in in vitro settings (Rohman et al., 2007; Stankus et al., 2008; Baker et al., 2009; Engelhardt et al., 2010; Ajalloueian et al., 2013, 2014; Sivaraman et al., 2015), in canine (Oberpenning et al., 1999; Jayo et al., 2008; Kwon, Yoo and Atala, 2008), porcine (Tu et al., 2013; Webster et al., 2013), rat (Stankus et

al., 2008; Jack et al., 2009; Gaudio et al., 2013; Horst et al., 2014; Kajbafzadeh et al., 2014), murine (Gomez et al., 2011) and human models (Atala et al., 2006). To date, reports have shown alternate results, highlighting the need for further studying solutions for urinary bladder regeneration.

1.4.5 Processing techniques

A variety of processing techniques have been described and applied for fabrication of matrices produced from natural or synthetic polymers. These include electrospinning (Baker et al., 2006), phase separation (Rowlands et al., 2007) gas foaming (Mooney et al., 1996), particulate leaching (McGlohorn et al., 2004; Baker et al., 2011), inkjet-printing (Roth et al., 2004). Such manufacturing processes can contribute to obtain scaffolds from biological or synthetic polymers. Cross-linking (chemical, physical or enzymatic) is the process that promotes material stabilisation by creating bonds between polymer chains and it can be required to improve mechanical properties of the scaffolds (Park et al., 2002; Wiesmann and Lammers, 2009; Campiglio et al., 2019; Lim, 2022). Scaffolds of different porosity and shapes have been fabricated using these techniques aiming to facilitate cell engraftment. It has been proposed that growth and other bioactive factors could be added to bioscaffolds with the intent to enhance angiogenesis and encourage vascularisation during the process of tissue regeneration (Mikos et al., 1993; Nomi et al., 2002; Wang et al., 2008; Kaully et al., 2009; Rohman et al., 2009; Chen, Zhang and Wu, 2010; Lee et al., 2010).

1.5 Thesis rationale

The previous paragraphs explained the clinical need for alternative solutions, including TE and RM technologies, for small-contracted bladders when conservative medical and minimally invasive treatments fail. The surgical procedure of urinary bladder auto-augmentation (detrusorotomy) has been introduced (section 1.2.1) alongside its known complications, which have impeded the widespread application of this surgical technique. The role of acellular biomatrices for urological surgical application, the status quo of their experimented applications, possible advantages and remaining open questions, have also been explained. The PABM was presented, alongside its decellularisation process, which allows the preservation of the biomechanical and biological properties of the full thickness originating tissue. The properties of PABM as detailed in section 1.4.3.2 suggest it may serve purpose for use in urological surgery and tissue-engineering applications.

1.5.1 Aim and objectives

The final aim of the present research was to investigate the PABM's biomaterial integration properties and tissue regeneration characteristics when applied in homologous surgical settings. Here, the potential of using PABM to reinforce the bulging mucosa in urinary bladder auto-augmentation was

examined. It was hypothesised that the use of this acellular matrix with integrative properties and physical properties (strength and compliance) homologous to the native tissue, would promote an adequate support and favourite a biological environment able to promote tissue regeneration. This potential surgical use for PABM was therefore tested in a large animal model of urinary bladder auto-augmentation, evaluating histological outcomes after 4 months in terms of integration of the biomaterial into the bladder and extent of cell and tissue regeneration.

In order to achieve these aims, the specific objectives of this project were as follow:

- To prepare and characterise PABM testing different decellularisation techniques for full-thickness porcine urinary bladders and investigate suitability for scaling up the decellularisation process.

- To determine local effect data studying biological response parameters for cross-linked versus non-crosslinked biomaterials when implanted as a urethral on-lay graft in a large animal model.
- To investigate biomaterial integration properties, and tissue regeneration characteristics, in a homologous surgical setting where the PABM is implanted to reinforce the bulging mucosa of auto-augmented urinary bladders.

In the following chapter, materials and methods are introduced and described in extenso.

Chapter 2
Materials and methods

2.1 General

2.1.1 Laboratories

Laboratory work was carried out at the Jack Birch Unit of Molecular Carcinogenesis (JBUMC), Department of Biology, University of York, UK. Large animal work was carried out at the Animal Facilities, University of Leeds, UK. Validation work to test the feasibility of scale up the decellularisation technique was carried out at Tissue Regenix Ltd manufacturing facilities, Leeds, UK. Image and quantitative analysis were performed at the Bioscience Technology Facility, Department of Biology, University of York.

2.1.2 Commercial suppliers, dissection equipment, surgical instruments, glassware and plastic-ware

All the manufacturers and suppliers are listed in the text or provided in Appendix I.

Tissue handling and dissection was performed using disposable scalpels (Scientific Laboratory Supplies; SLS), reusable forceps and scissors. After use, dissecting forceps and scissors were decontaminated in an ultrasonic bath (Ultra Wave) in a 1:40 (v/v) solution of Ultrawave Ultraclean M Formula (SLS) for 10 minutes. Then, reusable instruments were rinsed, dried, lubricated with Instol spray (Cell Path) before being packaged in autoclave pouches (Dr Buylines).

After use, glassware and reusable plasticware were washed with de-ionised water (dH_2O) to prevent exposure to detergents and sterilised before use (Section 2.1.4). Single use plastic-ware including 5ml Bijoux, 30ml Universal tubes were Sterilin brand and supplied by SLS. Pasteur plastic pipettes (2 ml) were supplied by SLS and Petri dishes (90 x 15 mm, 150 x 15 mm) were from Thermo Fisher Scientific. Sample pots (150ml) and sterile serological pipettes were obtained from Sarstedt. Glass Pasteur pipettes (SLS) were packaged in metal cans and autoclaved before use (Section 2.1.4). Pipette tips and microfuge tubes were supplied by Starlab.

2.1.3 Reagents, stock solutions and buffers

Recipes for all stock solutions, buffers and their constituents are provided in the text or in Appendix II. Chemical reagents were supplied by Fisher or Sigma, unless otherwise stated. General laboratory solutions were prepared using dH_2O. Decellularisation solutions were prepared with ultra-pure water

from a Purelab Ultra Genetic (Elga) ultraviolet water purification unit. A precision balance (GR-200) was used to weight chemicals. A magnetic stirrer was used to facilitate dissolution. Solutions were placed on a hotplate (60ºC) if required. Liquid volumes were measured using measuring cylinders, and solutions were made in Duran bottles unless otherwise stated. When indicated, pH of solutions was measured using a HI 991001 pH meter (Hanna Instruments) and it was adjusted as required using 6 M HCl or 6 M NaOH.

2.1.4 Sterilisation

Dissection equipment, glassware, plasticware, pipette tips, microfuge tubes were sterilised by autoclave (121ºC and 1 bar for 50 minutes), then oven-dried at 80ºC. Glass Pasteur pipettes were autoclaved in metal pipette containers (Jencons).

Heat-stable solutions were autoclaved at 121°C for 20 minutes.

Heat-labile solutions were sterilised by syringe filtration through nitrocellulose filters with 0.2µM pore size (Sartorius).

2.1.5 Aseptic procedures

All aseptic procedures were performed in Class II laminar air flow safety hoods with HEPA filters. The hoods were either recycling (Medical Air Technology) or externally ducted (Envair). Hood working surfaces were cleaned with 1% v/v Virkon® (SLS), followed by 70% v/v ethanol (Fisher) before and after use. Materials entering the safety hoods were sprayed with 70% v/v ethanol.

2.2 Porcine bladder procurement, transportation, preparatory dissection and storage

Porcine bladders were obtained from the local abattoir (Alec Traves Ltd Abattoir). Whole bladders were removed from the animal at the time of death and provided in a sealed leak-proof plastic bag within less than 10 minutes from slaughter. More than 50% extra bladders than needed for experiments were ordered and collected. This was in consideration of any eventual unsuitability of bladders for processing, mainly secondary to size or damage. Bladders were either immediately inspected, placed in Sterilin pots with transport medium (Bolland et al., 2007), before being transported to the laboratory facility or were transported immediately to the laboratory, without transport medium, for processing.

In a class II safety cabinet, under aseptic conditions, each bladder was transferred into a 150 x 15 mm Petri dish and rinsed with wash buffer. If not inspected at the abattoir site, each bladder was then

inspected to ensure it was free from damage and suitable for being used. Any excess of fatty and connective tissue was removed by using sterile reusable scissors and forceps and appropriately disposed.

If the whole intact bladder was planned for decellularisation by gentle inflation and submersion method (2.3.3), it was slowly filled up to 500 ml of hypotonic buffer in a 1 L wide-mouthed container using a 50 ml syringe and a pair of blue disposable plastic 12 cm haemostatic forceps (Fisher Scientific). The same forceps were used to keep closed the bladder neck after having verified that no air was trapped within the bladder. The bladder was then immersed in the hypotonic buffer. The container was closed tight and sealed with parafilm to avoid any spillage. Bladder was incubated for 24h at 4 ºC (Figure 2.1).

Each bladder for decellularisation by flat-bed method was initially laid flat to allow orientation. In order to identifying the ventral surface, each bladder was rotated about its longitudinal (apex-to-neck) axis until symmetrical, so that one ureter was on each side of the bladder and the longitudinal connective tissue band was visible and running down the midline of the tissue (ventral surface facing upwards). With the ventral surface facing upwards, each bladder was then dissected into a flat sheet by:

1. removing the bladder neck by cutting through both bladder layers just below the ureters,
2. removing the apex by cutting approximately the same length as the previous incision, through both bladder layers,
3. cutting longitudinally through one bladder layer along the ventral connective tissue band.

Each bladder was then opened into a flat sheet, rectangular in shape. Removed tissue was discarded. To allow recognition of the bladder orientation, a small piece of bladder tissue was left towards the apex site.

Following such preparatory dissection, the excess of moisture was removed from the surface of each bladder by allowing it to air-dry just to the point where no moisture is visible on its surface. Some gauze (or blue roll paper 20 cm x 20 cm) were disinfected by adding 70% ethanol for 10 minutes and allowing the gauze to air dry. Each bladder was put on a gauze moistened with PBS and placed in a 120 ml Sarstedt Sterile container before being stored at -20 ºC (Figure 2.2).

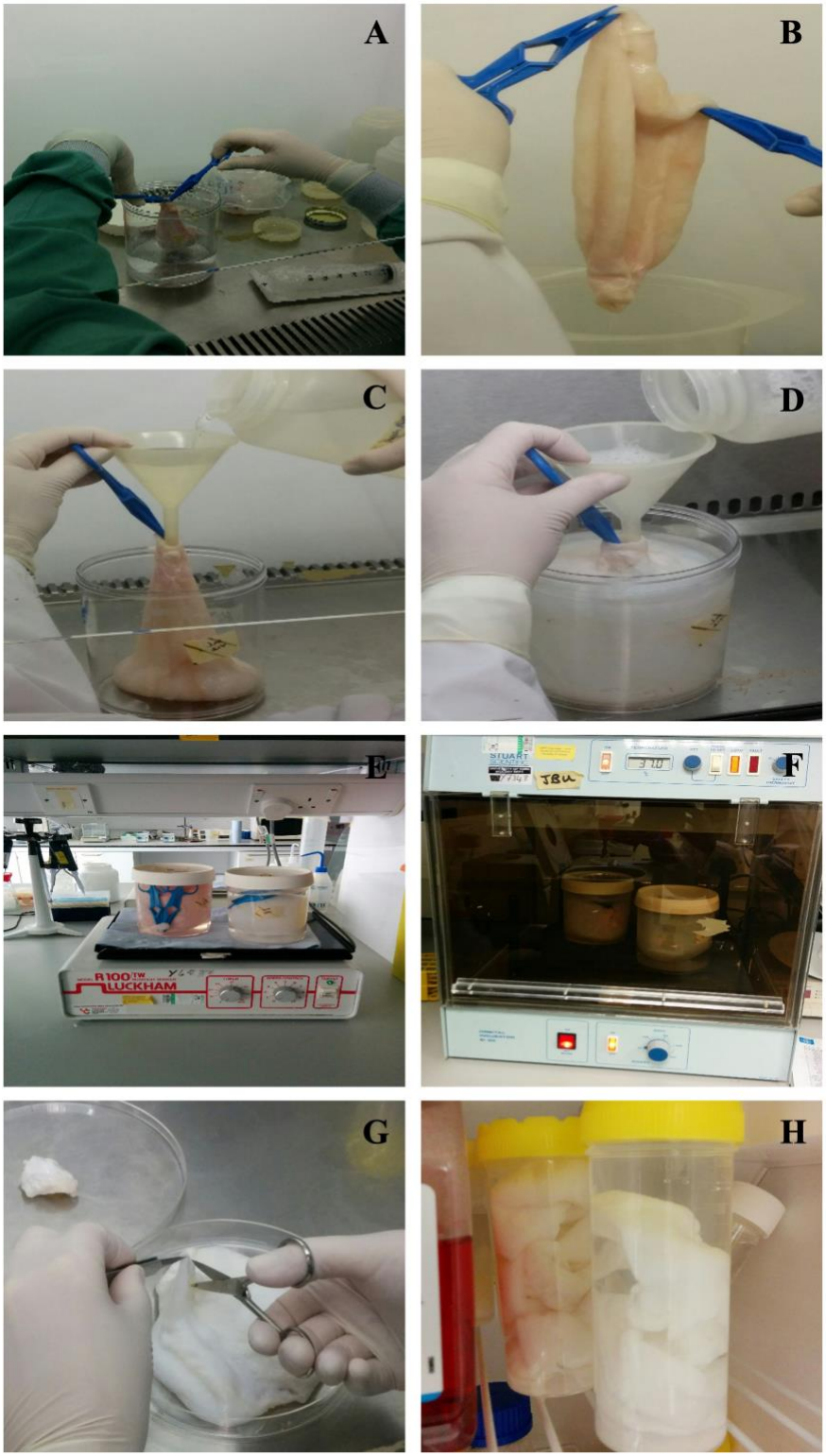

Figure 2.1 Decellularisation of intact porcine bladders.

Bladders were distended with up to 500 ml of solution prior to immersion (A, B, C, D). Use of the clamps allowed the bladders to maintain the distended status through the decellularisation steps (E, F). G and H illustrate the final dissection into flattened sheets and their storage at 4°C.

Figure 2.2 Dissection of porcine urinary bladder into a flat sheet.

(A, B, C) The ventral aspect of the bladder was recognisable by the presence of a longitudinal line of connective tissue (B). A small piece of bladder tissue was left towards the apex site to allow recognition of the bladder orientation (C). Each bladder sheet was placed on a gauze moistened with sterile PBS in a 120 ml Sarstedt Sterile container and stored at -20 ºC (D, E).

2.3 Porcine bladder decellularisation

2.3.1 Stock solutions

Ethanol, 70 % (v/v): 700 ml ethanol was made up to 1 L using deionised water and stored at ambient temperature for up to 6 months.

Alcohol, 90 % (v/v): 1350 ml denaturated alcohol was made up to 1.5 L using deionised water.

Sodium hydroxide solution, 6 M: 120 g NaOH pellets were dissolved into deionised water. The solution was made up to 500 ml and stored at ambient temperature.

Hydrochloric acid, 6 M: 500 ml HCl (6 M) was aliquoted from the stock solution. The solution was stored at room temperature.

Phosphate buffered saline (PBS): PBS tablets were dissolved into deionised water. The solution was made up to 1 L, autoclaved and stored at room temperature for up to 1 month.

EDTA solution, 10 % (w/v): 100 g EDTA were dissolved in 900 ml deionised water using a magnetic stirrer and hotplate turned on to ~60 °C to allow the EDTA to completely dissolve. The solution was made up to 1 L using deionised water, autoclaved at 121°C for 20 minutes and stored at ambient temperature for up to 6 months.

Sodium Dodecyl Sulphate (SDS) solution, 10 % (w/v): in a fume hood, 100 g SDS were dissolved in 900 ml deionised water using a magnetic stirrer. The solution was made up to 1 L using deionised water, filter-sterilised into sterile Universals (10 ml/Universal) using a filter with a pore size of 0.2 µm and stored at ambient temperature for up to 6 months.

$MgCl_2$ solution, 1 M: 203.3 g magnesium chloride hexahydrate [$MgCl_2(H_2O)6$] were dissolved in 700 ml deionised water using a magnetic stirrer. The solution was made up to 1 L using deionised water, autoclaved at 121°C for 20 minutes (section 2.1.4) and stored at ambient temperature for up to 6 months.

Tris-HCl, 2 M (pH 7.5): 242.38 g Tris were dissolved in 600 ml deionised water using a magnetic stirrer and hotplate turned on to ~60 °C. After cooling, pH was adjusted to 7.5 by adding hydrochloric acid (6 M). The solution was made up to 1L using deionised water, autoclaved as above (section 2.1.4) and stored at ambient temperature for up to 6 months.

Tris-HCl, 2 M (pH 8): 242.38 g Tris were dissolved in 600 ml deionised water using a magnetic stirrer and hotplate turned on to ~60 °C. After cooling, pH was adjusted to 8 by adding hydrochloric acid (6

M). Solution was made up to 1 L using deionised water, autoclaved and stored at ambient temperature for up to 6 months.

2.3.2 Working solutions

Transport medium (0.01 M HEPES, 20 KIU/ml aprotinin): aseptically, aprotinin (1 ml, 10000 KIU/ml) and HEPES (5 ml, 1 M) were added to 500 ml Hank's Balanced Salt Solution (HBSS) with Ca^{2+}/Mg^{2+}, $NaHCO_3$, and phenol red. This was aseptically aliquoted into five sterile 250 ml Sterilin pots (100 ml per pot) and stored for up to 3 months at 4°C.

Wash buffer (with EDTA): to make up 1 L of buffer, 10 PBS tablets and 10 ml EDTA stock solution were added to 989 ml of deionised water. Buffer was autoclaved and stored at ambient temperature for up to 6 months. Aseptically, in a class II safety cabinet, 1 ml aprotinin was added immediately before use.

Wash buffer (no EDTA): to make up 1 L of buffer, 10 PBS tablets were added to 999 ml of deionised water. Buffer was autoclaved and stored at ambient temperature for up to 6 months. Aseptically, 1 ml aprotinin was added immediately before use.

Hypotonic buffer: 5 ml Tris-HCl (2M, pH 8) stock solution and 10 ml EDTA stock solution were added to 984 ml of deionised water, autoclaved and stored at ambient temperature for up to 6 months. Aseptically, 1 ml aprotinin was added immediately before use.

SDS buffer: 5 ml Tris-HCl (2M, pH 8) stock solution and 10 ml EDTA stock solution were added to 974 ml of deionised water, autoclaved and stored at ambient temperature for up to 6 months. Before use, 10 ml SDS stock solution were added followed by 1 ml aprotinin added aseptically.

Nuclease solution.1 (used in the decellularisation of whole porcine bladders as in section 2.3.3): aseptically, 25 ml Tris solution (pH 7.5) and 10 ml MgCl2 (1 M) solution were added to 965 ml deionised water. The solution was autoclaved and stored for up to 1 month at ambient temperature. Aseptically, 50 mg bovine serum albumin (BSA) were added in a 10 ml aliquot of the solution. This step was performed immediately before use. BSA solution, 10 ml RNase A (100 U/ml), and 5 ml DNase I (10000 U/ml) were added and filter-sterilised into the nuclease solution.

Nuclease solution.2 (used in the decellularisation of full-thickness porcine bladder flat sheets as in section 2.3.4): 25 ml Tris-HCl (pH 7.5) stock solution and 10 ml $MgCl_2$ stock solution were added to 965 ml of deionised water, autoclaved and stored at ambient temperature for up to 6 months. Aseptically, 4 µl of benzonase (250 U/µl) were added just before use. The solution was used within 10 minutes of preparation.

Hypertonic buffer: using a magnetic stirrer, 87.66 g NaCl and 6.057 g Tris were dissolved in 800 ml of deionised water. By adding hydrochloric acid (6 M), pH was adjusted to 7.5. Solution was made up to 1 L using deionised water, autoclaved and stored at ambient temperature for up to 6 months.

Peracetic acid solution, 0.1 % (v/v): PBS tablets were dissolved in 800 ml of ELGA water. In a fume cupboard, 2.8 ml peracetic acid (36-40%) were added. By adding NaOH (6 M), pH was adjusted to 7.2. Solution was made up to 1 L using deionised water and used within 1 hour of preparation.

2.3.3 Decellularisation of full-thickness entire porcine bladders

This method was based on the procedure developed by Bolland and colleagues (2007). All materials were sterilised by autoclave before use (2.1.4).

Whole porcine bladders incubated for 24h at 4 ºC in hypotonic buffer (Day 1) were placed back in a class II safety cabinet. Under aseptic conditions, the hypotonic buffer was removed from the bladder, transferred to a large baker with Vyrkon and discarded the day after. With the use of a sterile funnel, the bladder was filled and immersed in SDS buffer as described above (2.2) and placed on an orbital shaker for 24h at ambient temperature (Day 2).

All subsequent steps were performed under the same aseptic conditions, in a class II safety cabinet (2.1.5). At completion of the indicated incubating time, each buffer was removed and discarded as above.

The bladder was subsequently washed in wash buffer (no EDTA) for 72h at 37 ºC on an orbital shaker (Grant PSU 10i shaker at 140 rpm or IKA KS 130 shaker at 160 rpm to allow gentle agitation) (Day 3-5).

Bladder was filled, immersed and incubated in nuclease solution for 24h at 37 ºC with gentle agitation (Day 6) and was then washed in wash buffer for 24h at 37 ºC without agitation (Day 7).

The following day, the bladder incubated in hypertonic buffer for 24h at 37 ºC with gentle agitation (Day 8).

Bladder was then washed in wash buffer for 24h at 37 ºC with gentle agitation (Day 9).

On the tenth day of the process, the wash buffer was removed, the bladder was filled with peracetic acid and incubated for 3h on an orbital shaker at ambient temperature. After removal of the peracetic acid, the bladder was placed in a large Petri dish (150 mm x 15 mm). The bladder neck was removed using reusable sterile scissors. The bladder was then dissected longitudinally, from the neck site to the base into a flattened sheet using a disposable sterile scalpel. One cm^2 specimens were taken from

the base site, the dome, the anterior and the posterior aspect of the bladder using the scalpel and were fixed in 10% Formalin (2.4.1.1).

The dissected bladder sheets were placed in Sterilin pots and washed with sterile PBS for 1h with gentle agitation at ambient temperature. This step was repeated for a total of three times (3 x 1h) using fresh Sterilin pots at each wash. The Sterilin pots were then labelled and stored with the bladder material at 4 ºC.

2.3.4 Decellularisation of full-thickness flat porcine bladder sheets

This method was based on the procedure developed by Ward et al. (2021). All steps were performed aseptically, in a class II safety cabinet (2.1.5).

All instruments were sterilised by autoclave before use (2.1.4).

Before starting the decellularisation process, the bladder sheets prepared and stored as described in section 2.2, were thawed at ambient temperature for 4 hours. In a class II safety cabinet, each bladder sheet was placed onto a sterile cork board (IKEA) with the urothelium facing downwards. In order to remove any residual contraction, a scalpel handle was used and gently pushed it over the bladder sheet. A guide plate (60 mm x 47 mm) was placed centrally onto the dorsal aspect of the rectangular bladder sheet (with the longest edge parallel to the longitudinal side of the bladder sheet). Using a disposable scalpel, the tissue was cut leaving a uniform 3 - 5 mm border around the guide plate. With the guide and help of the indentations of the guide plate, the pins (total length of the needles = 55 mm) were inserted through the tissue and into the cork board. The four corner pins were placed first. The guide plate was removed leaving the pins in situ. With the help of a pair of forceps, the pins were slightly removed from the cork board and the bladder tissue was moved up the pins. While keeping the pins in the tissue, those were detached from the cork board. At this point, it was possible to hold the tissue within the pins and gently, slowly and gradually start stretching and moving it onto the frame (144 mm x 140 mm). By moving opposing pairs, the corner pins were placed first, subsequently the midpoints of the edges and finally all the other pairs of pins.

The tissue was at greatest risk of tearing when the corner pins were being moved: this could be minimised by moving some of the adjacent pins. During the process, in order to avoid the tissue to become too dry, the sheets were kept moisturized by gently applying drops of sterile PBS. Using Spencer Wells blue plastic forceps, aseptically, each frame/stretched bladder sheet was picked up and placed it into an autoclaved container.

The hypotonic buffer was placed into the container and covered with the lid. Each container (with frame and bladder) was secured with Parafilm and placed at 4 ºC for 24 hours (Day 1).

One 230 x 230 x 110 mm container was used for 1 frame/bladder requiring 2.0 – 2.5 L of each buffer to allow the tissue to be entirely submerged. One 270 x 270 x 125 mm container was used for 2 frames/bladders requiring 6.5 L of each buffer to allow both frames/tissues to be entirely submerged.

Aseptically, for subsequent steps of the process and for each container/frame/bladder, the lid of the container was removed and, using plastic forceps, the frame was moved onto the upturned lid. The old buffer was emptied from the container. Using forceps, the frame/bladder was placed back into the empty container. The required buffer was placed into the container, which was covered with the lid. Each container (with frame and bladder) was placed at the required temperature (4°C, 37°C, or at ambient temperature). If required, containers were placed on an orbital shaker with gentle agitation. Following the hypotonic buffer, the solutions subsequently used were: SDS buffer (Day 2), wash buffer (no EDTA) (Day 3), nuclease solution (Day 4), wash buffer with EDTA (Day 5-7), hypertonic buffer (Day 8), wash buffer with EDTA (Day 9), peracetic acid solution and PBS × 4 (Day 10-11).

Following the peracetic acid solution step, in a class II safety cabinet, each bladder was removed from its container and using forceps all the pins used to secure the tissue to the frame were removed.

Final dissection: using sterile scissors, the outside border was removed by cutting between the points where the pins were previously placed in. Using a sterile disposable scalpel, provided with a graduated measure on the reverse of the handle (Swann Morton), the central region (8 cm x 8 cm) was isolated from the remaining tissue. This corresponded with the region of tissue sufficiently stretched and decellularised. each decellularised bladder sheet was transferred into a fresh Sarstedt 120 ml sterile container and fill with PBS solution. Each Sarstedt 120 ml sterile container was placed on an orbital shaker (gentle agitation) at ambient temperature for 1 hour (50 – 70 minutes) and the step was repeated twice more. On the final day of the process, each bladder sheet was aseptically transferred into a fresh Sarstedt 120 ml sterile container filled with 100 ml PBS solution and cover with the lid. Containers were then labelled with a batch processing label and stored at 4 ºC (Figure 2.3).

The process alongside equipment, stock solutions, decellularisation buffers, chemicals and reagents is detailed in the developed SOP provided in Appendix II.

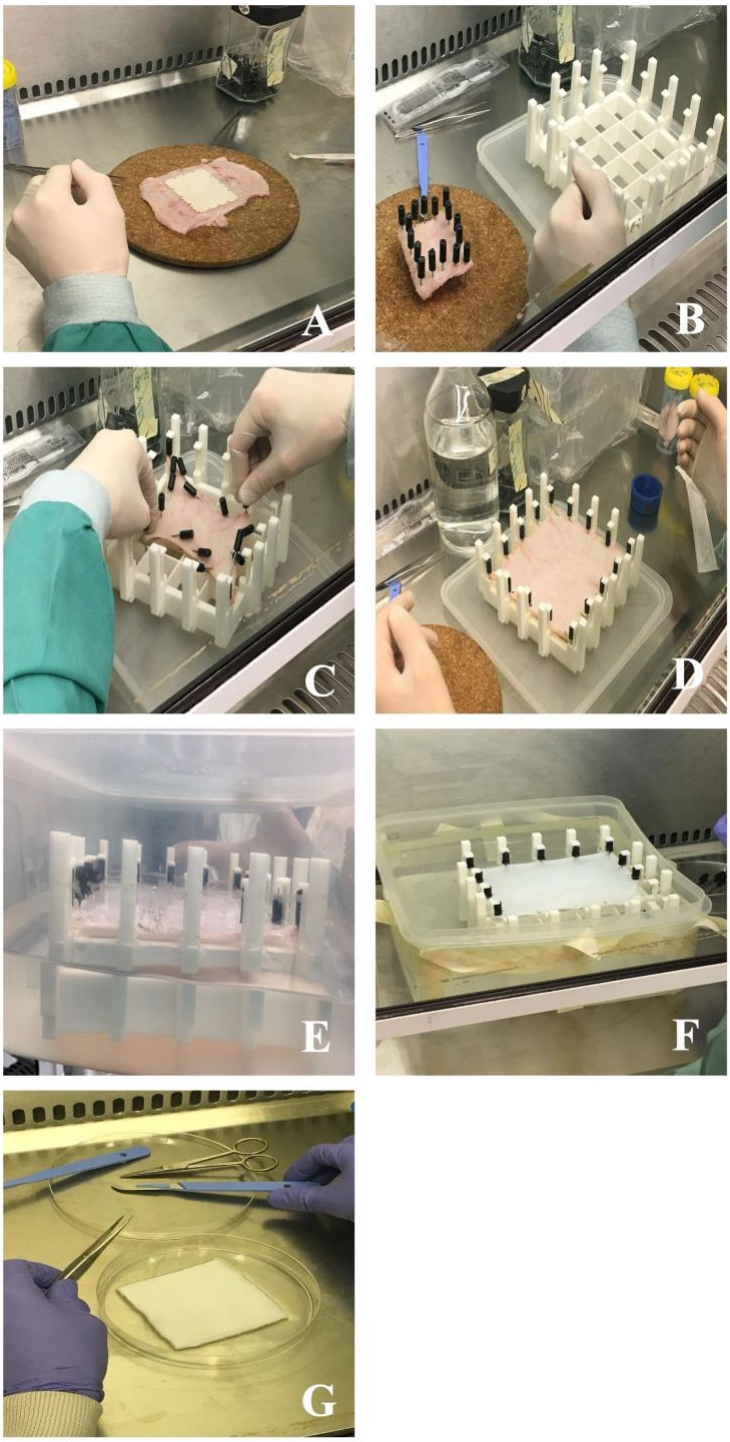

Figure 2.3 Decellularisation steps for porcine bladder flattened sheets.

The guide plate was placed centrally onto the dorsal aspect of the rectangular bladder sheet with the longest edge parallel to the longitudinal side of the bladder sheet (urothelium facing downwards onto the cork board) (A). Transfer of the bladder with pins onto the frame is shown in B, C, D. Stretched tissue was submerged in adequate volume of serial buffers (E). Along the process, a change of tissue colour was observed (pink to white) (F). Final 8 cm x 8 cm PABM sheet is shown in G.

2.4 Tissue processing and analysis

2.4.1 Histology

2.4.1.1 Fixation, dehydration, paraffin wax embedding and sectioning

Fresh and decellularised porcine bladders samples were placed at ambient temperature in neutral buffered formalin (NBF) (10% formalin (v/v) in PBS). At least, 1:10 tissue: formalin ratio was maintained to allow adequate fixation and preservation of the tissue features. Samples measuring less than 1 cm^3 were kept in NBF for about 18-24 h. Samples with dimensions between 1-3 cm^3 were fixed for an average of 72 h. Entire bladders were kept in NBF for 5 days.

After fixation, samples were placed into the same volume of fresh 70% ethanol and stored until histological processing.

Tissues were eclosed in embedding cassettes and dehydrated by submersion in fresh 70% ethanol, 100% ethanol (step repeated for a total of three washes), isopropanol (step repeated once), xylene (step repeated for a total of four washes), molten paraffin wax (Shandon) at 60ºC (step repeated for a total of four wax changes).

Samples were positioned and oriented to ensure that the fresh and decellularised bladder tissue would be sectioned perpendicularly to the surface of the entire bladder wall. Specimens in embedding moulds were set on a cold plate at -12ºC. Each mould was filled with molten wax and the labelled tissue cassette was placed on top to form the block lid.

Sections representing a cross-section of the entire bladder wall were created using a Leica RM2135 microtome set to 5 μm cutting thickness. Sections were carefully positioned on the surface of a floatation warm bath before being collected onto electrostatically charged Superfrost Plus glass slides to air dry. Once dry, sections were melted on a 50ºC hot plate (RA Lamb) to allow tissue sections to adhere to the glass slide and were stored at ambient temperature.

2.4.1.2 De-waxing, re-hydration, staining, de-hydration and mounting

With the help of a slide holder, sections were de-waxed using two 10-minute and two 1-minute xylene washes. Sequential rehydration was obtained using three 1-minute absolute ethanol washes, a 1-minute 70% (v/v) ethanol wash and by being placed in running tap water for 1-2 minutes.

<u>Haematoxylin and eosin (H&E)</u>

H&E staining was used to assess the presence and distribution of cells across sections of the porcine bladder wall in native, decellularised and regenerated tissue. Haematoxylin staining allowed visualisation of cell nuclei (dark blue). Eosin pink-stained cytoplasm, collagen and muscle fibres. Dewaxed and rehydrated sections were immersed in haematoxylin for 2 minutes, rinsed in running tap water for 1 minute (or until the water ran clear), immersed in Scott's water for 1 minute, rinsed in running tap water for 1 minute, counterstained in 1% (w/v) aqueous eosin for 30 seconds and rinsed in running tap water for 1 minute (or until the water ran clear).

After staining, sections were dehydrated in a 1-minute 70% (v/v) ethanol wash, three 1-minute absolute ethanol washes, and two 1-minute xylene washes.

Sections were then quickly dipped in Histoclear and mounted by placing a drop of DPX mountant (Sigma) on each section followed by sealing under a coverslip. By carefully pressing on the coverslip, all visible air-bubbles were removed.

Hoechst 33258

Hoechst 33258 (pentahydrate (bis-benzimide)) staining was used to visualise DNA in decellularised and native porcine bladder tissue sections. Hoechst 33258 is a fluorescent dye that intercalates with double-stranded DNA and emits blue fluorescence when excited by ultraviolet light, allowing visualisation of DNA. It binds and intercalates. Therefore, cell nuclei can be identified and visualised as blue dots using fluorescent microscopy.

After baking, dewaxing and re-hydrating, each tissue section was immersed in 5 ml Hoechst 33258 (1/10000 in PBS) dye solution in a rectangular compartmentalised dish quadriPERM for 5 minutes on an orbital shaker at ambient temperature. This step was followed by a 5-minute wash in PBS (5 ml/slide) on an orbital shaker at ambient temperature. Each slide was then immersed in 5 ml of dH_2O for 5 minute and kept at ambient temperature on an orbital shaker.

The following steps were performed in the dark.

Sections were left to air dry for at least 15 minutes, or longer if needed. Sections were mounted by placing a drop of Anti-Fade (AF) fluorescence mounting medium on each section, followed by covering with a coverslip. Air-bubbles were removed applying gentle pressure on the coverslip. Air-drying transparent nail polish was used to seal coverslips on glass microscopes slides. The nail polish was applied along the sides of the coverslip onto the slide. This step allowed to secure the position of the coverslip and to prevent leakage of the mounting medium. Slides were left to air-dry in the dark for at least 15 minutes and stored wrapped in foil to maintain dark conditions. Sections were viewed

with epifluorescence illumination using an Olympus BX60 microscope. Excitation and emission filters were selected for an optimal fluorescence detection.

2.4.2 Immunohistochemistry

Immunohistochemical techniques were used to selectively identify the presence, location and distribution of antigenic markers (proteins) in tissue samples.

The sequence of steps used are summarised as follows: dewaxing and re-hydration of FFPE tissue sections mounted on glass slide (section 2.3.1.2), blocking (if required), antigen retrieval (AR), application of primary antibody, addition of secondary antibody that binds the primary antibody, application of a chromogen agent and counter-staining to detect the localisation of the primary antibody.

2.4.2.1 Antibodies

Antibodies stocks were stored at –80ºC and working solutions at 4ºC. Primary antibodies were diluted in Tris-buffered saline (TBS) containing 0.1% (w/v) sodium azide and 0.1% (w/v) bovine serum albumin and titrated to optimise contrast between positively stained tissue and non-specific background. The highest primary antibody dilution was used to prevent waste.

To secure quality control, a positive (tissue known to expresses the protein of interest), and a negative (no primary antibody) control were processed with each series.

To minimise non-specific background staining, blocking of any endogenous peroxidase was performed by a 10-minute bath in 3% (v/v) hydrogen peroxide followed by a 10-minute wash in running tap water. Blocking step was performed unless otherwise specified.

2.4.2.2 Antigen retrieval methods

Below are provided physical and chemical AR methods used to pretreat tissue to retrieve antigens masked by fixation and to facilitate antibody binding.

a) Trypsinisation

100 ml of 0.1% $CaCl_2$ pH 7.8 was pre-warmed in a microwave or in a warm incubator set at 37°C. Just before use, 0.1g of trypsin was added to the solution and mixed well to completely dissolve trypsin powder. Slides were incubated for 10 min in the 0.1% (w/v) trypsin solution at 37°C in a water bath.

b) Microwave (Citric Acid)

Slides were placed in a Pyrex dish with 350 ml of 10 mM citric acid buffer pH 6.0. Small glass weights were placed on the top of slides and the Pyrex dish was covered with cling film with some punch holes in it. Slides were then microwaved at 800 W for 13 minutes. Once completed, the dish was laid on ice to allow cooling.

c) Trypsin and Microwave

This resulted in a combination of the two methods above. Sections were first trypsinised for 1 minute as in a). Slides were washed in dH_2O and microwaved in 10 mM citric acid buffer pH 6.0 as in b).

d) Microwave (EDTA)

Slides were placed in a Pyrex dish with 350 ml of 1 mM EDTA buffer pH 8.0. Small glass weights were placed on the top of slides and the Pyrex dish was covered with cling film with some punch holes in it. Slides were then microwaved at 800 W for 13 minutes. Once completed, the dish was laid on ice to allow slides to cool.

e) Pressure Cooker

2.5L of ELGA H_2O were poured into the pressure cooker pan. Plastic Coplin staining jars containing slides in the required buffer were placed in the pressure cooker at 50kPa for 10 minutes. Once completed, the Coplin jars were placed on ice to allow cooling.

2.4.2.3 Immunoperoxidase method

Preparation and primary antibody

Slides were applied to Sequenza cover-plates in TBS to secure good sealing. Slides with cover-plates were inserted in Shandon Sequenza racks (Thermo Fisher Scientific) and wells were filled with TBS to check the formation of a good seal. 100 µl of avidin (Vector Laboratories) were added to each coverplate well to block endogenous avidin binding and left incubating at ambient temperature for 10 minutes. Slides were washed twice with TBS. 100 µl of biotin (Vector Laboratories) were added and left incubating for 10 minutes at ambient temperature. Two further TBS washes were performed per each slide. To prevent any non-specific antibody binding, 100 µl of appropriate serum (10% (v/v) in TBS) was applied to each slide and incubated at ambient temperature for 5 minutes. Normal rabbit serum was used for mouse primary antibody and normal goat serum was used for rabbit primary antibody. 100 µl of primary antibody at the predetermined concentration was then added to all slides except for the negative controls that received 100 µl of TBS only. Slides were incubated overnight at 4°C.

Secondary antibody

Three TBS washes were performed to remove unbound primary antibody. 100 µl of appropriate biotinylated secondary antibody was added to each slide and incubated for 30 minutes at ambient temperature. Rabbit anti-mouse secondary antibody was used for a mouse primary antibody and goat anti-rabbit secondary for a rabbit primary antibody. Unbound secondary antibody was removed by two TBS washes.

Chromogen application

Streptavidin-biotin-horseradish peroxidase complex (StrepAB/HRP) (VECTASTAIN® ABC Kit, Vector Laboratories) was preprepared 30 minutes before its use and was applied (100 µl) to each slide for 30 minutes at ambient temperature. Two TBS-washes and one dH_2O-wash followed. 200 µl of diaminobenzidine (DAB) solution, obtained by dissolving Sigma Fast DAB tablets in 5 ml dH_2O, were added to the sections and incubated for 15 minutes at ambient temperature. To not allow sections to dry, slides were promptly twice-washed with dH_2O before being removed from cover-plates and placed in staining racks in dH_2O.

2.4.2.4 ImmPRESS™ Excel method (polymer kit for mouse or rabbit primary antibodies only)

Slides were applied to Sequenza cover-plates in a TBST bath and proper seal was checked filling the wells with TBST (technique described above).

Each sample was incubated for 20 minutes with 100 µl of 2.5% normal horse serum at ambient temperature. 100 µl of primary antibody (mouse or rabbit) pre-diluted in TBST were then added and incubated at 4°C overnight. Slides were washed three times with TBST. 100 µl of amplifier antibody was applied and incubated at ambient temperature for 15 minutes. After two TBST washes, 100 µl ImmPRESS Excel reagent was applied for 30 minutes at ambient temperature. Two TBST washes and one dH_2O followed. Equal quantity of ImmPACT DAB reagent 1 and reagent 2 were mixed by vortexing, and 100 µl of the solution was added to each slide for 5 minutes. Slides were rinsed in dH_2O and then in tap water before counterstaining step (2.3.2.5).

2.4.2.5 Counterstaining

Slides in the staining rack were counter-stained in haematoxylin, blued in running tap water for 2 minutes, dehydrated and mounted using DPX and coverslips as described for H&E staining (Section 2.4.1.2).

The resulting brown colour of the DAB reagent was used to identify antigen expression using microscopy (2.4.3.1).

2.4.3 Imaging analysis

2.4.3.1 Photo-microscopy

H&E-stained and IHC tissue sections were observed with bright-field illumination using an Olympus BX60 microscope equipped with x4, x10 and x20 objectives. Labelled Hoechst 33258-stained slides were viewed using epifluorescence illumination with an Olympus BX60 microscope with x20 and x40 oil objectives. Olympus immersion oil was used. Images were captured using an Olympus DP50 digital camera and processed using Image-Pro®Plus software (Media Cybernetics).

2.4.3.2 Zeiss slide scanner and TissueGnostics StrataQuest software

To facilitate quantitative analysis, a Zeiss Axio Scan.Z1 microscope slide scanner was used to scan labelled slides. The resulting images were stored as CZI image files.

To quantify protein expression on immunohistochemically labelled tissue slides, StrataQuest software (version 6.0.0.123 and version 7.0.1.178) on the TissueGnostic image analysis platform (Vienna, Austria) was applied to CZI files.

Haematoxylin staining was used as a master marker for nuclear detection in cell identification. The average nuclear size, discrimination area, discrimination grey and background threshold were specified. The auto-detection function was used to set the intensity of the master marker (nuclear haematoxylin) and the immunohistochemical staining (DAB label) to identify the different cell type-associated markers. Standard shape 0.1 x 0.1 mm^2 non-overlapping regions of interest (ROIs) were defined. Settings were optimised and the same conditions applied to analyse all image files. To quality control measurements, forward and backward gating was used. Results of the analysis were visualised as dot plot scattergrams and histograms. Raw data were imported into GraphPad Prism for statistical evaluation.

2.5 DNA extraction, purification and quantification assay (absorbance method)

To determine the amount of residual nucleic acid (dsDNA, ssDNA, ssRNA) in the produced PABM, extraction and purification of total DNA from both PABM samples produced at the JBU laboratory and PABM samples produced at the medical equipment manufacturing facilities of TRX Ltd in Garforth (UK). The DNA assay exploits the property of the DNA to absorb at a wavelength of 260 nm and 280 nm and determines the concentration of DNA in porcine tissue (native and decellularised) by absorbance at these wavelengths. At the JBU, a NanoDrop™ ND-1000 spectrophotometer was

used to perform a calculation-based absorbance reading at 260 nm to give the required concentration (ng/µl).

Unprocessed fresh tissue samples were analysed for DNA content (positive control). A negative control (AE buffer) was also included. Sample were processed and analysed in triplicate. The procedure was performed using Qiagen DNeasy® Blood and Tissue Kit (cat. Nos. 69504 and 69506).

2.5.1 Tissue sample preparation

Each tissue was placed onto a new Petri dish. With the help of a sterile disposable scalpel and reusable sterile forceps a 2 mm x 2 mm small piece was cut. Each small piece of PABM had a weight of approximately 10 mg.

2.5.2 DNA extraction and purification

Samples were placed in a 1.5 ml microcentrifuge tube. 180 µl of a tissue lysis buffer (ATL buffer) and 20 µl of proteinase K solution were added. Samples were mixed by vortexing and incubated at 56 ºC on a preheated heather block for 4 h (or until completely lysed). During incubation, samples were vortexed twice. A 15-second mix by vortexing was performed at the end of the incubation time just before proceeding to the following step. 200 µl of buffer AL (supplied within the kit as ready for use) were then added, and samples were mixed thoroughly by vortexing. Subsequently, 200 µl of absolute ethanol was added, and samples were mixed thoroughly by vortexing. The mixture was then pipetted into DNeasy Mini spin column (provided with the kit) placed in a 2 ml collection tube (provided with the kit). Those were centrifuged at 8000 rpm (revolutions per minute) for 1 minute. The flow-through and the collection tube were discarded, and the spin column was placed in a new 2 ml collection tube. 500 µl of buffer AW1 were added, and the mixture was centrifuged at 8000 rpm for 1 minute. As above, the flow-through and the collection tube were discarded, and the spin column was placed in a new 2 ml collection tube. 500 µl of buffer AW2 were added, and the mixture was centrifuged at 14000 rpm for 3 minutes. Buffers AW1 and AW2 were supplied concentrated and required dilution with absolute ethanol according to the supplier instructions in order to obtain the working solution. The flow-through and the collection tube were again discarded, and the spin column was transferred to a new pre-labelled 1.5 ml microcentrifuge tube. To elute the DNA, 100 µl of buffer AE (provided with the kit) were added to the centre of the spin column membrane that was incubated at ambient temperature for 1 minute and then centrifuged for 1 minute.

2.5.3 DNA quantification

Samples were quantified using the NanoDrop™ ND-1000 spectrophotometer. Before starting, the system was cleaned, calibrated and blanked. To prevent cross-contamination cleaning and blanking steps were repeated between measurements. 1.2 μL of each sample was carefully pipetted directly onto the measurement pedestal. Three measurements were taken per each sample and the mean of these readings was calculated.

2.6 Sterility testing

Sterility testing is a critical quality control process to detect and measure microbial contamination levels in a biomedical product.

2.6.1 Nutrient broth

Working in a class II safety cabinet, 0.5 cm × 0.5 cm samples were obtained from decellularised and native porcine bladder tissue. Positive and negative controls were processed with each series. Three replicates were included per tissue sample. Samples were added to 5 ml Lysogeny Broth (LB) and placed in an incubator shaker at 37°C.

2.6.2 Optical density

Samples were analysed for microbial growth at 24 h and more than 72 h. Analysis was performed by measuring the optical density at 600 nm (OD_{600}) based on absorbance detection mode using a BioPhotometer.

2.7 Cytotoxicity testing

To fulfill requirements of an industry-relevant Analytical Quality Control (AQC) of the PABM produced (section 2.3.4), cytotoxicity testing was performed. As per request of the commercial partner Tissue Regenix, the contact cytotoxicity test was performed by an external company (Nelson Laboratories, LLC, Salt Lake City, U.S.A.). The Minimal Essential Media Elution test was designed and performed by Nelson Laboratories to determine the cytotoxicity of extractable substances. In summary, an extract of the test article was added to cell monolayers and incubated. The cell monolayers were examined and scored based on the degree of cellular destruction. Testing was performed in compliance with US FDA good manufacturing practice (GMP) regulations 21 CFR Parts 210, 211 and 820. The procedure is detailed in Appendix III.

2.8 Graphical and statistical analysis

Data were imported, organised, analysed and graphically represented using Microsoft® Excel 2000 or GraphPad Prism (version 9.0.2(161)).

Chapter 3

Towards an improved and scalable process of porcine bladder decellularisation

3.1 Background

Acellular matrices (Section 1.4.3) are biomaterials derived from animal or human tissues, that are processed to remove cellular components, including DNA and RNA, while preserving the extracellular matrix structure (ECM) (Schmidt and Baier, 2000). The resulting lack of immunogenicity (Allaire et al., 1994) and the recognised characteristic of being highly conserved across species (Van Der Rest and Garrone, 1991), make the ECM suitable for autologous, allogeneic and potentially xenogeneic applications.

PABM, introduced in Section 1.4.3.2, is a full-thickness natural acellular matrix, developed via a patented process (Bolland et al., 2007). This decellularisation process (distension by inflation and immersion) differs from other described bladder decellularisation techniques as it was applied to a whole full-thickness porcine bladder. In fact, to reduce originating tissue thickness and achieve satisfactory decellularisation, other groups utilised delamination of the bladder wall to obtain split-thickness tissue (Chen, Yoo and Atala, 1999; Badylak et al., 2000; Rosario et al., 2008; Davis et al., 2011; Keane, Swinehart and Badylak, 2015).

PABM was shown to retain the inherent major structural components and physical characteristics, including strength and compliance, of the originating full-thickness porcine bladder tissue (Bolland et al., 2007). The matrix resulted biocompatible with bladder-derived cells and was thought to have potential for use in urological surgery and tissue-engineering applications (Bolland et al., 2007).

A scalable and reproducible manufacturing process that allows for the transfer from the benchtop to an industrial scale of tissue engineering strategies in general (Rustad et al., 2010) and more specifically of this biomatrix production (Ward et al., 2021) is highly desirable. Such transition from the laboratory to the market, facilitated by scalable manufacturing processes, should produce biomaterials in large quantities without compromising their functional properties. This need led to the development of a decellularisation technique for full-thickness porcine bladder sheets via stretching on a 3D printed flat-bed rig (Ward et al., 2021) (Appendix V). Such technique exploited the regional and directional anisotropy in the biomechanical and histological characteristics of the

porcine bladder to calculate and achieve sufficient tissue stretching/thinning in order to facilitate adequate diffusion of the solutions, and obtain satisfactory decellularisation (Korossis et al., 2009).

3.2 Aim and objectives

The aim of the study reported in this chapter was to test, implement and transfer a more scalable decellularisation technique for full-thickness porcine urinary bladders.

Objectives:

To decellularise porcine bladders using the decellularisation method of distension by inflation and immersion and evaluate histology and presence of residual DNA in the produced PABM.

To perform decellularisation on porcine bladder sheets using an implemented decellularisation method through distension on a flat-bed rig at the Jack Birch Unit academic laboratory facility and evaluating histology, presence of residual DNA and sterility of the produced PABM.

To transfer knowledge of decellularisation of porcine bladders' sheets process through distension on a flat-bed rig at the Tissue Regenix Ltd manufacturing facility and perform Quality Control (QC) analysis of the produced PABM.

3.3 Experimental Approach

3.3.1 Decellularisation of full-thickness, intact porcine bladders: distension by inflation and immersion

Five bladders were collected from Traves abattoir (A Traves & Son Ltd) and transported to the JBU laboratory in transport medium according to the method described in Section 2.2. All subsequent work was carried out aseptically in a class II safety cabinet. Excess tissue was removed from the bladders that were left intact as outlined in Section 2.2. Bladders underwent decellularisation using the method (Bolland et al., 2007) detailed in Section 2.3.3. Filling volumes of 500 ml in a sequential series of sterile extraction buffers, including detergents and a nuclease solution were used to lyse and remove cell components, and render the tissue acellular. At the end of the procedure, the decellularised bladders were dissected open in a flattened sheet. Bladders' measurements were not recorded. A total of about one litre of each solution was used per bladder.

3.3.1.1 Biomaterial assessment

Square samples, approximately 0.5 cm x 0.5 cm in size, were taken for histological analysis from fresh and decellularised porcine bladders at the level of the base, dome, anterior and posterior walls.

Samples were fixed in NBF, processed, embedded in paraffin wax and sectioned, as described in Section 2.4.1.1. Tissue sections were then de-waxed, re-hydrated, stained with either H&E or Hoechst 33258 before being dehydrated and mounted as detailed in Section 2.4.1.2. Slides were respectively evaluated via bright-field microscopy or fluoroscopy (Section 2.4.3.1).

3.3.2 Decellularisation of full-thickness, porcine bladder sheets on flat-bed rig - at the laboratory facility of the Jack Birch Unit for Molecular Carcinogenesis

To produce an acellular matrix from porcine bladders using a decellularisation technique by distension on a flat-bed rig, bladders were collected from the abattoir and transported to the laboratory without transport medium according to the method described in Section 2.2.

All subsequent work was carried out aseptically in a class II safety cabinet. Bladders were inspected and the excess tissue was removed. The bladders were dissected flat, then rinsed with wash buffer, air dried for about 10 min, placed into Sterilin pots, and frozen at -20 °C (Section 2.2).

On day one of the decellularisation process, bladders were thawed at ambient temperature for at least 4 h. The bladders were decellularised as described above in Section 2.3.4 and stored at -4°C.

3.3.2.1 Biomaterial assessment

Square samples, approximately 0.5 cm x 0.5 cm in size, were taken for histological analysis from fresh bladders and decellularised sheets. Samples were fixed in NBF, processed, embedded in paraffin wax and sectioned, as described in Section 2.4.1.1. Tissue sections were then de-waxed, re-hydrated, stained with either H&E or Hoechst 33258 before being dehydrated and mounted as detailed in Section 2.4.1.2. Slides were respectively evaluated via bright-field microscopy or fluoroscopy (Section 2.4.3.1).

Samples for total DNA extraction and quantification were taken from fresh and decellularised bladder tissue, processed using Qiagen DNeasy Blood and Tissue Kit and analysed using Nanodrop Spectrophotometer, as described in Section 2.5.

End preparation sterility testing was performed using LB medium (Section 2.6.1), and Optical Density (OD600) was evaluated by BioPhotometer (Section 2.6.2).

Cytotoxicity testing of extractable substances in the produced PABM was performed by an external laboratory facility (Nelson Laboratories, Salt Lake City, UT, USA) on request of the commercial partner (TRX Ltd) (Section 2.7). The Minimal Essential Media (MEM) Elution test was used to determine any cytotoxic effect of the produced PABM. An extract of the test article was added to cell

monolayers before incubation. The cell monolayers were examined and scored based on the degree of cellular destruction. Testing was performed in compliance with US FDA good manufacturing practice (GMP) regulations, with all test method acceptance criteria reported as met. The details of the procedure are provided in Appendix III.

3.3.3 Decellularisation of full-thickness, porcine bladder sheet on flat-bed rig - at the TRX facility

To transfer the decellularisation process by distension on a flat-bed rig to a manufacturing site of a commercial partner and to scale up the production of PABM, fifteen bladders were collected from the abattoir and transported to the laboratory without transport medium according to the method described in Section 2.2.

Bladders were inspected and the excess tissue was removed (Section 2.2). Three out of fifteen resulted suitable for decellularisation process based on dimensions and general conditions. The bladders were dissected flat, then rinsed with wash buffer, air dried for about 10 min, placed into Sterilin pots, and frozen at -20 °C (Section 2.2).

On day one of the decellularisation process, bladders were thawed at ambient temperature for at least 4 h. The bladders were decellularised as described above in Section 2.3.4. On request of the industrial partner, the following exceptions to the protocol were made:

Aprotinin was not used.
Sterilisation step (by peracetic acid) was not performed.

Produced PABM sheets were stored at -4°C.

3.3.3.1 Biomaterial assessment

QC analysis of the matrices produced at TRX facilities was performed at the JBU laboratory.

Square samples, approximately 0.5 cm x 0.5 cm in size, were taken for histological analysis from fresh bladders and decellularised sheets as indicated in Figure 3.1. Samples were fixed in neutral buffered formalin (NBF), processed, embedded in paraffin wax and sectioned, as described in Sections 2.4.1.1. Tissue sections were then de-waxed, re-hydrated, stained with either H&E or Hoechst 33258 before being dehydrated and mounted as detailed in section 2.4.1.2. Slides were respectively evaluated via bright-field microscopy or fluoroscopy (Section 2.4.3.1).

Samples for total DNA extraction and quantification were taken from fresh and decellularised bladder tissue, processed using Qiagen DNeasy Blood and Tissue Kit and analysed using a Nanodrop Spectrophotometer, as described in Section 2.5.

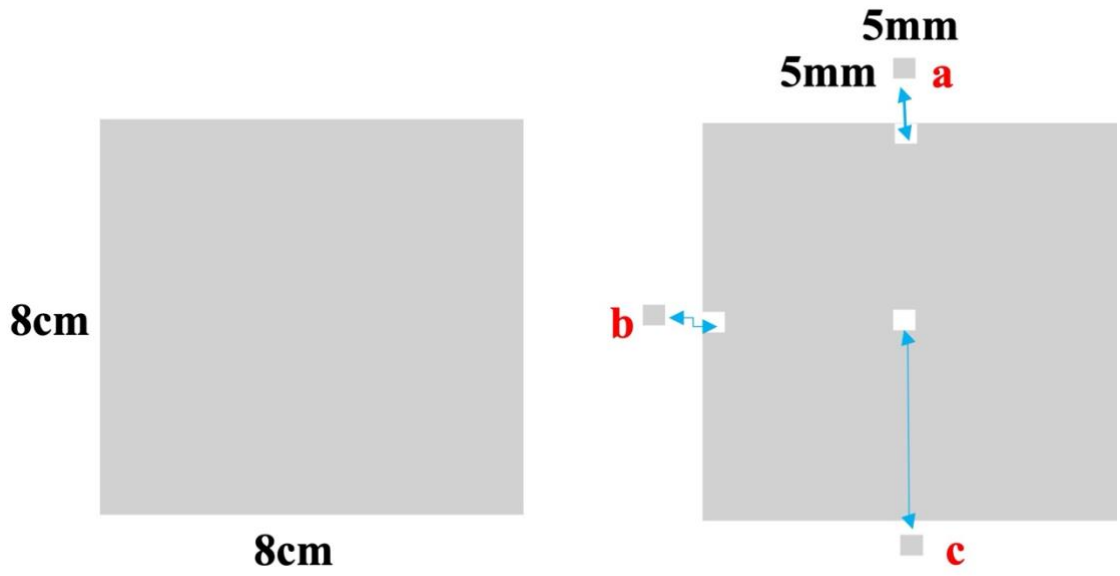

Figure 3.1 PABM tissue sampling.

Scheme illustrating tissue sampling applied to the 8 cm x 8 cm PABM sheets produced at TRX and the regions from which the three 5 mm x 5 mm samples of PABM were taken for analysis.

3.4 Results

3.4.1 Decellularisation of full-thickness, intact porcine bladders: distension by inflation and immersion

Upon inspection, two of the collected bladders resulted suitable for processing and were decellularised using the method of distension by inflation and immersion (section 2.6 and 2.7). At each step of the process, 500 ml of solution were used to distend the bladders, which were placed in a jar containing further 500 ml of the same decellularisation solution (Figure 2.1). A total of about one litre of solution was used at each decellularisation step. Bladders were subsequently processed and histologically assessed for presence of cellularity.

Both decellularised bladders showed absence of any residual urothelium with some cellular remnants identified at the level of the bladder wall. Specifically, nuclear material was found in a specimen taken from the posterior wall of the first bladder and from the base of the second processed bladder.

Figure 3.2 shows images of sections taken from the second decellularised bladder compared with fresh control samples, stained with H&E. No urothelial cells were identified in the decellularised samples. Some evidence of residual nuclear material is noticeable in Figure 3.2B (base) suggesting that the tissue was only partially decellularised.

Similarly, some residual nuclear material Hoechst 33258-stained was detected in tissue sample taken at the level of the posterior wall for the first decellularised bladder and the base of the second bladder (Figure 3.3).

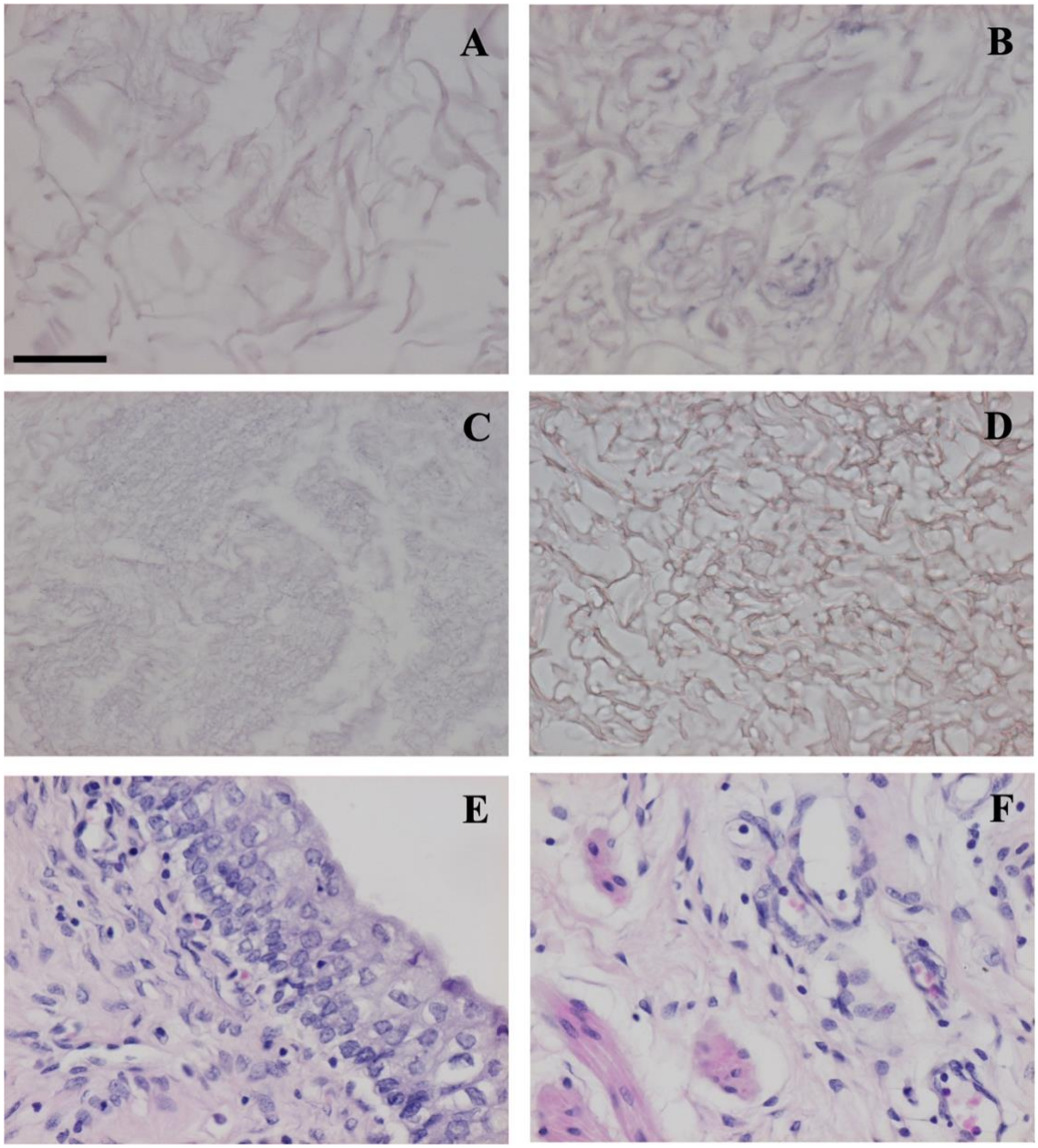

Figure 3.2 Micrographs of H&E-stained sections from a porcine bladder decellularised using the distension by inflation method.

A is a section from the anterior wall, B is a section from the base, C is a section from the dome and D is a section from the posterior wall. E and F are native controls showing urothelium and detrusor muscle. Some residual nuclear material was noted in sample B (Base). Images were captured at 60× magnification. Scale bar: 50μm.

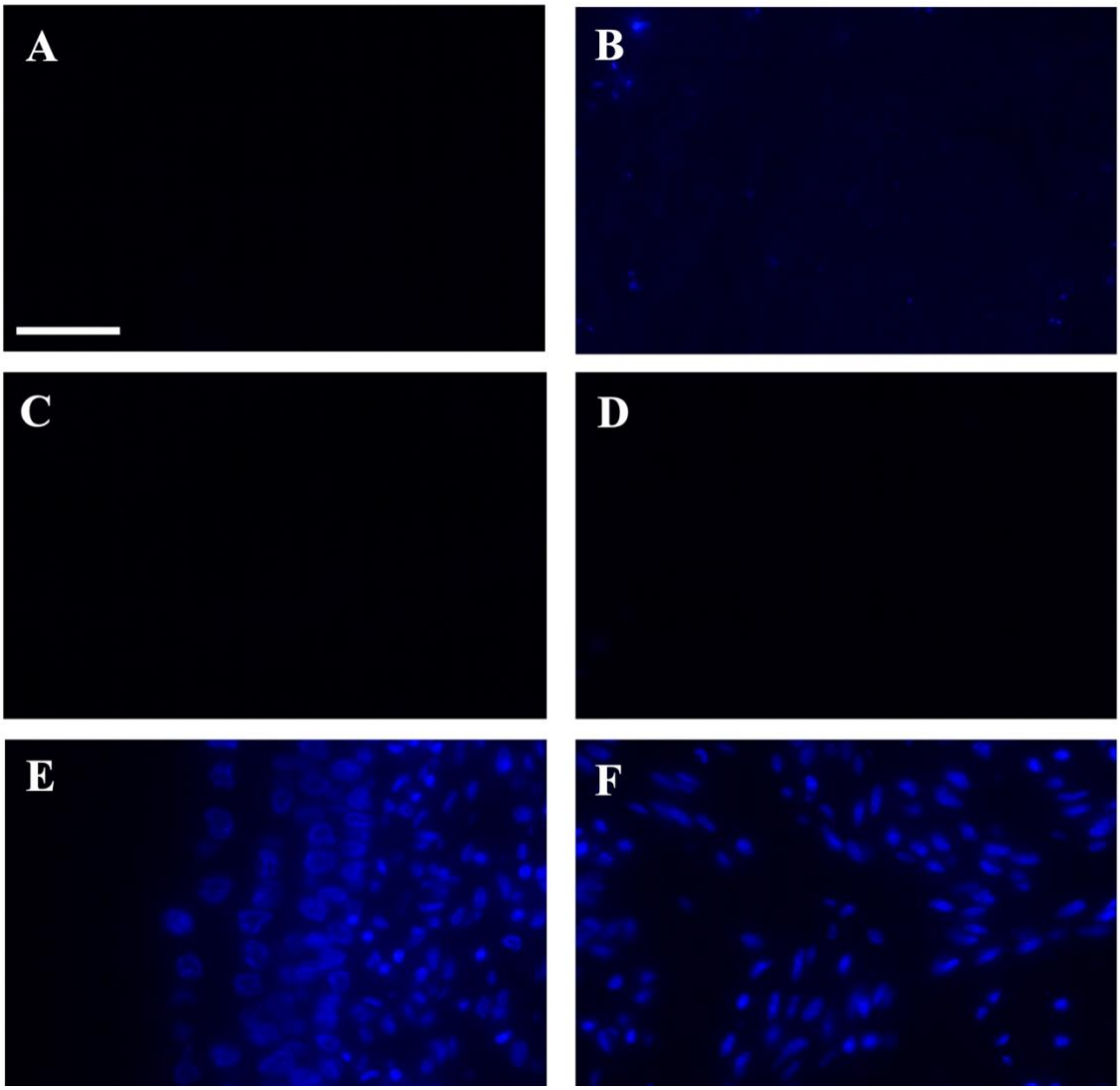

Figure 3.3 Micrographs of Hoechst 33258 stained sections from a porcine bladder decellularised using the distension by inflation method.

A is a section from the anterior wall, B is a section from the base, C is a section from the dome and D is a section from the posterior wall. E and F are native controls showing urothelium and detrusor muscle. Evidence of some residual nuclear material was found in sample B (Base). Images were captured at 60× magnification, scale bar 50 µm. Exposure time: 1/35 sec.

3.4.2 Decellularisation of full-thickness, porcine bladder sheets on flat-bed rig - at the laboratory facility of the Jack Birch Unit for Molecular Carcinogenesis

In total, six porcine bladders were decellularised subdivided in two batches of three bladders, using the method of stretching bladder tissue on a flat-bed rig. Therefore, two batches of three 8cm x 8cm PABM sheets were produced. At each step of the process, stretched bladder tissue was placed into a large container filled with about two litres of decellularisation buffer, to allow the tissue to be fully immersed in the solution (Figure 2.2 and 2.3). Bladders were subsequently processed and histologically assessed for presence of cellularity.

Figure 3.4 and 3.5 show images of sections taken from decellularised bladders (two batches of three bladders with three replicates per each bladder) stained with H&E. No urothelial cells were identified in the decellularised samples. No evidence of nuclear material or residual cell fragment was noted across the processed samples.

No nuclear Hoechst 33258 staining was detected in sections from decellularised bladder tissue at the detailed settings (Figure 3.6). For comparison, positive controls are showed in Figure 3.2 and 3.3.

A NanoDrop Spectrophotometer was used to quantify the DNA purified and extracted from samples of decellularised and native porcine bladder tissue. Acquired data confirmed adequate decellularisation. Data (mean ± SD) relative to the quantified DNA content in comparison to native controls is shown in Figure 3.8 for the three bladders decellularised in each of the two batches of the decellularisation process, for a total of six bladders.

End of preparation sterility testing was performed, and the Optical Density (OD600) was evaluated by BioPhotometer. No growth was detected in decellularised material, compared with positive control porcine bladder tissue. Data expressed in mean ± SD is shown in Figure 3.9 for the two batches of porcine bladders decellularised.

Furthermore, Minimal Essential Media (MEM) Elution test was performed at an external facility (Nelson Laboratories, LLC) to assess biomaterial cytotoxicity. Pre- and post-extracts were found clear, with no particulates present. Post-extracts did not show any changes in colour. Overall, no evidence of cellular destruction was seen for any sample (the full report is provided in Appendix III).

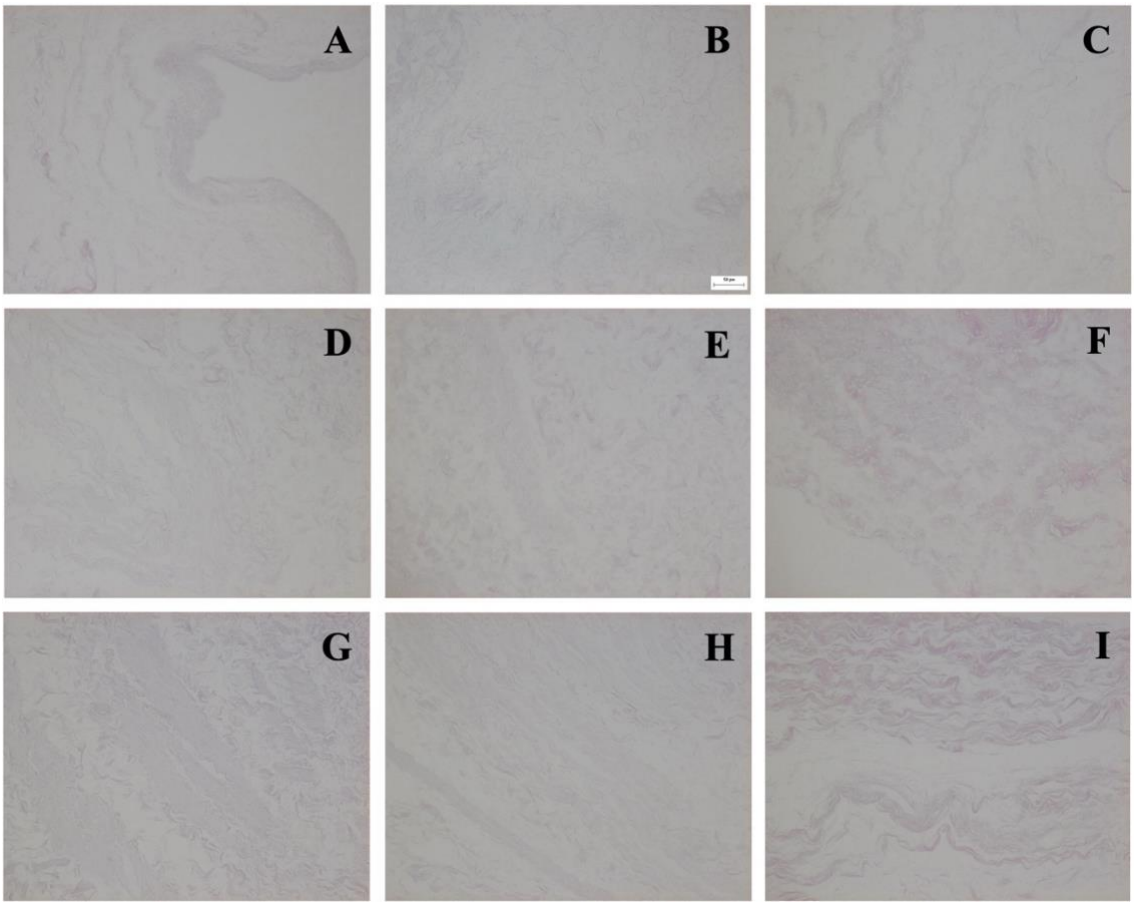

Figure 3.4 Micrographs of H&E-stained sections from the first batch of three bladders decellularised stretched onto a flat-bed apparatus at the JBU.

Absence of nuclear haematoxylin staining was detected in three samples per each decellularised bladder and are here shown. Respectively, micrographs of the H&E results for three replicates of the first bladder are illustrated in A, B, C. Micrographs of three replicates of the second bladder are reported in D, E, F. G, H, I illustrate H&E findings in three replicates of the third bladder decellularised with the flat-bed technique at the JBU. Scale bar: 50µm. A micrograph of control tissue (porcine bladder) is shown in Figure 3.2.

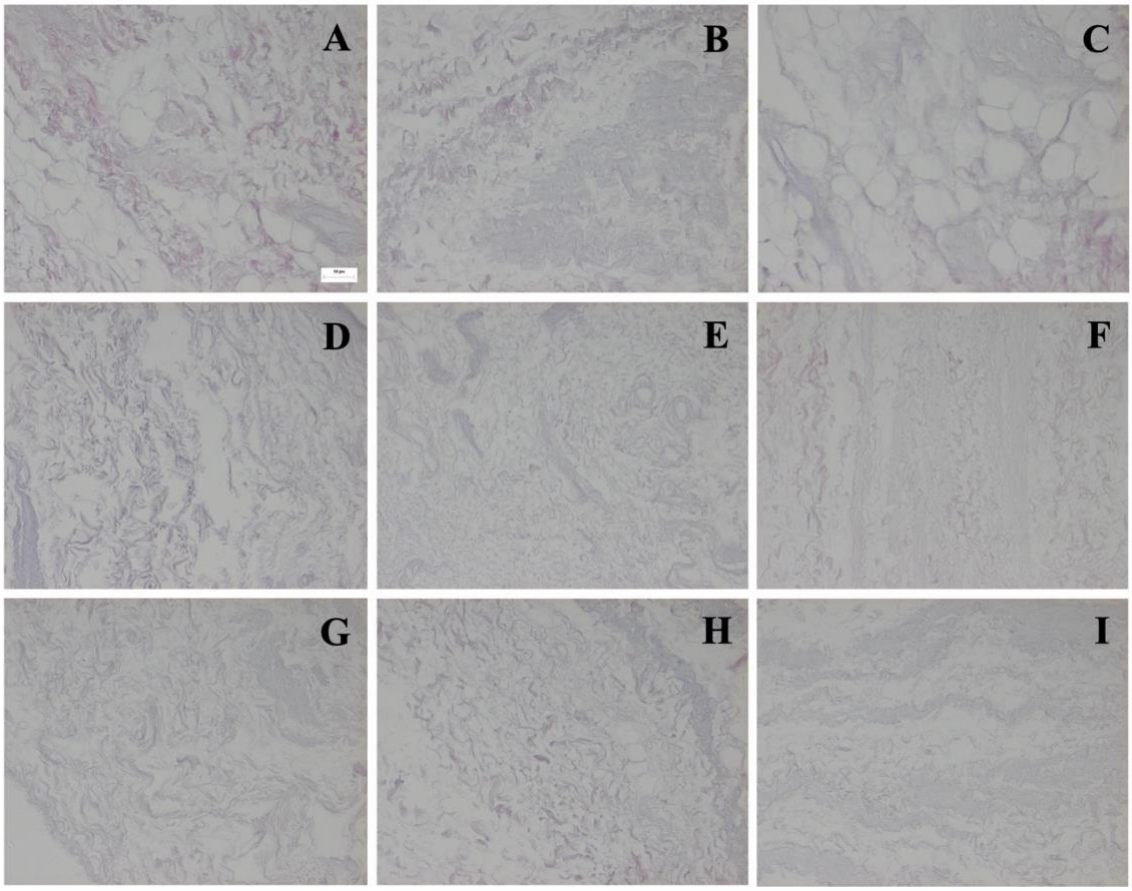

Figure 3.5 Micrographs of H&E-stained sections from the second batch of three bladders decellularised via the flat-bed method at the JBU.

No nuclear haematoxylin staining was detected in three samples per each decellularised bladder and are here shown. Respectively, micrographs of the H&E results for three replicates of the first bladder from the second batch are illustrated in A, B, C. Micrographs of three replicates of the second bladder of the second batch are reported in D, E, F. G, H, I illustrate H&E findings in three replicates of the third bladder of the second batch of porcine bladders decellularised with the flat-bed technique at the JBU. Scale bar: 50µm. A micrograph of control tissue (porcine bladder) is shown in Figure 3.2.

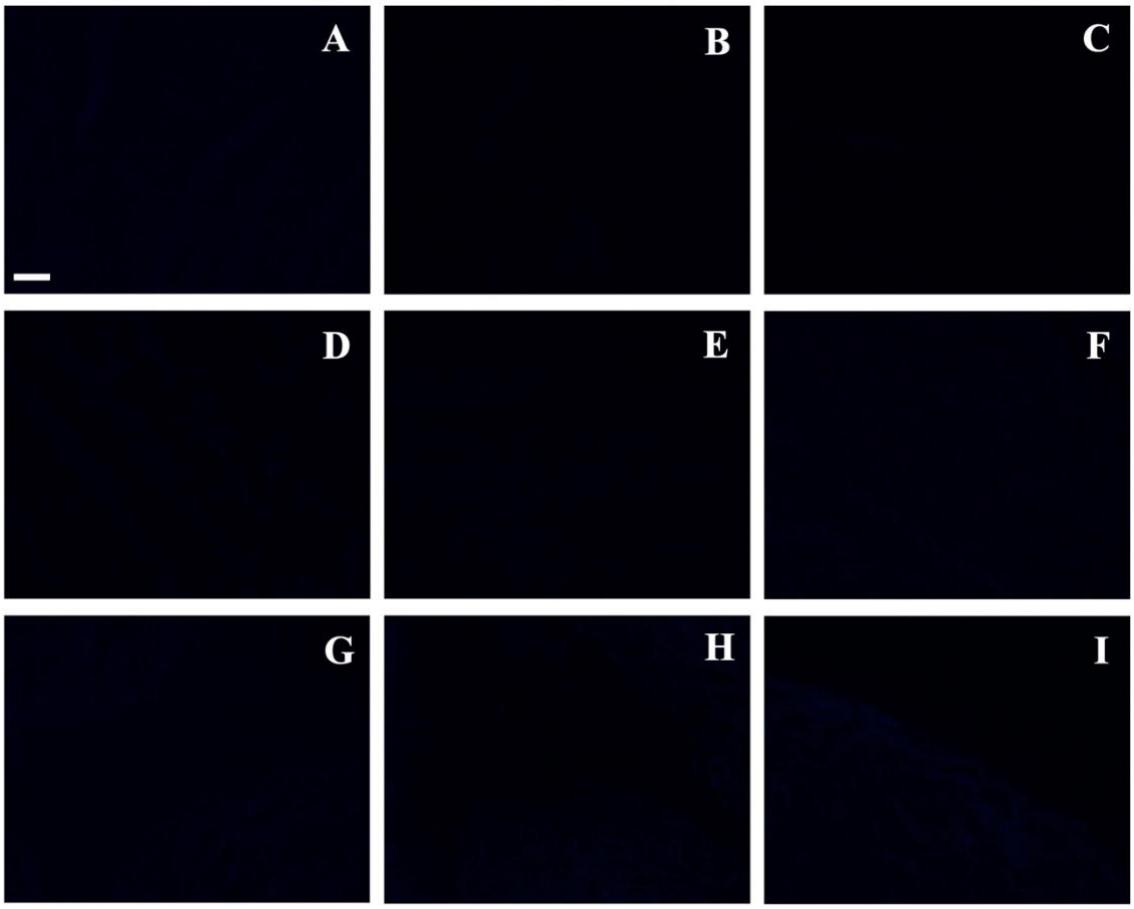

Figure 3.6 Micrographs of Hoechst 33258 stained sections from the first batch of three bladders decellularised using the flat-bed method at the JBU.

Three samples per each decellularised bladder are here shown indicating absence of nuclear Hoechst 33258 staining. Respectively, micrographs of three replicates of the first bladder from the first batch are illustrated in A, B, C. Micrographs of three replicates of the second bladder are reported in D, E, F. G, H, I illustrate Hoechst 33258 findings in three replicates of the third bladder decellularised with the flat-bed technique at the JBU. Images were captured at 60× magnification, scale bar 50 µm. Exposure time: 1/35 sec. A micrograph of control tissue (porcine bladder) is shown in Figure 3.3.

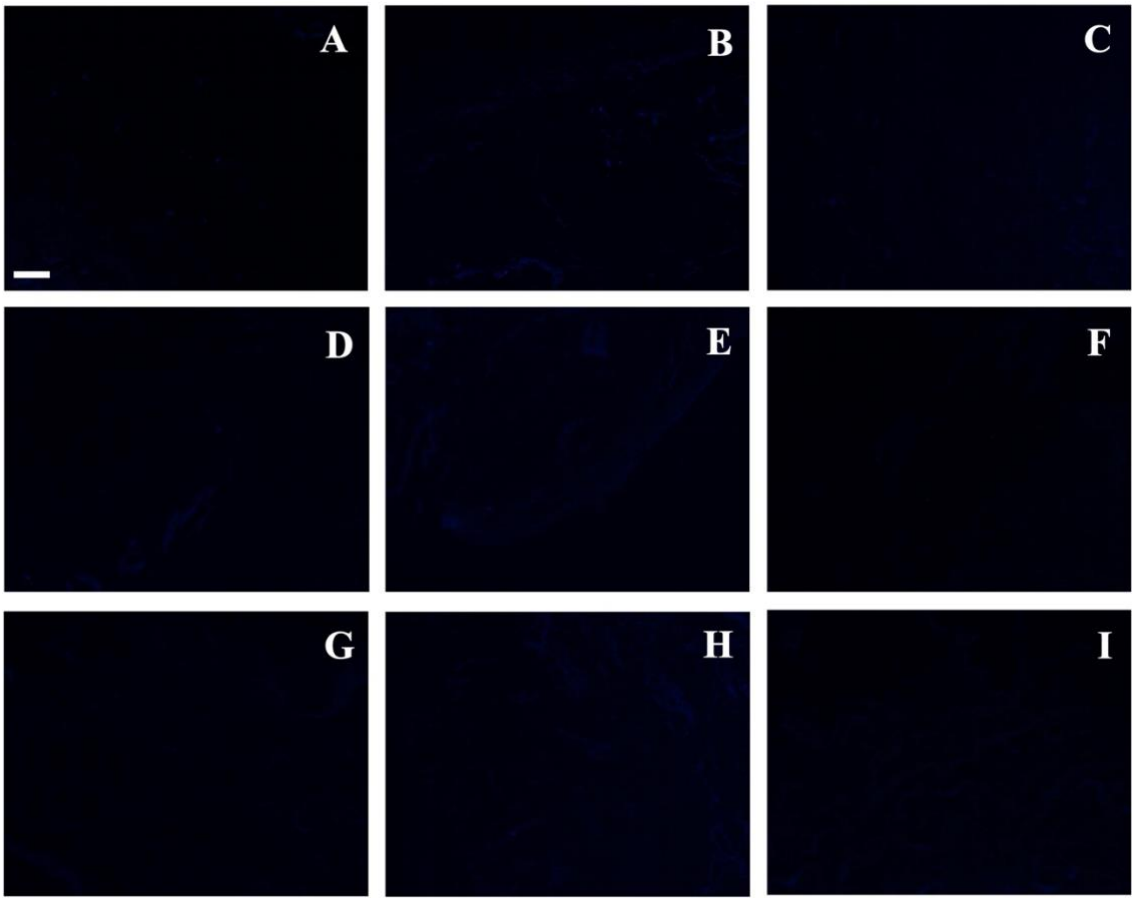

Figure 3.7 Micrographs of Hoechst 33258 stained sections from the second batch of three bladders decellularised using the flat-bed method at the JBU.

No nuclear Hoechst 33258 staining was detected. Three samples per each decellularised bladder are here shown. Respectively, micrographs of three replicates of the first bladder from the second batch are illustrated in A, B, C. Micrographs of three replicates of the second bladder from the second batch are reported in D, E, F. G, H, I illustrate Hoechst 33258 findings in three replicates of the third bladder from the second batch of porcine bladders decellularised with the flat-bed technique at the JBU. Images were captured at 60× magnification, scale bar 50 µm. Exposure time: 1/35 sec. A micrograph of control tissue (porcine bladder) is shown in Figure 3.3.

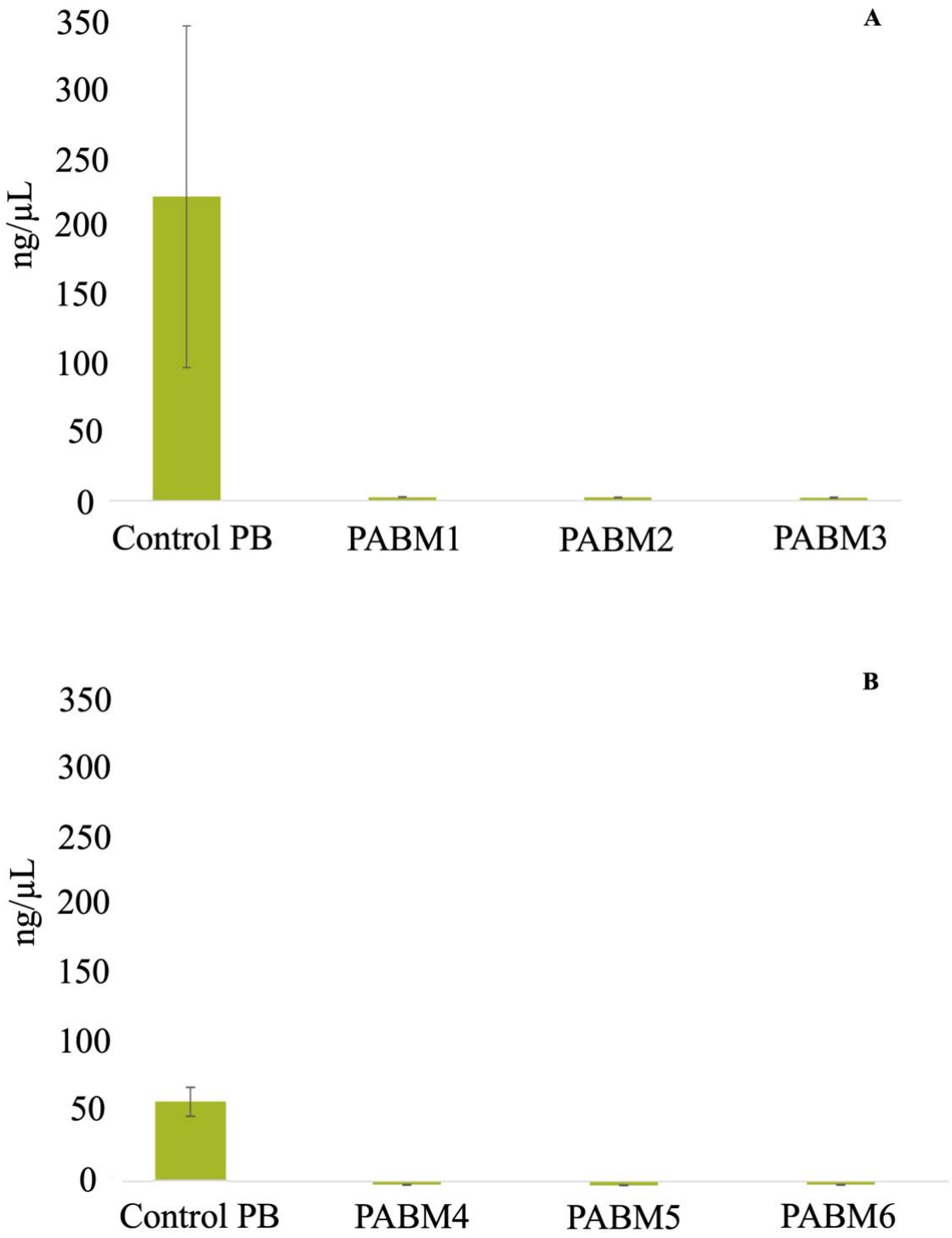

Figure 3.8 Quantification via NanoDrop Spectrophotometer of the DNA content of samples taken from bladders decellularised using the flat-bed method.

Two batches (A, B) of three bladders underwent decellularisation. n = 3 replicates were weighed, processed and analysed per each decellularised and fresh tissue (control porcine bladder). DNA quantification is presented as ng/µL as each sample weighed 10 mg. Data expressed in Means and SD, showing satisfactory removal of nuclear material.

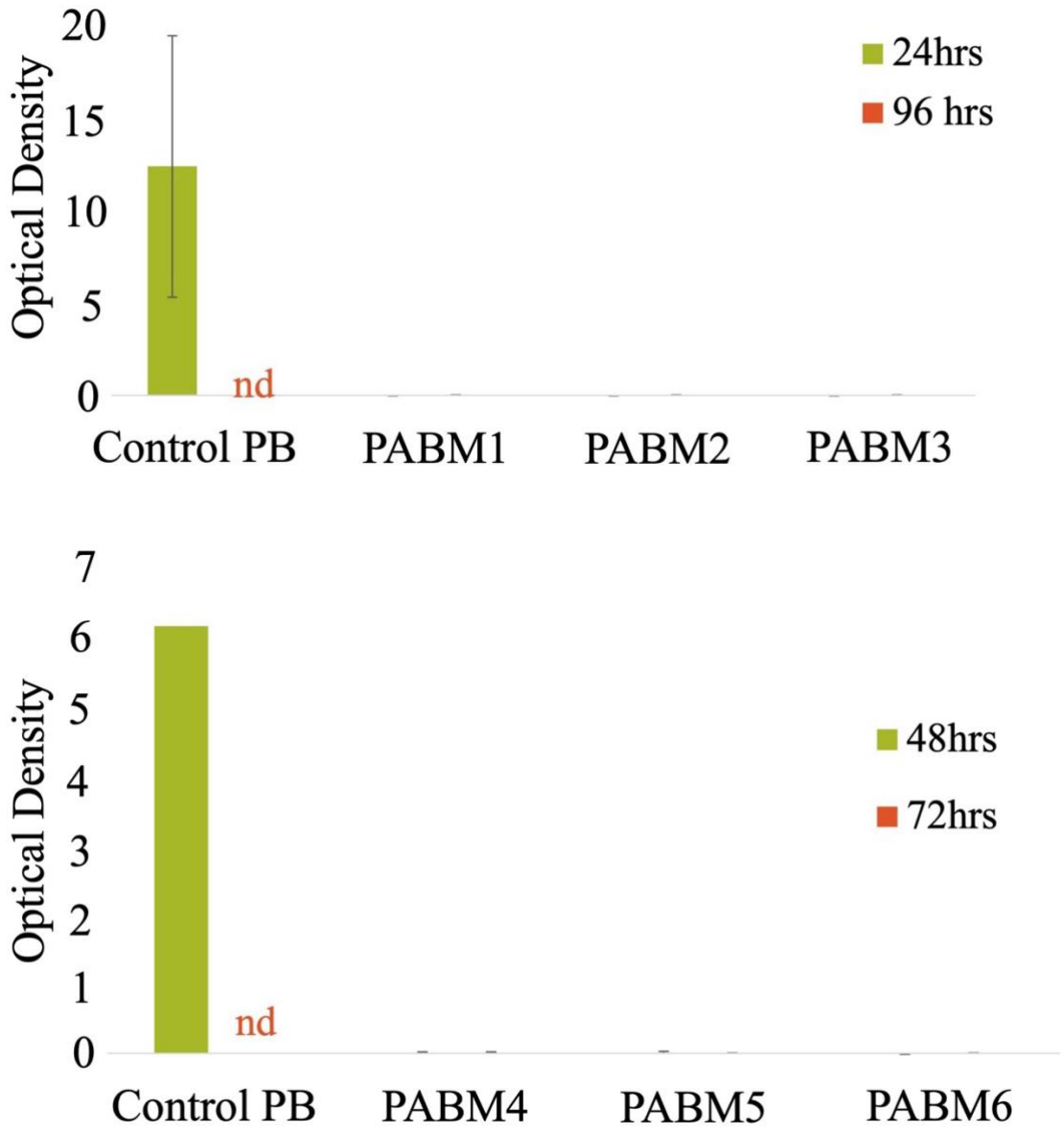

Figure 3.9 Sterility testing of the samples taken from bladders decellularised using the flat-bed method at the JBU.

No evidence of microbial growth was noted representing absence of contamination within samples. Means and SD were calculated from n = 3 replicates per bladder sample.

3.4.3 Decellularisation of full-thickness, porcine bladder sheet on flat-bed rig - at the TRX facility

Using the method of stretching porcine bladder tissue on a flat-bed apparatus, three porcine bladders were decellularised at the manufacturing facilities of Tissue Regenix Group plc (Unit 1&2, Astley Way, Astley Lane Industrial Estate, Swillington, Leeds LS26 8XT (UK)) by three different operators. Therefore, one batch of three 8 cm x 8 cm PABM sheets was produced. At each step of the process, stretched bladder tissue was placed into a large container filled with about two litres of decellularisation buffer, to allow the tissue to be fully immersed in the solution. Bladders were subsequently processed and histologically assessed for presence of cellularity. The test facility for the Quality Control analysis was the Jack Birch Unit, Department of Biology (M0), University of York, Heslington, York YO10 5DD (UK).

Images of sections taken from decellularised bladders samples (formalin fixed, paraffine embedded) stained with Haematoxylin and Eosin are shown in Figure 3.10. No urothelial cells were identified in the decellularised samples. No evidence of nuclear material or residual cell fragment was noted across the processed samples, compared to positive control porcine bladder (Figure 3.10L).

Absence of nuclear Hoechst 33258 staining was detected in sections from decellularised bladder tissue (Figure 3.11). For comparison, positive control is shown in Figure 3.11L.

A NanoDrop Spectrophotometer was used to quantify the DNA purified and extracted from samples of decellularised and native porcine bladder tissue. Data (Mean ± SD) relative to the quantified DNA content are shown in Figure 3.12 for the three bladders decellularised at the TRX facility in comparison to native control samples. Adequate removal of nuclear material was detected in the decellularised tissue.

The present results confirmed completion of knowledge transfer and application of the decellularisation process following the JBU SOP: Porcine Bladders procurement, dissection and storage. Decellularisation of full-thickness flat porcine bladder sheets. Version 2-2017 (Appendix II). Based on the QC analysis performed at the Jack Birch Unit (academic laboratory facility), the PABM produced at Tissue Regenix Group (commercial manufacturing facility) resulted adequately decellularised, with no evidence of residual DNA material.

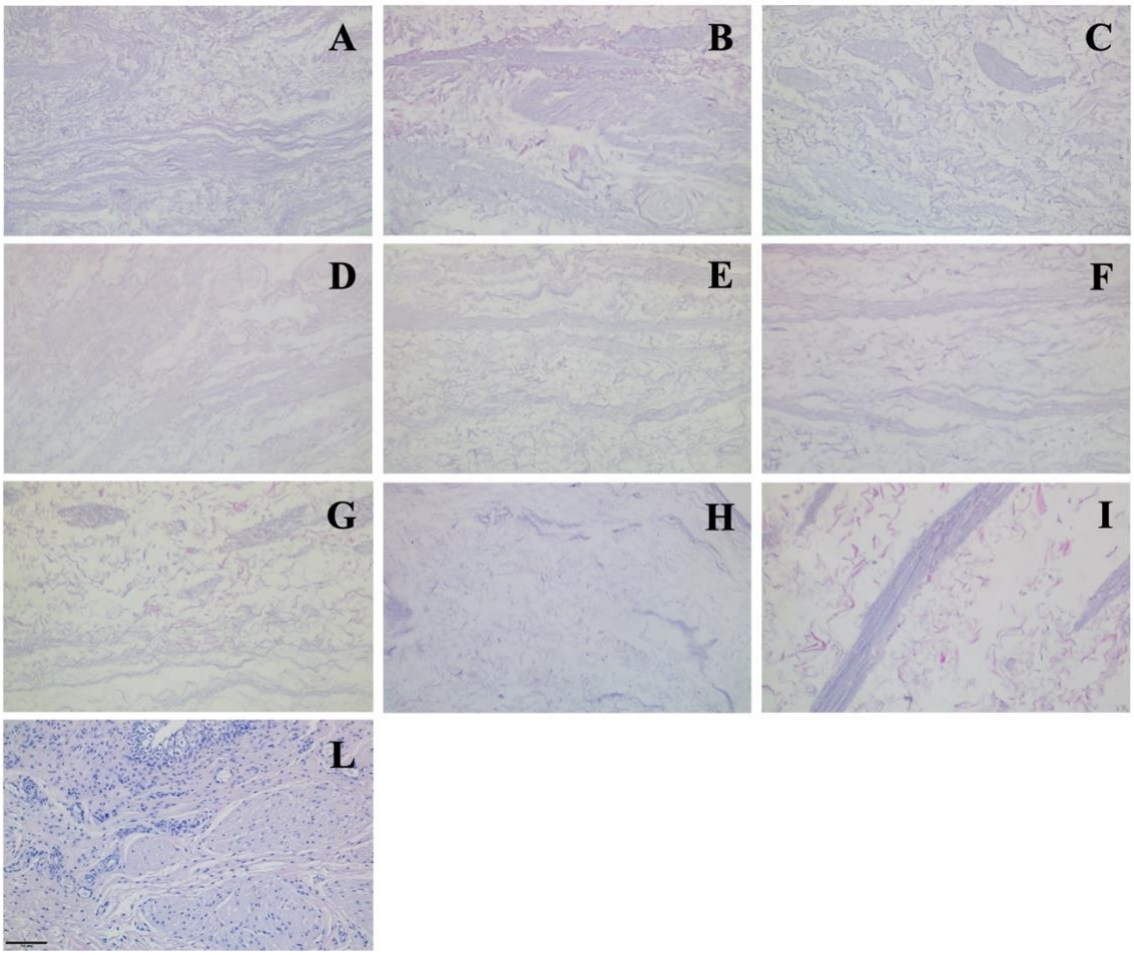

Figure 3.10 Micrographs of H&E staining of porcine bladder tissue decellularised at a commercial partner manufacturing site using the flat-bed method.

Three samples from each produced PABM are here shown. Respectively, micrographs of the H&E results for three replicates of the first bladder are illustrated in A, B, C. Micrographs of three replicates of the second bladder are reported in D, E, F. G, H, I illustrate H&E findings in three replicates of the third bladder decellularised with the flat-bed technique at the TRX facility. No evidence of nuclear haematoxylin staining was detected in the decellularised tissue samples, compared with a positive control porcine bladder (L). Scale bar: 100µm.

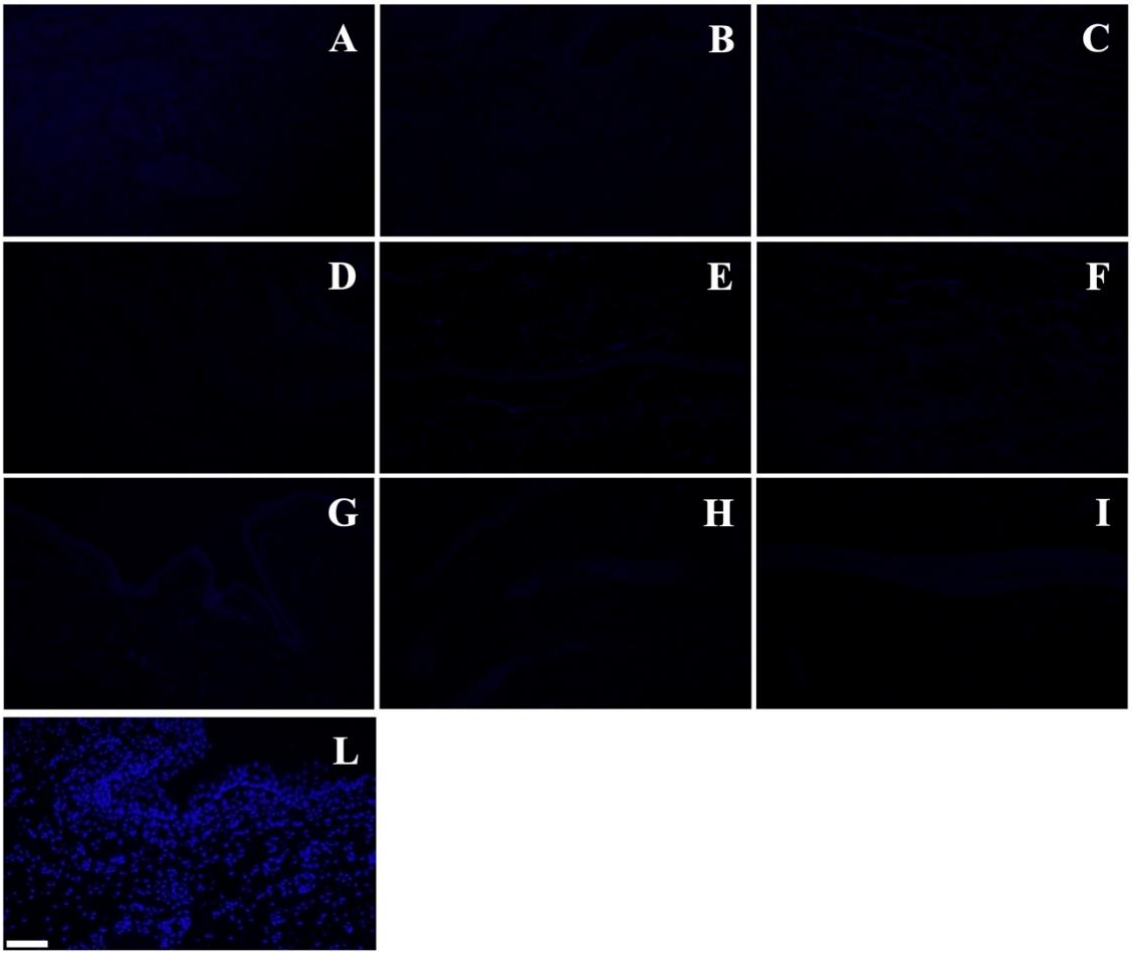

Figure 3.11 Micrographs of Hoechst 33258 staining of porcine bladder tissue decellularised at a commercial partner manufacturing site using the flat-bed method.

Three samples are here reported per each produced PABM, showing no detection of nuclear staining in the decellularised tissue. Respectively, micrographs of three replicates of the first bladder are illustrated in A, B, C. Micrographs of three replicates of the second bladder are reported in D, E, F. G, H, I illustrate Hoechst 33258 findings in three replicates of the third bladder decellularised with the flat-bed technique at the TRX facility. For comparison, microscopic appearances in a positive control porcine bladder are shown in L. Scale bar: 100µm. Exposure time: 1/35 sec.

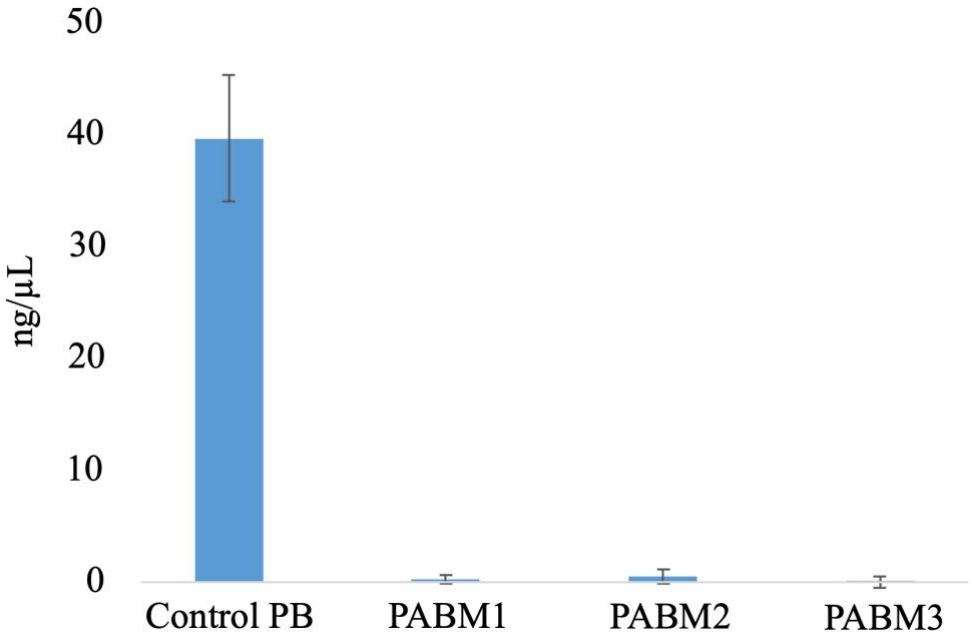

Figure 3.12 Quantification via NanoDrop Spectrophotometer of the DNA content of samples taken from three bladders decellularised using the transferred flat-bed method at the commercial partner manufacturing site.

Means and SD were calculated from n = 3 replicates per bladder sample. DNA quantification is presented as ng/µL as each sample weighed 10 mg. Adequate nuclear material removal was detected in decellularised tissue, compared to positive control - porcine bladder (PB).

3.5 Discussion

The purpose of this chapter was to compare decellularisation methods for full-thickness porcine bladders using intact bladders (Bolland et al., 2007) and dissected sheets (Ward et al., 2021) and evaluate the transferability and scalability of the process for biomaterial production.

The technical decellularisation steps included a combination of chemical and physical methods. Several parameters have been recognised as critical to allow the chemical solutions to diffuse effectively through the decellularising tissue, with the tissue thickness being directly correlated to such diffusion distance. As the bladder wall is a densely organised and thick tissue (5 mm - 1 cm), it is a barrier to diffusion for achieving full decellularisation. In studies elsewhere, a physical method such as tissue delamination has been used to develop a thinner tissue for decellularisation of the urinary bladder and other tissues (Badylak et al., 1989; Lun et al., 2010; Davis et al., 2011).

In the first decellularisation method tested in this chapter (Bolland et al., 2007), the limit presented by the thickness of the originating tissue was obviated by filling and distending the entire porcine bladder by utilising its natural mechanical stretching property, and applying biaxial strain to the bladder wall .

As applied to full-thickness entire bladders, inflation to distend the bladder produced a biomaterial that was previously shown retaining properties such as strength and compliance of the originating tissue. The lamina propria of the bladder wall is mainly composed of collagen fibers, which provide the function of maintaining the shape of the organ and securing its compliance (calculated dividing volume by pressure). As following decellularisation, the lamina propria remained intact, no statistical difference was found in the burst pressure of decellularised bladders in comparison to fresh ones. Furthermore, there was no difference in the ultimate tensile strength or in the ability to retain sutures when the decellularised bladder tissue was compared to native tissue, however, the decellularised matrix resulted slightly stiffer than the fresh tissue. This was represented by an increase in the collagen phase slope and decrease in the failure strain values when the biomatrix was compared to fresh bladder tissue (Bolland et al., 2007). Further studies could be performed to evaluating the decrease in extensibility its significance. A bladder scaffold's mechanical properties have been recognised as a crucial factor that could influence the quality of bladder regeneration (Jokandan et al., 2018). Therefore, the PABM property of retaining strength and compliance of the native full-thickness bladder makes it an ideal candidate in bladder reconstruction surgical settings.

However, microscopic histological analysis of the decellularised tissue, including H&E and Hoechst 33258 staining, showed evidence of residual nuclear material. Inadequate decellularisation, with

retention of cellular remnants within the extracellular matrix, can evoke a proinflammatory host response and can also affect tissue remodelling outcomes (Keane et al., 2012; Keane, Swinehart and Badylak, 2015; Keane, Saldin and Badylak, 2016).

One of the potential limits of the inflation method resides in the variability in dimensions between bladders (size and capacity). Utilising the same filling/bathing volume of solutions, independently from the dimensions of the bladder, revealed the risk of inadequate distension leading to suboptimal decellularisation.

The second decellularisation method here tested, obviated the need to keep the intact bladder distended by stretching flat porcine bladder sheets to reduce tissue thickness. The limit represented by variability in the initial dimensions of the bladders was overcome by dissecting bladders into sheets of discrete dimensions and shape.

In a previous study, which used uniaxial mechanical testing, correlations between histological and mechanical characteristics of the whole bladder highlighted the presence of regional and directional anisotropy in the stress/force - strain/elongation behaviour, meaning that the bladder stretches in different directions in an inhomogeneous manner (Korossis et al., 2009). Stress-strain behaviours observed by the authors by using uniaxial mechanical testing, correlated and informed on the whole organ pressure-volume behaviour. Overall, the bladder was found more distensible along the transverse direction, with increased compliance described at the dorsal and ventral region levels, compared to the trigone and the lower body. This means that at the same pressure, those regions deform more (Korossis et al., 2009; Zanetti et al., 2012; Borsdorf et al., 2019). These findings of an increased compliance and increased level of deformation along the transverse direction correlated with the histological observation of elastin being predominantly oriented in this direction, and being mainly present in the dorsal, ventral and lateral regions. The lower body of the bladder and the trigone were found being the least able to distend, retaining the original tissue thickness (Korossis et al., 2009). Such anisotropy of the passive mechanical properties of the bladder was subsequently considered when mathematically modelling tissue stretching, by defining the correlation between bladder size and capacity, and the biaxial deformation state (biaxial strain) required to reduce thickness and, ultimately, to facilitate the decellularisation chemical solutions to penetrate effectively (Ward et al., 2021) (Appendix V). Authors there identified that the model of a tissue area of 47 mm x 60 mm with a 5 mm border was adequate for a bladder sheet to achieve the required deformation state to facilitate decellularisation, and provide a final 8 cm x 8 cm decellularised tissue. Therefore, the decellularisation method by stretching bladder sheets on a flat-bed rig of known dimensions, using five discrete points along each edge of the tissue overcomes the need to keep the whole bladder

distended to replicate the deformation state and reduces the variability of decellularisation results by applying similar deformation forces to a tissue of known dimensions (Ward et al., 2021) (Appendix V).

Six bladder sheets were here decellularised in total. The technique and the available equipment was scalable as it allowed three bladders to be processed simultaneously by a single operator. Analysis of the decellularised tissue showed adequate removal of cellular/nuclear material (Figure 3.4 – 3.8). The absence of contamination within samples validated the disinfection process via peracetic acid (Figure 3.9). Furthermore, samples of the decellularised tissues were found not cytotoxic (Section 3.4.2 and Appendix III).

In an industrial manufacturing setting, it has been considered not feasible to process fresh bladders straight after collection. Therefore, the process of decellularisation on a flat-bed rig implemented the initial decellularisation method by not placing bladders in a transport medium upon collection and by including the possibility of storage by freezing the bladders before processing. The transport medium was used originally to preserve bladder tissue, particularly the viability of the urothelial cells (Southgate, Masters and Trejdosiewicz, 2002). This step was considered potentially unnecessary for bladders planned for decellularisation, as cells, including urothelial cells, are removed during the process. Results presented here show that adequately decellularised tissue was obtained even when this step was omitted. At an industrial level, this could streamline the collection step and reduce costs. However, information about the potential tissue damage secondary to the implemented transport method has yet to be acquired, specifically regarding tissue mechanical properties. This has the potential to be further evaluated. Biomechanical characterisation of the tissue transported with or without transport medium could include low strain-rate uniaxial tensile loading to failure test to inform on the stress-strain behaviour of specimens, and suture retention strength testing to measure the suture pull-out force using an Howden tensile machine (Korossis et al., 2002; Bolland et al., 2007).

The transfer of knowledge from an academic laboratory setting to an industrial manufacturing facility of the decellularisation process (flat-bed rig method) was part of the present study. A collaboration with a commercial partner (TRX Ltd) was established to test the feasibility of the method's scalability. Three porcine bladders of the 15 collected/delivered were found suitable for processing. One bladder was utilised as a control. The remaining bladders were discarded as they were considered too small. The decellularisation process was performed by three different operators at the manufacturing site. At the request of the commercial partner, the applied protocol differed from the one applied at the academic facility:

- Aprotinin was not used,
- The sterilisation step using peracetic acid was omitted.

Aprotinin is a small basic protein (bovine pancreatic trypsin inhibitor) with an antifibrinolytic function that inhibits proteolytic enzymes. At a clinical level, its use in heart and liver surgery has been discontinued due to the observed increased risk of complications and death that raised concerns about its safety and toxicity (Schneeweiss et al., 2008; Shaw et al., 2008). Such suspension was lifted by the European Medicines Agency (EMA) in 2014. In research settings, aprotinin is used as an enzyme inhibitor to prevent protein degradation during cell lysis (Coffin and Gaudette, 2016). It has been used vastly in decellularisation protocols for several tissues (Stapleton et al., 2008b; Yoeruek et al., 2012; de Lima Santos et al., 2020). The protocol reported by Stapleton and colleagues has recently been applied with the minor modification of the omission of aprotinin (Kara Özenler et al., 2021).

Three methods have been tested in this chapter. Two protocols included the use of aprotinin as an antifibrinolytic, which was omitted during the decellularisation process performed at the manufacturing facility. The results presented here were comparable across the three methods applied. Further histoarchitectural and mechanical characterisation with a comparison between the produced PABMs could provide additional information.

In the decellularisation protocol here applied, disinfection by peracetic acid was used. Peracetic acid was utilised as a disinfectant and decellularisation agent, as it can inactivate viruses, bacteria and endotoxins, solubilise cell membranes, and remove residual DNA material with minimal effect on the ECM (Gilpin and Yang, 2017; Zhang, Brown and Hu, 2019; Kuzin et al., 2023). It is considered economical, degrades into nontoxic products (acetic acid and water), and is active at low temperatures and low concentrations, but it could affect morphological characteristics and mechanical properties of the matrix (Hodde and Hiles, 2002; Huang et al., 2004; Hodde et al., 2007; Yoganarasimha et al., 2014; Keane, Saldin and Badylak, 2016). However, this step was omitted when the method was used in a manufacturing setting. This modification was applied to comply with the current requirements of the commercial partner. Terminal sterilisation is required for a biomaterial composed of ECM to be classified as a medical-grade device and to be applied clinically (Crapo, Gilbert and Badylak, 2011; Keane, Saldin and Badylak, 2016), as failing to achieve satisfactory removal of microorganisms could lead to a proinflammatory host response and compromise clinical outcomes (Daly et al., 2012). The US Food and Drug Administration (FDA) indicated safety guidelines for terminal sterilisation and approved several methods used to sterilise decellularised ECMs. Those include incubation in acid or solvents, depyrogenation, exposure to ethylene oxide, gamma irradiation and electron beam irradiation. However, such processes can damage ECM components by compromising mechanical properties (Crapo, Gilbert and Badylak, 2011; Keane, Saldin and Badylak, 2016). Of these, ethylene

oxide can cause an unwanted host immune response and is known to be a human carcinogen (Jackson, Windler and Simon, 1990; Jinot et al., 2018). Gamma irradiation and electronic radiation can increase ECM degradation, causing changes in tissue strength. Residual peroxidated lipids produced by these ionising radiations have also been linked to cytotoxicity. The optimal sterilisation method able to preserve the structural and mechanical characteristics of an ECM-based scaffold, like PABM, fulfilling industrial manufacturing requirements while adhering to safety and regulatory guidelines still needs to be determined. Further studies to test and compare sterilisation methods dedicated to the PABM could facilitate its production.

Currently, available equipment allows for the simultaneous processing of three bladder sheets. However, a few implementations could facilitate the industrial-scale production of the PABM. An upgrade of the 3D-printed apparatus to allow for the use of more than three rigs at the same time could be considered. This would require a subsequent adjustment to the bathing solutions' volume and container dimensions. Tests leading to the determination of the minimum volumes required to obtain adequate decellularisation of the bladder sheets would be beneficial. In this series, a corkboard was used as a dissecting surface and as a temporary support for inserting of the pins. Suppose a material alternative to the corkboard needs to be selected to be more suitable for a commercial manufacturing process. In that case, the choice should include a material/surface that is suitable for autoclaving, resistant to cutting instruments, and compliant with the currently used pins. Insulating materials and hard foams could be evaluated. Although cork is considered a natural, sustainable, eco-friendly material, more efficient alternatives could be explored.

One of the most critical steps of the current method resides in stretching the porcine bladder sheet. This is operator-dependent and carries the risk of tearing the tissue making it unsuitable for further processing. An alternative option could involve a supervised automation of the step. A robotic machine could be programmed to perform this specific task, with an algorithm designed using data on tissue stretching characteristics. Furthermore, sensors could be applied at every step of the process to the tissue pinned to a plate that gradually expands to the required size. Sensors could be used to acquire real-time data to continue training the model in a feedback mode to provide "personalised" stretching and improve results. This will ensure adequate stretching force is applied at any time at any region/point of every single tissue sheet. Therefore, with the use of real-time data-driven technology to automate and streamline the process, a more consistent stretching force could be applied under supervision to the bladder, reducing potential tissue damage and enhancing accuracy, consistency and efficiency. Further benefits of exploring and deploying such technological solution of an automated system could include improved safety, easy scalability, and the provision of data insights to enhance decision-making.

In this chapter, a decellularisation process implemented in an academic facility was tested and subsequently transferred to an industrial setting via collaboration with an external commercial partner. Overall, the biomaterial manufacturing process was implemented. This was observed while increasing the number of operators performing the process simultaneously, implementing quality control measures, and ensuring compliance with regulatory guidelines.

In the next chapter, PABM tissue integration characteristics will be studied and compared to those of a commercially available cross-linked biomatrix (Permacol™) in an in vivo setting.

Chapter 4

Augmentation of the insufficient tissue bed for surgical repair of hypospadias using acellular matrix grafts: a proof of concept study

The present Chapter 4 is included as the original research article published by the thesis' author and colleagues in 2021 (Morgante et al., 2021). Therefore, it differs in writing style from the other thesis chapters. The surgical part of the study presented here was not part of this thesis project and was not performed by the thesis author. The qualitative (histology and immunohistochemistry evaluation) and quantitative analysis were part of this thesis project. The thesis author contributed with optimising the histological and immunohistochemical evaluation to complete the qualitative analysis, and planning, designing, optimising and performing the quantitative analysis.

4.1 Introduction

Decellularised tissue matrices offer a promising natural biomaterial in surgical situations where there is either an inherent lack of a tissue bed for repair, or where the healthy tissue bed is compromised by trauma or fibrotic scarring.

One such need is encountered in surgical repair for hypospadias. With reported frequencies of 0.3 to 7.0 per 1000 live births, hypospadias is one of the most common genitourinary birth defects, requiring revision in as many as 1in 300 boys (Faure et al., 2016; Abbas et al., 2017). Hypospadias is associated with the development of a foreshortened urethra resulting in an aberrantly-positioned external orifice (meatus) on the ventral aspect of the penis. Surgical repair is the mainstay treatment for the majority of infants with hypospadias, but can require multiple procedures and is frequently associated with unsatisfactory results and complications, including the formation of urethral fistulas, stenosis and dehiscence or rupture of the repair. The underlying pathophysiology of many complications is the inherent lack of healthy host vascularised tissue, with tension on these inadequate tissues resulting in poor healing and dehiscence of the wound (Springer and Subramaniam, 2012a). Retrospective reviews of patient outcome following two-stage repair for severe hypospadias have reported complication rates from 58 to 68% (McNamara et al., 2015; Stanasel et al., 2015; Faure et al., 2016).

Fistulas and strictures are particularly difficult to manage due to a lack, or poor quality of tissue at the site of repair.

Post-operative complications increase with the severity of the anomaly (Long et al., 2017) and patients with severe hypospadias often require extra tissue to repair the urethra (Abbas et al., 2017). Autologous free tissue grafts have been used clinically for urethral reconstruction, including skin from genital and extra-genital regions (Schwentner et al., 2011; Altarac, Papeš and Bracka, 2012), with buccal mucosa the most commonly used (Duckett et al., 1995; Stein, Schröder and Thüroff, 2006; Cruz-Diaz, Castellan and Gosalbez, 2013). Problems most commonly associated with the use of autologous free tissue grafts include graft size, donor site morbidity and graft contracture (Barbagli et al., 2010). Preclinical studies aimed at improving hypospadias repair outcomes by applying novel biomaterials and tissue-engineering techniques have met limited success (Faure et al., 2016). Such approaches have included the use of biomaterials of synthetic or natural derivation, either unseeded or cell-seeded in both flat and tubularised configurations in rabbits, dogs or rats (80 preclinical studies reviewed in Versteegden et al. (2017)). A range of acellular biological scaffolds derived from allogeneic and xenogeneic sources using different decellularisation processes have been used in these pre-clinical studies including porcine small intestinal submucosa (SIS, Surgisis®), Alloderm®, decellularised bladder submucosa and decellularised urethra (Versteegden et al., 2017). Due to a lack of controlled preclinical studies, however, the efficacy of these approaches has been difficult to determine. Although pre-clinical studies in animals have tended to suggest better results and reduced complications when acellular matrices are combined with cells, such findings have not been confirmed in the limited number of clinical studies (Versteegden et al., 2017). However, a major confounder is the tendency to test novel approaches clinically only after standard surgical procedures have failed.

The ideal biomaterial to enhance urethral tissue repair would provide a suitable template to replicate the biological and biomechanical functional properties of the host tissue by allowing progressive ingrowth of periurethral tissue components, without inducing an adverse host response that would lead to fibrosis and contracture. The size of the defect and the extent to which endogenous cells can infiltrate and organise within a graft material have been reported as key limitations. In male rabbits, a 0.5 cm tubularised decellularised matrix of porcine bladder submucosa was reported to be the maximum length able to support normal tissue formation (Dorin et al., 2008). However, it is important to highlight that different decellularisation methods are utilised by different research groups and different protocols can have varying effects on the extent of cell and DNA removal, composition of the extracellular matrix and biomechanical attributes of the resultant biological scaffold matrix

resulting in variations in the potential for constructive tissue remodelling (Crapo, Gilbert and Badylak, 2011; Keane, Swinehart and Badylak, 2015).

We have developed proprietary decellularisation processes using low concentration sodium dodecyl sulphate (0.1% (w/v) SDS) and proteinase inhibitors for the production of a range of porcine and human tissue specific biological scaffolds including cardiac valves (Booth et al., 2002; Vafaee et al., 2018), dermis (Hogg et al., 2015), arteries (Wilshaw et al., 2012) and musculoskeletal tissues (Stapleton et al., 2008b; Jones et al., 2017). Importantly, these processes preserve the biomechanical and biological tissue properties. Preclinical (Paniagua Gutierrez et al., 2015) and clinical (da Costa et al., 2009; Greaves et al., 2013, 2015; Kimmel and Gittleman, 2017) studies have clearly demonstrated the utility of this approach. We have adapted this process for full thickness porcine bladder to create an acellular porcine bladder biomaterial (PABM) particularly aimed at urological applications (Bolland et al., 2007). Using an ex vivo model in which human urinary tract tissue was combined with PABM in organ culture, we have previously associated host M2-polarised CD163+ tissue macrophages with the pioneering events of cellular infiltration and integration at the tissue:decellularised biomaterial interface (Bullers et al., 2014).

It is reported that Permacol™ (aka Pelvicol™), a commercial cross-linked collagen acellular matrix derived from porcine dermis and licenced for surgical use, may reduce the complications of primary complex hypospadias repair when used as a peri-urethral graft (Springer and Subramaniam, 2012a). In the off-label study, it was suggested that the graft supported the urethroplasty as a splint, but there was no scope for the histological outcome to be assessed. Our previous in vitro studies have indicated that unlike PABM (Bullers et al., 2014), Permacol™ lacks cell integrative properties (Kimuli, Eardley and Southgate, 2004). In order to help inform future clinical development, the aim of this study was to evaluate gross and histological outcomes of incorporating PABM or Permacol™ as peri-urethral grafts in an experimental large animal model. The male juvenile pig was chosen as the animal species because of the anatomical size and physiological similarity to male children. The cellular response to the implanted scaffolds at 3 months was studied using CD163 (M2 macrophages) with progenitor markers of haematopoietic (CD34), leucocyte (CD45) and myofibroblast (αSMA) lineages to assess the cell-integrative properties of non-crosslinked and cross-linked natural biomaterial matrices.

4.2 Materials and methods

4.2.1 Biomaterials

For PABM production, pig bladders were collected from a local abattoir (Traves & Son Ltd, Escrick) on ice in Transport Medium consisting of Hank's balanced salt solution (Gibco) containing 10 mm

HEPES pH 7.6 (Gibco) and 20 kallikrein inhibiting units/ml aprotinin (Trasylol®, Nordic Pharma) (Southgate et al., 1994). PABM, a full-thickness porcine acellular bladder matrix, was produced aseptically using the decellularisation procedure described by Bolland et al. (Bolland et al., 2007), including a terminal disinfection stage with peracetic acid. PABM was batch-tested by histology and Hoechst 33258 staining of sections from multiple samples to confirm the absence of cells or double-stranded DNA. Contact cytotoxicity tests conducted in vitro as described (Bolland et al., 2007) confirmed both sterility and absence of toxic by-products.

Permacol™ was purchased from Medtronic (Watford, UK).

4.2.2 Animal husbandry, analgesia and anaesthesia

Large White Landrace Hybrid male pigs 14 weeks old of approximately 15–20 kg weight were ear-tagged for identification and housed in pairs with unlimited access to water. Assessment of the animals was performed at least twice daily and animals were weighed every two weeks.

All experimental procedures were approved by the local Animal Welfare and Ethical Review Body and were conducted at the University of Leeds animal surgical facility under a project licence granted by the UK Home Office, in accordance with the Animal Scientific Procedures Act 1986. Details to fulfil the essential and recommended ARRIVE 2.0 guidelines for reporting animal studies is available as Supplementary Information (Appendix VI).

Food was withheld 16 h prior to surgery. Initial sedation was performed using intramuscular Midazolam 0.32 mg/kg (Hypnovel Roche, UK) and Azeperone 2.25 mg/kg (Stresnil Elanco Animla Health). An over-the-needle cannula (18 g Venflon) was inserted and secured in an ear vein. In some animals, where combination of Midazolam and Azeperone did not produce enough sedation to allow intravenous catheterisation, 2.5% Isoflurane in oxygen was delivered via a snout mask for no more than 1 min attached to an anaesthetic machine. This deepened the state of sedation enough to allow intravenous catheterisation of an ear vein. Following intravenous catheterisation, general anaesthesia was induced by intravenous injection of Propofol 4.0 mg/kg or to effect (Propofol Plus, Zoetis UK Limited). A 7–8 mm ID endo-tracheal tube (Sims Portex Limited) was introduced and anaesthesia maintained using Isoflurane (2.0 – 3.0% in oxygen).

An eye lubricant was applied and the skin was prepared for aseptic surgery using 5% Chlorhexidine (Vetasept, Animalcare Limited). A long acting antibiotic injection, Amoxicillin 15 mg/kg body weight (Ampoxypen LA 150 mg/ml Suspension for Injection, MSD Animal Ltd.) and a non-steroidal anti-inflammatory drug, Carprofen 4 mg/kg body weight (Rimadyl small animal solution for injection, Zoeist UK Ltd.) were given subcutaneously as separate injections before the start of the surgery.

During the surgical procedure, 0.9% NaCl (Vetivex 1 9 mg/ml, Dechra Veterinary Products) was infused via the ear vein cannula at a rate of 40 ml/kg body weight.

At the end of the surgical procedure, 3 ml of local anaesthetic (0.5% Marcaine, AstraZeneca UK) was infiltrated locally and an opioid analgesic Buprenorphine 20 μg/kg body weight (Vetergesic 0.3 mg/ml solution for injection, CEVA Animal Health Ltd) was administered as intramuscular injection to provide postoperative pain relief. Further post-operative analgesia was dependent on animal behaviour and was provided either by Buprenorphine or Carprofen alone.

Humane euthanasia involved sedation with Midazolam and Azeperone as described above followed by an overdose of barbiturate (phenobarbital sodium 200 mg/ml solution; Euthatal, Merial Animal Health Ltd).

4.2.3 Implantation of PABM and Permacol™ as on-lay urethral free graft

Surgery was performed on 12 pigs (mean weight 16.59 kg ± 1.25 SD), with six animals receiving implants of PABM and six of Permacol™. The study was designed so that procedures were carried out on half the animals (three PABM and three Permacol™) followed by a 5 month gap in order to enable the first series to be analysed and inform the second series.

Under anaesthesia and complete aseptic conditions, a 5 cm midline incision was made caudally, approximately 5 cm from the preputial sac. The peri-urethral plane was opened and a 3.0 by 1.5 cm^2 graft of PABM or Permacol™ was positioned and secured with eight to ten dissolvable Vicryl™ (polyglactin 910; Ethicon) sutures, consistent with the surgical procedure reported in children (Springer and Subramaniam, 2012b). Two non-dissolvable polypropylene (Prolene™, Ethicon) sutures were placed at either end of the graft in the opened superficial fascia in order to mark the implant site. The rest of the superficial fascia was closed using Vicryl™ interrupted sutures. Skin closure was achieved using absorbable suture in a continuous closure. Two further Prolene™ sutures were placed as external markers of the closure to enable location of the implant site after 3 months.

Euthanasia was performed 3 months post-operatively as planned and, following external inspection, implants with surrounding tissues were removed for analysis. Guided by the marker sutures, incisions were made and the graft and surrounding tissues removed en bloc, extending from the subcutaneous fat to the deep aspect of the penile shaft. During tissue collection from the first cohort of pigs, free movement of the penile shaft within the sheath of surrounding fascia and peri-urethral tissues made it difficult to register the orientation of the graft in relation to the penile structures for histology. To overcome this during tissue collection from the second set of pigs, the penile shaft and surrounding

tissues were clamped before cutting through these structures beyond the site of the clamps. Clamps were replaced by sutures once the tissue was removed from the animal and prior to fixation.

Antigen	Distribution	Antibody clone	Supplier	Concentration
CD34	Haematopoietic, vascular and other lineages	EP373Y	Abcam	1:1000
CD45	Leucocyte lineage marker	K252-1E4	Serotec	1:150
CD163	Expressed by monocytes and macrophages of M2 tissue-remodelling phenotype	2A10/11	Serotec	1:200
SMA	Vascular structures & myofibroblasts	1A4	Sigma	1:4000
MAC387	Recently tissue infiltrating monocytes and macrophages	MAC387	AbD Serotec	1:150

Table 4.1 Primary porcine-reactive monoclonal antibodies used for immunohistochemistry.

All immunohistochemistry was performed on serial zinc-fixed tissue sections with exception of anti-CD34 which was applied to antigen-retrieved tissue sections from formalin-fixed paraffin wax-embedded tissues processed in parallel.

4.2.4 Histology and immunohistochemistry evaluation: qualitative and quantitative analysis

Harvested tissues were divided in two to enable separate fixation in 10% (v/v) formalin in phosphate buffered saline and in zinc salts. Equivalent samples of non-implanted PABM and Permacol™ were processed in parallel. Following fixation, tissues were processed routinely into paraffin wax and 5 μm sections were collected onto slides. Standard haematoxylin and eosin staining was performed to evaluate the position and histological appearance of grafts and peri-urethral tissues. Staining with DNA intercalating Hoechst 33258 (0.1 μg/ml) was performed to assess tissue and graft cellularity.

Immunohistochemistry was performed, in some cases on serial sections, to identify the nature of the cell populations surrounding or infiltrating the implants. For this purpose, antibodies were selected against CD34 (haematopoietic progenitor marker), CD45 (leucocyte/macrophage lineage marker), CD163 (monocytes/macrophages of an M2 tissue-remodelling phenotype), MAC387 (recently infiltrated macrophages) and anti-smooth muscle actin (αSMA expressed by myofibroblasts and smooth muscle cells of vascular structures). Antibodies were selected on the basis of immunoreactivity against paraffin wax-embedded porcine tissues as listed in Table 4.1. All antibodies were titrated for use, with appropriate positive and negative (irrelevant and no primary antibody) controls included in all series. All antibody labelling was performed on zinc-fixed tissues without antigen retrieval, except in the case of anti-CD34, where formalin-fixed paraffin wax-embedded sections were used.

For zinc-fixed tissue sections, blocking of all free avidin/biotin sites (kit from Vector Laboratories) and secondary antibody binding sites (10% (v/v) rabbit serum; Dako) was performed before incubation overnight at 4°C with primary antibody. The secondary antibody, biotinylated rabbit anti-mouse immunoglobulin (Dako) was pre-incubated with 10% (v/v) swine serum (Dako) to eliminate cross-reactivity with porcine tissue. Bound antibody was detected using the Vectastain® ABC kit (Vector Laboratories), with 3,3′-diaminobenzidine (DAB; SigmaFAST™ 3,3′-diaminobenzidine tablets) as chromogen.

For formalin-fixed sections, endogenous peroxidase was blocked with 3% (v/v) hydrogen peroxide, then antigen retrieval was performed by microwave boiling in 1 mM ethylenediamine tetra-acetic acid (pH 8.0) for 10 min. Secondary antibody binding sites were blocked with 2.5% (v/v) horse serum (Dako) before incubation overnight at 4°C with primary (anti-CD34) antibody. Bound primary antibody was detected using an Amplifier™ antibody, followed by ImmPRESS™ Excel amplified horseradish peroxidase (HRP) polymer reagent and ImmPACT™ DAB EqV substrate as the chromogen (ImmPRESS™ Excel Amplified HRP Polymer Staining Kit; Vector Laboratories).

Following labelling, all sections were counterstained in Mayer's haematoxylin, dehydrated and mounted in 1,3-diethyl-8-phenylxanthine (DPX; Sigma-Aldrich).

Immunohistology was analysed to characterise and quantify the extent and type of cellularisation and tissue integration versus host reaction to the two implanted biomaterials (PABM and Permacol™). The analysis focused on the extent of cellular integration (cell type and density), presence and extent of any encapsulation process, and the number and distribution of immunolabelled cells. For analysis, labelled slides were scanned on a Zeiss Axioscan Microscope and the resulting CZI image files were subjected to supervised semi-automated analysis using StrataQuest software (version 6.0.0.123) on the TissueGnostics image analysis platform (Vienna, Austria). The auto-detection function was used to set the colour intensity of the master marker (nuclear haematoxylin) and DAB label to identify the different cell type-associated markers. Five non-overlapping 0.1 × 0.1 mm^2 regions of interest (ROIs) were defined within each implanted biomaterial (PABM and Permacol™) and nuclei were detected automatically within the five equal-sized ROIs. Following optimisation, the same conditions were applied to all image files. Raw data were imported into GraphPad Prism for statistical evaluation.

4.3 Results

4.3.1 Survival and health of surgical recipients

The procedure is illustrated schematically in Figure 4.1A to D. Surgery proceeded according to plan with biomaterials positioned as on-lay urethral grafts (Figure 4.1E – G). All pigs survived the immediate and long-term post-operative period with no complications; voiding was normal and there were no episodes of urinary retention, urinary tract or wound infections. Upon termination at 3 months, the body weight of the animals ranged from 55 to 62 kg (mean 56.12 kg). Gross anatomy, as examined at the time of dissection and harvesting of tissue around the graft, was similar to control animals, with no substantial scarring, fibrosis or encapsulation. Macroscopically PABM grafts appeared fully integrated and could only be identified from the positioning of the non-absorbable marker sutures (Figure 4.1H), whilst Permacol™ grafts remained readily apparent (Figure 4.1I).

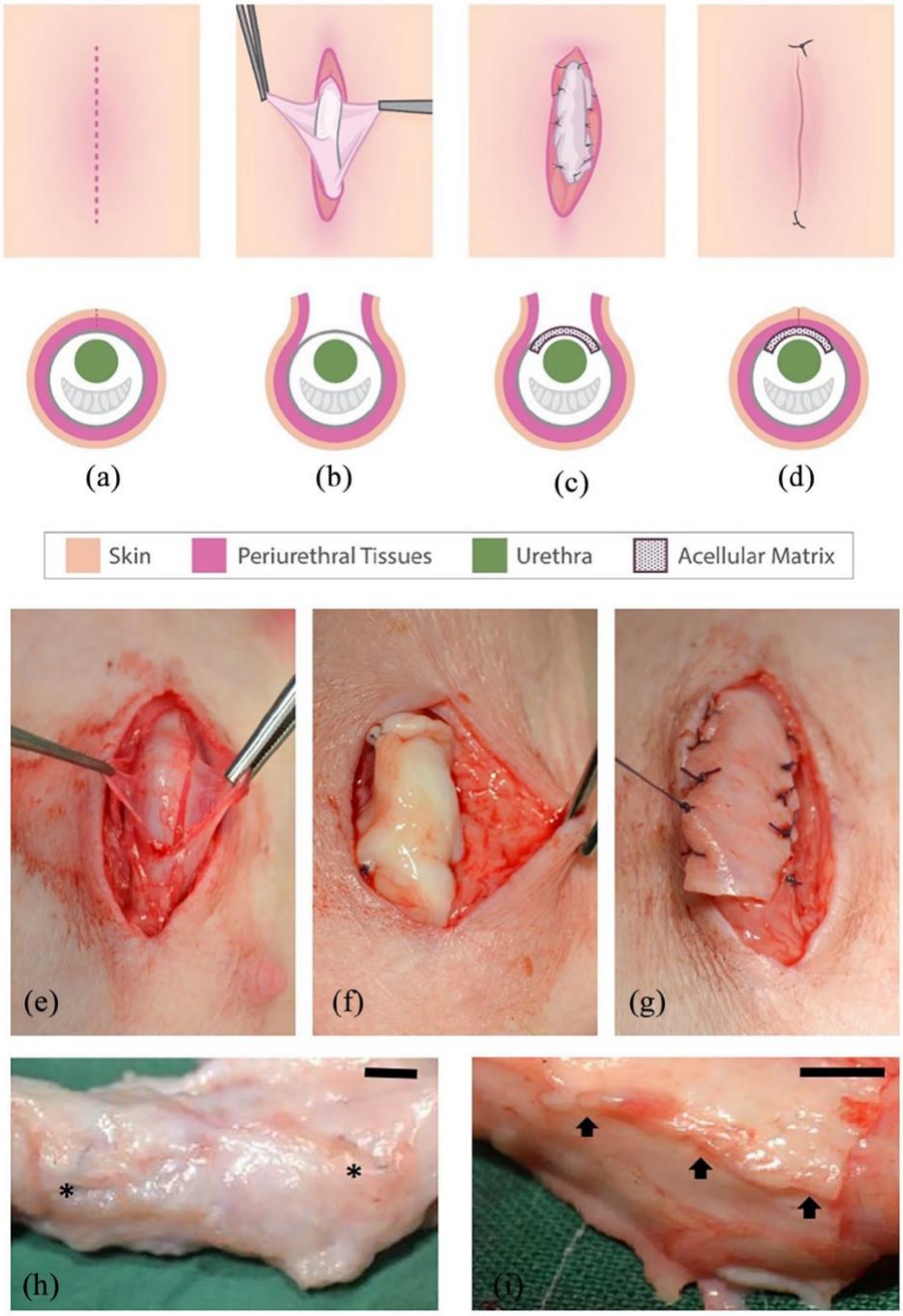

Figure 4.1 Surgical placement of biomaterial implant (PABM or Permacol™) within the peri-urethral fascia.

Surgery was performed on 12 large white landrace hybrid male pigs 14 weeks old and mean weight of 16.59 kg (± 1.25 (SD)). Six animals received implants of PABM and six of Permacol™: (a)-(d) Schematic of the surgical procedure. An incision (red dashed line in (a)) was made approximately 5 cm caudally from the preputial sac. The superficial adipose tissue was dissected (b) to reveal the peri-urethral tissues and fascia. The fascia was opened (b) in order that either PABM or Permacol™ could be sutured in place using eight Vicryl™ sutures, with two non-absorbable 3'0 Prolene® marker sutures positioned at either end of the graft (c). Subcutaneous fat was then opposed followed by skin

closure (d) achieved with 5'0 Monocryl (Ethicon) or Vicryl™ continuous suture with two external Prolene® marker sutures at the caudal and cranial end of incision (d). (e)-(g) Intraoperative stages from surgery reflecting schematic parts (b) and (c) with insertion in part (c) of PABM (f) or Permacol™ (g). (h) and (i): at harvest, the grafted tissue area was removed en bloc for histological analysis using the delineating permanent marker sutures as guides for PABM (h) and Pelvicol (i). In (h) arrows highlight the persistence of Permacol™; in (i) asterisks highlight the position of permanent sutures used to mark the position of the graft. Scale bar 1 cm.

4.3.2 Extent and patterns of cellularisation

Following dissection and histological evaluation, the biomaterial implants were identified in all 12 animals, as illustrated in Figure 4.2A and B. Samples of non-grafted PABM or Permacol™ processed in parallel for haematoxylin and eosin (H&E) stain and immunohistochemistry revealed multidirectional collagen bundles and an absence of cells that provided a morphological reference for identifying the implanted grafts.

Histologically, there was no widespread inflammation associated with any graft and there was no detection of any MAC387+ cells, which would have been indicative of recently infiltrated macrophages. In one Permacol™ graft, a small localised reaction of giant cells within a thin capsule was found coincident with the Prolene™ marker suture and provided an internal control for the potential for foreign body reaction. In addition, occasional foci of lymphocytes were observed at the edges of Permacol™ samples which, based on location, frequency and distribution, related to the position of the Vicryl™ absorbable sutures used to attach the grafts.

Varying extents of cellularisation were apparent within the implant sections analysed from the 12 grafts. Implanted PABM grafts revealed cells present uniformly throughout the implant (Figure 4.2C). There was evidence of vascularisation at the periphery and within the graft. This was highlighted by αSMA immunolabelling, which was detected on vascular elements as well as by a majority of cells within the PABM grafts (Figure 4.2E). In the case of PABM implants, there were no lymphocytic aggregates found and no evidence of any encapsulation-like reaction around the periphery of the implant (Figure 4.2F). An absence of cellularisation was typical of Permacol™ grafts, where cells accumulated at the edge of the implant and showed very limited, sparse infiltration (Figure 4.2D). Where present, cells showed a tendency to infiltrate along natural pathways within the Permacol™ grafts, sparsely infiltrating between collagen bundles (H&E shown in Figure 4.2D). Evidence of a partial encapsulation-like reaction, where cells accumulated at the interface between the Permacol™ graft and host tissue, was apparent in some regions. This partial encapsulation reaction exclusive to the Permacol™ implants was particularly evident when sections were immunolabelled with antibodies to αSMA (Figure 4.2F). As measured from scans of all six Permacol implants, the capsule involved between 6 and 44% (min - max range) of the perimeter of the visualised implanted biomaterial (mean ± SD: 19.5% ± 12.59, n = 6). The average thickness of the identified capsule was 216 µm ± 96 (mean ± SD, n = 6; min - max range: 20 - 500µm).

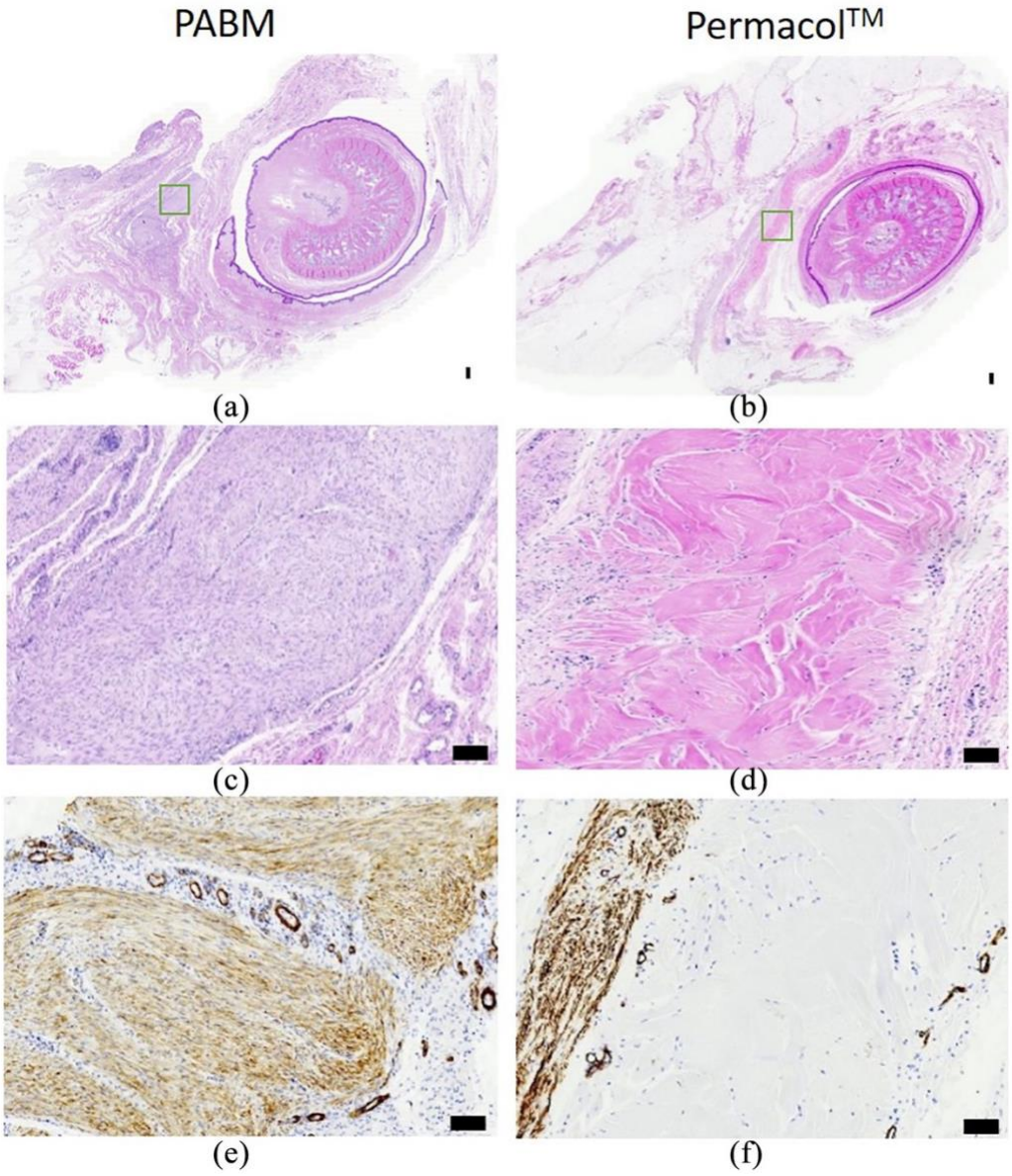

Figure 4.2 Histology of on-lay graft implants after 3 months.

PABM (left column) or Permacol™ (right column): (a)-(d)) H&E-stained sections of peri-urethral penile tissue showing PABM and Permacol™ implants at low power (a) & (b), with boxes (green) marking the position of implant regions illustrated at higher magnification in (c) & (d) (by H&E) and (e) & (f) (by IHC) to examine differences in the extent of cellularisation of each biomaterial. Note the extensive infiltration by cells in PABM (c) marked by haematoxylin-stained nuclei (blue dots), compared to the absence of cells across the Permacol™ graft (pink) in (d). Immunolabelling with anti-αSMA indicates differences in distribution of vessels and αSMA+ cells between PABM (e) and Permacol™ (f) implants. PABM implants showed extensive cellular infiltration and neovascularisation, whereas Permacol™ implants showed cells and vessels retained along the edges of the implant. Note partial encapsulation evident along one edge of Permacol™ (f).

4.3.3 The nature and abundance of infiltrating cell populations

An objective quantitative analysis of immunohistochemically-labelled tissue sections was carried out. Total cell counts confirmed significantly higher cell densities in PABM than in Permacol™ implanted grafts (Figure 4.3). The cell count per ROI is shown for each animal to illustrate the extent of variation between animals and across the grafts (Figure 4.3A). The density of infiltrating cells expressed as the mean total number of cells per $mm^2 \pm$ SEM was 5309 ± 78 for PABM versus 906 ± 32 for Permacol™ ($n = 6$ animals per group; Figure 4.3B). This difference was statistically significant ($p < 0.0001$, determined using Welch's t-test).

To determine if, separate from the total cell count, there were shifts in the relative proportions of the different major cell types infiltrating PABM and Permacol™, the percentages of cells expressing CD34, CD45, CD163 and αSMA was examined. Whereas percentages of cells expressing αSMA, CD45 and CD163 were assessed in serial sections, the antibody to CD34 required a different tissue fixation to be immunoreactive and hence was counted in equivalent but non-related areas. The relative quantification revealed 40% CD34: 20% CD163: 40% αSMA positive cells in PABM, compared to 40% CD34: 20% CD163: 40% CD45 positive cells in Permacol™. In other words, although both biomaterials were infiltrated by cells expressing CD34+ and/or CD163+ cells in a similar ratio, the remaining 40% of the infiltrating population showed a significant switch from predominantly CD45+ in Permacol™ to αSMA+ in PABM (Figure 4.4).

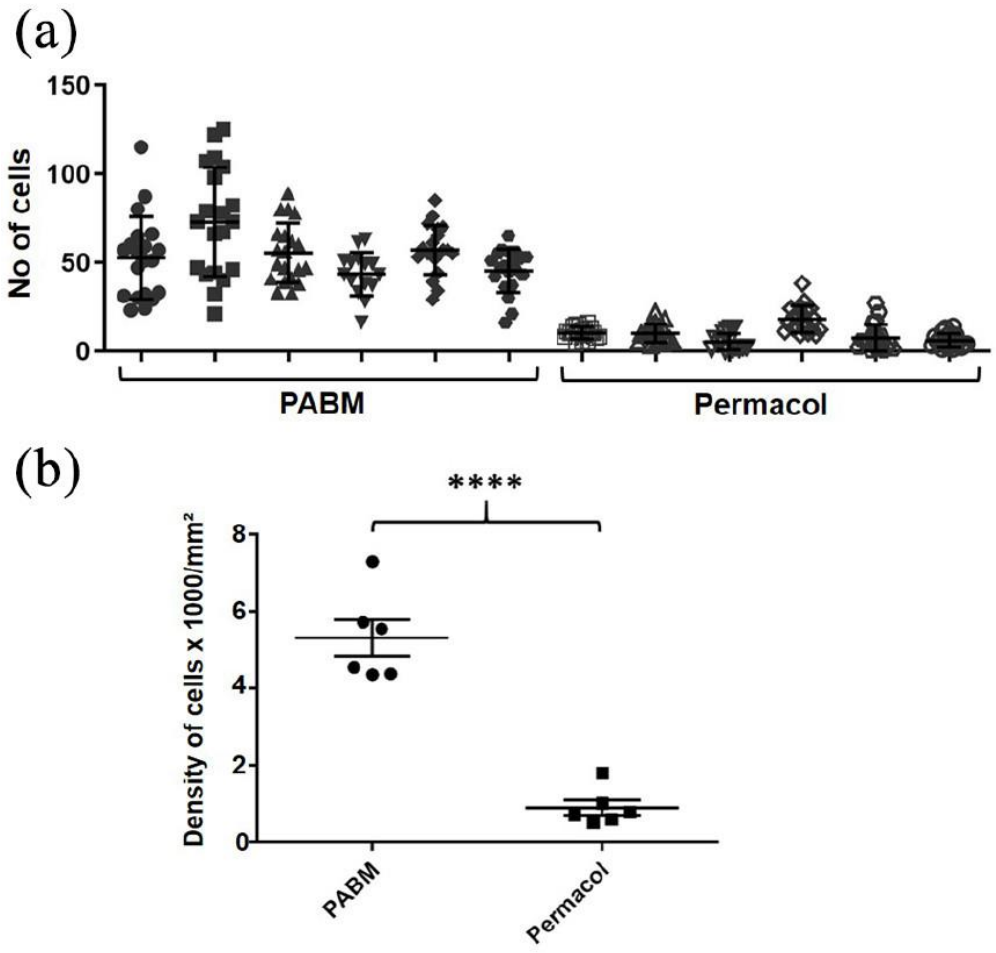

Figure 4.3 Implant cell density.

(a) scatter plot for number of cells detected within the biomaterial implant for each animal displayed individually, showing mean and SD. Using tissue analysis software, nuclei were detected automatically within 20 non-overlapping equal-sized regions of interest (ROIs) for each PABM and Permacol™ implant. Data are displayed for the individual animals to show the variance within and across grafts. Filled symbols represent PABM data and empty symbols represent Permacol™ data and (b) combined data from all animals displayed as mean number of cells per mm² (± SEM) in PABM versus Permacol™ (5309 ± 78 vs 906 ± 32; $p < 0.0001$; $n = 6$ animals per group).

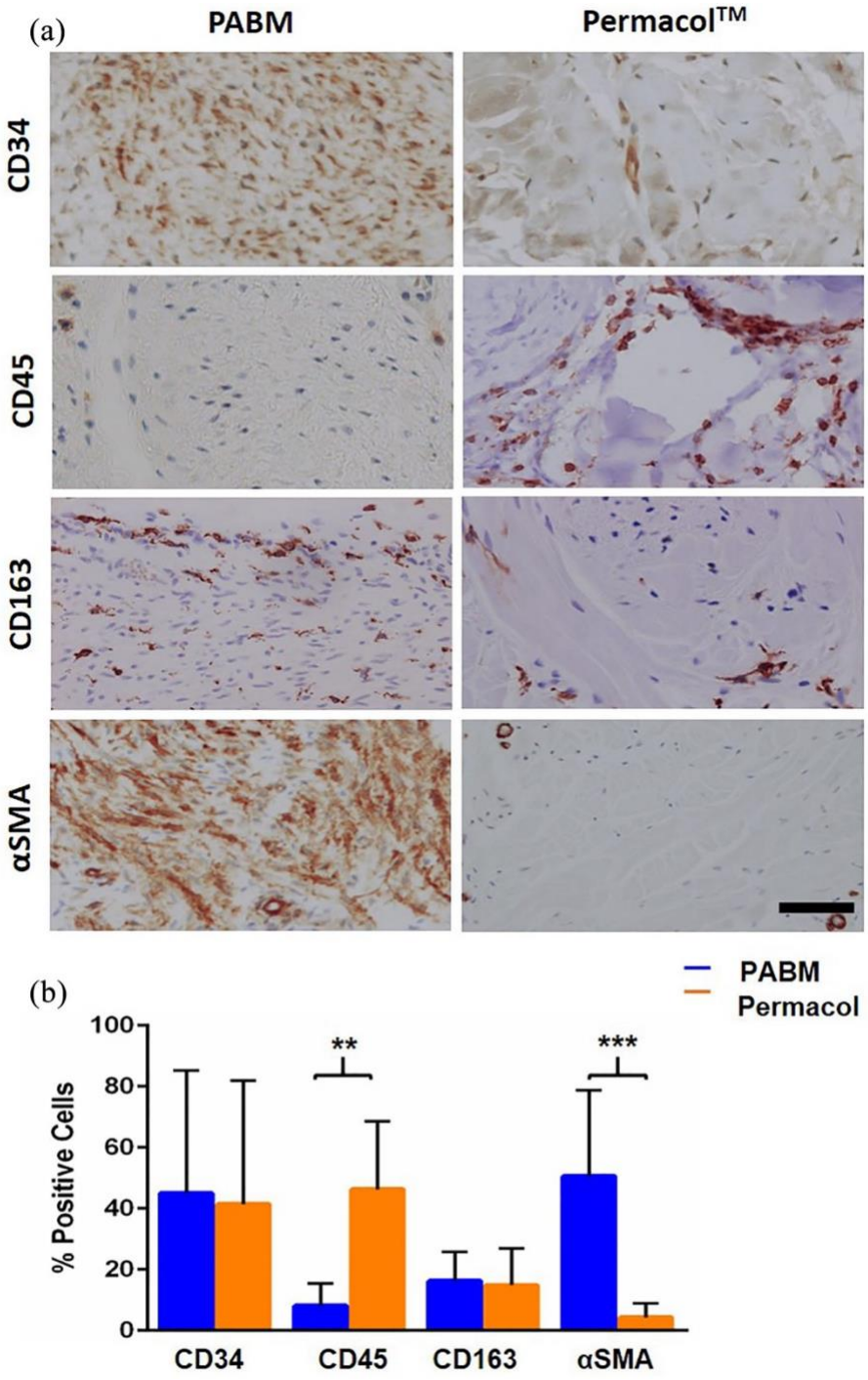

Figure 4.4 Distribution of infiltrating cell types in implants.

(a) immunohistochemistry of Permacol™ and PABM implants labelled with antibodies against CD34, CD45, CD163 and αSMA to identify lineages of infiltrating host cell populations. Scale bar 100 µm and (b) quantification of the relative proportion of different cell types in PABM and Permacol™ samples identified using cell type lineage markers. Supervised automated image analysis using StrataQuest software was used to quantify cell numbers from 5 individual ROIs per implant for each marker. Data expressed as mean ± SD.

4.4 Discussion

The aim of hypospadias repair is to provide a good cosmetic and functional outcome, resulting in a penis devoid of ventral curvature and the patient being able to pass urine from the tip of the penis with a good stream. Our study investigated the concept that an acellular matrix graft inserted into a peri-urethral position would become tissue-integrated, augmenting a deficient tissue bed on the ventral aspect and reducing the potential for surgical complications. By being positioned peri-urethrally, our approach differs in surgical approach from other studies where acellular matrices, either alone or seeded with cells, have been used as in-lay grafts in urethral reconstruction in both animal and human studies (Versteegden et al., 2017).

In this present study aimed at acquiring proof-of-concept evidence towards clinical translation, we have demonstrated that implanting decellularised tissue matrices into the peri-urethral stroma in a large animal surgical model is well-tolerated and does not provoke an inflammatory response. We compared two porcine matrices that varied in their different surgical handling characteristics from highly compliant (PABM) to stiff (Permacol™). The handling differences are supported by mechanical evidence, as the Young's modulus for Permacol™, reported to be 50 – 100 MPa (Cavallo et al., 2015), is considerably higher than the 2 – 3 MPa we found for native porcine bladder (Korossis et al., 2009), albeit that some stiffening occurs following decellularization (Bolland et al., 2007). Nevertheless, how different tissue derivations and/or processing affects biomaterial properties and influences implantation outcomes is an incomplete science. Bladder and dermal matrices both contain collagens type I and III, but whereas type III collagen is associated in the bladder with healthy compliance (Aitken and Bägli, 2009a), in the dermis it is associated with rigidity and scarring (Tanaka et al., 2009), reflecting negative implications for (dermal) scaffold design (Khan and Bayat, 2019). This highlights the need for further basic studies to inform intelligent scaffold design, alongside empirical, translation-focused studies of the type reported here.

Externally, both porcine-derived biomaterials used gave acceptable results. Nevertheless, there were important biological differences in the host response to the two materials. Implants of PABM had become fully incorporated within the three-month period to leave no macroscopic residue. Histologically, the marked PABM graft region was extensively vascularised and completely infiltrated by cells. This agrees with independent reports of non-cross-linked matrices in terms of superior host tissue integration and cellular infiltration accompanied by neo-vascularisation (Macleod et al., 2005; Butler et al., 2010). By contrast, Permacol™ implants persisted macroscopically and the bulk material remained acellular at 3 months. Permacol™ is terminally-sterilised by gamma radiation and chemically cross-linked by hexamethylene diisocyanate (Khor, 1997), the latter producing stable

urea groups by the interaction of amine groups with isocyanate (Olde Damink et al., 1995). Cross-linking is known to limit scaffold degradation (Stanasel et al., 2015) and to inhibit host cells from infiltrating matrix grafts, including Permacol™. Although we might predict acellular matrix properties to reflect tissue-specific differences, it seems axiomatic that observed differences in results between Permacol™ and PABM were dominated by the influence of cross-linking. Supporting this point, we have shown previously that cells fail to infiltrate PABM cross-linked by gamma-radiation (Bullers et al., 2014).

Cells expressing αSMA+ were present both as vascular smooth muscle cells in association with blood vessels and as spindle-shaped myofibroblasts. The myofibroblasts were present either within the PABM or in the case of Permacol™, at the neo-vascularised interface of the biomaterial and native host tissue where they formed an incomplete capsule-like structure. An encapsulation response to Permacol™ has been described in some studies (Valentin et al., 2006; Butler et al., 2010), albeit with exceptions (de Castro Brás et al., 2010). The myofibroblast is recognised as an essential effector of both healthy tissue regeneration through matrix remodelling and pathological fibrosis, although how this balance is regulated is not fully understood (Hinz, 2016; Pakshir and Hinz, 2018). Our observations suggest that the physical cross-linking of the matrix might define whether recruited myofibroblasts formed a boundary at the edge of the implant or infiltrated the matrix.

Given the difference in extent of cellular infiltration into Permacol™ and PABM, we were interested in whether there was any relative shift in infiltrating cell types. Historically, any evaluation of cellularisation in implanted biomaterials has been performed using qualitative or semi-quantitative approaches. In the field of histology and immunohistochemistry, it is well known that different observers see and report the same tissue sample differently (Taylor, 1994; Rhodes et al., 2000; Sirota, 2005). To overcome this limitation, we performed an objective quantitative analysis of immunohistochemically-labelled biomaterials 3 months post-implantation. Although restricted by the limited availability of reliable porcine-reactive antibodies, we were nevertheless able to examine the major infiltrating cell lineages as identified by expression of CD34 (to identify progenitor cells of multiple lineages, particularly haematopoietic (Sidney et al., 2014)); CD45 (as a pan-leucocyte marker); CD163 (macrophages of M2 phenotype) and αSMA (vascular and other smooth muscle cells, including myofibroblasts). These different markers revealed that after 3 months, both implanted biomaterials contained a similar proportion of CD34+ and CD163+ cells, making up about 60% of the total cellular infiltrate. The presence of CD163-expressing cells further indicated that both acellular collagen matrices promoted a remodelling, regenerative (M2), rather than inflammatory (M1) macrophage response, as observed previously with PABM in human ex vivo studies (Bullers et al., 2014). The remainder 40% infiltrating population was different between matrices, being

constituted by spindle-shaped αSMA+ cells in PABM versus diffuse lymphoid CD45+ cells in Permacol™. This reveals key differences in recellularisation biology and outcome between the two matrices, discussed below.

Irrespective of matrix tissue derivation (bladder or dermal) or cross-linked status, neither acellular matrix tested provoked an acute reactive or rejection response upon implantation. Nevertheless, the presence of a diffuse infiltrating CD45+ population in Permacol™ was indicative of a low level, chronic inflammatory state, as was reinforced by the presence of enhanced acute local reactions at permanent and resorbable suture sites. Thus, although implanted acellular matrices were not themselves inflammatory and promoted an M2-type macrophage phenotype, the PABM was the more benign material, possibly as a result of being non-cross-linked. The absence of innate immune-activating signals in PABM fits with our previous observations using a novel ex vivo human tissue:PABM interface model, where early (< 10 days) 'pioneering' cellular events involved recruitment of tissue-resident macrophages and polarisation to an M2 CD163+ remodelling phenotype (Bullers et al., 2014). The ability of PABM as a non-cross-linked allogeneic material to promote a fully integrative response perforce rests on the quality of matrix production, including absence of innate immune-inducing 'danger' signals such as DNA. This clearly needs stringent quality-control during batch production if the material is to be taken forward for clinical use. This also raises the question of sterilisation, as most terminal sterilisation methods involve cross-linking, such as by gamma-radiation, which our previous results indicate may impact negatively on tissue integrative properties (Bullers et al., 2014).

The availability of PABM and Permacol™ as biomaterials with contrasting properties of host integration/remodelling versus persistence may suit different surgical applications. The process of chemical cross-linking results in a product that remains rigid but flexible and resistant to degradative processes and therefore maintains strength and 3D structure. This resilience of Permacol™ was exploited by Springer and Subramaniam to support urethral repair where Permacol™ was incorporated as a periurethral splint in 12 boys undergoing urethrocutaneous fistula repair (10) or redo urethroplasty (2) (Springer and Subramaniam, 2012b). Apart from one instance of late wound infection, no recurrence of fistula or stricture was noticed in the cohort at a median follow-up of 2.5 years. The results supported the principle of managing complications from hypospadias surgery by incorporating a suitable biomaterial into the surgical procedure when local tissues are insufficient or inadequate. The clinical nature of the study meant that outcomes were observational only, with no possibility of obtaining follow-up histological evidence of the extent or nature of any tissue integration. Our present study highlights the importance of studying histological outcomes in a clinically-relevant in vivo model, as the eventual fate of the cross-linked implant material in the

clinical study (Springer and Subramaniam, 2012b) is unknown. On a related point, our study demonstrates that even in the case of natural non-cross-linked tissue matrices, the complete remodelling and integration events take place over a longer timescale than the 3 months typically reported for in vivo models.

In addition to its superior integration, other benefits of PABM are its compliance, malleability and ability to hold sutures. In accordance with the recognised ideal characteristics of a biomaterial for urethral use (O'Brien, 2011), PABM provided a functional strong and supple scaffold when placed in the peri-urethral plane in a simple porcine urethroplasty model. From its characteristics, it is predicted that in primary hypospadias repair, where insufficient native tissue is available, PABM may fulfil an unmet surgical and clinical need as a scaffold for augmentation of the native tissue in order to prevent subsequent complications, such as urethral fistulae and strictures.

In conclusion, this study provides proof of principle evidence that implanted non-crosslinked acellular matrices become readily incorporated, meaning they may be useful to augment an inadequate tissue bed to support primary surgical repair. In the particular case of hypospadias, the successful incorporation of an on-lay graft of acellular matrix during the primary surgery may improve the quality of repair, leading to reduced complications. It is clear that natural acellular tissue matrices offer promising new biomaterials to support reconstructive and regenerative surgery, but that many of their advanced physical and biological properties are negatively affected by cross-linking as a result of conventional chemical- or radiation-induced terminal sterilisation procedures. If natural acellular matrices are to meet their full clinical potential it is important to evaluate the safety/efficacy outcomes from both ex vivo (Bullers et al., 2014) and in vivo studies and use these to define new criteria for the regulated production of such materials for clinical use.

In the next chapter, the homologous use of PABM as a non-cross-linked biomatrix will be tested in an in vivo large animal surgical model of urinary bladder auto-augmentation, and biomaterial integration and tissue regeneration characteristics will be evaluated.

Chapter 5
Homologous use of an acellular bladder matrix (PABM) in a porcine surgical model of urinary bladder auto-augmentation

5.1 Aim and objectives

The clinical need for urinary bladder augmentation alongside the attempted and currently available solutions has been illustrated in Sections 1.2 – 1.4 and related subsections. The known complications and limitations have also been highlighted. The concept and technical specificities of urinary bladder auto-augmentation have been introduced (Section 1.2.1). The need for alternative solutions involving tissue engineering and regenerative medicine to overcome ongoing complications and shortfalls has been there explained.

The properties of PABM as detailed in Section 1.4.3.2, supported by the results presented in Chapter 3 and Chapter 4 suggest it may serve purpose for surgical applications in urinary tract reconstruction (Morgante et al., 2021).

Here, the main aim was to examine the potential of using PABM as a free graft in a setting of urinary bladder auto-augmentation. It was hypothesised that the use of this highly compliant acellular matrix with integrative properties and physical properties homologous to the native tissue, would provide an initial physical support by reinforcing the exposed mucosa, while promoting tissue regeneration.

Specific objectives were:

- To evaluate the feasibility of performing bladder auto-augmentation in a large animal surgical model (cadaver) and to investigate the possibility of using the omentum as a vascular graft.
- To test a new surgical protocol by performing bladder auto-augmentation reinforcing the bulging mucosa by applying PABM in a series of large animals.
- To investigate tissue integration properties, extent of cell and tissue regeneration of the implanted PABM in auto-augmented urinary bladders, by examining histological outcomes.

5.2 Experimental approach

5.2.1 Legal and ethical obligations

An application for a Project Licence (PPL) was made to the Home Office under the Animals (Scientific Procedures) Act 1986 containing full details of any possible procedures that may have been necessary to carry out on the experimental animals. All personnel working with the animals under the Project Licence, within the designated establishment for animal research, underwent Home Office Training and assessment from an accredited licensee training course to obtain a Home Office Personal Licence (PIL) to carry out regulated procedures.

5.2.2 Surgical Protocol Development

At the Animal Facility (Central Biomedical Services - University of Leeds) one 25 Kg Large White Landrace Hybrid female pig underwent humane euthanasia as a planned culling procedure. The animal was placed supine on a surgical bed and the skin of the lower abdomen was shaved.

A lower midline abdominal skin incision was made with a size 15 disposable scalpel. The abdomen was opened by layers. The peritoneum was opened, and the bladder was exposed through the surgical wound. Bladder auto-augmentation (detrusorotomy) was carefully performed in the midline with micro-blade and micro-scissors. A lozenge-shaped area of 4 cm (length) x 3 cm (width) of bladder mucosa was exposed until bulging (Figure 5.2).

The omentum was identified cranially. This resulted of an insufficient length to be able to reach the position of the urinary bladder. Attempt was made by the operating surgeons to pedunculate the omentum with the aim to obtain a longer vascularised tissue able to cover the PABM graft during the surgery. The pedunculated tissue obtained resulted of insufficient physical characteristics and potentially dangerous for the bowel of the animals. The abdomen was closed in layers and the carcass properly disposed.

Such findings further inform the experimental surgical plan. In consideration of the guiding principles of the ethical framework for the use of animals in research (Russell and Burch; Hubrecht and Carter, 2019), decision was made to proceed with one animal series with the application of PABM only on the exposed mucosa of the auto-augmented urinary bladders.

In the Figure 5.1 below the experimental surgical pathway is summarised.

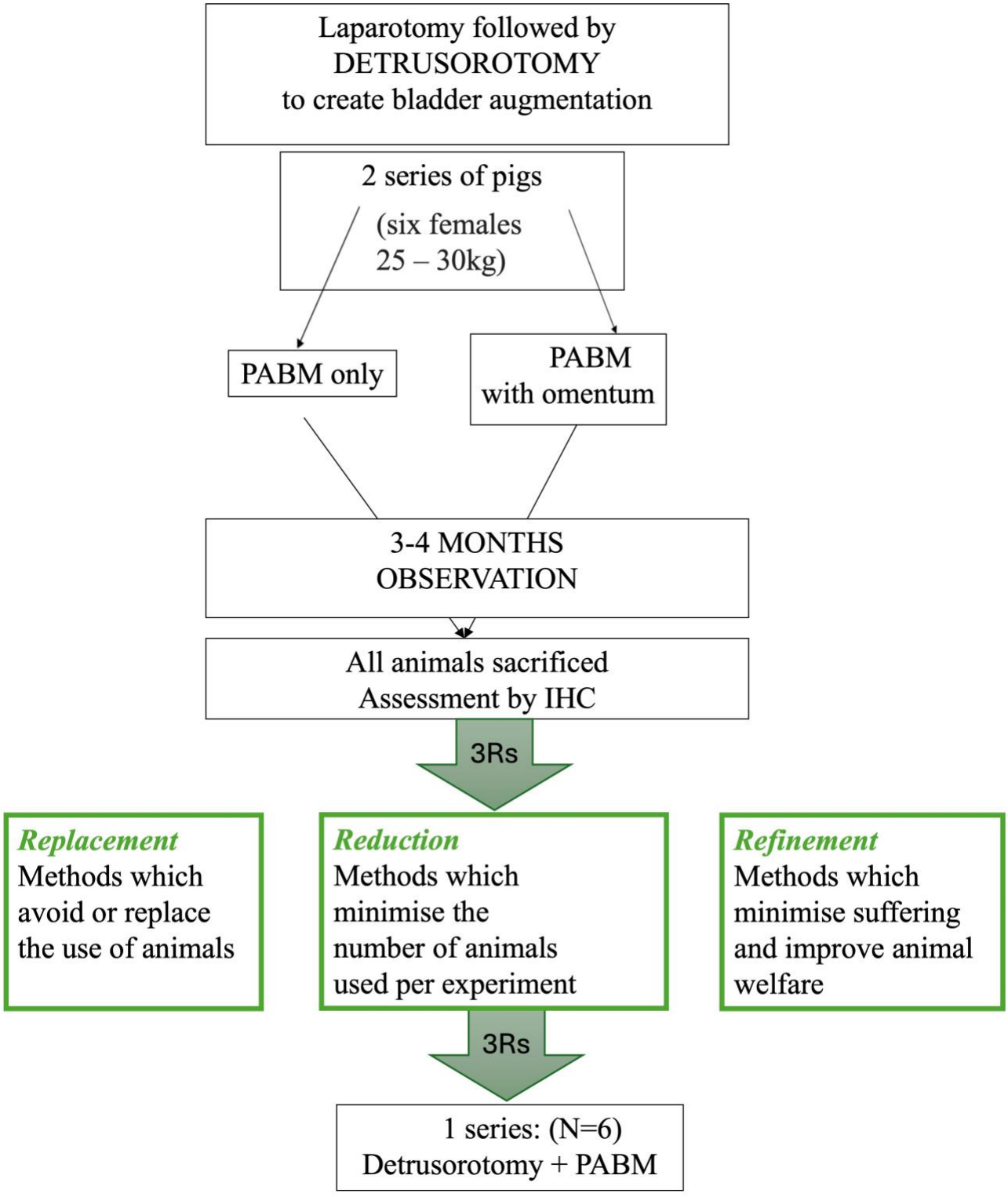

Figure 5.1 Schematic diagram illustrating the initial surgical experimental plan.

Two methods of urinary bladder auto-augmentation were initially included: with PABM graft only and with PABM graft + omentum. Based on the intraoperative technical findings (Figure 5.2 below) and in respect of the principles of the 3Rs, decision was made to proceed with detrusorotomy with PABM only in one series of six animals.

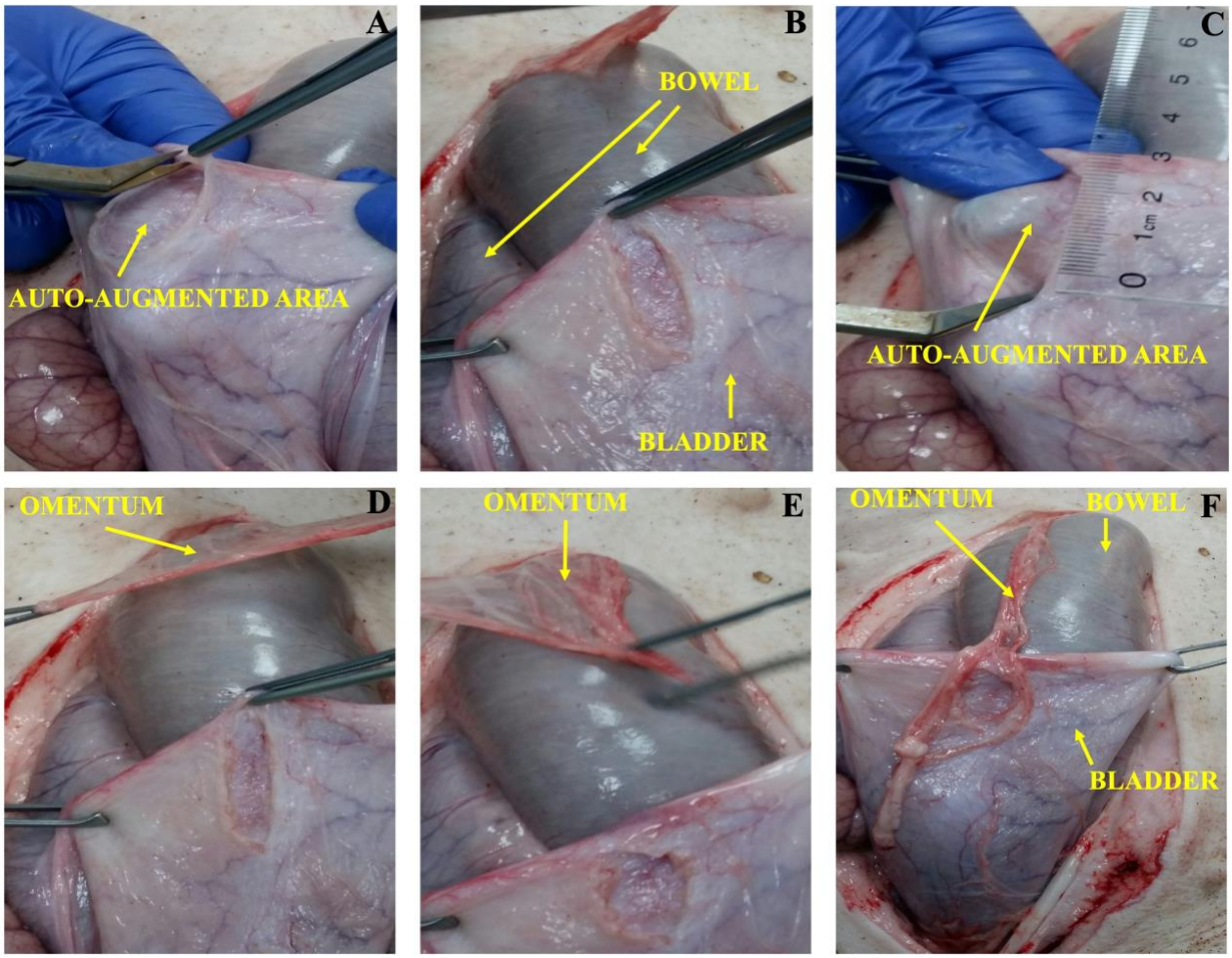

Figure 5.2 Development of a surgical large animal model of bladder auto-augmentation.

Intraoperative images showing the development of a model of urinary bladder auto-augmentation by detrusorotomy (A, B, C) in a large animal model (deceased Landrace pig). The possibility of utilising the omentum as a vascular support to the acellular matrix was also tested and resulted not feasible (D, E, F).

5.2.3 Animal husbandry

Six female pigs, Large White Hybrid (LWH) with an initial weight of approximately 20 Kg, were purchased from a local farm and transported to the surgical animals' facility. Animals were identified by number and labelled with ear tags. On arrival, pigs were inspected by a veterinary consultant, and they were housed in pens with sawdust and hay bedding. The pens were checked, cleaned and replenished daily by the facility's technical staff. Experimental animals had access to water and were regularly fed daily with a ready-made food mix (Figure 5.3). Animals were moved to and from the pens by using pig boards. All pigs received a prophylactic dose of antibiotics. Animals were allowed at least two weeks of acclimatisation.

Figure 5.3 Landrace female pigs.

Image showing Landrace female pigs hosted in a pen at the Animal Facility (Central Biomedical Services - University of Leeds).

5.2.4 Surgical procedure

5.2.4.1 Surgical instruments

Surgical instrument packs were arranged prior to the surgical procedures. After use, instruments were cleaned, dried, repacked, and autoclaved at 121˚C (1 bar) for 20 minutes.

5.2.4.2 Sedation, Anaesthesia and Analgesia

The day before the planned surgery, food was halved in quantity. On the day of surgery, the pig was restrained and sedated by intramuscular injection (neck) of Hypnovel (Midazolam) and Stresnil (Azaperone), and left in a quiet environment for 15-20 minutes to let it calm and sleep. A snout-mask containing an Isoflurane-soaked gauze was used to induce light anaesthesia. The animal was then weighed before been transported to the anaesthetic room on a trolley. A local anaesthetic cream was applied to the pinna of both ears to prepare the introduction of an intravenous cannula into an ear vein. The animal was given atropine sulphate and a Venflon peripheral intravenous catheter ported 18 G, 45 mm winged was introduced into an ear vein and secured with a drop of glue and sticky tape. Anaesthesia was induced using Propofol and maintained by 1.5 - 2.5% Isoflurane in Oxygen, delivered via a 6 mm endotracheal tube attached to the anaesthetic machine and a ventilator. The animal was given a dose of Amoxicillin antibiotic and Rimadyl, a non-steroidal anti-inflammatory agent: both provided via subcutaneous injection (Left groin). A 0.9% w/v Sodium Chloride infusion was started and continued along the surgical time. Eyes were protected by giving Lacri-lube. Marcain (Local Anaesthesia) was infiltrated into the wound. Analgesia (Rymadyl) and antibiotic therapy (Amoxicillin) were administered post-operatively as required.

5.2.4.3 Preparation for surgery

The surgical team wore surgical clothes, shoes and overshoes, caps (Barrier) and masks (LiteOne). The anaesthetised animal was place supine and the skin on the lower abdomen was properly shaved (Figure 5.4A). The animal was transferred from the anaesthetic room into the surgical room. The surgical table was broken longitudinally to ensure the animal could not roll. A plate electrode (Conmed) was placed onto flank skin and attached to the diathermy machine. In an adjacent scrub room, surgeons scrubbed using Chlorhexidine wash (Hibiscrub), worn sterile, disposable surgical gowns (3M) and ultratouch sterile gloves powder free, non-latex (Biogel). The animal's skin was prepared with Chlorhexidine solution (Vetasept). A reusable 307 cm x 254 cm drape with incise pouch was used to limit the surgical field. The monopolar diathermy (Unomedical) was connected and set up (set up level: 15).

5.2.4.4 Surgical procedure

A lower midline abdominal skin incision (length = 6 cm) was made with a size 15 disposable scalpel (Swann Morton) on a mark pen (Maddis) drawn line (Figure 5.4B). The abdomen was opened in layers using monopolar diathermy. The peritoneum was opened and the bladder was exposed through the surgical wound. The bladder was stabilised and exposed by applying a stay-suture (5/0 Prolene) secured using a big clip (Figure 5.4C). Bladder auto-augmentation was carefully performed in the midline with micro-blade, micro-scissors and monopolar diathermy. A lozenge-shaped area of 4 cm (length) x 2-2.5 cm (width) of bladder mucosa was exposed and left bulging (Figure 5.5 and Table 5.4). A sterile PABM sheet, cut to the required dimensions, was fixed in place with 12 stiches (5/0 Vicryl) (Figure 5.6). The six required patches were taken from the six 8 cm x 8 cm PABM sheets produced as described in Section 2.3.4, 3.3.2 and 3.4.2. Four cardinal stiches of non-absorbable suture were applied for marking purposes (2/0 Prolene (Ethicon)) (Figure 5.6). The abdomen was closed in layers, with continuous 2/0 Vicryl (Ethicon) suture to the peritoneum and interrupted 2/0 Vicryl sutures to the muscle. To prevent the risk of post-surgical ventral hernia development, a Vicryl mesh (Ethicon) was left in situ and secured applying interrupted 2/0 Vicryl sutures (Figure 5.4D). The skin was then closed using a subcuticular 3/0 Monocryl (Ethicon) suture. Opsite spray (Smith and Nephew) was applied to the skin at the end of the procedure (Figure 5.4E).

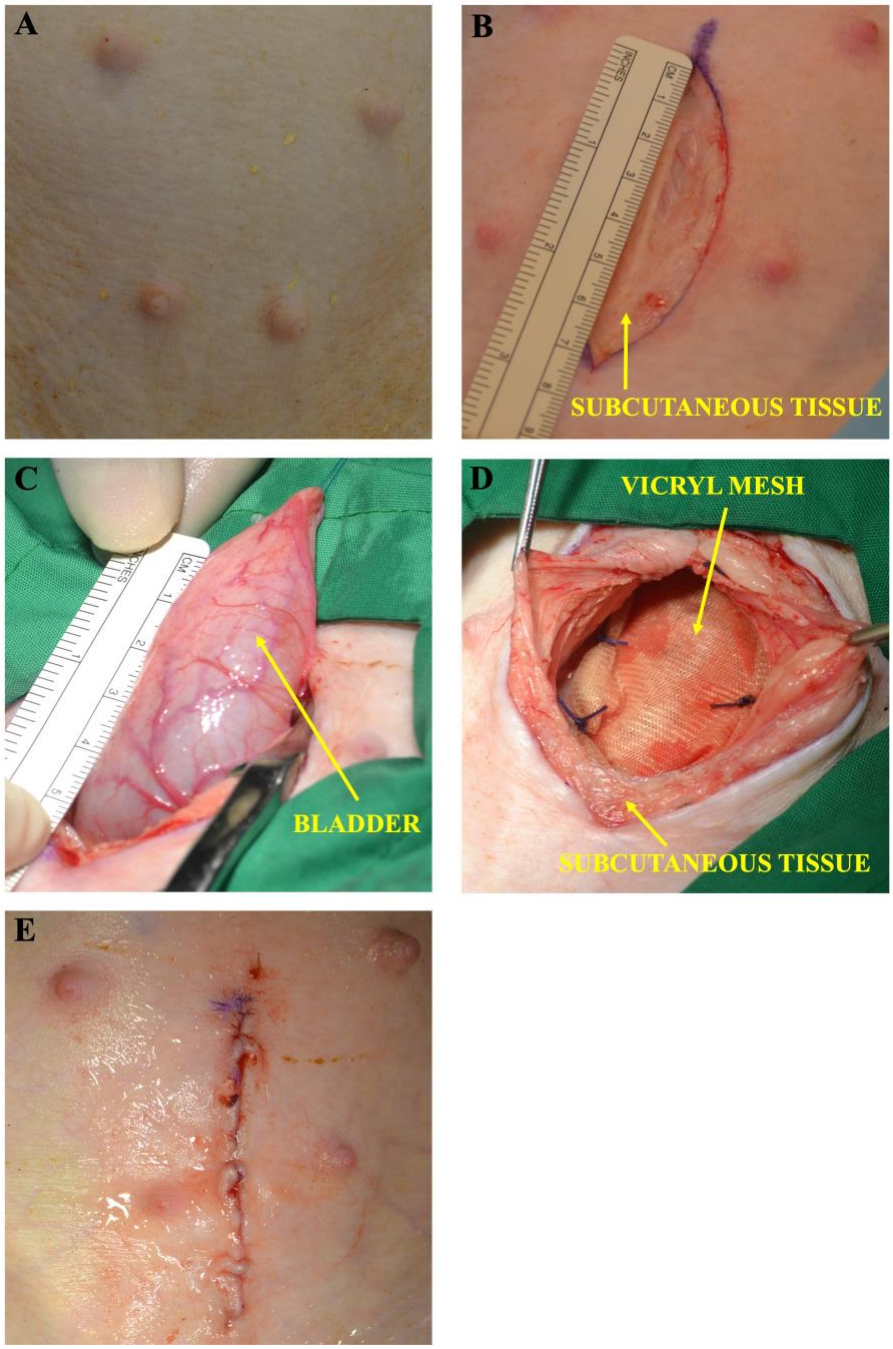

Figure 5.4 Surgical procedure (I).

Pictures showing the shaved skin on the lower abdomen of anaesthetised animal (supine position) (A), the lower midline abdominal skin incision (length = 6 cm) made (B), the peritoneum opened, with the bladder exposed through the surgical wound and stabilised by applying a stay-suture (5/0 Prolene) (C). To avoid the risk of post-surgical ventral hernia development, a Vicryl mesh (Ethicon) was left in situ and secured applying interrupted 2/0 Vicryl sutures (D). Skin closure was obtained using a subcuticular 3/0 Monocryl (Ethicon) suture. Opsite spray (Smith and Nephew) was applied to the skin at the end of the procedure (E).

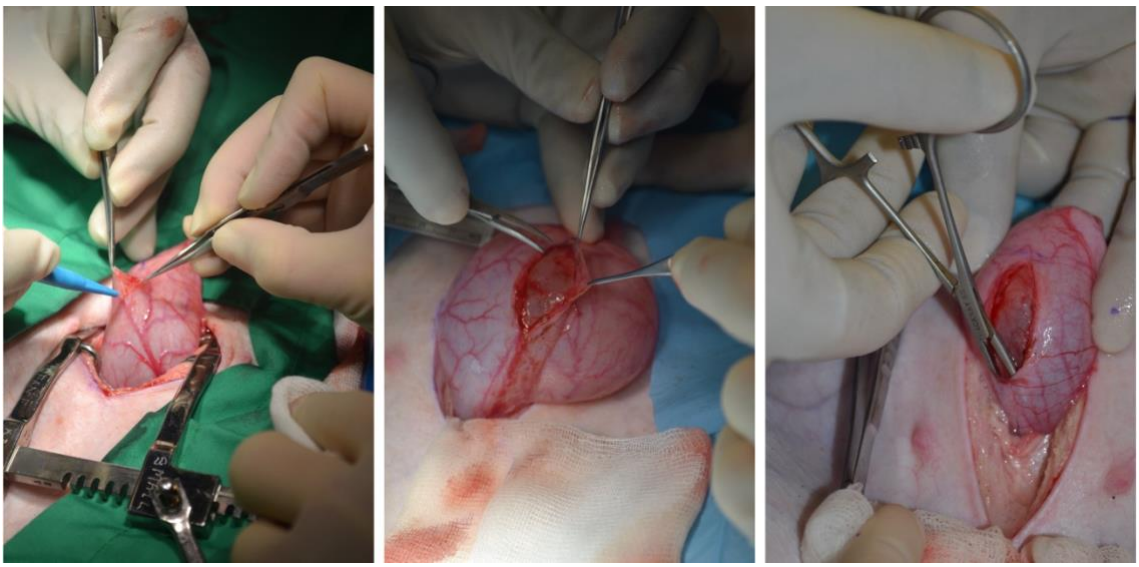

Figure 5.5 Surgical procedure (II).

Bladder auto-augmentation performed in the midline with micro-blade, micro-scissors and monopolar diathermy. A lozenge-shaped area of 4 cm (length) x 2-2.5 cm (width) of bladder mucosa was exposed and left bulging.

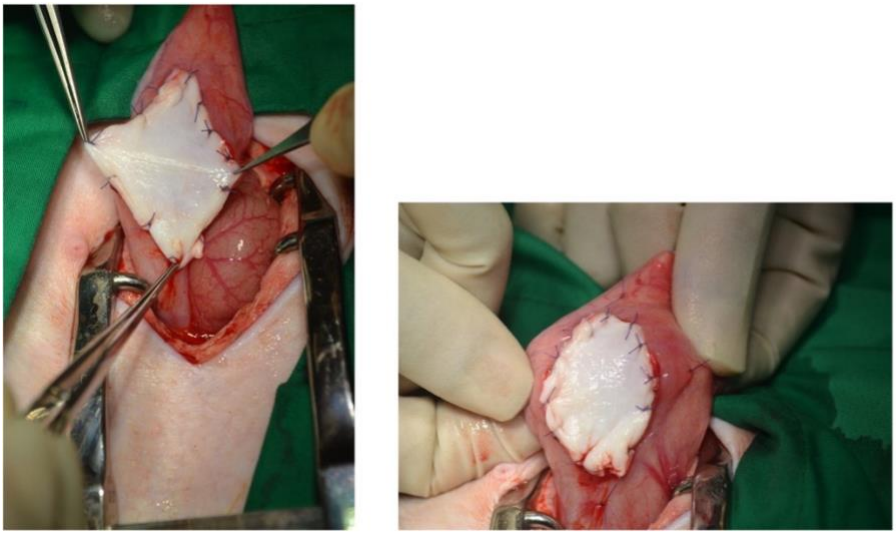

Figure 5.6 Surgical procedure (III).

A sterile PABM sheet was cut to fit the defect size and was fixed in place with 12 stiches (5/0 Vicryl). Four cardinal stiches of non-absorbable suture applied for marking purposes (2/0 Prolene (Ethicon)).

5.2.5 Post-operative care

Once extubated, pigs were returned to the pens and kept warm using warmer lamps (Figure 5.7). For the welfare of the animals, analgesia and antibiotics were given to the pigs post-operatively as prescribed by the vet. Members of the surgical and technical staff monitored the animals with particular interest towards any signs of distress, urinary symptoms and alteration in eating and drinking habits.

Figure 5.7 Post-operative care.

Image showing pigs, standing and feeding, returned to the pen and kept under warm lamps.

5.2.6 Follow up

A four-month follow up was chosen to ensure that some persistent material would remain within the explanted tissue to help investigate any ongoing remodelling process.

An operation note was completed for each pig and attached to their individual care plans. Weight gain was plotted over the four months to assess for any long-term complications. All animals were monitored and evaluated at least twice a day.

5.2.7 End of Protocol

Experimental animals that were four months post-bladder auto-augmentation were initially sedated. An ear vein was cannulated and barbiturate was administered intravenously to overdose (Schedule 1 euthanasia). The animals were taken to another room, the abdomen was opened and the augmented bladders excised in toto: total cystectomy (*en bloc* resection) was performed using Metzenbaum scissor straight 150 mm. The rest of the intra-abdominal structures were examined to ensure no damage or inflammation had occurred. In consideration of reduction, refinement and replacement, it was made known to other groups in allied laboratories that 5 pigs were to be put down, and so other parts of the pig were removed for non-related research projects.

5.2.8 Assessment of the auto-augmented bladder

The bladder was excised en bloc with the ureters, distally to the bladder neck. It was immediately inspected and placed into a 5 L specimen bucket (Jokey Plastik). A freshly made 10% formalin was poured into the lumen using a 50 ml bladder syringe until the bladder reached distension. Urethra and ureters were closed with 2/0 Vicryl free ligatures to secure and keep the filled status of the urinary bladder during the fixation process. The bucket was then filled with 10% formalin to bathe the organ completely (Figure 5.8). This was to ensure that the bladder maintained its shape during the fixation process and to minimise shrinkage of the tissue. The bucket was transported to the laboratory and after 5 days, the bladder was removed and photographed.

The augmented region was identified via non-absorbable sutures in situ. The bladder was gently opened longitudinally along the posterior ligament (from the urethra to the apex) in correspondence of the surface opposite the area involved in the surgery, and a full-thickness sample was excised as control (Figure 5.9). A dissection and classification method was developed to facilitate bladder tissue assessment. Therefore, a quadrant of the augmented area and the surrounding native bladder tissue was excised, measured and photographed (Figure 5.10). Following the same method, the quadrant was cut into multiple sub-segments according to a pre-studied grid pattern, so that every sample contained full-thickness tissue comprising of native urothelium and either implanted graft or normal

tissue. Each sub-segment was approximately 1 cm wide and was given an individual alphanumeric code, so it could be cross-referenced to its original position within the bladder (Figure 5.11). The samples were stored in 70% ethanol. They were then embedded in paraffin wax, recording the orientation (Figure 5.11), microtomed (5µm sections) as detailed in Section 2.4.11. Tissue sections were dewaxed, rehydrated and then subjected to staining and immunohistochemical testing according to standard protocols (Sections 2.4.1.2 and 2.4.2). Photo-microscopy (Section 2.4.3) was performed to assess and record results. Native tissue was used as control for comparison.

Stains and antibodies (listed in Table 5.1) were chosen with the following main purposes:

1) H&E Staining: to evaluate location of the implanted biomaterial, the overall bladder structure including the continuity of the urothelial layer, and the general recellularisation pattern of the auto-augmented area with PABM.
2) Hoechst 33258 Staining, which intercalates with double-stranded DNA, to identify nuclei and evaluate pattern of recellularisation.
3) α-SMA, SM22α and Myo11hc: to define the phenotype of the cells, particularly to assess for the presence and distribution of smooth muscle cells, myofibroblasts and myoepithelial cells, including identification of blood vessels.
4) ki-67: to assess the normality of the tissues, specifically to identify proliferative cells.
5) UP3a and CK20.8: to evaluate the integrity of the urothelium and the preservation of its unique function.
6) CD163: to evaluate the presence of phenotype M2 macrophages, which have been associated with a pro-regenerative environment.
7) NFP: to evaluate the neurogenesis.

A section of the biomaterial only was also processed. For every IHC experiment a negative control (no primary antibody) and or an irrelevant antibody was performed alongside a section of appropriate positive control, which utilised the same anti mouse/rabbit secondary antibody.

Analysis of immunohistology aimed to characterise and measure the cellular type and integration and the tissue response to the implanted acellular matrix. The quantitative analysis focused on cell type, density, and immunolabelled cells' number and distribution. Slides were scanned using a Zeiss Axioscan Microscope, and the resulting CZI files were analysed using StrataQuest software (version 7.0.1.178) on the TissueGnostics image analysis platform. The colour intensity of markers (nuclear haematoxylin and DAB) was set using the auto-detection function, and 150 non-overlapping ROIs (0.1 x 0.1 mm^2) were delineated within each animal. Nuclei were automatically detected within these regions. Data were then statistically evaluated using GraphPad Prism (Section 2.8).

Figure 5.8 Fixation process of the excised urinary bladders.

Figure showing an excised bladder placed into a 5 L specimen bucket (Jokey Plastik), while a freshly made 10% formalin was poured into the lumen using a 50 ml bladder syringe until the bladder reached distension. Urethra and ureters were closed with 2/0 Vicryl free ligatures to maintain the filled status of the urinary bladder during the fixation process. The bucket was filled with 10% formalin to bath the organ completely.

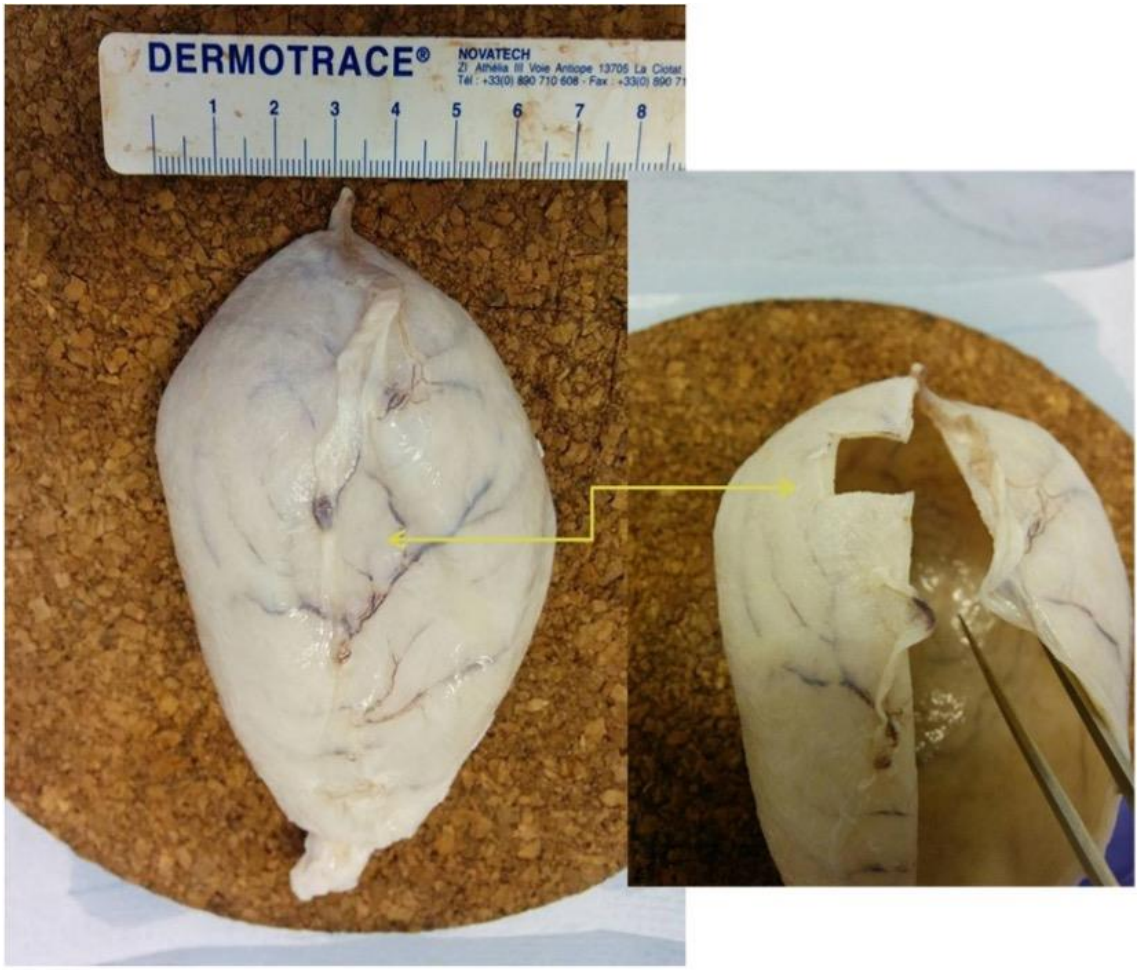

Figure 5.9 Porcine Urinary Bladder NBF fixed.

Images showing the posterior bladder wall and the area where the control sample was taken.

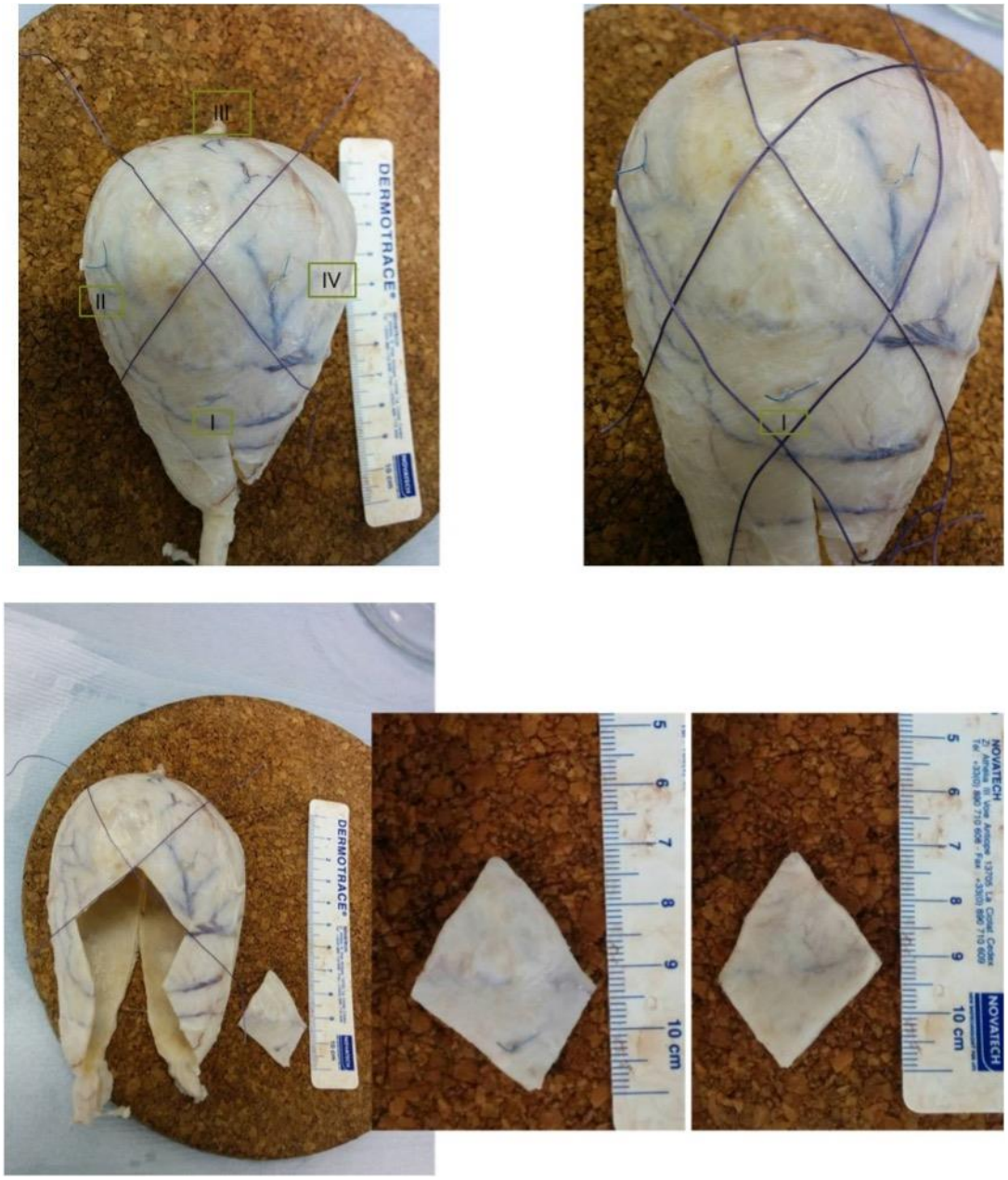

Figure 5.10 Dissection of the Porcine Urinary Bladder NBF fixed.

Images showing how four quadrants of interest were identified on the anterior wall of the porcine bladder in correspondence to the area site of auto-augmentation and PABM implant. Quadrant I was dissected for further investigations (external and internal aspect showed).

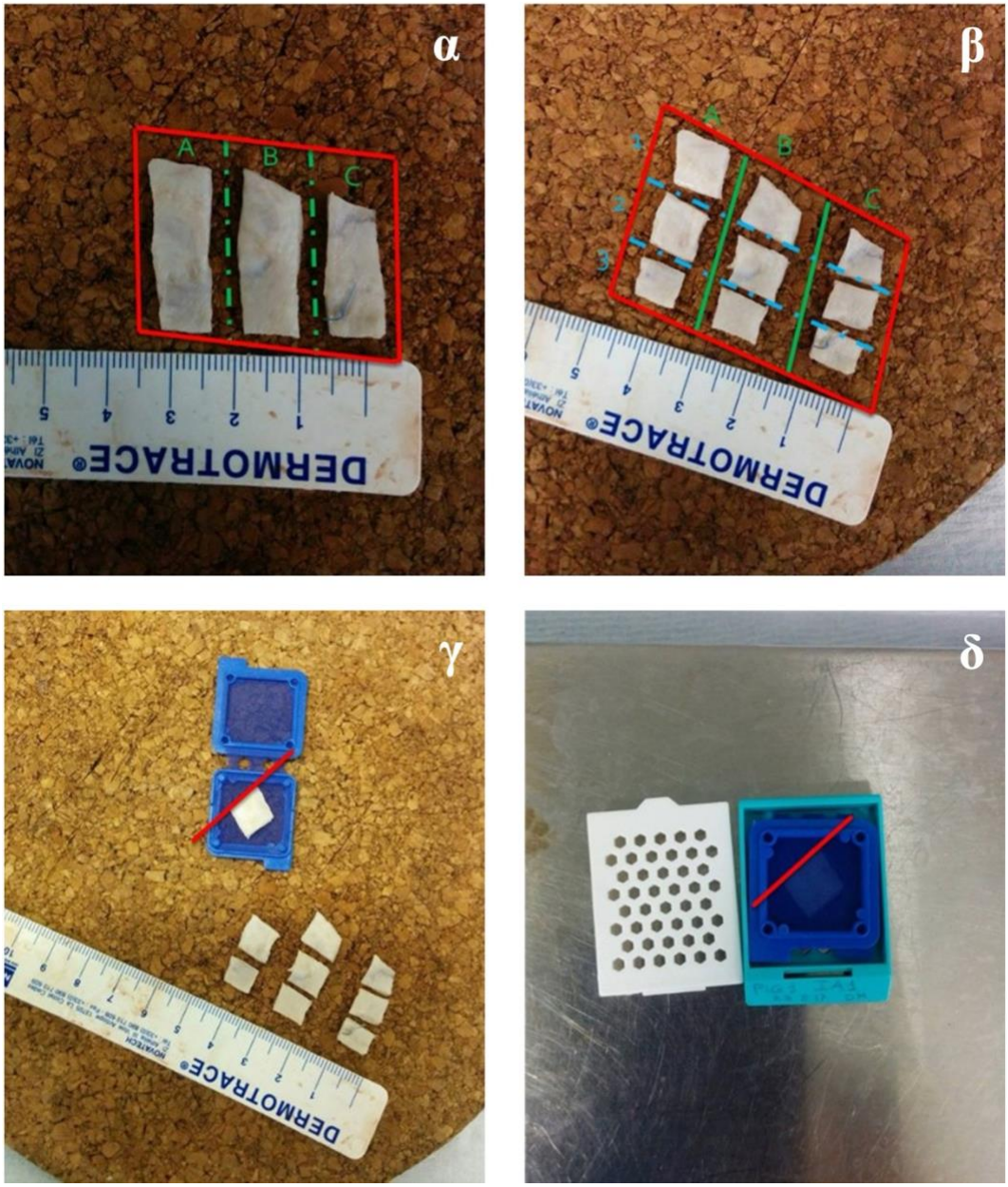

Figure 5.11 Dissection of Quadrant I.

Images α and β showing the developed dissection method. Quadrant 1 was further dissected in segments A, B, C and sub-segments 1, 2, 3. Images γ and δ showing method of orientation of fixed and dissected samples, in preparation for paraffin wax embedding.

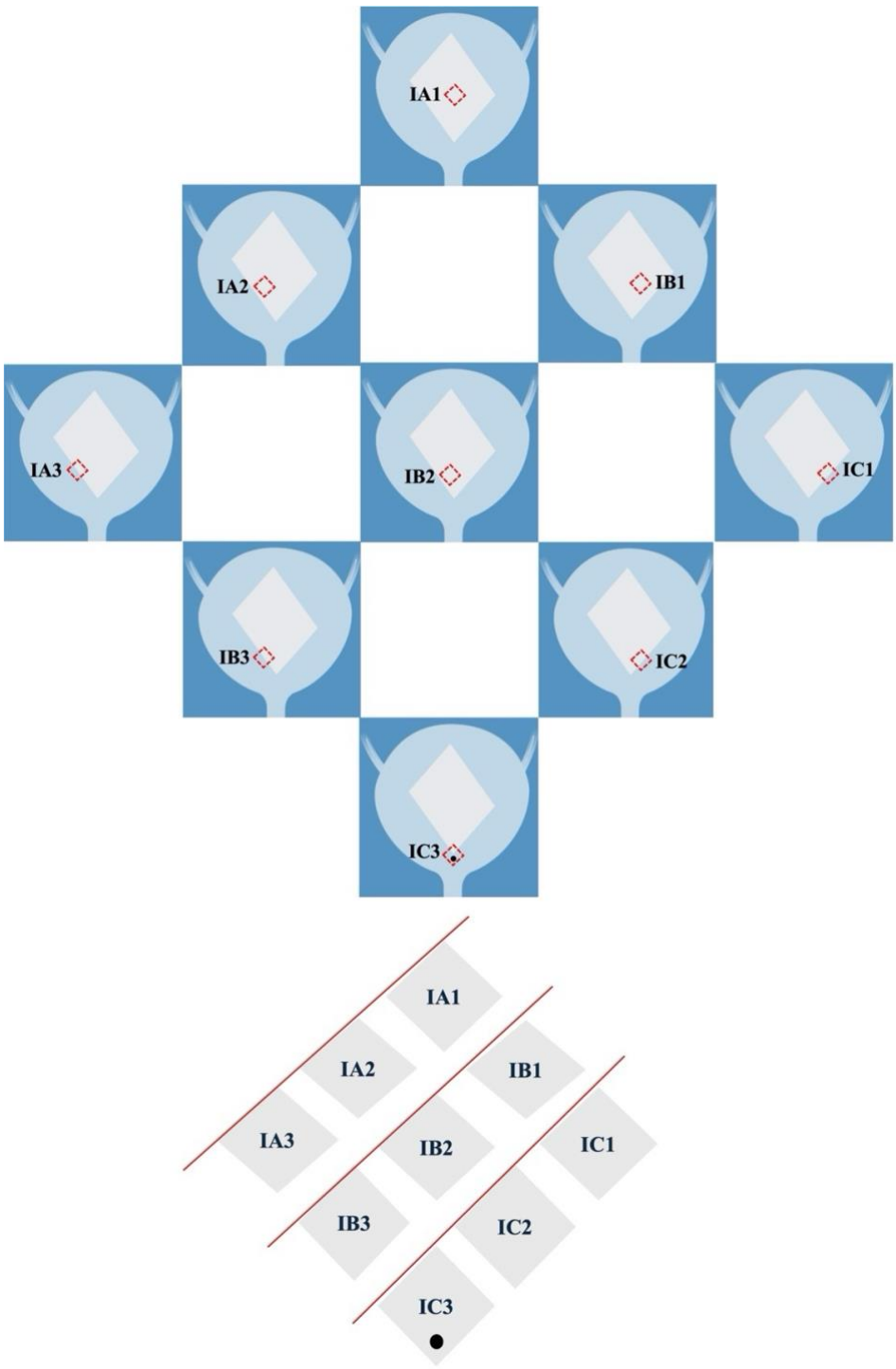

Figure 5.12 Schematic representation of the identified subsegments in correlation to their position at the time of surgery within the bladder and the implanted PABM graft.

The individual alphanumeric code shown was used for classification purposes and to cross-reference a sample to its original position within the bladder. Black dot in IC3 indicates the non-absorbable stitch placed at the time of surgery as a marker.

Antigen	Distribution	Antibody clone	Supplier	Concentration
αSMA	Smooth muscles (myoepithelial cells & myofibroblasts)	1A4	Sigma	1:4000
SM22α / Transgelin 1	Differentiated smooth muscle cells	10H12	Leica/Novocastra	1:50
Myo11hc	Vascular smooth muscle cells/cells derived from smooth muscle lineages	Polyclonal	Abcam	1:4000
CD163	Macrophages of M2 tissue-remodelling phenotype	EPR14336	Abcam	1:8000
Ki67	Proliferating cells	MM1	Leica/Novocastra	1:600
NFP	Neurons (axons) of the central and peripheral nervous system	2F11	DAKO	1:200
UPIIIa	Differentiated Urothelium	AU1	Progen	1:200
CK20.8	Normal Urothelium	KS20.8	Novocastra	1:50

Table 5.1 Primary porcine-reactive monoclonal antibodies used for immunohistochemistry.

All immunohistochemistry was performed on serial formalin-fixed tissue sections.

5.3 Results

5.3.1 Legal and ethical obligations

The application for a Home Office Project Licence was successful (PPL P564844F6). The author operated with Personal Licence (PIL I0B43D4E0).

5.3.2 Survival and health of surgical recipients

Surgery was performed in all animals and proceeding according to plan (Figure 5.5 and 5.6). The weight of the animals at surgery was recorded with a Mean ± SD of 24.3 Kg +/- 1.2 (Table 5.2). All animals survived the immediate post-operative period with no complications relating to the surgery and the biomaterial implantation. No distress and urinary symptoms were observed in our series. All animals had an uneventful long term post-operative period but one. One pig (case study #102), on day 16 post-operative was noted to have a swollen area in correspondence of the surgical wound. The animal looked otherwise in good general conditions and did not seem to be in any discomfort. Thinking of a possibility of a ventral incisional hernia, the decision was taken to perform surgery in the following 48 hours in the best interest of the animal and the research. Case study #102 is discussed in a dedicated Section below (5.3.4.1). The remaining five animals completed the 4-month follow up and after Schedule 1 procedure, all the bladders were harvest for further examination. The dimensions of the urinary bladders were recorded at the time of the surgery, at Schedule 1 and after fixation. The size of the implanted acellular grafts and the dimensions of the area included within the four non-absorbable stiches were also documented. Results have been shown and summarised in Table 5.3 and Table 5.4 below, showing an overall regular and healthy growth pattern of the urinary bladders across all animals during the study period. An overall regular growth of the area site of the PABM implant was observed with time, except for case study #799. In this recipient despite a regular growth of the whole bladder (in line with all the other animals), a small reduction of the dimension of the area between non-absorbable stiches was noted alongside a potential shift of the biomaterial position. No shrinkage was recorded after fixation of the urinary bladders.

Case study	Weight at Operation / Kg	Weight at Schedule 1 / Kg
1 (766)	24	64.3
2 (777)	22	70.2
3 (799)	26	79.6
4 (803)	24	69.8
5 (822)	25	72.1
6 (102)	24.7	24.9*

* All animals except case study 102 underwent Schedule 1 after a 4-month follow-up; case study 102 underwent Schedule 1 18 days post-surgery.

Table 5.2 Animal weight (kg).

Mean ± SD of the six animals' weight at operation was 24.3 ± 1.2. Mean ± SD of the five animals' weight at Schedule 1 after a 4-month follow up was 71.2 ± 4.9, confirming a healthy regular growth of the recipients.

Case Study	Dimensions of the bladder at surgery (length x width) / cm x cm	Dimensions of the bladder at harvest (fresh) (length x width) / cm x cm	Dimensions of bladder after fixation (length x width) / cm x cm
1 (766)	6 x 4.5	10 x 6.5	10 x 6.5
2 (777)	7 x 5.5	11 x 7	11 x 7
3 (799)	6 x 5	10 x 6.5	10 x 6.5
4 (803)	7 x 5	12 x 7	12 x 7
5 (822)	6 x 4.5	10 x 6.5	10 x 6.5

Table 5.3 Dimensions (length x width) of porcine bladders (cm x cm).

Mean ± SD of the dimensions of the bladders at surgery was 31.5 cm^2 ± 5.099. Mean ± SD of the dimensions of the bladder at Schedule 1 resulted 71.2 cm^2 ± SD 8.8431. Mean ± SD of the bladders after fixation was 71.2 cm^2 SD 8.8431. ANOVA between the three groups was calculated (p value 0.00000). Data suggest a normal growth of the overall bladder recorded during the study period in all recipients. No tissue shrinkage was noted after fixation.

Case Study	Size of implanted PABM graft at surgery / cm x cm	Area between non-absorbable stiches at surgery / cm x cm	Area between non-absorbable stiches at harvest (fresh bladder) / cm	Area between non-absorbable stiches after fixation / cm
1 (766)	4 x 2.5	5.5 x 3.5	7 x 4	7 x 4
2 (777)	4 x 2.5	5.5 x 3.5	8 x 4.5	8 x 4.5
3 (799)	4 x 2	5.5 x 3.5	4 x 3	4 x 3
4 (803)	4 x 2.5	5.5 x 3.5	6.5 x 4.5	6.5 x 4.5
5 (822)	4 x 2	5.5 x 3.5	6.5 x 4	6.5 x 4

Table 5.4 Dimensions (length x width) of PABM grafts and areas between markers (cm x cm).

Mean ± SD of the dimensions (length x width) of the implanted PABM grafts at surgery was 9.2 cm^2 ± 1.0954. Mean ± SD of the areas between non-absorbable stiches at surgery was 19.25 cm^2 ± SD 0. Mean ± SD of the areas between non-absorbable stiches at harvest (fresh bladders) was 26.25 cm^2 ± SD 8.807. Mean ± SD of the areas between non-absorbable stiches after fixation was 26.25 cm^2 ± SD 8.807. ANOVA between the three groups (at surgery, at Schedule 1 and after fixation) representing the areas defined by the non-absorbable marker stiches was calculated and resulted not statistically significant (p value 0.24617).

Macroscopic appearances

Gross anatomy of the 5 explants (at 4-month from surgery) was examined at harvest. No significant scarring, fibrosis or encapsulation were noted. The absorbable sutures were no longer identifiable. The area of auto-augmentation and biomaterial implantation was identified using the presence of the 4 non-absorbable sutures. No pathological adhesions were noted between the bladders and the surrounding intra-abdominal structures in all animals. The PABM grafts resulted fully integrated and could not be properly identified macroscopically. Some changes and minimal discoloration were noted after fixation in the most central area of the implantation site, with an otherwise uniform surrounding tissue. Intact appearances of the internal aspect of the bladders were found with no discontinuity or superficial damages identifiable (Figures 5.13-5.17). Results were comparable across all animals. A potential movement of the implanted PABM area was observed in case study #799 (Figure 5.15).

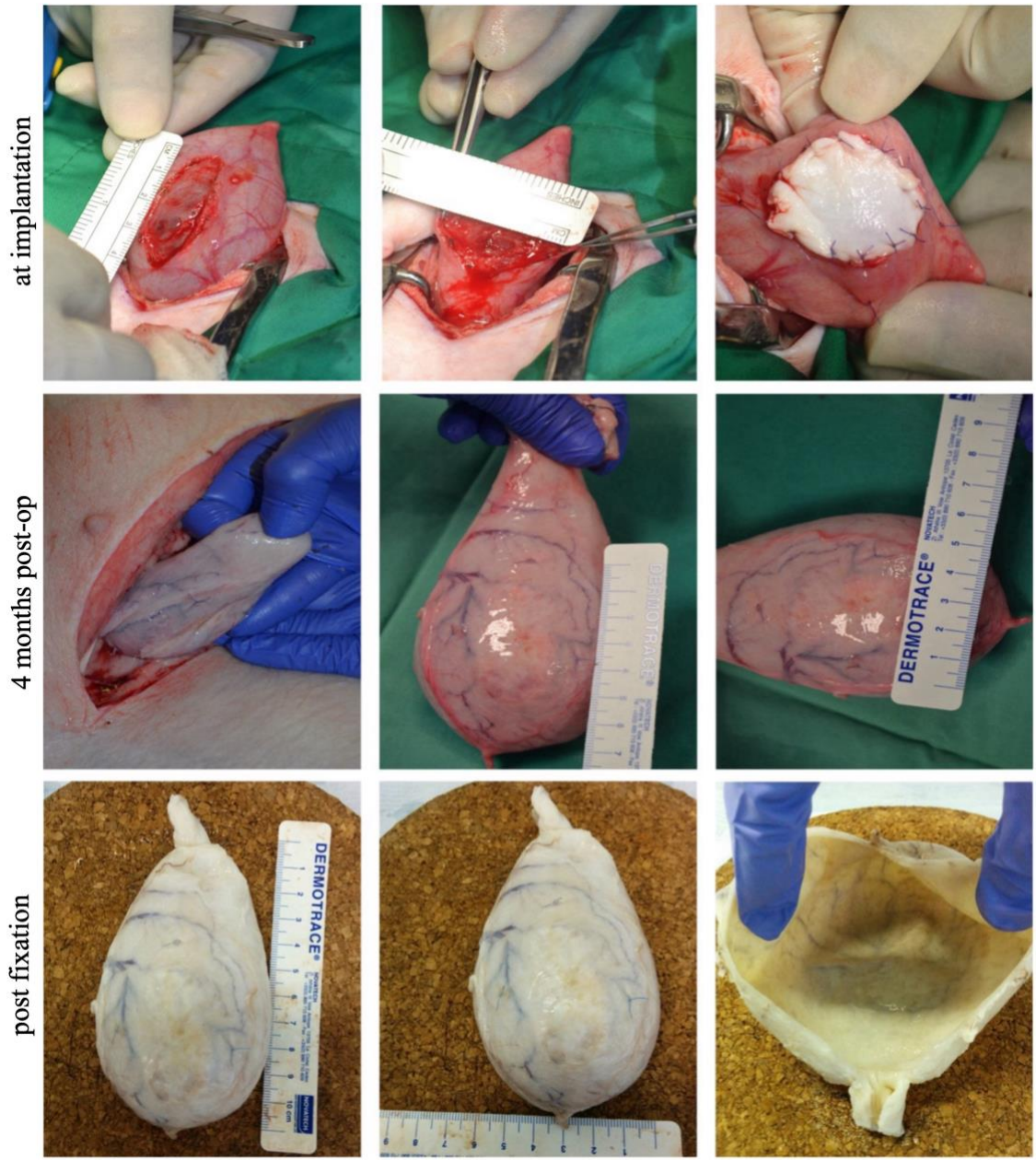

Figure 5.13 Case Study #766 at surgery , at harvest 4-months post-implantation, and macroscopic appearances of the explant after fixation in formalin.

The dissolvable sutures were no longer present and the marker sutures (non-absorbable material) were still in situ. At the time of the cystectomy, there was no evidence of adhesions, fibrosis or scarring. No PABM graft was clearly visible, with no defined separation noticeable between the graft site and the surrounding tissue. However, a central slightly discoloured area was noted after fixation, with no discontinuity between the surrounding tissues. Macroscopic intact appearances of the internal aspect of the auto-augmented area, site of PABM implant are also shown.

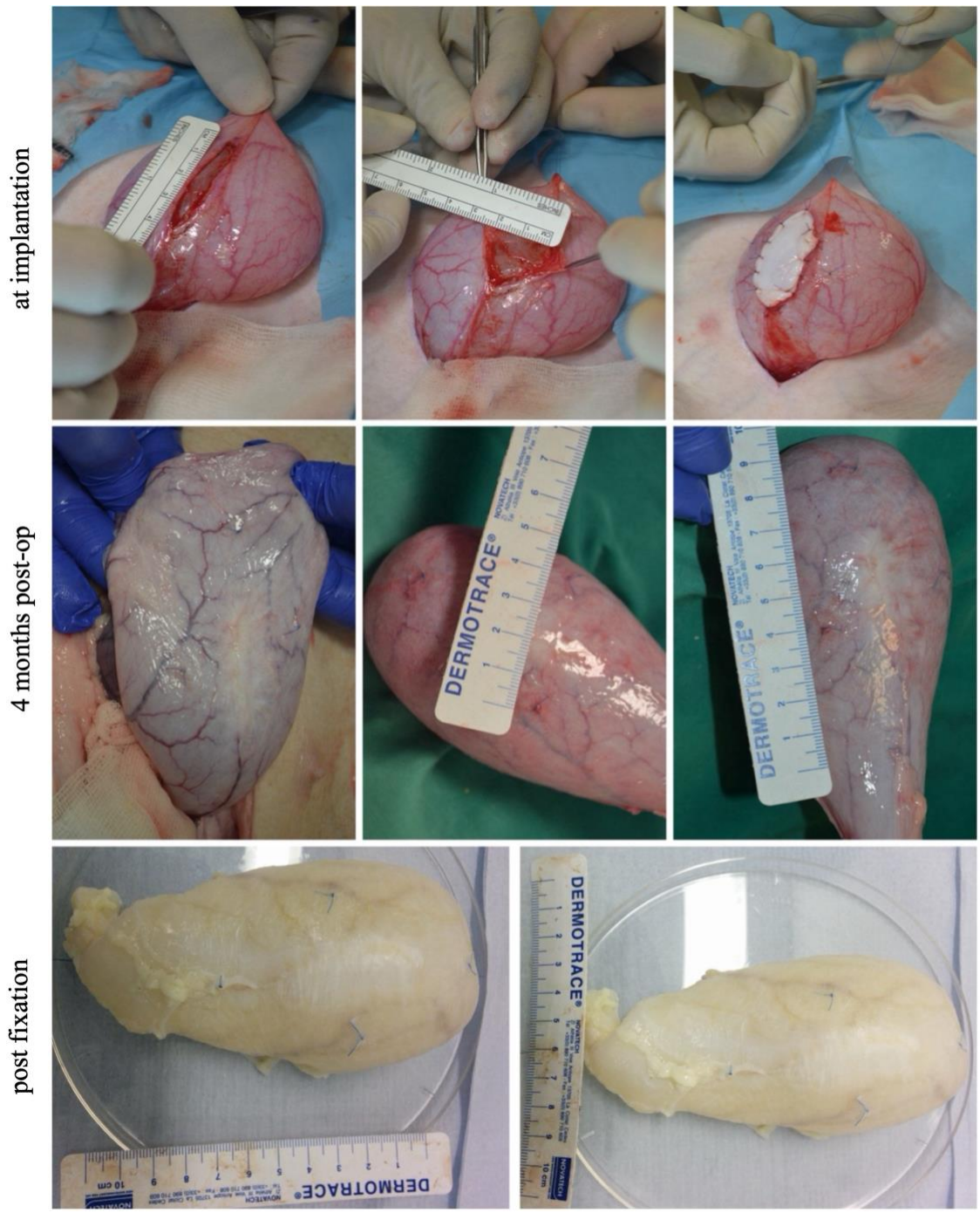

Figure 5.14 Correlation of the macroscopic appearances of the urinary bladder in case study #777 at surgery, at harvest and after fixation.

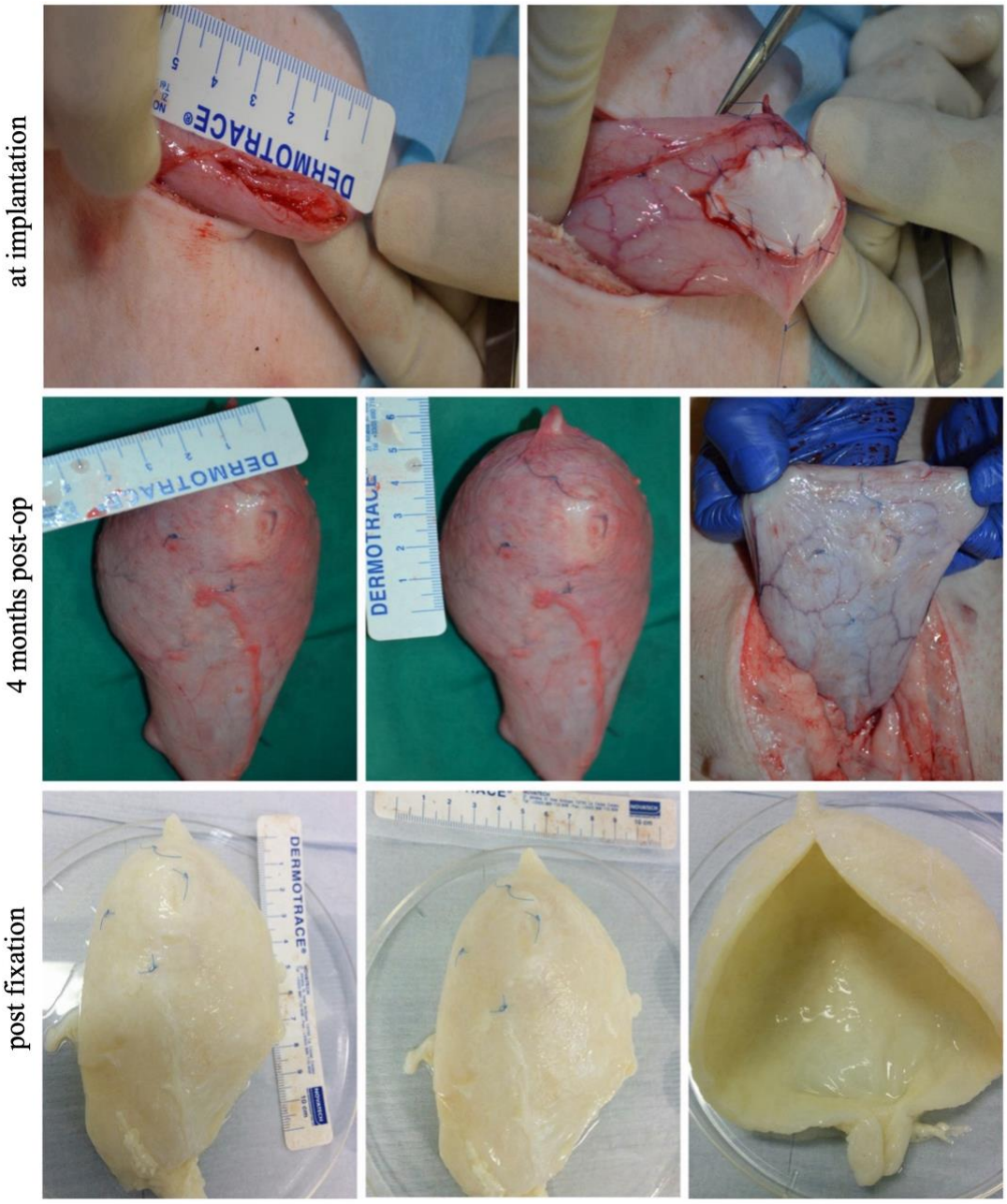

Figure 5.15 Correlation for case study #799 at surgery, at harvest and after fixation.

Macroscopic appearances of the area between non-absorbable sutures suggested a potential movement of the core area of the implanted biomatrix, surrounded by an otherwise healthy-looking bladder tissue.

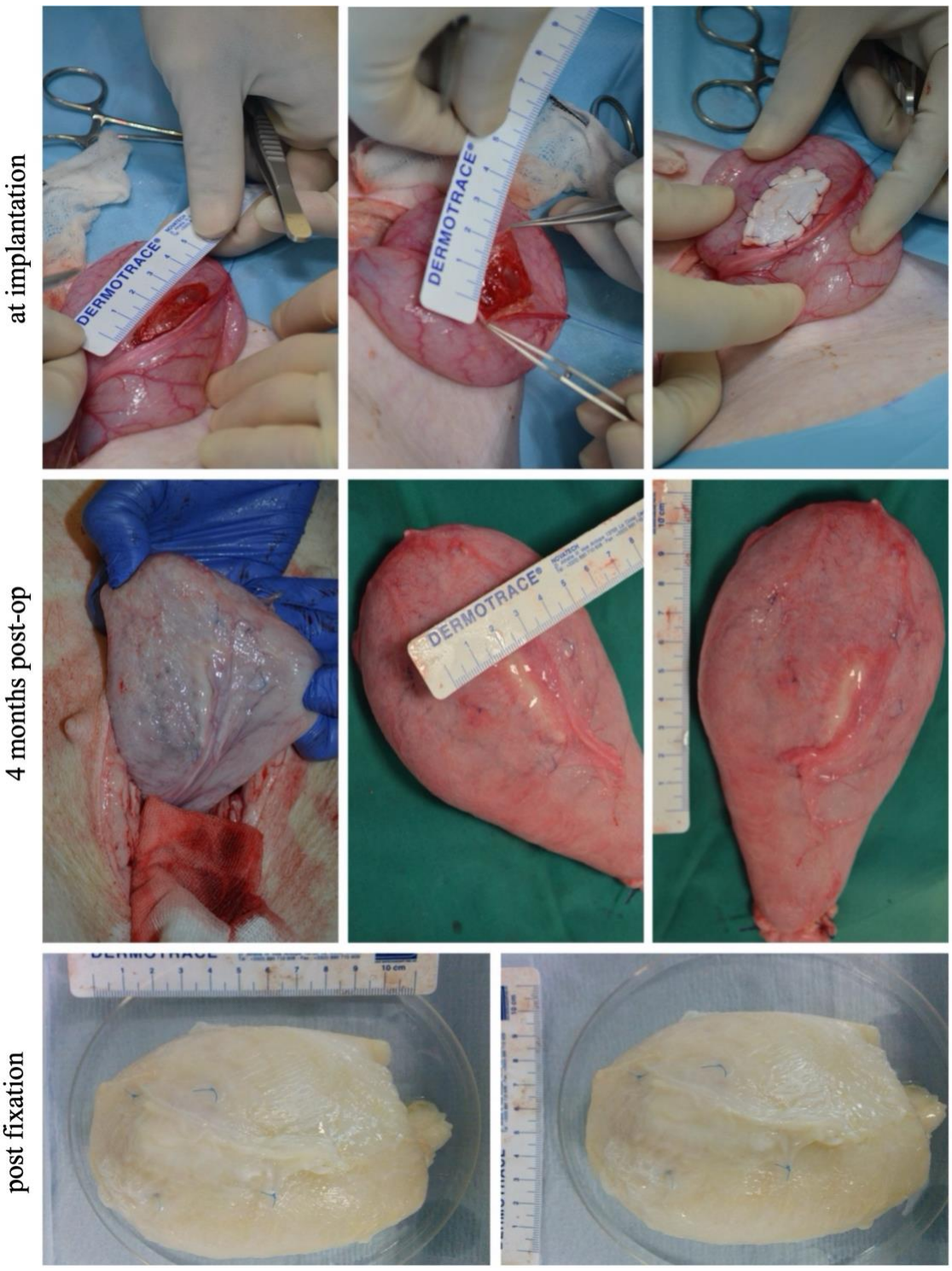

Figure 5.16 Correlation of the macroscopic findings at surgery, at harvest and after fixation for case study #803.

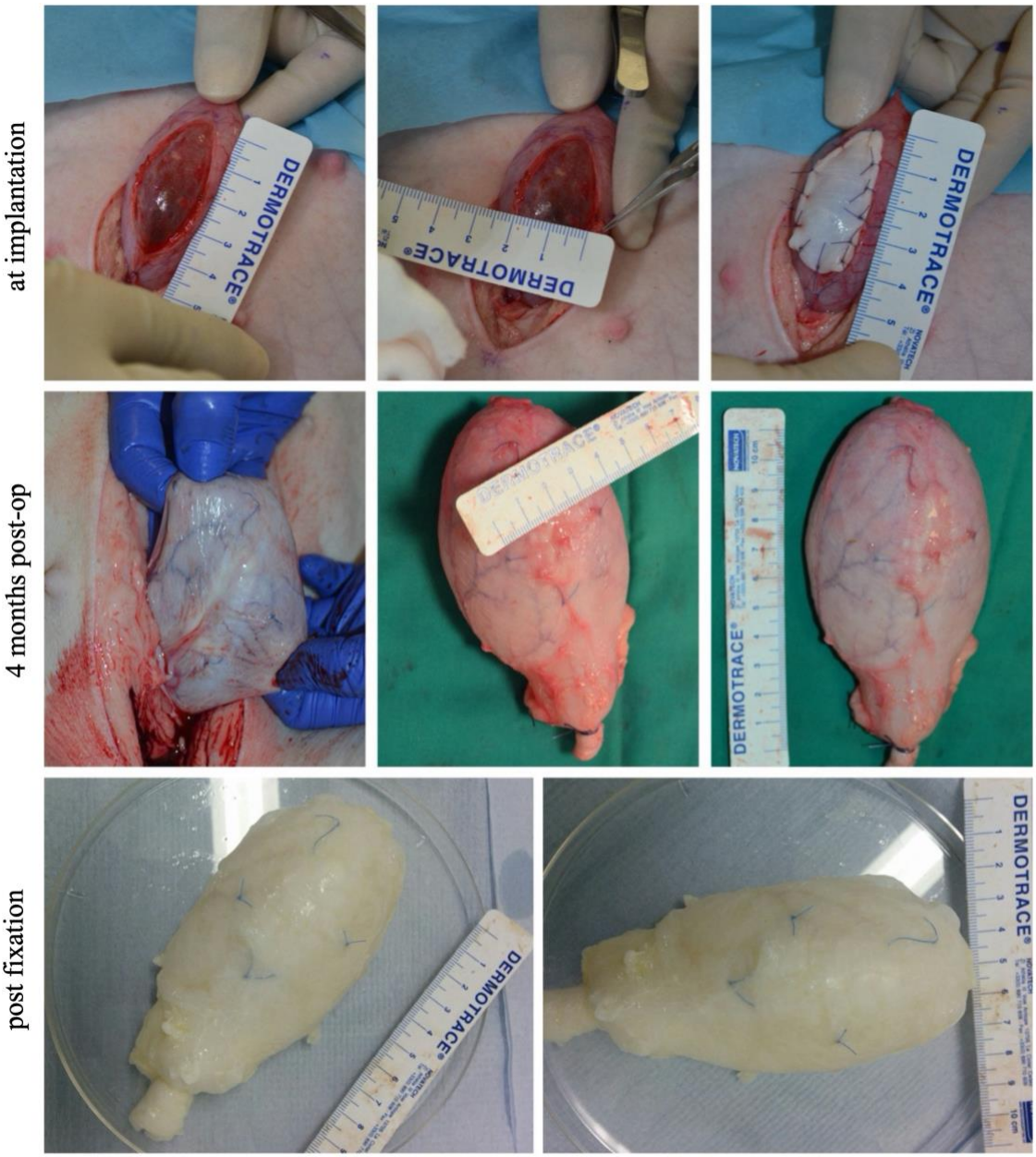

Figure 5.17 Macroscopic appearances of the urinary bladder in case study #822 at surgery, at harvest and after fixation.

5.3.3 Histology and immunohistochemistry

The area site of bladder auto-augmentation and biomaterial implantation in the five animals who completed a 4-month follow-up, was identifiable using a combination of H&E staining and immunohistochemistry. Sections of PABM alone from the patches used for the surgery were evaluated using same staining and immunolabelling. No cells were detected in sections of PABM alone on the H&E and Hoechst 33258 staining. Collagen bundles were however identified (Figure 5.18). The findings from H&E and immunohistochemistry were evaluated in comparison to those obtained in the control tissue (Figure 5.19). Guided by the applied dissection scheme (Figure 5.12), it was possible to identify in the sub-segment IA1 elements of tissue regeneration (recellularised PABM area) (Figures 5.20, 5.22 - 5.25). The sub-segment IA1 was therefore chosen for further analysis and tissue characterisation of all five bladders via IHC.

Evidence of a good recellularisation pattern within the implanted PABM was noted in sections from all 5 bladders analysed via H&E, Hoechst 33258 stain and αSMA labelling. Bladder specimens histologically showed no signs of acute or chronic inflammation. No signs of fragmentation or condensation at the nuclear level were noted on the H&E samples, suggesting no evidence of apoptosis. The αSMA localisation was found related to the regenerating bladder wall and the vasculature, revealing a good pattern of neo-angiogenesis (Figures 5.26-5.31). A continuous urothelium lined both the native bladder tissue and the auto-augmented regions were PABM was applied on the exposed mucosa (Figures 5.20-5.26 and Figure 5.29). The urothelium was found not damaged, with UP3a and CK20.8 appropriately expressed on the apical surface of superficial urothelial cells (Figure 5.32). In some small areas a superficial cell loss was noted, probably as a result of processing of the tissues. The urothelium also characteristically appeared non-quiescent, with consistent expression of ki-67 across samples (Figure 5.32). No clear demarcation between the native tissue and the implanted biomaterial area was noted, but a transition zone (TZ) was identified as a continuity between native-looking tissue and the regenerating area. No evidence of fibrotic capsule or adverse effects were noted at this interface level. The presence of NFP positive cells were detected at the interface between the native tissue and the implanted biomaterial a swell as within the implanted PABM area. Such findings revealed not just the presence of de novo innervation but confirmed the presence of a healthy regenerative environment (Figure 5.33). In the process of assessing the nature of the cells present at the level of the implanted PABM area, CD163 immunolabeling was performed. This revealed the presence of a more pro-regenerative pattern of cells of the monocytes-macrophages lineage (M2 macrophages phenotype) (Figures 5.26-5.31).

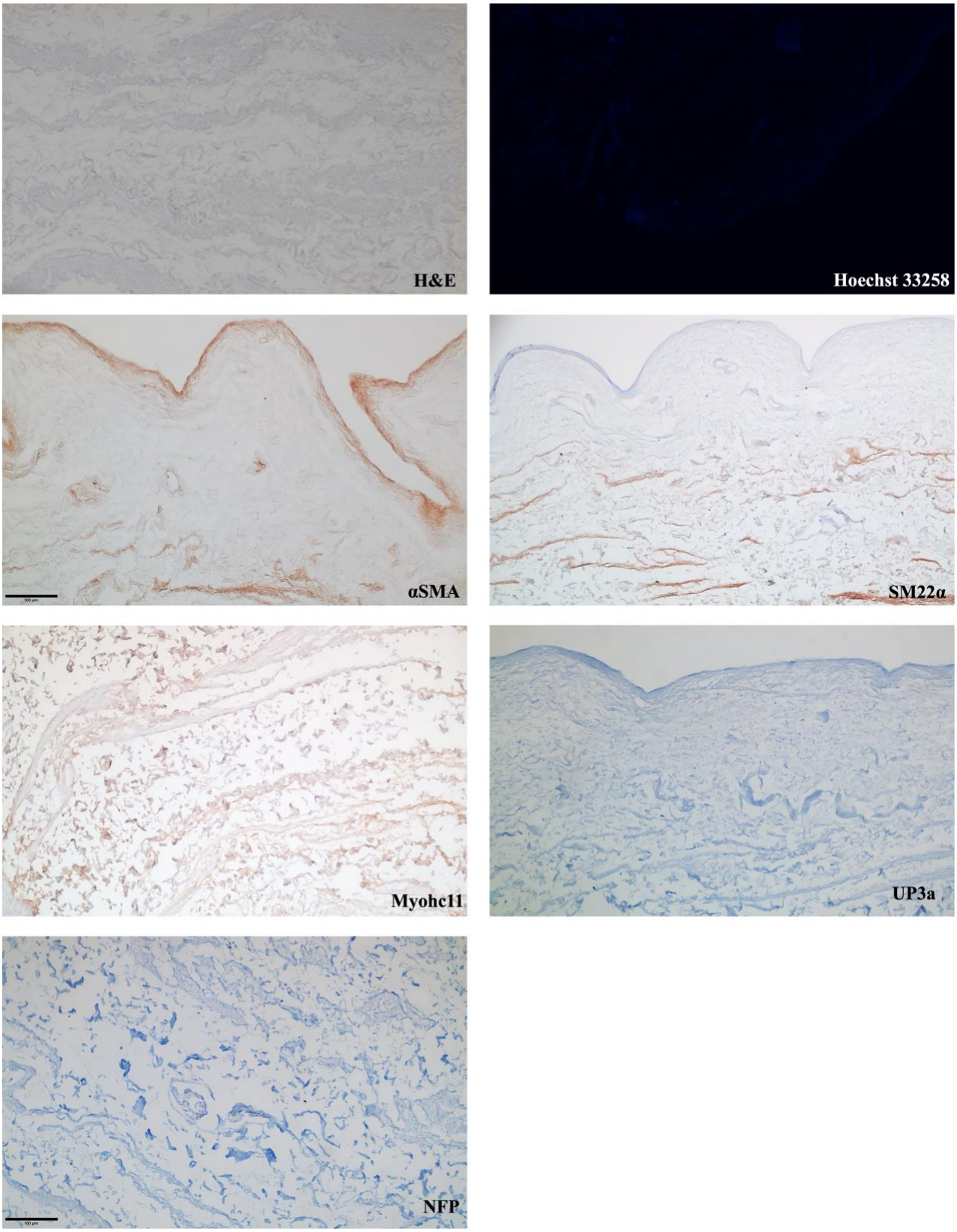

Figure 5.18 H&E staining, Hoechst 33258 staining and immunolabelling of the PABM.

Images showing no nuclear staining detected in the decellularised tissue with retention of the ECM (collagen bundles and structural proteins. (Scale bar: 100 µm).

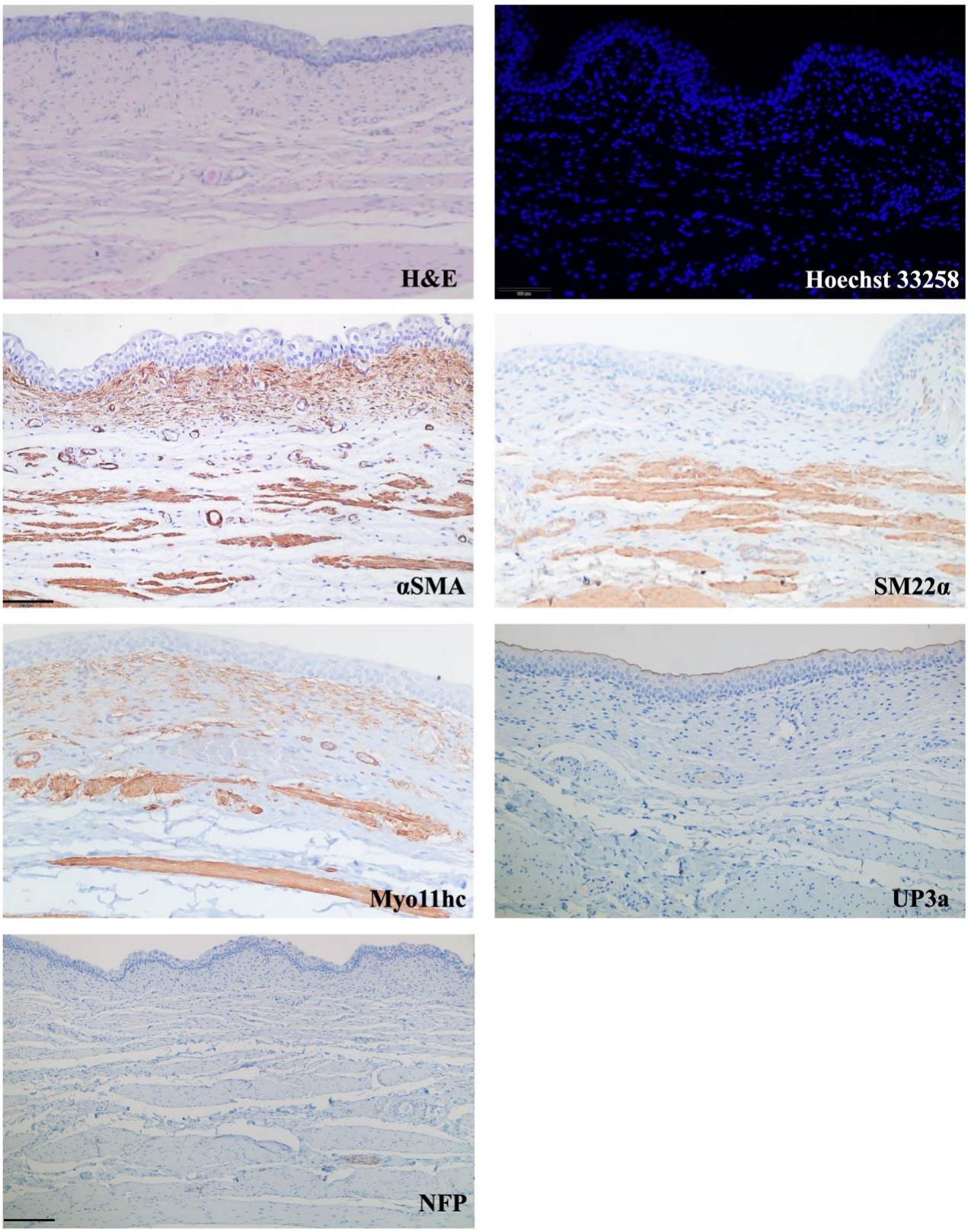

Figure 5.19 Microscopic appearances of a normal urinary bladder tissue.

Micrographs showing H&E staining, Hoechst 33258 staining and immunostaining of positive control samples is here provided (Scale bar: 100 µm. Scale bar: 200 µm in NFP).

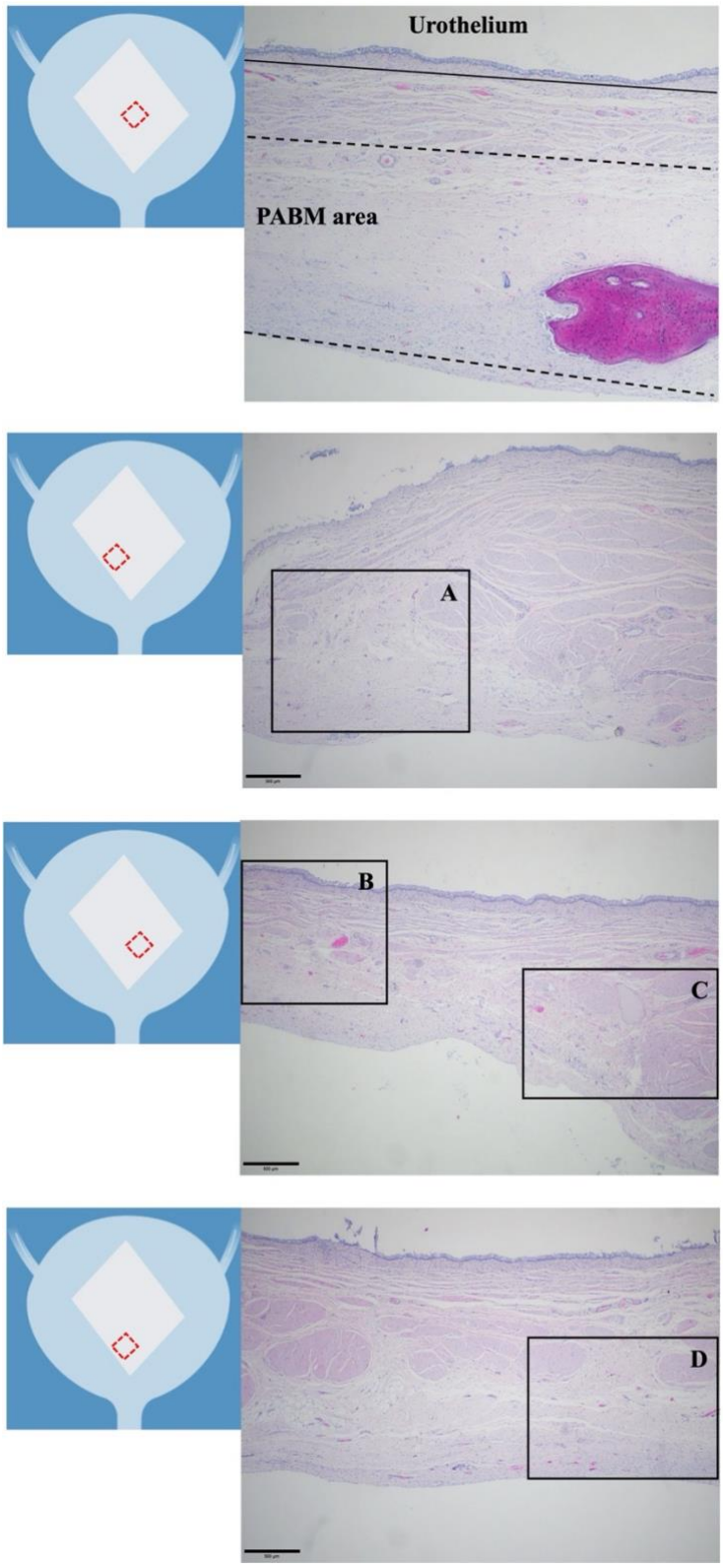

Figure 5.20 Histological overview (haematoxylin and eosin staining) in case study #766.

The urothelium, a transition zone and the regenerated PABM area are shown. The transition zone (TZ) was defined as the interface between normal-looking bladder tissue and tissue with recellularisation features. (Scale bar: 500 μm). ROI A, B, C, D are illustrated at a higher magnification in below Figure 5.21.

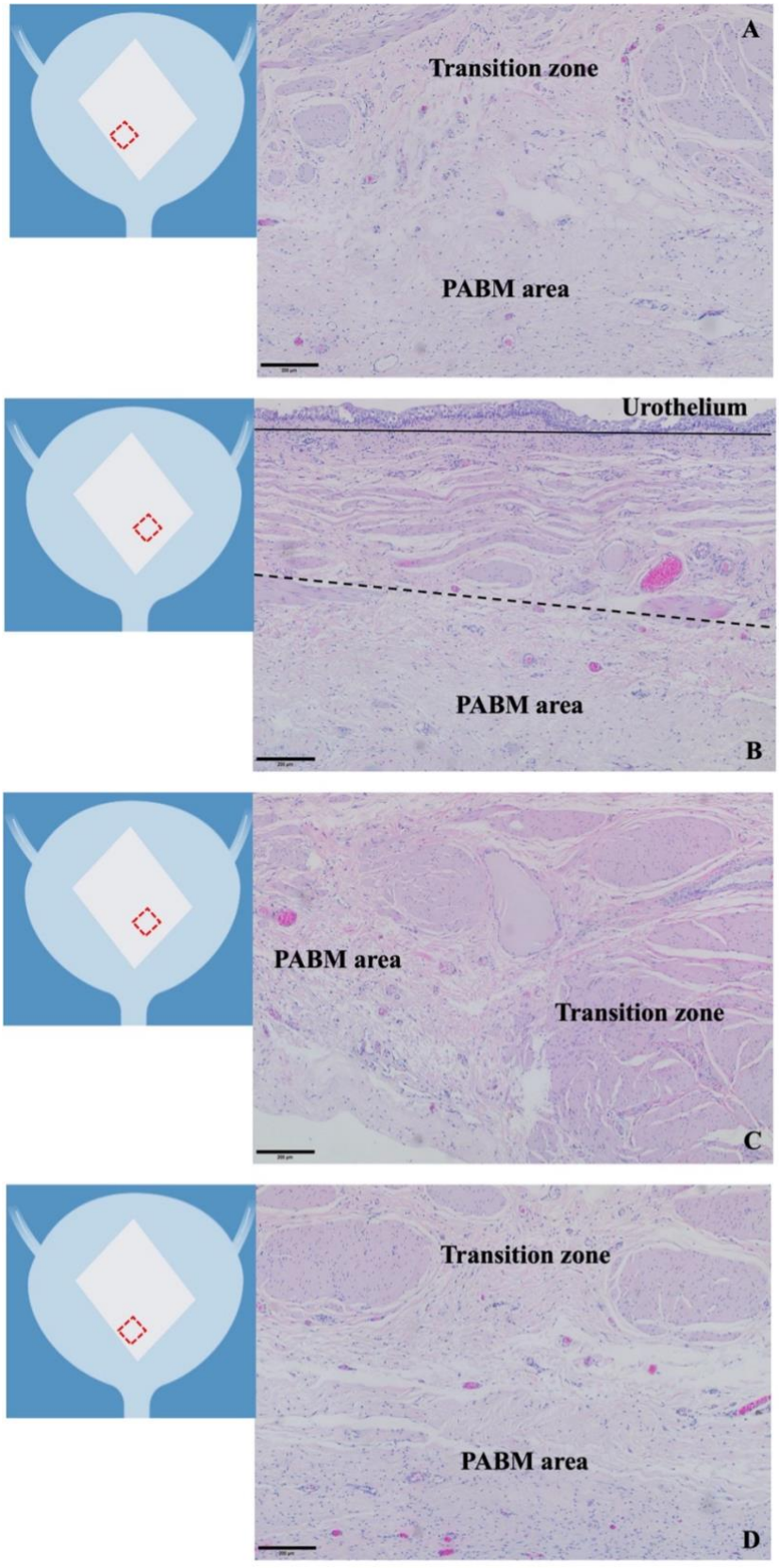

Figure 5.21 Histological overview of ROIs A, B, C, D in case study #766.

(Scale bar: 200 μm).

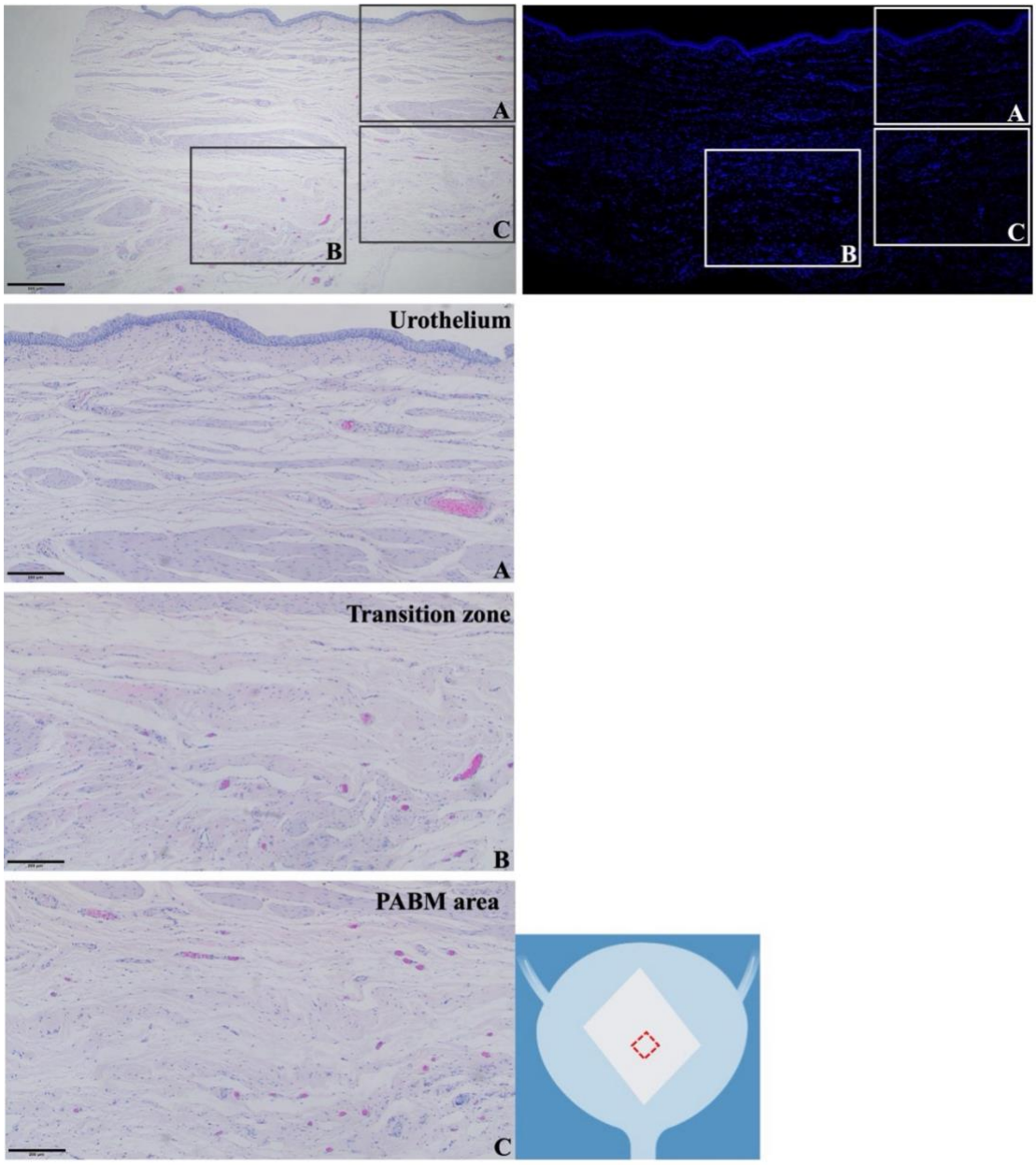

Figure 5.22 Representative histological overview in case study #777.

Micrographs showing H&E and Hoechst 33258 staining. (Scale bar: 500 μm and 200 μm).

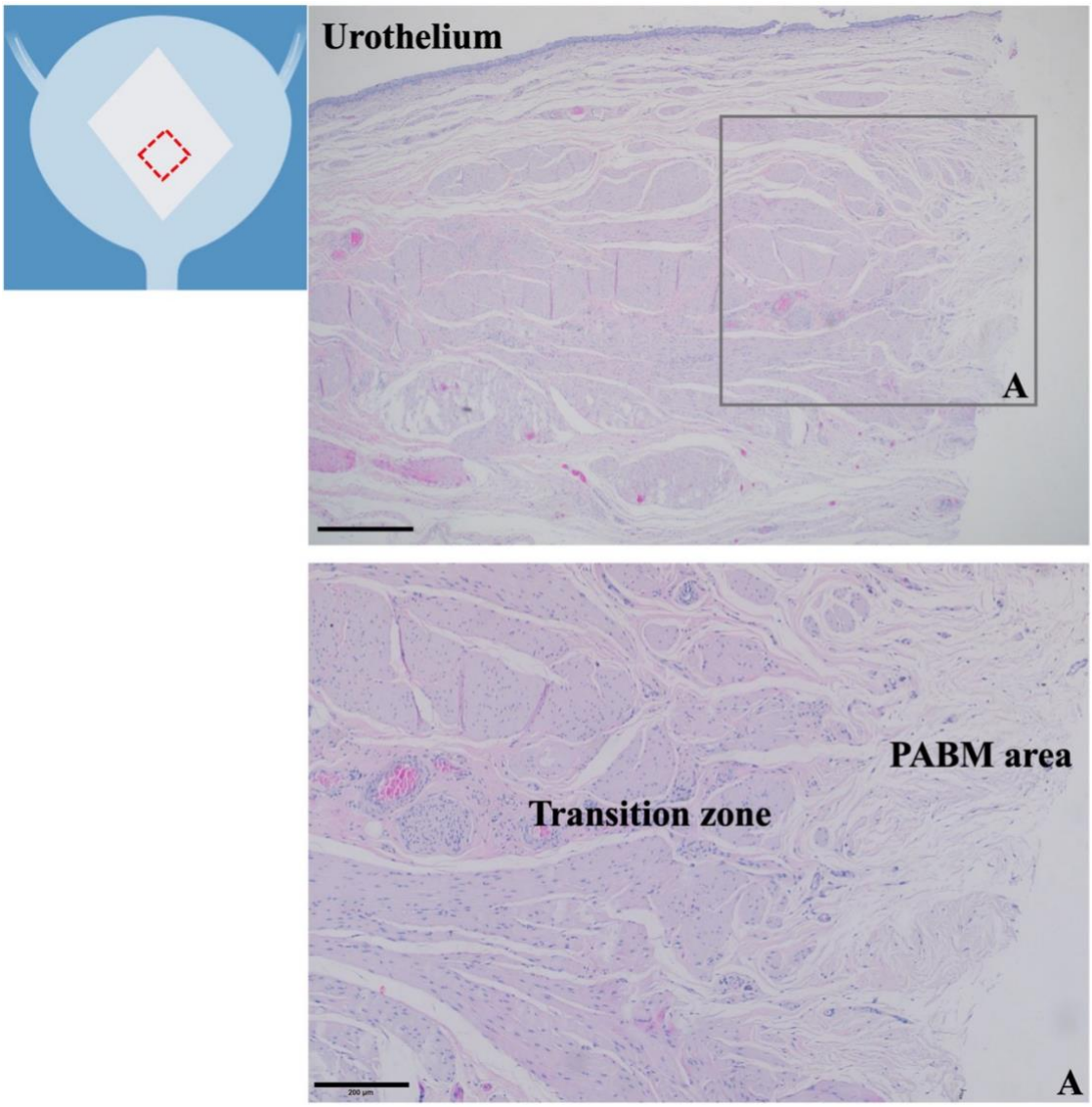

Figure 5.23 Representative histological overview in case study #799.

Micrographs showing haematoxylin and eosin staining at 4 months from surgery. (Scale bar: 500 μm and 200 μm).

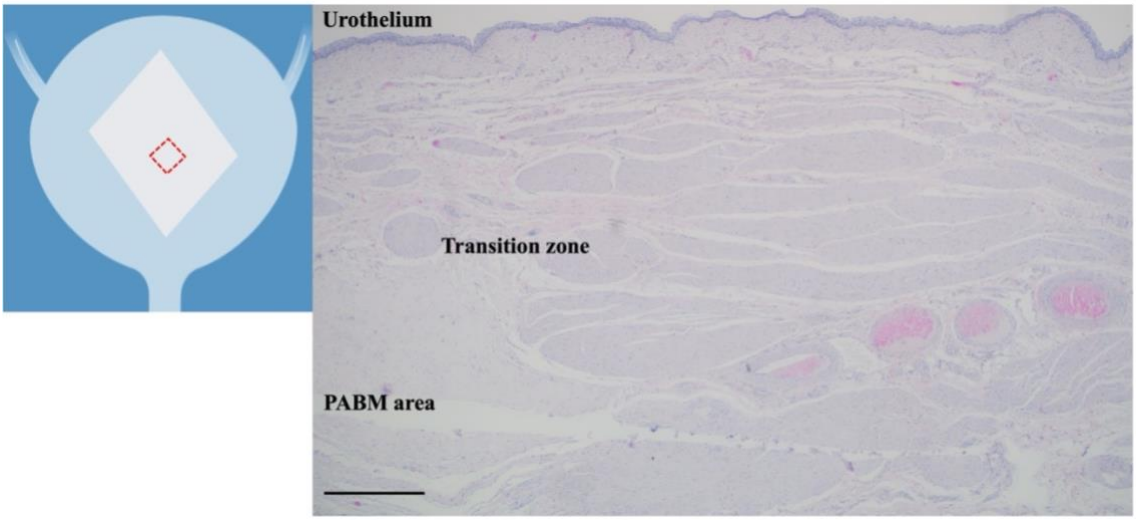

Figure 5.24 Representative histological overview in case study #803.

Micrograph showing haematoxylin and eosin staining after 4 months from surgery. (Scale bar: 500 μm).

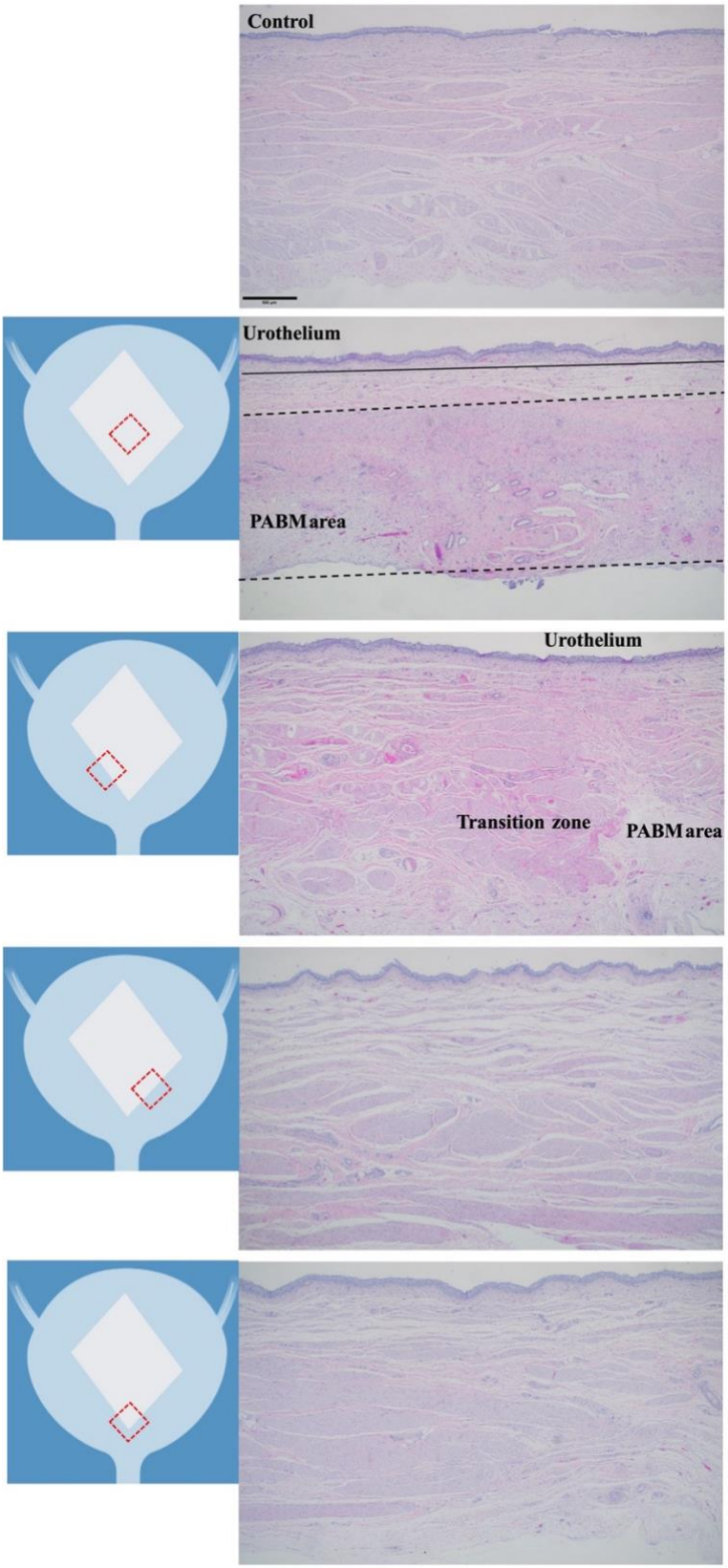

Figure 5.25 Representative histological overview in case study #822.

Micrographs showing haematoxylin and eosin staining at 4 months from surgery. (Scale bar 500 μm).

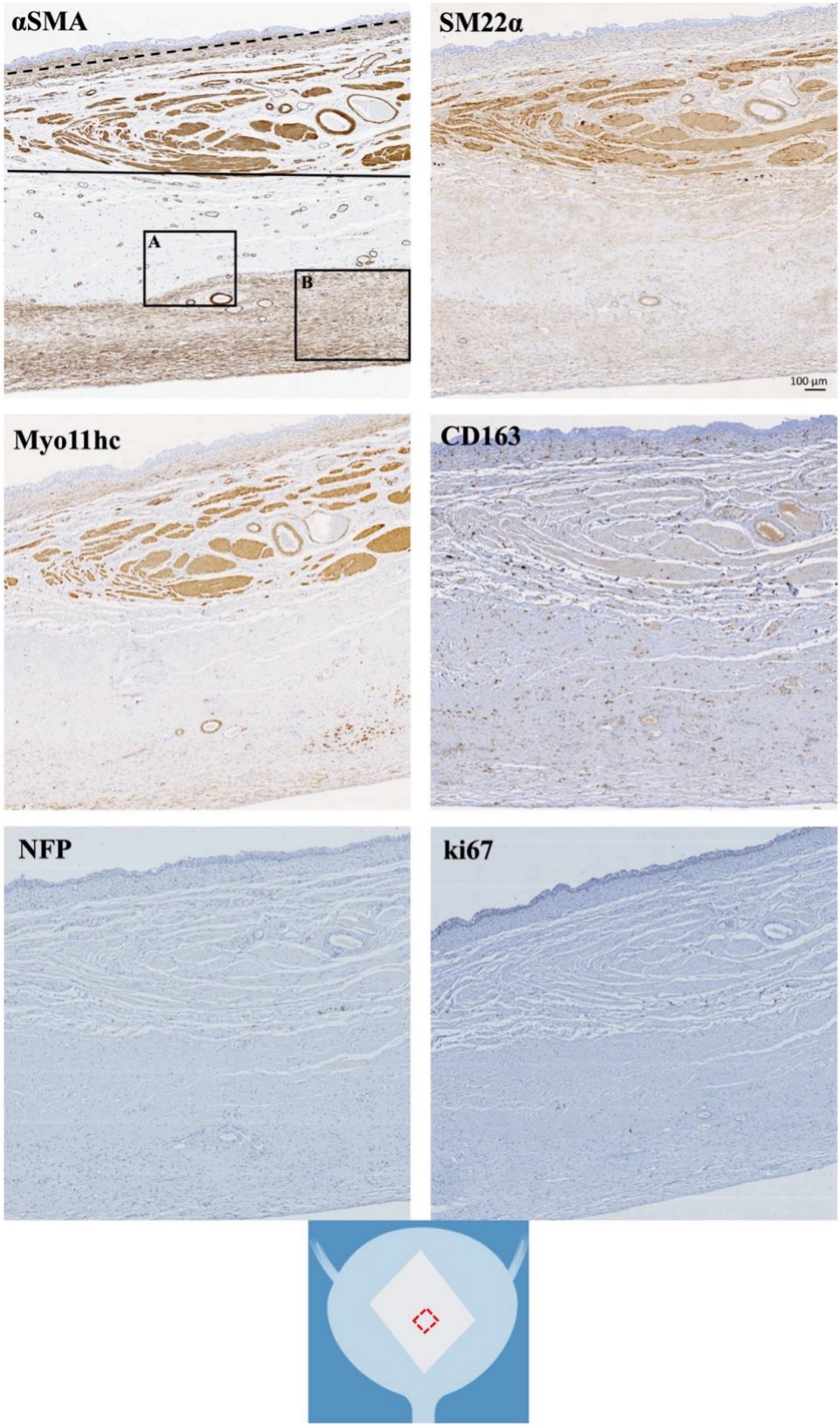

Figure 5.26 IHC findings of the sub-segment IA1 in case study #766.

(Scale bar: 100 µm). The highlighted ROIs A and B are presented in Figures 5.27 and 5.28.

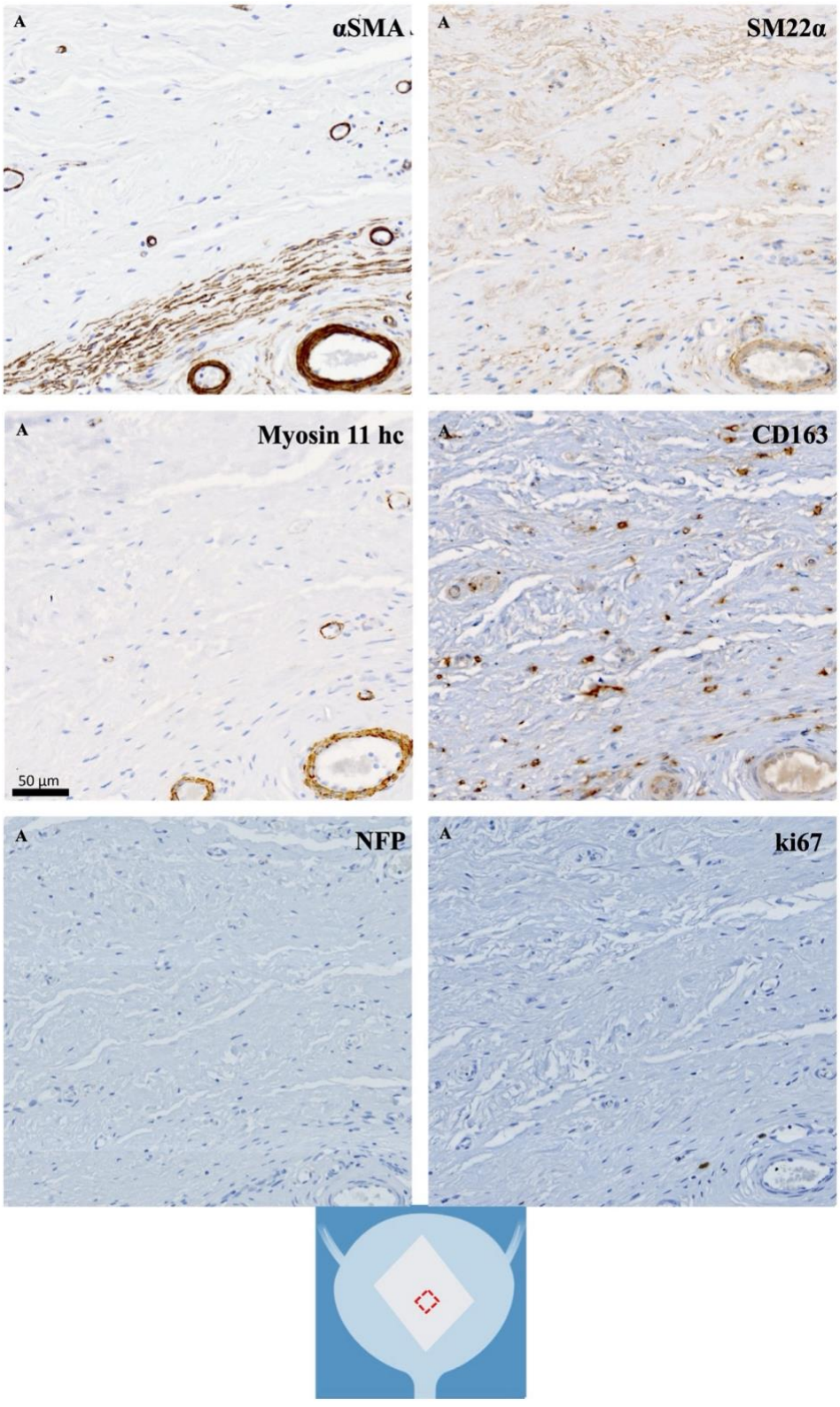

Figure 5.27 Immunohistochemical findings in the ROI A in case study #766.

Within the regenerated site of the acellular biomaterial implantation, the presence of blood vessels and muscular structures (aSMA, SM22, Myo11hc), M2 macrophages (CD163), sparse neuronal cells (NFP) and proliferating ki67+ cells were identified. (Scale bar: 50 µm).

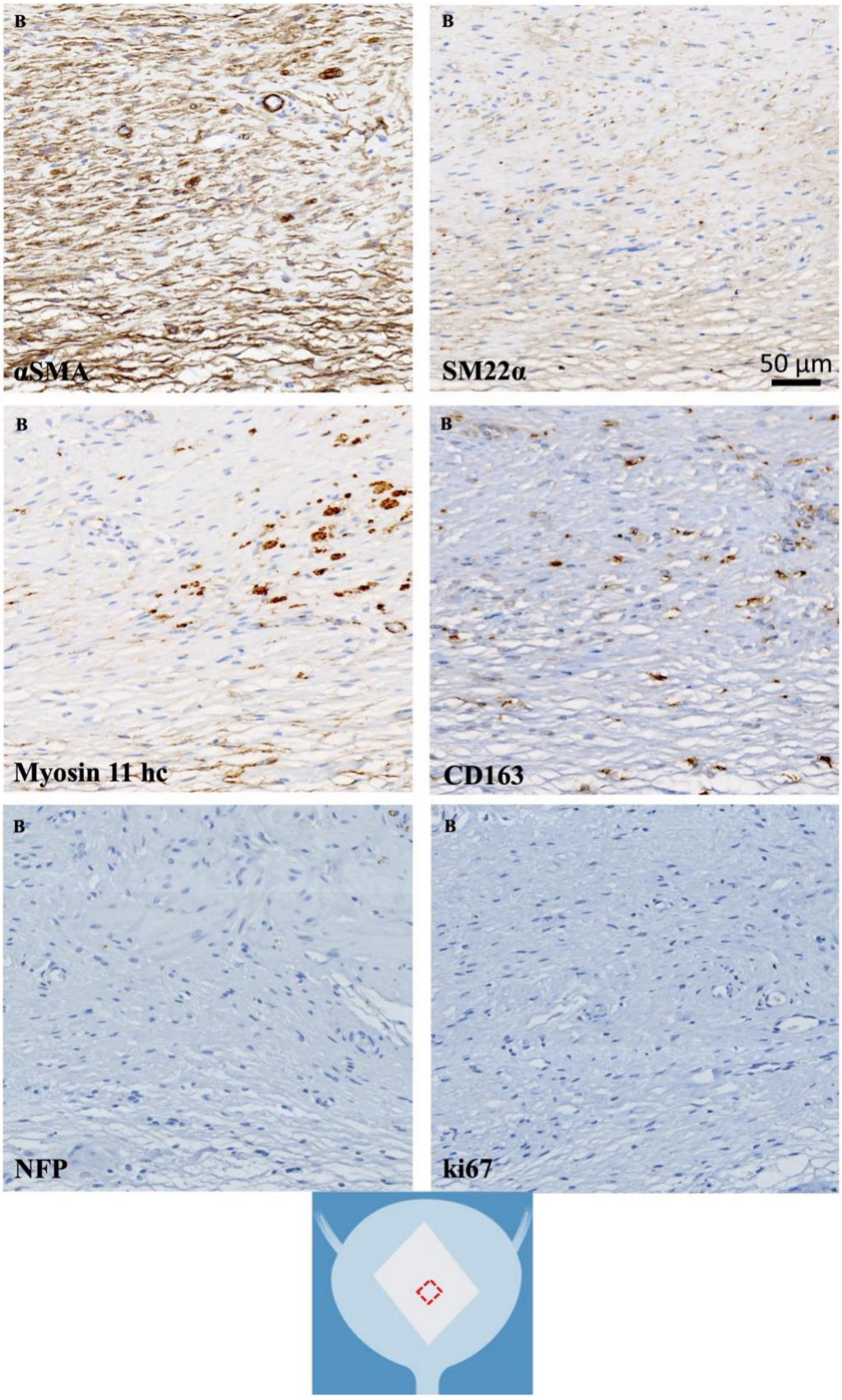

Figure 5.28 Representative immunohistochemical overview at higher magnification of the ROI B in case study #766.

(Scale bar 50 µm).

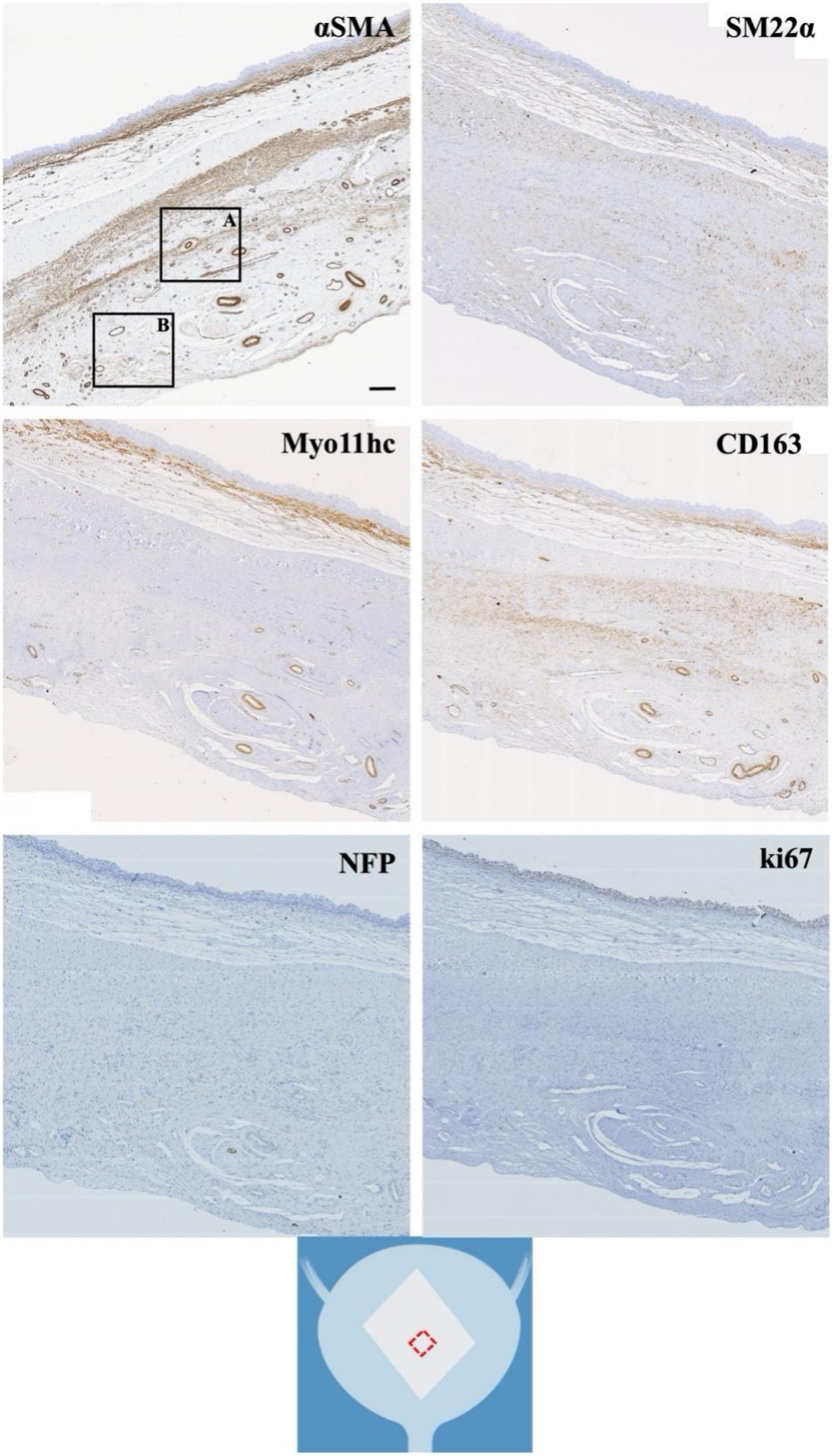

Figure 5.29 IHC findings of the regenerating PABM area in case study #822.

(Scale bar: 100 μm). The highlighted ROIs A and B are presented at a higher magnification in Figures 5.30-5.31.

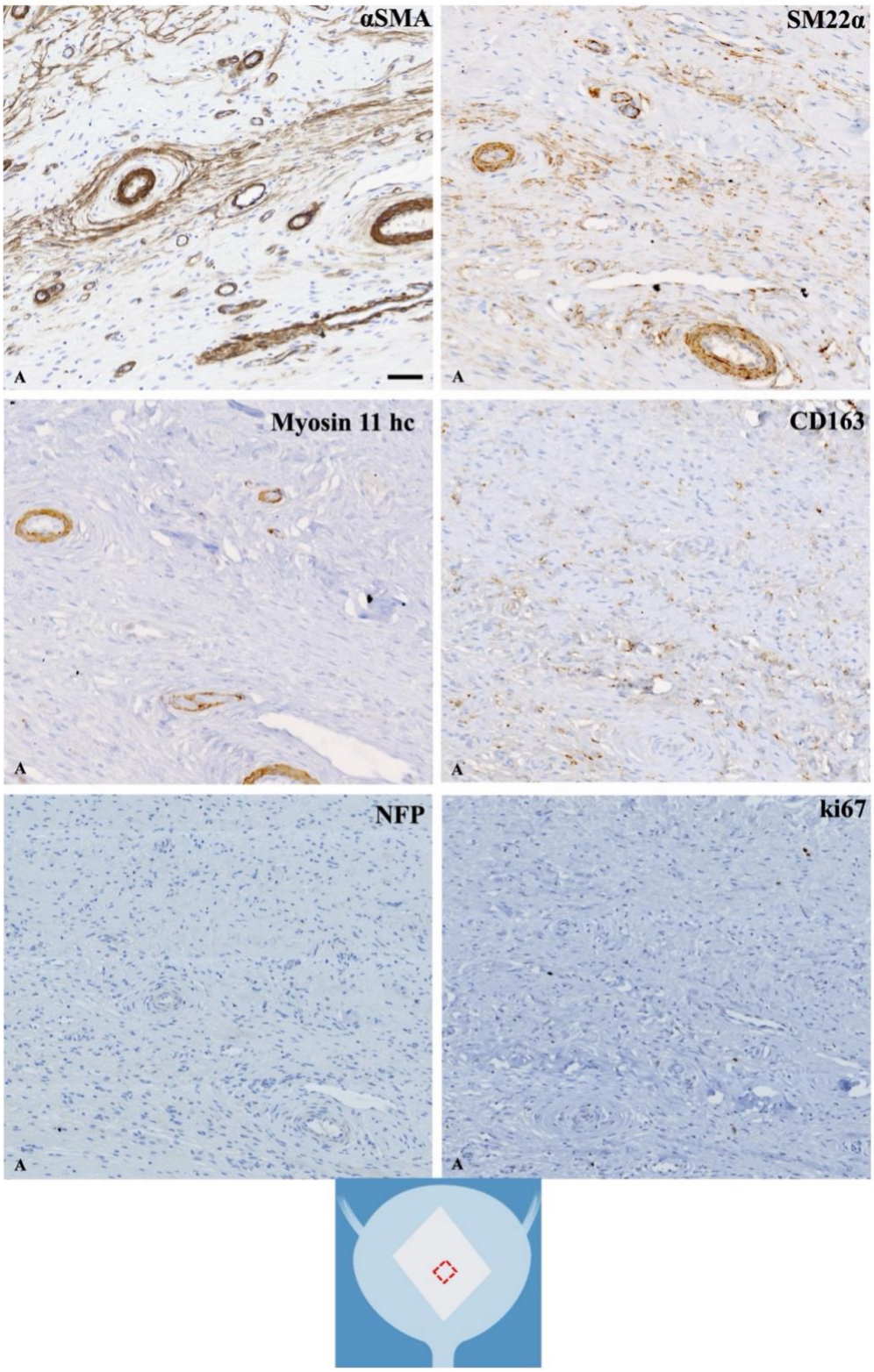

Figure 5.30 Representative immunohistochemical overview of the ROI A in case study #822.

Micrographs show the presence of vascular and muscular structures (aSMA, SM22, Myo11hc), M2 macrophages (CD163), neuronal cells (NFP) and proliferative cells (ki67) at the implanted PABM area. (Scale Bar 50 µm).

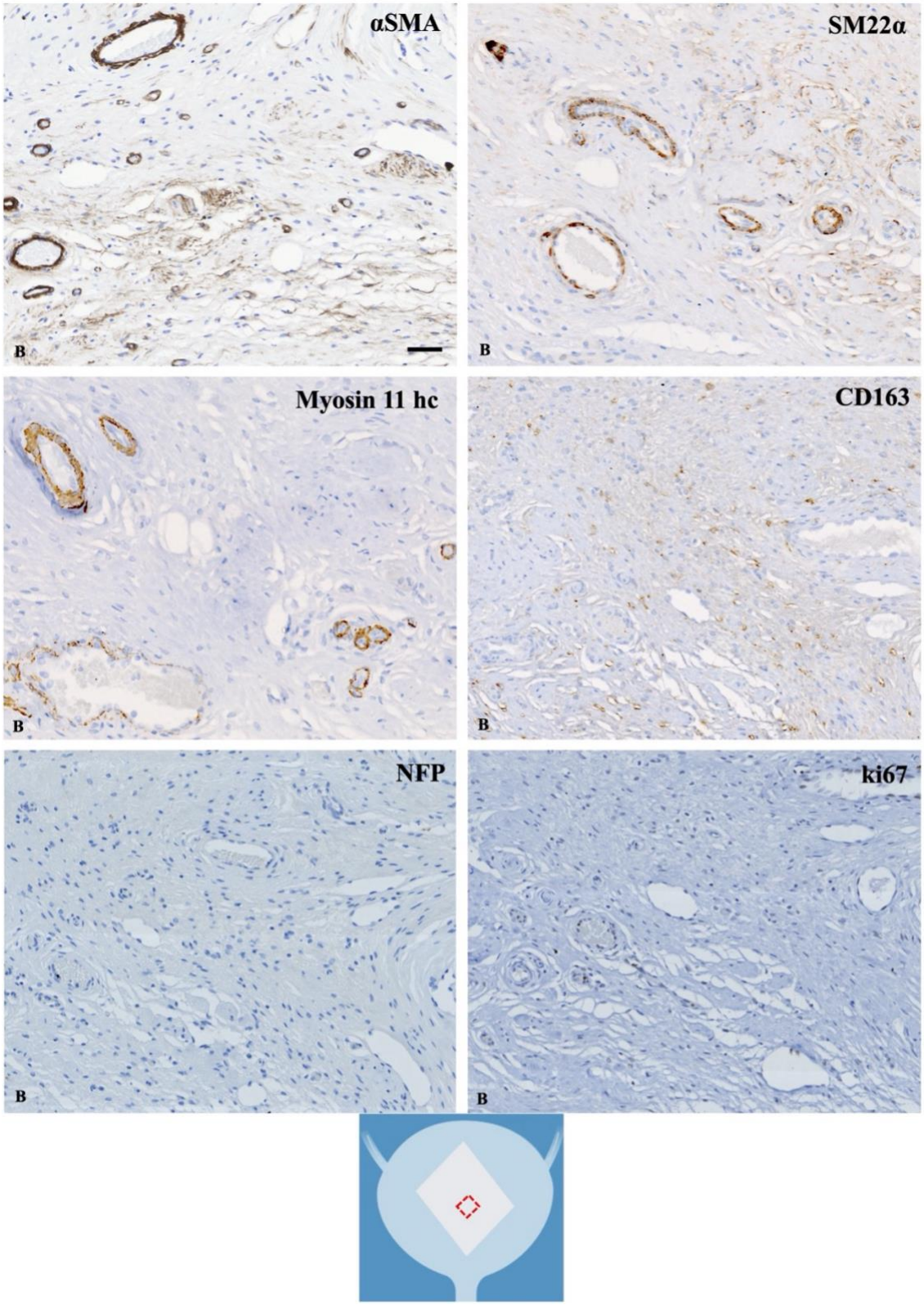

Figure 5.31 Representative immunohistochemical overview of the ROI B in case study #822.

Micrographs illustrate tissue characterisation. (Scale bar: 50 µm).

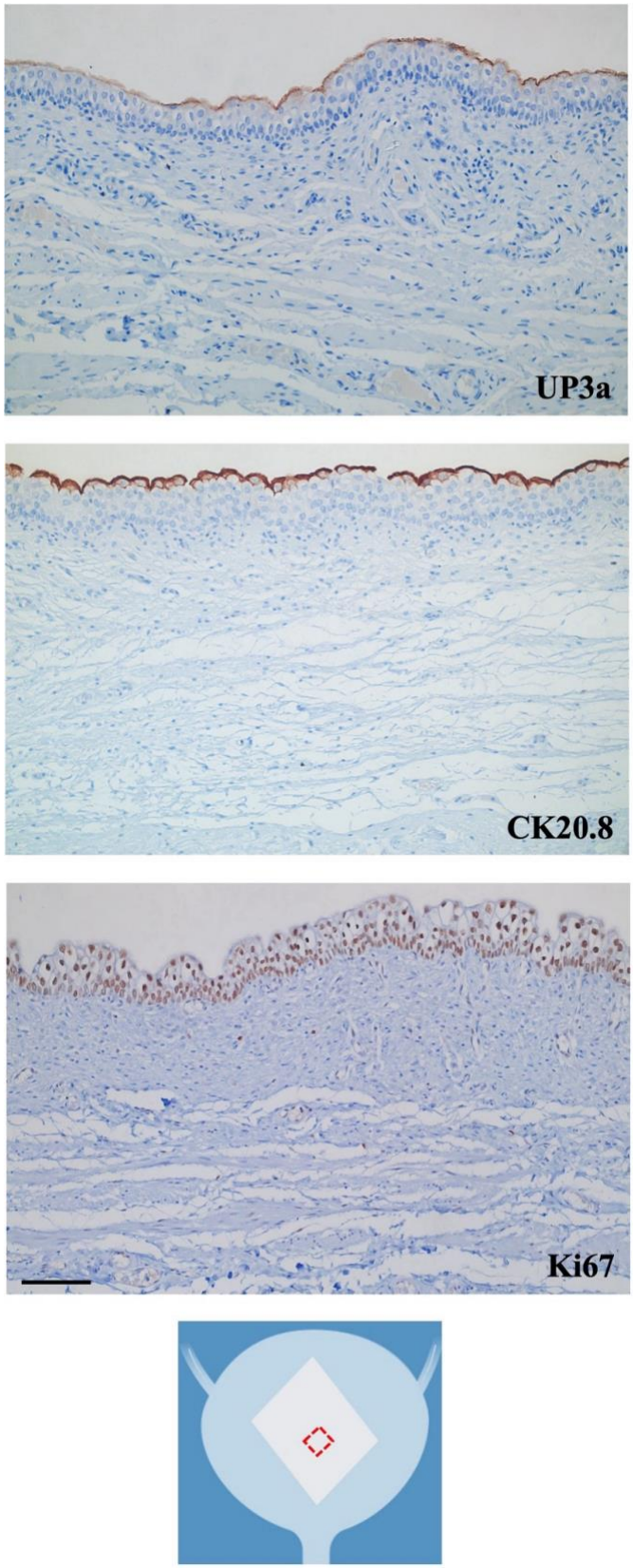

Figure 5.32 Urothelium at the implant site after 4 months from surgery.

Micrographs showing the presence of a normal intact, differentiated, proliferating urothelium in correspondence to the regenerated PABM area (Scale bar 100 μm).

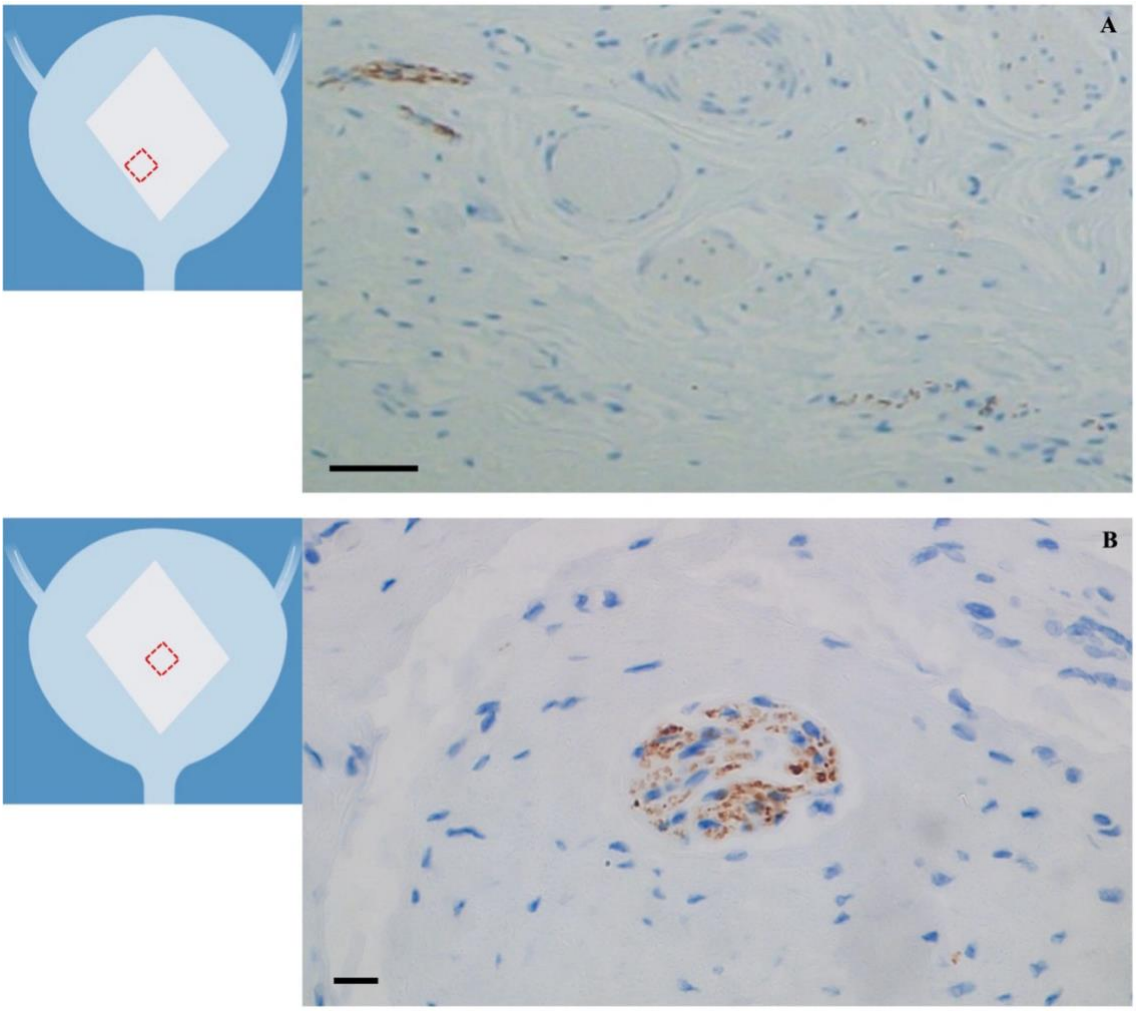

Figure 5.33 De novo neurogenesis.

Figure illustrating the findings of NFP + cells at the level of the regenerated PABM area (B; scale bar: 20µm) and at the level of the TZ (A; scale bar: 50µm). The presence, location and organisation of such nerve structures informed on a healthy regenerative micro-environment able to promote de novo neurogenesis at the biomaterial site.

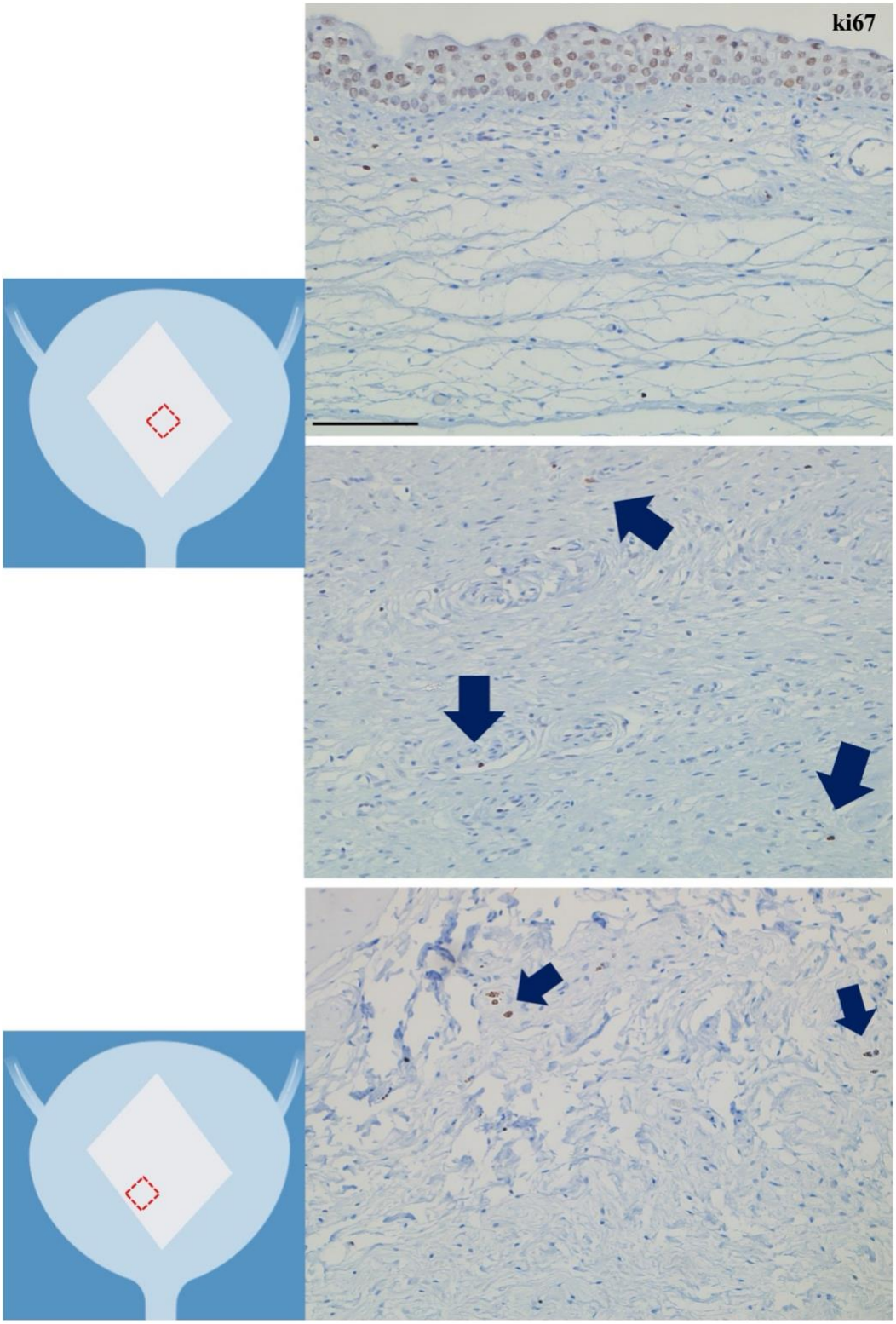

Figure 5.34 Proliferative ki67+ cells.

Micrographs showing findings of proliferative ki67+ cells at the level of the PABM area, the urothelium above it, and at interface between the implanted biomaterial and the native-looking tissue (TZ). (Scale bar: 100μm).

5.3.3.1 Case study #102

On day 16 post-surgery, the animal was noted to have a swollen area in correspondence of the surgical wound, while looking otherwise in good general conditions. As explained in Section 5.3.2, in consideration of the principles of research animal welfare, decision was made to proceed with a surgical exploration. At the evaluation under anaesthesia, the wound was seen to be well healed. A non-reducible swollen area (15 cm diameter), with a dark-blue pointed spot in the centre of a red inflamed area (2 cm of diameter) was noted in correspondence of the previous surgical incision (Figure 5.35A). The inner red area was not present the day before the surgery. Skin incision was performed in correspondence of the pointed area along the previous surgical incision, with immediate observation of faecaloid fluid material coming out from the incision site, suggesting a bowel perforation (Figure 5.35B). The skin incision was enlarged, and evidence of a subcutaneous/supra-fascial sac (depth = 12 cm ca) fully filled of bowel content was found. Accurate and generous cleaning with gauzes and normal saline was provided. Evidence of spots of necrotic tissue was noted on the internal aspect of the sac (Figure 5.35C). On the deeper site of the cavity the previously applied mesh was noted with the relative stiches still in situ (Figure 5.35D). Gentle and cautious dissection was performed around the cavity, which appeared to have very thick and inflamed walls, with a little almost perforated part in correspondence of the dark-blue pointed spot previously noted and described. No abdominal hernia was identified.

Decision was taken by the consultant vet and the surgeon/author to proceed with Schedule 1. Such decision was guided by the indications and limitations provided by the Project Licence that allowed animals to undergo only one further surgery and only to repair an incisional hernia (minor procedure).

The peritoneal cavity was then opened, and the presence of multiple bowel adhesions was noted. A small bowel loop was found to craniocaudally cross the abdomen and to be attached with several adhesion bands to the internal aspect of the abdominal wall, creating a fistula with the previously observed neo-cavity. The urinary bladder, site of the primary surgery, was found healthy, not involved in the diseased process and completely free from adhesions. The auto-augmentation site looked healthy, macroscopically completely healed, with no signs of adverse reactions. The absorbable stitches (5/0 Vicryl) put in place between the PABM and the bladder during the first surgery were still appreciable (Figure 5.35E-F).

After cautious dissection, excision en bloc of the bladder was performed. The specimen was briefly macroscopically examined before being placed in 10% formalin for fixation. The whole bladder was immersed in the fixative fluid. Interrupted 2/0 Vicryl sutures were applied to close the abdominal

wound. After cleaning, the carcass was disposed as per protocol. Pictures were taken alongside all the described steps of the surgery for documentation.

A different scheme of dissection (Figure 5.36) was applied to this case study compared with the method applied for the five pigs who completed the 4-month follow up.

Specimens from case study #102 were processed alongside all specimens that were obtained from the other five animals, and were used as an internal control to acquire potential significant information. This was performed in order to compare appearances at 1 and 4 months after implantation. Those data were evaluated and included even with the limitation of being related only to one animal.

A uniform urothelium was detected and a good pattern of cellularisation was noted in correspondence with the area site of biomaterial implantation. A transition zone was well identified at the interface between native-looking tissue and the implanted PABM, with no evidence of any adverse reaction or fibrotic capsule formation. An initial microscopic examination suggested a lower concentration of cells at the transition zone in comparison with specimens from the 4-month follow-up group. Such an interface resulted in more demarking and easier definition when microscopic appearances were compared to findings four months after surgery, where no clear demarcation was identifiable (Figure 5.37).

Via ki67 immunolabeling, it was possible to identify proliferative cells within the PABM area and the urothelium (Figure 5.38). Evidence of M2 pro-regenerative macrophages (CD163+ cells) was detected within the area where PABM was implanted and at the transition zone (Figure 5.39).

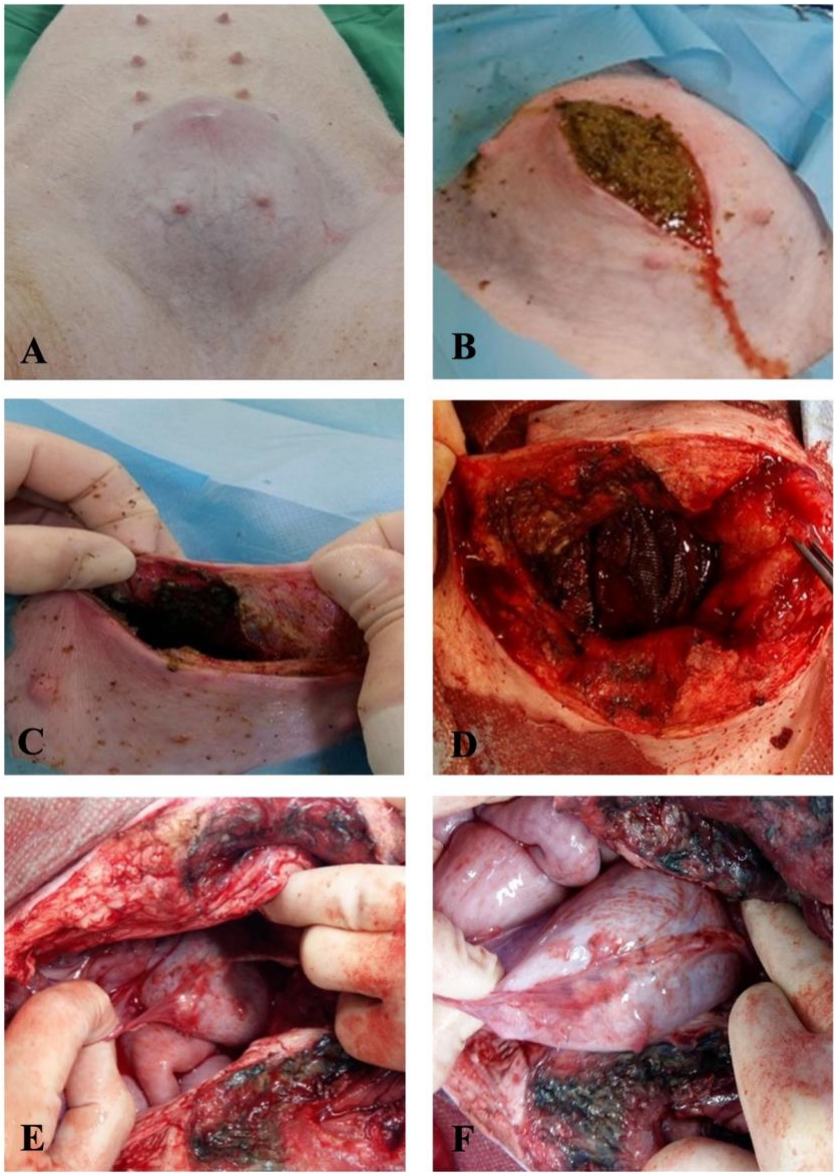

Figure 5.35 Case study #102.

Images showing a swollen area (A) noted in correspondence of the surgical wound in case study #102 on day 16 post-op. The animal did not show any clinical symptoms or signs of discomfort. Faecaloid fluid material (B) was observed after a skin incision was made in correspondence of the pointed area, along the previous surgical incision. Spots of necrotic tissue (C) were identified after accurate cleaning of the involved area. The previously applied mesh, with the stiches still in situ, was visible at the deeper site of the cavity (D). The urinary bladder was found healthy. It was not involved in the diseased process and was completely free from adhesions. The auto-augmentation site looked healthy too, macroscopically completely healed, with no signs of adverse reactions. The absorbable stitches (5/0 Vicryl) put in place during the first surgery between the PABM and the bladder were still appreciable (E, F).

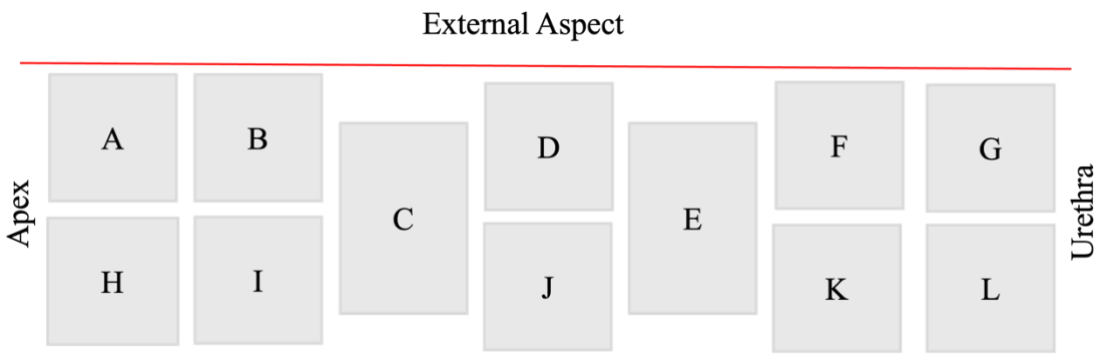

Figure 5.36 Scheme of dissection in case study #102.

The bladder was retrieved and processed after 18 days from the biomaterial implantation.

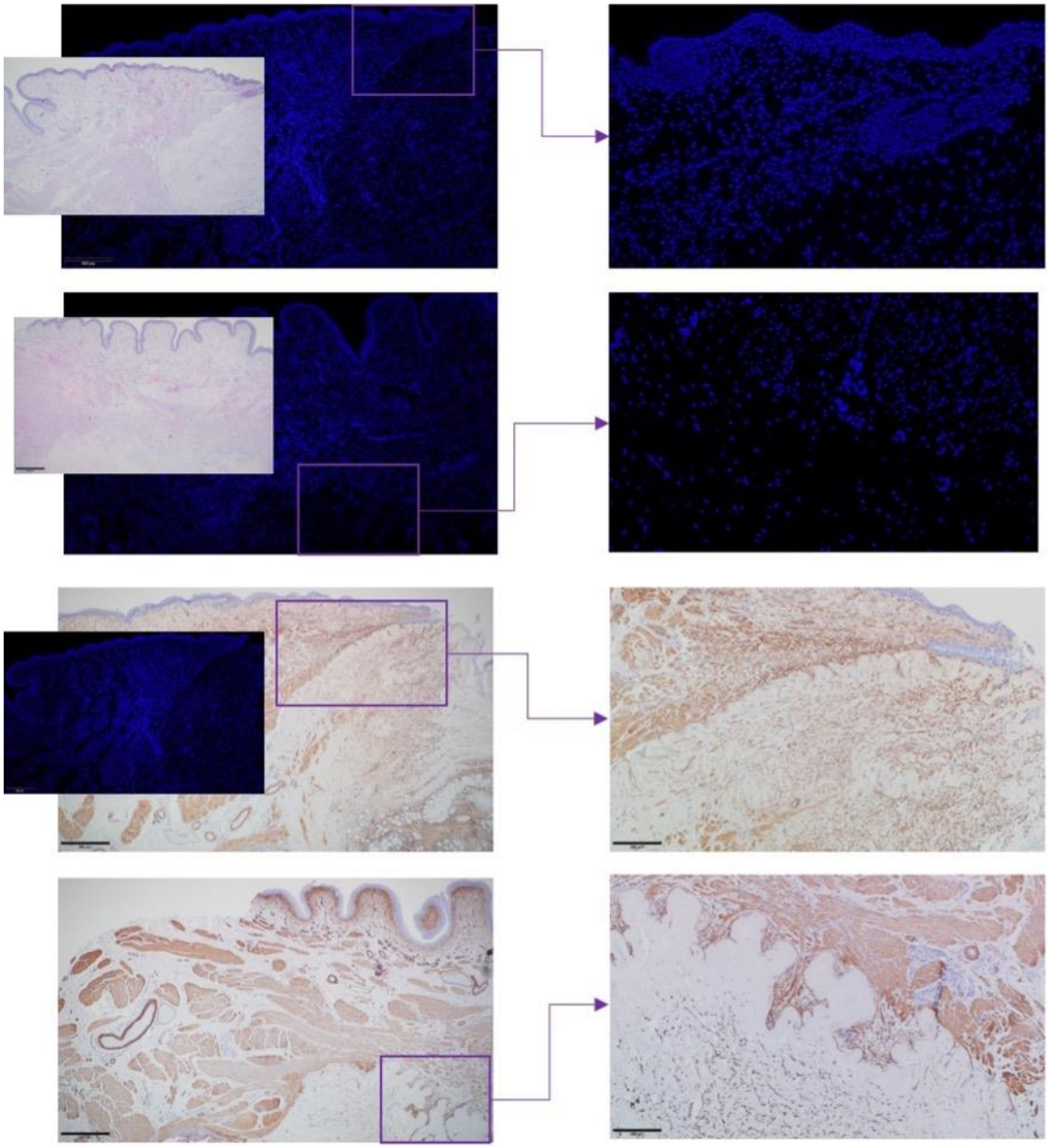

Figure 5.37 Recellularisation pattern in case study#102.

Images showing the re-cellularisation pattern assessed via Hoechst 33258 and H&E staining in two different samples from case #102, at 18 days from the biomaterial implantation. A uniform urothelium, a transition zone and the PABM area are here identified. αSMA expression is also shown with evidence of neo-angiogenesis and no evidence of any encapsulation process at the interface between native-looking bladder tissue and the implanted PABM (Scale bar: 500 µm and 200 µm).

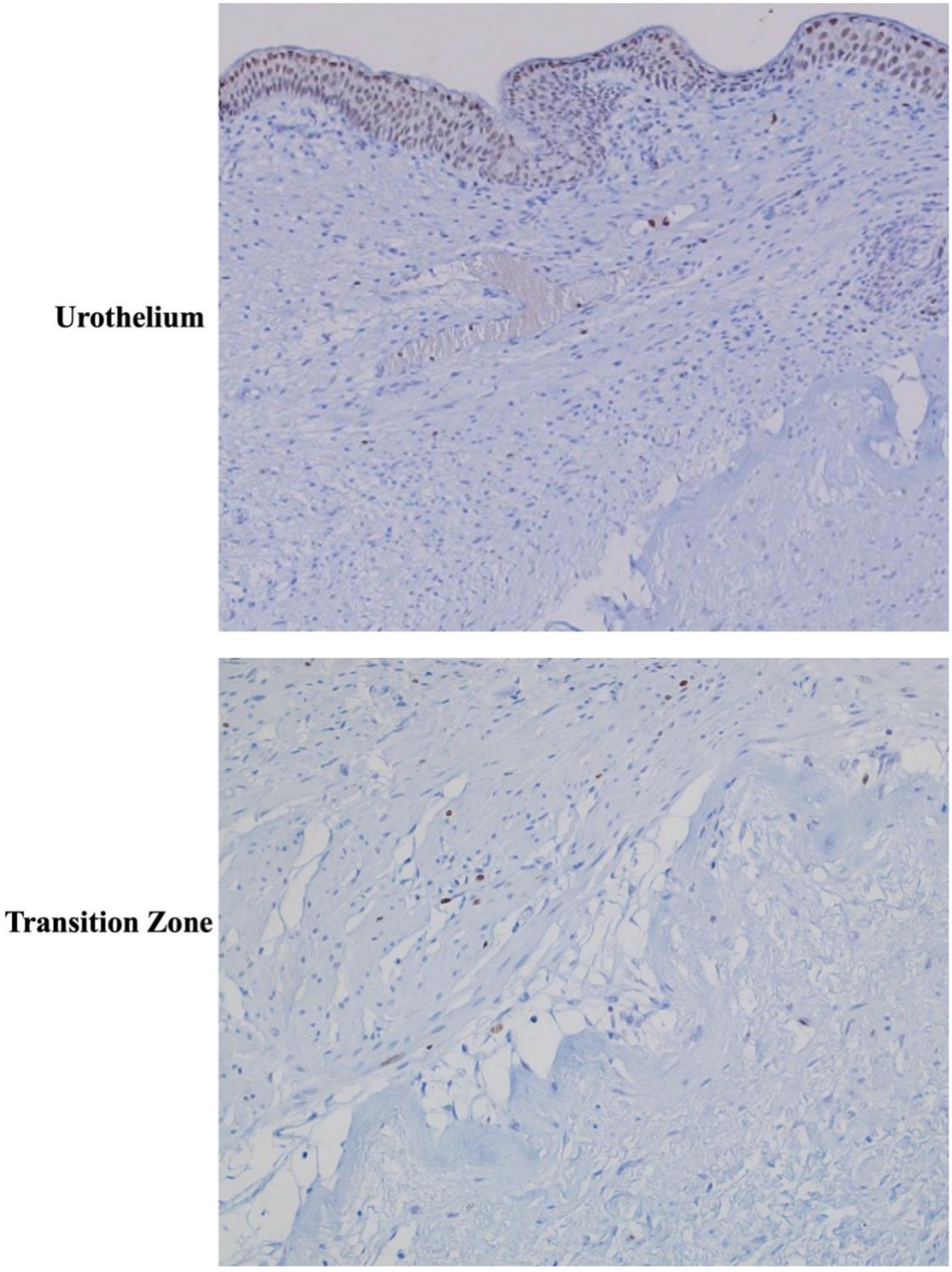

Figure 5.38 ki67 labelling in case study #102.

Images showing evidence of proliferative cells found within the urothelium, the transition zone and the regenerating area at a 18 day-follow-up.

Transition Zone

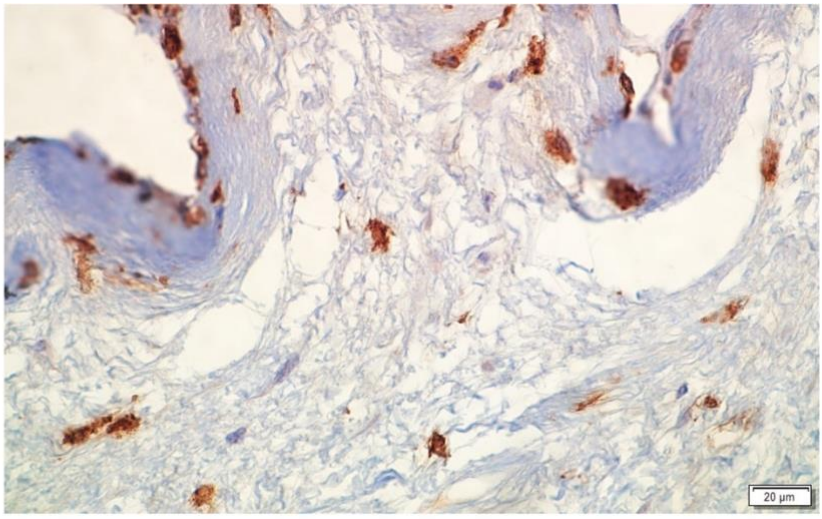

PABM Area

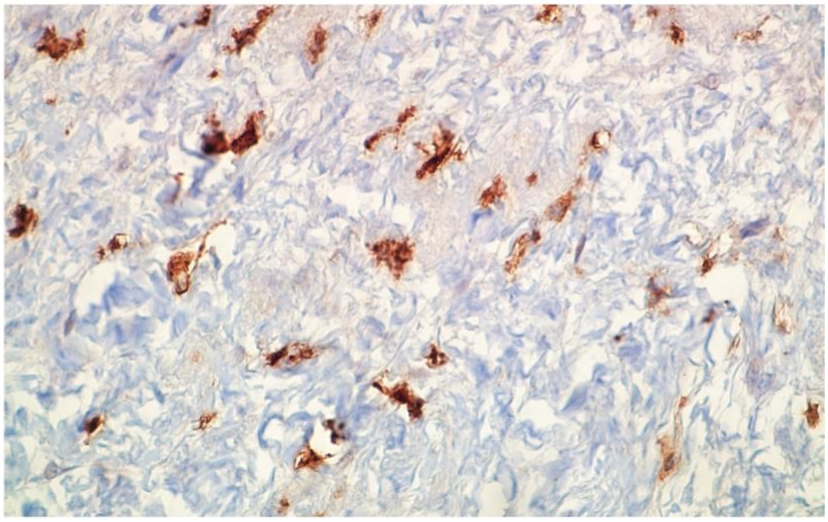

Figure 5.39 CD163 expression in case study #102.

Micrographs showing CD163 expression, suggesting the presence of a more pro-regenerative macrophages phenotype detected at the level of the transition zone and the implanted PABM area after 18 days from surgery. (Scale bar: 20 µm).

5.3.4 Quantitative Analysis

A quantitative analysis was conducted on tissue sections labelled with immunohistochemistry for all animals.

The total cell count showed an overall uniform recellularisation pattern across recipients. The variation in cell count per ROI among animals is illustrated in Figure 5.40A.

The mean total number of cells per mm^2 ± SEM was calculated to show the density of infiltrating cells (Figure 5.40B).

Additionally, the percentages of cells expressing specific markers were examined to determine the relative proportions of different cell types infiltrating the PABM. The analysis revealed that more than 50% of the cells were αSMA+ across animals, except for case study #799. A higher percentage of CD163+ and ki67+ infiltrating cells were found in case study #102 (18 days FU), which also revealed a lower percentage of SM22α+ and NFP+ cells if compared to the recipients which completed the 4-month FU (Figure 5.41).

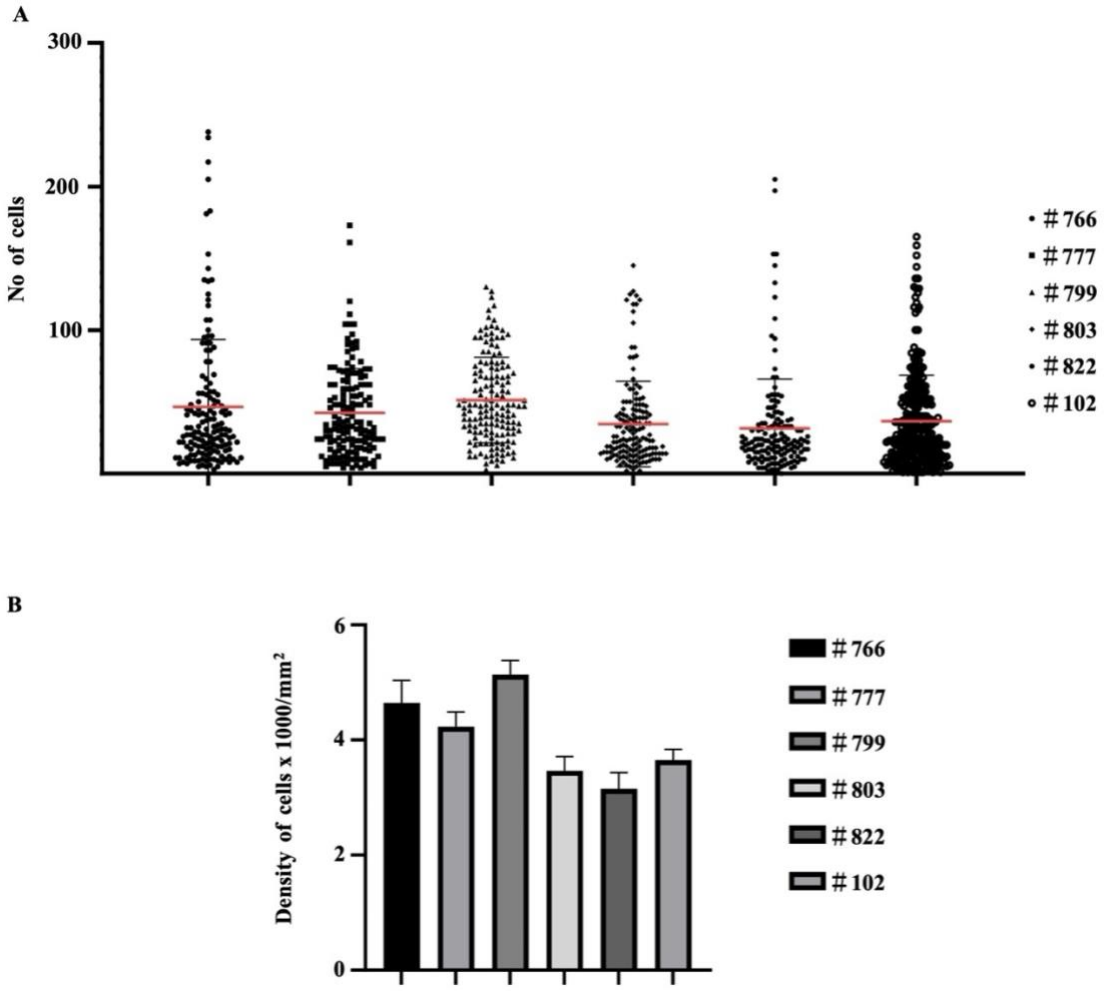

Figure 5.40 Quantitative Analysis.

A) scatter plot representing the total number of cells detected within the analysed ROIs of the regenerating biomaterial area. Data is shown per animal and is expressed as Mean ± SD. B) Implant cell density: data per each animals reported as mean number of cells per mm² (± SEM).

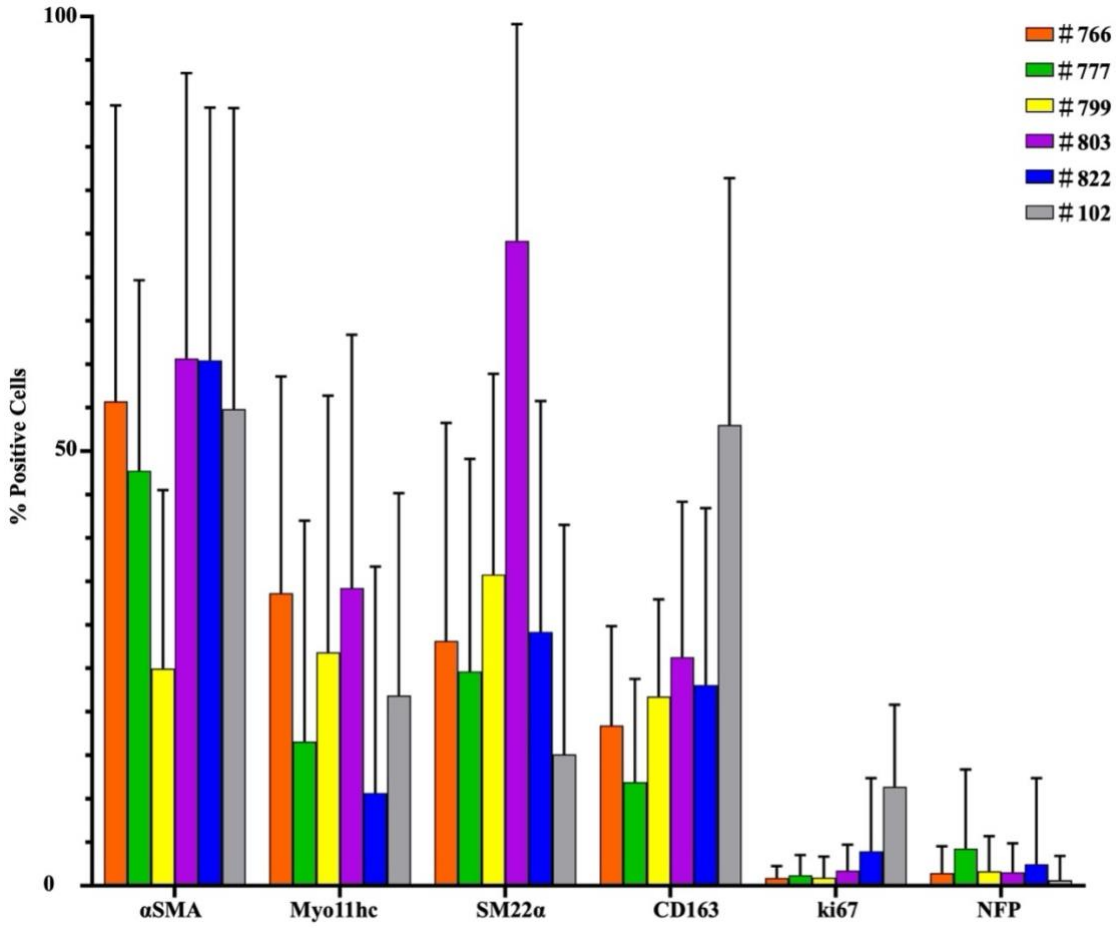

Figure 5.41 Quantification of the relative proportion of different cell types identified using immunolabelling in the regenerated PABM samples.

Cell numbers were quantified from 25 individual, standard, non-overlapping ROIs per each marker for implant. Data expressed as mean ± SD.

5.4 Discussion

Urinary bladder auto-augmentation aims at improving the bladder capacity by splitting the bladder wall and leaving the mucosa bulging to create a diverticulum-like structure (Johnson et al., 1994; Stothers et al., 1994). The resulting more capacious reservoir allows the urine to be stored at a low pressure reducing the risk of kidney damage in patients with small, contracted, poorly functioning bladders. The main aim of the present study was to investigate the potential of using a highly compliant acellular matrix (PABM) as a free graft in a homologous surgical setting of urinary bladder auto-augmentation. It was hypothesised that the PABM would provide the initial physical support by reinforcing the bulging mucosa and would promote tissue regeneration, reducing the potential surgical complications (Perovic et al., 2002; MacNeily et al., 2003; Gurocak et al., 2007; Rivas et al., 1996; Ehdaie et al., 2013). This was achieved by performing bladder auto-augmentation with implantation of PABM in 6 large Landrace female pigs and assessing biomaterial integration properties and tissue regeneration characteristics after a 4-month follow-up (FU).

This series demonstrated that the animals well tolerated the procedure of urinary bladder auto-augmentation with the PABM implant, with no post-operative morbidity. They passed urine per urethra with no signs of any discomfort. During the follow-up, all animals behaved normally except one, which showed bullying and aggressive behaviour, requiring the animals to be hosted in smaller groups (2 or 3 individuals in each pen). They went on to grow as expected for a pig of this breed (Table 5.2).

One animal was sacrificed after 18 days due to a complication not directly related to the procedure of bladder auto-augmentation and biomaterial implantation but potentially secondary to the closure steps and the insertion of the mesh (case study #102). The collection and processing of all the bladders allowed an internal comparison between the five animals who completed a 4-month FU and the animal sacrificed at 18 days, providing some information on the early stages of the tissue recellularisation and regeneration process. As the first bladder was harvested in a semi-emergency setting, it was placed in 10 % formalin in a 150 ml container. The bladder did not retain the filled status. The fixation method was implemented by filling the bladder with formalin and closing the urethra and the ureters to maintain organ distension, placing the organ in a large container (5 L), and allowing the bladder to be fully submerged in NBF. The dissection scheme used for case study #102 (Figure 5.36) was based on a previous experience (Turner et al., 2011) and differed from the dissection and classification method used in the remaining five bladders fixed in a filled status. The five bladders were therefore subjected to the same dissection plan to allow to navigate through the tissue (Figure 5.10-5.12). Such systematic approach kept into consideration the geometric

characteristics of the bladder wall defect created during the detrusorotomy and those of the implanted PABM patch. It facilitated tissue orientation and enabled analysis across bladders.

The main macroscopic and microscopic findings can be summarised as follows:

- Complete integration of the biomaterial with no evidence of any encapsulation process.
- No evidence of any adverse inflammatory response and necrosis.
- Presence of a continuous urothelium.
- Evidence of new structures within the implant area, including vessels, nerves and muscle bundles.
- Proliferating cells confirming a healthy environment.
- Pro-regenerative macrophage phenotype.

Macroscopically, all PABM implants became fully incorporated. At harvest, it was impossible to assess the true size of the graft after 4-month follow-up as no clear discontinuity was found between the native tissue and the site undergone auto-augmentation and PABM implantation. There was no evidence of fibrosis/scarring on the fresh bladders, with the auto-augmented areas feeling soft.

The histological analysis performed allowed the identification of a good pattern of cellularisation where PABM was applied, with evidence of neo-angiogenesis and de novo neurogenesis, confirming a healthy regenerative environment at the interface between native tissue and implanted biomaterial, and within the PABM area. No adverse reaction was noted, and no inflammation or fibrotic capsule formation were identified at the interface between the implanted biomaterial and the native tissue.

A uniform and healthy urothelium was found in all our samples. The assessment of the cytokeratin and uroplakin expression profiles (markers of terminal differentiation) did clarify that the epithelium lining both native areas and the auto-augmented areas where the PABM was applied, was a normal urothelium. This allowed to exclude at the status quo any phenotypical changes in response to the surgery or to the presence of the implanted biomaterial. αSMA was here tested to evaluate the presence of myofibroblast and vascular structure. Further IHC was performed to try to distinguish between neo-vascularisation and re-vascularisation and to better characterise muscular structures (Myo11hc, SM22α). The findings of neo-angiogenesis, visible in αSMA immunolabeling, correlates with the absence of any chondroid or bony metaplasia, as metaplasia can be attributed to ischemia due to a lack of angiogenesis in the regenerated tissue (Chang et al., 2004).

The presence of a more pro-regenerative macrophages phenotype was indicated by the presence of CD163+ cells (M2 macrophages) across samples. This is in line with what reported in in vitro studies,

where it was observed that the infiltration of decellularised biomaterials (PABM) is pioneered by macrophages. It was there suggested that the natural components of the PABM play an active role in polarising macrophages toward a CD163+ phenotype, with PPARγ activation identified as a potential pathway (Bullers et al., 2014). PPARγ is the peroxisome proliferator activated receptor γ, a nuclear hormone receptor that has been described to have also a role in the transitional cytodifferentiation of the urothelium by inducing expression of cytokeratin and uroplakin genes (Varley et al., 2004b, 2004a; Hustler et al., 2018). CD163+ macrophages (M2 macrophages) prevent tissue fibrosis after damage and initiate tissue regeneration and remodelling due to their anti-inflammatory and repair activities, highlighting their significance in regenerative medicine (Odegaard and Chawla, 2011; Sica and Mantovani, 2012; Chazaud, 2014; Rőszer, 2015; Wynn and Vannella, 2016; Zhang et al., 2023; Sheikh et al., 2015; Li et al., 2016).

As highlighted in Chapter 4, a qualitative or semi-quantitative evaluation has been historically performed to evaluate recellularisation in implanted biomaterials. To overcome the limitations linked to a subjective immunohistochemistry assessment leading towards a more standardised material assessment (Rhodes et al., 2000; Sirota, 2005; Taylor, 1994), and based on a previous experience (Morgante et al., 2021), an objective quantitative analysis was performed. This facilitated the evaluation of the degree of the cellularity in the area where tissue regeneration may had occurred and the analysis of the infiltrating cell types within the most central zone of the implants across pigs. If the recorded overall growth of the urinary bladders is considered, data shown that more than the 83% of the initial PABM was not recognisable after four months from the biomaterial implantation and was substituted by a normal-looking bladder tissue (Table 5.4). This is in line with recent reviews that highlighted the biodegradability as a crucial factor in bladder reconstruction studies, especially in the paediatric field (Casarin, Morlacco and Dal Moro, 2022). However, appearances observed in case study #799 suggested the possibility that the graft had moved cranially. Such consideration correlates macroscopic findings with the quantitative evaluation of cell density and cell type, suggesting that in case study #799 sub-segment IA1 captured the regenerating interface between native-looking tissue and the biomaterial. Therefore, extending the analysis to the remaining quadrants could provide support to the current findings further information.

The analysis of the percentages of cells expressing specific markers contributed to determining the relative proportions of different cell types infiltrating the PABM after implantation. A higher percentage of CD163+ and ki67+ infiltrating cells were found in case study #102 (18 days FU), which also revealed a lower percentage of SM22α+ and NFP+ cells if compared to the recipients who completed the 4-month FU (Figure 5.41). Such findings of changes in relative proportions of different markers after 4 months and 18 days from implantation provided significant information and offered

an internal comparison of the regenerative process at different timeframes, despite the limitation of the difference in the numbers of the case studies in the two groups (N = 5 and N = 1). Such observation could be further investigated in future animal studies.

Furthermore, IHC and quantitative data suggested the hypothesis that immunolabeled cells co-expressed different markers at the captured timeframe of the tissue regeneration process (e.g. co-localisation of CD163 and αSMA) (Figure 5.41). Further characterisation with co-labelling techniques, and advancement in the TissueGnostics technology to allow processing and comparison of wider tissue areas could allow additional data collection to support or confute the speculation of newly characterised regenerative (transient?) cell populations.

Based on the results of anti-αSMA immunolabelling at 4 month FU, it can be hypothesised that most of the fibroblasts in the PABM area were activated as myofibroblasts (similar results were noted in case study #102 sacrificed at 18 days post-operation (N = 1)). Such process of fibroblasts activation towards acquisition of a smooth muscle cell-like phenotype has been thought been in response to TGF-β1 stimulation (Hu and Phan, 2013; Micallef et al., 2012).

Historically, limited information and data on the immuno-labelling of porcine tissue have been available (Furukawa, Nagaike and Ozaki, 2017). Despite such limitations, the immunohistochemical work conducted in this study contributed to increasing the technical knowledge for histopathological examination within formalin fixed paraffin embedded porcine tissue. Advances in the availability of species-specific markers will contribute to further expanding the immune characterisation of the regenerating tissue (e.g., T cells, M1 macrophages).

It has been recognised that despite many limitations, animal models have been critical in advancing the understanding of the pathophysiological mechanisms of lower urinary tract functions (Kitta et al., 2020, 2018). In biomedical research, mice and rats represent 95% circa of all laboratory animals, with mice the most commonly utilised (Hickman et al., 2017). As recently reported (Gray, Guido and Kugadas, 2022), such rodent models are often unsuited for applying size-relevant surgical techniques used in patients. Furthermore, they cannot represent disease characteristics seen in humans, and fail to address translatable immune-related outcomes. Thus, recently, there has been an increased scientific need to develop translational pre-clinical large animal models. More specifically, pigs have gained significant scientific attention as translational models because they share important proteomic, genomic, and immunologic similarities to humans, including macrophages similarities (Bassols et al., 2014; Kapetanovic et al., 2012; Fairbairn et al., 2011). Pigs have also been used in experimental surgery due to the similarities to humans in terms of size and anatomy (Turner et al., 2011). Although,

it is recognised that the larger the animal model, the more difficult the study is due to the associated animal ethics issues, laboratory facility, and budget (Shen et al., 2021).

In this study, pigs and their bladders were therefore chosen as experimental model. This choice was further supported by evidence of the pig model becoming the main species for developing implantable bladder devices, and in consideration of the observation that the size of the pig bladder capacity is similar to that of humans (Chen et al., 2015; Parsons et al., 2012). In the surgical study presented in this Chapter, a patch of 4 cm x 2-2.5 cm of PABM was implanted in an auto-augmented bladder. Four non-absorbable sutures were left in place at the time of the initial surgery as marker points (0.5 - 1 cm ca from the biomaterial). At harvest, the area between the non-absorbable sutures was larger due to natural growth of the urinary bladder with age/size (Tables 5.3 and 5.4). Upon processing, no tissue shrinkage was observed (Tables 5.3 and 5.4). This is in contrast with other studies where tissue shrinkage was observed being up to 20% after fixation in formalin (Tran et al., 2015).

In addition, in this surgical experience it was planned not to insert any urinary bladder catheters or distension-balloons. This was to encourage the immediate recovery of the natural filling/emptying - storage/voiding cycle in the operated animals. It has been suggested that mechanical stimulation contributes to modulate the phenotype of tissue constructs in vitro (Kim et al., 1999; Kim and Mooney, 2000; Heise et al., 2009) and in vivo (Boruch et al., 2010). This is in line with the experience reported in this study, where it was observed how an early restoration of the filling/emptying physiologic bladder conditions did not implicate post-surgical complications (perforation, leakage, peritonitis), and potentially improved tissue remodelling, differentiation into both urothelium and smooth muscle, and vascularisation. These results support the concept that mechanical stimulation play a significant role in constructive remodelling and tissue regeneration (Boruch et al., 2010).

Aim of this study was specifically to assess the tissue integration and regeneration of PABM as homologous implanted natural material. Thus, normal, non-pathological porcine urinary bladders were used. It is proposed that future studies based on a diseased model could be considered to gain further results. As introduced above, the urinary bladder serves as a storage and elimination organ for urine; hence, symptoms of failure to store urine or empty the bladder can include incontinence, frequency and retention. As mentioned and recently reviewed, several animal models have been used to study a variety of bladder disorders, including rodents, rabbits, felines, canines, pigs, and mini pigs (Shen et al., 2021) and a broad range of biomaterials, both biologic and synthetic, have been applied to attempt urinary bladder regeneration (Morgante and Southgate, 2022; Wang, Zhang and Liao, 2021; Casarin, Morlacco and Dal Moro, 2022). The use of synthetic scaffolds allows to manipulate important chemical and physical characteristics such as degradation rate, pore structure, chemical properties, and stiffness, providing flexibility in both chemistry and manufacturing processes. On the

other hand, the use of synthetic materials alone in bladder reconstruction has been reported linked to complications such as urine leakage, graft shrinkage, collapse and cicatrisation) (Jack et al., 2009). Furthermore, the lack of bioactive factors and the formation of acidic degradation products are disadvantages of synthetic materials.

So far, promising natural acellular scaffolds have been applied with different outcomes. It was thought that acellular scaffolds can act as a temporary support allowing spontaneous regeneration of urothelial cells but it was noted that a cell-based approach (pre-seeded scaffold) with the eventual combination of specific growth factors would be necessary to obtain regeneration of smooth muscle cells, nerves and vessels (Wang, Zhang and Liao, 2021; Adamowicz et al., 2011; Kikuno et al., 2009). Conversely, the findings here shown challenge this, as confirmed the achievement of differentiated muscular structures, as well as the presence of neo-vessels when an acellular unseeded matrix was used.

In terms of cell source, autologous donor cells were reported being a primary source, due to the reduced risk of rejection and subsequent complications (Cilento et al., 1994; Turner et al., 2008). Specifically, in urinary bladder tissue engineering both urothelial cells and smooth muscle cells are required. However, cells isolated from neuropathic bladders did not show growth, contract ability, adherence proper of normal cells and reduced capacity for in vitro proliferation and differentiation (Lin et al., 2004; Subramaniam et al., 2011; Keay et al., 2000, 2003).

Overall, this study challenges the concept that cells implanted on the biomaterial is a necessity, a requirement to warranty structural and functional property of the regenerated bladder and highlights the fact that PABM can create a healthy and pro-regenerative environment for cell migration and proliferation.

In conclusion, these first surgical results support an application for PABM in providing the required support for the exposed mucosa in homologous urinary bladder auto-augmentation. The cellular integration properties of PABM combined with its natural strength and compliance make it a candidate biomaterial suitable for use in reconstructive urological surgery.

Chapter 6

Final discussion and conclusions

6.1 Overview

Several congenital and acquired disorders affecting the lower urinary tract require surgical reconstruction. However, the current gold standard procedures are associated with complications. As the main limitation resides in the lack of autologous good quality tissue available, alternative solutions have been proposed including regenerative medicine and tissue engineering. A range of degradable and non-degradable, synthetic and natural biomaterials, either seeded and unseeded have been tested for reconstructive purposes, but typically resulted in fibrosis and graft contracture leading over time to mechanical failure (Adamowicz et al., 2019; Casarin, Morlacco and Dal Moro, 2022; Atala, 2011). The ideal material should be biodegradable, biocompatible and non-immunogenic, retain physical and mechanical properties of the originating tissue, meet the surgical requirements in terms of strength, elasticity and manipulability and promote cell regeneration (Abbas et al., 2017; Casarin, Morlacco and Dal Moro, 2021; Serrano-Aroca, Vera-Donoso and Moreno-Manzano, 2018; Farhat and Yeger, 2008; Singh, Bivalacqua and Sopko, 2018; Casarin, Morlacco and Dal Moro, 2022). More specifically, in the paediatric urological field, a high regenerative capacity associated to the absence for the need of a prolonged catheterisation are preferable (Chan et al., 2020; Horst et al., 2019). Natural acellular matrices have the potential benefit of retaining the physical, biochemical and biomechanical properties of the originating tissue (Sara et al., 2010; Bolland et al., 2007).

The overall aim of this study was to evaluate in vivo the tissue integration properties and recellularisation characteristics of a non-cross-linked natural acellular matrix (PABM) developed by a decellularisation process applied to full-thickness porcine bladders (Bolland et al., 2007; Ward et al., 2021).

The general hypothesis was that the PABM would be fit for homologous use in the surgical setting of the urinary tract, including urethral repair and bladder auto-augmentation. In the latter application, it was hypothesised that PABM would provide the initial required supporting function to the exposed bladder mucosa, while supplying an environment able to promote cellular migration and regeneration.

Two different processes for sufficiently stretching the bladders to achieve full decellularisation were applied. An initial empirical inflation of the intact bladder (Bolland et al., 2007) was advanced to a more precise use of a flat-bed apparatus to deliver the necessary biaxial strain to dissected bladder

sheets (Ward et al., 2021). The results showed residual nuclear materials when bladders were decellularised with the first method. This could be due to the variation in individual bladder size and the filling volumes used. Furthermore, the initially tested method was considered not suitable for scaling up at an industrial manufacturing level. Thus, the second method was used at the JBU to produce six 8 x 8cm PABM sheets, which resulted adequately decellularised and sterile. Based on these results, the six produced biomatrices were implanted to cover the exposed bladder mucosa in a large animal model of urinary bladder auto-augmentation (detrusorotomy) and the bladder tissue was harvest, processed and analysed to assess tissue regeneration characteristics after a four month FU. One animal required to be sacrificed at an early stage, providing a useful understanding of the tissue regeneration process. The qualitative and quantitative analysis performed allowed the identification of a good pattern of cellularisation where PABM was applied. The evidence of neo-angiogenesis, de novo neurogenesis and M2-polarised macrophages confirmed a healthy regenerative environment within the implanted biomaterial area. No adverse reaction was noted, with no inflammation or fibrotic capsule formation identified at the interface between the implanted biomaterial and the native tissue. A uniform and differentiated urothelium was found in all samples. The objective quantitative analysis performed suggested that some cells were co-expressing more than one marker, highlighting the opportunity for further tissue characterisation, within the limitations related to the antibodies available for porcine tissue immunolabelling.

These tissue integration characteristics of PABM were confirmed when a comparison was performed with the tissue regeneration properties of a cross-linked, commercially available biomaterial (Permacol™), following an in vivo study of hypospadias repair (Chapter 4) (Morgante et al., 2021). The results obtained in this study were in line with published data suggesting that cross-linking is a causative factor for foreign body reaction and for a lower level of recellularisation (Itoh et al., 2002; Ayyildiz et al., 2006).

One open question about tissue-derived matrices is whether they are most appropriate for use in homologous settings due to their intrinsic properties, including biochemical, architectural, biomechanical and biological features. In this study, bladder-derived PABM was tested in two settings, one homologous (Chapter 5) and one related but non-homologous (Chapter 4). In both models no adverse reactions occurred, and tissue regeneration with angiogenesis were found. These results were achieved without the need of providing additional vascularisation at the time of surgery or supplying the patch with supplementary factors (e.g. growth factors), or prior in vitro or ex vivo cell-seeding. This research underpins the concept that a 3D environment derived from a full-thickness urinary bladder is more effective in supporting bladder tissue regeneration post-implantation (tissue-specific), than biomaterials originating from a different organ (SIS), or biomatrices obtained by

processes that alterate the 3D structure of the originating bladder tissue (UBM, UBS) (Feil et al., 2006; Lin et al., 2014; Freytes et al., 2004; Gilbert et al., 2008). The regenerated tissue characteristics observed in this study in terms of cell repopulation and neovascularisation are supported by the concept that the composition and structure of the ECM are unique to individual tissues and, therefore, strongly influence cell attachment, migration and proliferation (Badylak, 2004). Alterating the collagen network can modify the mechanical environment to which the cells are exposed during the regenerating process. Therefore, the observation that PABM retains the ultrastructure of the urinary bladder in terms of the amount and organisation of collagen, porosity and mechanical properties supports the presented findings of angiogenesis, neurogenesis and enhanced development of smooth muscle structures and functional urothelium. The general features of PABM in terms of strength, compliance, and ability to retain sutures make it suitable for surgical application. While the results observed in a homologous setting suggest that PABM is suitable for bladder use, the results observed in a related but non-homologous model show its possible applications in different surgical settings. PABM was here shown to have not only ideal surgical properties but also ideal biological properties, as it was proven to be non-inflammatory, pro-regenerative, and pro-neovascularisation. Its full potential in surgical applications is yet to be established, and more research in different tissue settings could be considered.

Overall findings presented in this study suggest that the PABM prominent bioactivity (cell adhesion, migration, activation) towards tissue regeneration is inherent. This is highlighted by the property of PABM of being capable of recruiting endogenous progenitor cells to the site of “injury” (auto-augmented area) and unlock the regenerative capability of such cells (Tang et al., 2023; Cipitria et al., 2017).

These first surgical results support an application for PABM in providing the required support for the exposed mucosa in homologous urinary bladder auto-augmentation. It is therefore possible to conclude that the cellular integration properties of PABM combined with its natural strength and compliance make it an ideal biomaterial for use in reconstructive urological surgery.

The field of biomaterials for medical use has seen remarkable progress, however, transitioning from laboratory research to widespread clinical use requires scalable manufacturing processes to produce biomaterials in large quantities while maintaining their functional properties. Thus, as the demand for biomaterials grows, the need for scalable manufacturing processes becomes increasingly critical to meet clinical needs. Quality control (QC) is a crucial aspect of manufacturing that ensures products meet specific quality standards. It involves various methods and procedures to maintain or improve product quality and prevent defective or damaged products from reaching patients. Therefore, as part

of this study, the suitability for scaling up the manufacturing process of PABM was evaluated. The process was transferred to an industrial facility. The results of the analytical quality control performed on the produced biomaterial supported such suitability and highlighted areas for further process optimisation, including sterilisation and storage methods (Freytes et al., 2004, 2008; Freytes and Badylak, 2006; Pokrywczynska et al., 2015). Although surgical results suggest adequate tissue mechanical properties, in terms of strength, compliance, ability to retain sutures and malleability, further mechanical testing could inform on the effects of the transport methods (without transport medium) and of the freezing/thawing process on the PABM.

6.2 Future research

Aim of this research was specifically to assess the tissue integration and regeneration properties of PABM as homologous implanted natural material. Thus, normal, non-pathological porcine models were used. It is proposed that future research directions could include the use of PABM in diseased large animal models before translation to a clinical setting. As mentioned and recently reviewed, several animal models have been used to study a variety of bladder disorders, including rodents, rabbits, felines, canines, pigs, and mini pigs (Shen et al., 2021). Diseased animal models are important to improve our understanding of the pathophysiology of a disease, and to test in vivo safety and efficacy of a new medical device before progressing to human clinical trials. As the size of the animal model increases, though, the study becomes more challenging due to concerns related to animal ethics, the need for adequate laboratory facilities, and budget constraints (Mukherjee et al., 2022; Robinson et al., 2019).

The possibility of adapting the decellularisation process to develop grafts from full-thickness human bladder could be pursued offering a further option for urethral and bladder tissue repair. The technology here optimised for pig bladders could be applied to human cadaveric bladders to obtain a bioequivalent human acellular bladder matrix (HABM), which could be translated into a surgical setting. Further studies to inform on the biomechanical properties of the human bladder tissue would support the optimisation of the strain needed to obtain satisfactory decellularisation. One of the major challenges to such progression resides in the sourcing of human cadaveric bladders.

Additional research directed at investigating the biological characteristics of the niche/microenvironment created by PABM when implanted in a homologous surgical setting will deepen the understanding of the molecular biology of the cells-biomaterial interaction. As the ECM-based microenvironment is linked to the biophysical properties of the matrix and biochemical extracellular stimuli to cells, future studies could include the assessment of 3D characteristics of

PABM via advanced imaging modalities (e.g. scanning electron microscopy and super resolution microscopy) to analyse the spatial relationships and interactions of the micro-components. Mass spectrometry-based global phosphoproteomics profiling could contribute to a better understanding of integrated signalling pathways and composite output of direct and indirect crosstalk between signalling pathways. Furthermore, single-cell analysis could be performed to overcome the limit of a bulk analysis and in consideration of the genetic and non-genetic heterogeneity at a single-cell level. Thus, it could include the use of flow cytometry, mass cytometry, single-cell RNA sequencing, and multiplexed single-cell measurement technologies. However, a main limitation is the lack of reliable antibodies for porcine protein targets.

Within the field of urologic tissue engineering, a pivotal concept lays on the dynamic reciprocity between implanted biomaterials and the host tissues. This interaction appears to be a fundamental element to regulate tissue remodelling events, that influence the efficacy of functional tissue repair (Gattazzo, Urciuolo and Bonaldo, 2014; Mauney and Adam, 2015). Key determinants such as scaffold composition and architecture, the host-immune response, mechanical stimuli, the presence of endogenous growth factors participate in bidirectional signalling cascades that modulate the successful integration of grafts and the generation of de novo tissue at implantation sites. Therefore, a clearer comprehension of these intricate processes could help to identify further avenues for optimising the use of PABM in surgical reparative settings.

List of references

Abbas, T. O. et al. (2017). Current Status of Tissue Engineering in the Management of Severe Hypospadias. *Frontiers in Pediatrics*, 5, p.283. [Online]. Available at: doi:10.3389/fped.2017.00283.

Abbott, R. D. and Kaplan, D. L. (2016). Engineering Biomaterials for Enhanced Tissue Regeneration. *Current Stem Cell Reports*, 2 (2), pp.140–146. [Online]. Available at: doi:10.1007/s40778-016-0039-3 [Accessed 21 June 2024].

Abuharb, A. I. et al. (2024). The Impact and Implications of Regenerative Medicine in Urology. *Cureus*, 16 (1), p.e52264. [Online]. Available at: doi:10.7759/cureus.52264.

Acharya, P. et al. (2004). Distribution of the tight junction proteins ZO-1, occludin, and claudin-4, -8, and -12 in bladder epithelium. *American Journal of Physiology. Renal Physiology*, 287 (2), pp.F305-318. [Online]. Available at: doi:10.1152/ajprenal.00341.2003.

Adamowicz, J. et al. (2011). Schwann cells - a new hope in tissue engineered urinary bladder innervation. A method of cell isolation. *Central European Journal of Urology*, 64 (2), pp.87–89. [Online]. Available at: doi:10.5173/ceju.2011.02.art8.

Adamowicz, J. et al. (2019). Reconstructive urology and tissue engineering: Converging developmental paths. *Journal of Tissue Engineering and Regenerative Medicine*, 13 (3), pp.522–533. [Online]. Available at: doi:10.1002/term.2812 [Accessed 30 June 2024].

Adelöw, C. et al. (2008). The effect of enzymatically degradable poly(ethylene glycol) hydrogels on smooth muscle cell phenotype. *Biomaterials*, 29 (3), pp.314–326. [Online]. Available at: doi:10.1016/j.biomaterials.2007.09.036.

Aitken, K. J. and Bägli, D. J. (2009a). The bladder extracellular matrix. Part I: architecture, development and disease. *Nature Reviews. Urology*, 6 (11), pp.596–611. [Online]. Available at: doi:10.1038/nrurol.2009.201.

Aitken, K. J. and Bägli, D. J. (2009b). The bladder extracellular matrix. Part II: regenerative applications. *Nature Reviews. Urology*, 6 (11), pp.612–621. [Online]. Available at: doi:10.1038/nrurol.2009.202.

Ajalloueian, F. et al. (2013). One-stage tissue engineering of bladder wall patches for an easy-to-use approach at the surgical table. *Tissue Engineering. Part C, Methods*, 19 (9), pp.688–696. [Online]. Available at: doi:10.1089/ten.TEC.2012.0633.

Ajalloueian, F. et al. (2014). Constructs of electrospun PLGA, compressed collagen and minced urothelium for minimally manipulated autologous bladder tissue expansion. *Biomaterials*, 35 (22), pp.5741–5748. [Online]. Available at: doi:10.1016/j.biomaterials.2014.04.002.

Ajalloueian, F. et al. (2018). Bladder biomechanics and the use of scaffolds for regenerative medicine in the urinary bladder. *Nature Reviews. Urology*, 15 (3), pp.155–174. [Online]. Available at: doi:10.1038/nrurol.2018.5.

Akbal, C. et al. (2006). Bladder augmentation with acellular dermal biomatrix in a diseased animal model. *The Journal of Urology*, 176 (4 Pt 2), pp.1706–1711. [Online]. Available at: doi:10.1016/j.juro.2006.04.085.

Aktuğ, T. et al. (2001). EXPERIMENTALLY PREFABRICATED BLADDER. *The Journal of Urology*, 165 (6, Part 1), pp.2055–2058. [Online]. Available at: doi:10.1016/S0022-5347(05)66293-3 [Accessed 15 June 2024].

Allaire, E. et al. (1994). Cell-free arterial grafts: morphologic characteristics of aortic isografts, allografts, and xenografts in rats. *Journal of Vascular Surgery*, 19 (3), pp.446–456. [Online]. Available at: doi:10.1016/s0741-5214(94)70071-0.

Altarac, S., Papeš, D. and Bracka, A. (2012). Two-stage hypospadias repair with inner preputial layer Wolfe graft (Aivar Bracka repair). *BJU international*, 110 (3), pp.460–473. [Online]. Available at: doi:10.1111/j.1464-410X.2012.11304.x.

Arimura, H. et al. (2005). Preparation of a hyaluronic acid hydrogel through polyion complex formation using cationic polylactide-based microspheres as a biodegradable cross-linking agent. *Journal of Biomaterials Science. Polymer Edition*, 16 (11), pp.1347–1358. [Online]. Available at: doi:10.1163/156856205774472353.

Ashley, R. A. et al. (2010). Regional variations in small intestinal submucosa evoke differences in inflammation with subsequent impact on tissue regeneration in the rat bladder augmentation model. *BJU international*, 105 (10), pp.1462–1468. [Online]. Available at: doi:10.1111/j.1464-410X.2009.08965.x.

Atala, A. (1998). Autologous cell transplantation for urologic reconstruction. *The Journal of Urology*, 159 (1), pp.2–3. [Online]. Available at: doi:10.1016/s0022-5347(01)63994-6.

Atala, A. (2001). Tissue engineering in urology. *Current Urology Reports*, 2 (1), pp.83–92. [Online]. Available at: doi:10.1007/s11934-001-0030-z.

Atala, A. et al. (2006). Tissue-engineered autologous bladders for patients needing cystoplasty. *Lancet (London, England)*, 367 (9518), pp.1241–1246. [Online]. Available at: doi:10.1016/S0140-6736(06)68438-9.

Atala, A. (2011). Tissue engineering of human bladder. *British Medical Bulletin*, 97, pp.81–104. [Online]. Available at: doi:10.1093/bmb/ldr003.

Ayyildiz, A. et al. (2006). Using porcine acellular collagen matrix (Pelvicol) in bladder augmentation: experimental study. *International Braz J Urol: Official Journal of the Brazilian Society of Urology*, 32 (1), pp.88–92; discussion 92-93. [Online]. Available at: doi:10.1590/s1677-55382006000100015.

Badylak, S. et al. (2000). Resorbable bioscaffold for esophageal repair in a dog model. *Journal of Pediatric Surgery*, 35 (7), pp.1097–1103. [Online]. Available at: doi:10.1053/jpsu.2000.7834.

Badylak, S. F. et al. (1989). Small intestinal submucosa as a large diameter vascular graft in the dog. *The Journal of Surgical Research*, 47 (1), pp.74–80. [Online]. Available at: doi:10.1016/0022-4804(89)90050-4.

Badylak, S. F. (2002). The extracellular matrix as a scaffold for tissue reconstruction. *Seminars in Cell & Developmental Biology*, 13 (5), pp.377–383. [Online]. Available at: doi:10.1016/s1084952102000940.

Badylak, S. F. (2004). Xenogeneic extracellular matrix as a scaffold for tissue reconstruction. *Transplant Immunology*, 12 (3–4), pp.367–377. [Online]. Available at: doi:10.1016/j.trim.2003.12.016.

Badylak, S. F. (2005). Regenerative medicine and developmental biology: the role of the extracellular matrix. *Anatomical Record. Part B, New Anatomist*, 287 (1), pp.36–41. [Online]. Available at: doi:10.1002/ar.b.20081.

Baker, S. C. et al. (2006). Characterisation of electrospun polystyrene scaffolds for three-dimensional in vitro biological studies. *Biomaterials*, 27 (16), pp.3136–3146. [Online]. Available at: doi:10.1016/j.biomaterials.2006.01.026.

Baker, S. C. et al. (2009). The relationship between the mechanical properties and cell behaviour on PLGA and PCL scaffolds for bladder tissue engineering. *Biomaterials*, 30 (7), pp.1321–1328. [Online]. Available at: doi:10.1016/j.biomaterials.2008.11.033.

Baker, S. C. et al. (2011). Cellular Integration and Vascularisation Promoted by a Resorbable, Particulate-Leached, Cross-Linked Poly(ε-caprolactone) Scaffold. *Macromolecular Bioscience*, 11 (5), pp.618–627. [Online]. Available at: doi:10.1002/mabi.201000415 [Accessed 15 June 2024].

Baker, S. C., Shabir, S. and Southgate, J. (2014). Biomimetic Urothelial Tissue Models for the in Vitro Evaluation of Barrier Physiology and Bladder Drug Efficacy. *Molecular Pharmaceutics*, 11 (7), pp.1964–1970. [Online]. Available at: doi:10.1021/mp500065m [Accessed 14 June 2024].

Baker, S. C. and Southgate, J. (2011). 11 - Bladder tissue regeneration. In: Bosworth, L. A. and Downes, S. (Eds). *Electrospinning for Tissue Regeneration*. Woodhead Publishing Series in Biomaterials. Woodhead Publishing. pp.225–241. [Online]. Available at: doi:10.1533/9780857092915.2.225 [Accessed 14 June 2024].

Barbagli, G. et al. (2010). Morbidity of oral mucosa graft harvesting from a single cheek. *European Urology*, 58 (1), pp.33–41. [Online]. Available at: doi:10.1016/j.eururo.2010.01.012.

Barski, D. et al. (2017). Bladder Reconstruction with Human Amniotic Membrane in a Xenograft Rat Model: A Preclinical Study. *International Journal of Medical Sciences*, 14 (4), pp.310–318. [Online]. Available at: doi:10.7150/ijms.18127.

Baskin, L. S. et al. (1996). Role of mesenchymal-epithelial interactions in normal bladder development. *The Journal of Urology*, 156 (5), pp.1820–1827.

Bassols, A. et al. (2014). The pig as an animal model for human pathologies: A proteomics perspective. *PROTEOMICS – Clinical Applications*, 8 (9–10), pp.715–731. [Online]. Available at: doi:10.1002/prca.201300099 [Accessed 29 June 2024].

Beier-Holgersen, R., Kirkeby, L. T. and Nordling, J. (1994). 'Clam' ileocystoplasty. *Scandinavian Journal of Urology and Nephrology*, 28 (1), pp.55–58. [Online]. Available at: doi:10.3109/00365599409180471.

Biers, S. M., Venn, S. N. and Greenwell, T. J. (2012). The past, present and future of augmentation cystoplasty. *BJU International*, 109 (9), pp.1280–1293. [Online]. Available at: doi:10.1111/j.1464-410X.2011.10650.x [Accessed 15 June 2024].

Birder, L. and Wyndaele, J.-J. (2013). From urothelial signalling to experiencing a sensation related to the urinary bladder. *Acta Physiologica (Oxford, England)*, 207 (1), pp.34–39. [Online]. Available at: doi:10.1111/apha.12011.

Blanco Bruned, J. L. et al. (2001). [Seromuscular colocystoplasty lined by urothelium. Experimental study in rats]. *Cirugia Pediatrica: Organo Oficial De La Sociedad Espanola De Cirugia Pediatrica*, 14 (4), pp.162–167.

Bohne, A. W. and Urwiller, K. L. (1957). Experience with urinary bladder regeneration. *The Journal of Urology*, 77 (5), pp.725–732. [Online]. Available at: doi:10.1016/S0022-5347(17)66624-2.

Bolin, S. R., Matthews, P. J. and Ridpath, J. F. (1991). Methods for detection and frequency of contamination of fetal calf serum with bovine viral diarrhea virus and antibodies against bovine viral diarrhea virus. *Journal of Veterinary Diagnostic Investigation: Official Publication of the American Association of Veterinary Laboratory Diagnosticians, Inc*, 3 (3), pp.199–203. [Online]. Available at: doi:10.1177/104063879100300302.

Bolland, F. et al. (2007). Development and characterisation of a full-thickness acellular porcine bladder matrix for tissue engineering. *Biomaterials*, 28 (6), pp.1061–1070. [Online]. Available at: doi:10.1016/j.biomaterials.2006.10.005.

Booth, C. et al. (2002). Tissue engineering of cardiac valve prostheses I: development and histological characterization of an acellular porcine scaffold. *The Journal of Heart Valve Disease*, 11 (4), pp.457–462.

Borsdorf, M. et al. (2019). Locational and Directional Dependencies of Smooth Muscle Properties in Pig Urinary Bladder. *Frontiers in Physiology*, 10, p.63. [Online]. Available at: doi:10.3389/fphys.2019.00063.

Boruch, A. V. et al. (2010). Constructive remodeling of biologic scaffolds is dependent on early exposure to physiologic bladder filling in a canine partial cystectomy model. *The Journal of Surgical Research*, 161 (2), pp.217–225. [Online]. Available at: doi:10.1016/j.jss.2009.02.014.

Brown, A. L. et al. (2002). 22 week assessment of bladder acellular matrix as a bladder augmentation material in a porcine model. *Biomaterials*, 23 (10), pp.2179–2190. [Online]. Available at: doi:10.1016/s0142-9612(01)00350-7.

Brown, A. L. et al. (2005). Bladder acellular matrix as a substrate for studying in vitro bladder smooth muscle-urothelial cell interactions. *Biomaterials*, 26 (5), pp.529–543. [Online]. Available at: doi:10.1016/j.biomaterials.2004.02.055.

Brown, B. N. et al. (2009). Macrophage phenotype and remodeling outcomes in response to biologic scaffolds with and without a cellular component. *Biomaterials*, 30 (8), pp.1482–1491. [Online]. Available at: doi:10.1016/j.biomaterials.2008.11.040.

Buckley, B. S., Lapitan, M. C. M. and Epidemiology Committee of the Fourth International Consultation on Incontinence, Paris, 2008. (2010). Prevalence of urinary incontinence in men, women, and children--current evidence: findings of the Fourth International Consultation on Incontinence. *Urology*, 76 (2), pp.265–270. [Online]. Available at: doi:10.1016/j.urology.2009.11.078.

Budzyn, J. et al. (2019). Bladder Augmentation (Enterocystoplasty): the Current State of a Historic Operation. *Current Urology Reports*, 20 (9), p.50. [Online]. Available at: doi:10.1007/s11934-019-0919-z.

Bullers, S. J. et al. (2014). The Human Tissue–Biomaterial Interface: A Role for PPARγ-Dependent Glucocorticoid Receptor Activation in Regulating the CD163+ M2 Macrophage Phenotype. *Tissue Engineering Part A*, 20 (17–18), pp.2390–2401. [Online]. Available at: doi:10.1089/ten.tea.2013.0628 [Accessed 17 June 2024].

Burton, B. et al. (2014). Bone embrittlement and collagen modifications due to high-dose gamma-irradiation sterilization. *Bone*, 61, pp.71–81. [Online]. Available at: doi:10.1016/j.bone.2014.01.006.

Butler, C. E. et al. (2010). Comparison of cross-linked and non-cross-linked porcine acellular dermal matrices for ventral hernia repair. *Journal of the American College of Surgeons*, 211 (3), pp.368–376. [Online]. Available at: doi:10.1016/j.jamcollsurg.2010.04.024.

Cain, M. P. and Rink, R. C. (2010). Augmentation for Neuropathic Bladder Dysfunction—A Thing of the Past? *The Journal of Urology*. [Online]. Available at: doi:10.1016/j.juro.2010.03.067 [Accessed 15 June 2024].

Caione, P. et al. (2006). In vivo bladder regeneration using small intestinal submucosa: experimental study. *Pediatric Surgery International*, 22 (7), pp.593–599. [Online]. Available at: doi:10.1007/s00383-006-1705-9 [Accessed 16 June 2024].

Caione, P. et al. (2012). Bladder augmentation using acellular collagen biomatrix: a pilot experience in exstrophic patients. *Pediatric Surgery International*, 28 (4), pp.421–428. [Online]. Available at: doi:10.1007/s00383-012-3063-0.

Cameron, A. P. (2016). Medical management of neurogenic bladder with oral therapy. *Translational Andrology and Urology*, 5 (1), pp.51–62. [Online]. Available at: doi:10.3978/j.issn.2223-4683.2015.12.07 [Accessed 15 June 2024].

Campiglio, C. E. et al. (2019). Cross-Linking Strategies for Electrospun Gelatin Scaffolds. *Materials*, 12 (15), p.2476. [Online]. Available at: doi:10.3390/ma12152476 [Accessed 21 June 2024].

Carpentier, A. and Chachques, J. C. (1985). Myocardial substitution with a stimulated skeletal muscle: first successful clinical case. *Lancet (London, England)*, 1 (8440), p.1267. [Online]. Available at: doi:10.1016/s0140-6736(85)92329-3.

Cartwright, P. C. and Snow, B. W. (1989a). Bladder autoaugmentation: early clinical experience. *The Journal of Urology*, 142 (2 Pt 2), pp.505–508; discussion 520-521. [Online]. Available at: doi:10.1016/s0022-5347(17)38798-0.

Cartwright, P. C. and Snow, B. W. (1989b). Bladder autoaugmentation: partial detrusor excision to augment the bladder without use of bowel. *The Journal of Urology*, 142 (4), pp.1050–1053. [Online]. Available at: doi:10.1016/s0022-5347(17)38985-1.

Casarin, M., Morlacco, A. and Dal Moro, F. (2021). Bladder Substitution: The Role of Tissue Engineering and Biomaterials. *Processes*, 9 (9), p.1643. [Online]. Available at: doi:10.3390/pr9091643 [Accessed 30 June 2024].

Casarin, M., Morlacco, A. and Dal Moro, F. (2022). Tissue Engineering and Regenerative Medicine in Pediatric Urology: Urethral and Urinary Bladder Reconstruction. *International Journal of Molecular Sciences*, 23 (12), p.6360. [Online]. Available at: doi:10.3390/ijms23126360.

de Castro Brás, L. E. et al. (2010). Effect of crosslinking on the performance of a collagen-derived biomaterial as an implant for soft tissue repair: a rodent model. *Journal of Biomedical Materials Research. Part B, Applied Biomaterials*, 95 (2), pp.239–249. [Online]. Available at: doi:10.1002/jbm.b.31704.

Cavallo, J. A. et al. (2015). Remodeling characteristics and biomechanical properties of a crosslinked versus a non-crosslinked porcine dermis scaffolds in a porcine model of ventral hernia repair. *Hernia: The Journal of Hernias and Abdominal Wall Surgery*, 19 (2), pp.207–218. [Online]. Available at: doi:10.1007/s10029-013-1070-2.

Cervigni, M. et al. (2017). A randomized, open-label, multicenter study of the efficacy and safety of intravesical hyaluronic acid and chondroitin sulfate versus dimethyl sulfoxide in women with bladder pain syndrome/interstitial cystitis. *Neurourology and Urodynamics*, 36 (4), pp.1178–1186. [Online]. Available at: doi:10.1002/nau.23091 [Accessed 14 June 2024].

Chamley-Campbell, J., Campbell, G. R. and Ross, R. (1979). The smooth muscle cell in culture. *Physiological Reviews*, 59 (1), pp.1–61. [Online]. Available at: doi:10.1152/physrev.1979.59.1.1.

Chan, Y. Y. et al. (2020). The current state of tissue engineering in the management of hypospadias. *Nature Reviews. Urology*, 17 (3), pp.162–175. [Online]. Available at: doi:10.1038/s41585-020-0281-4.

Chang, S. L. et al. (1998). Role of type III collagen in bladder filling. *Neurourology and Urodynamics*, 17 (2), pp.135–145. [Online]. Available at: doi:10.1002/(SICI)1520-6777(1998)17:2<135::AID-NAU7>3.0.CO;2-E [Accessed 14 June 2024].

Chang, S. L. et al. (1999). Roles of the lamina propria and the detrusor in tension transfer during bladder filling. *Scandinavian Journal of Urology and Nephrology. Supplementum*, 201, pp.38–45. [Online]. Available at: doi:10.1080/003655999750042132.

Chang, Y. et al. (2004). Tissue regeneration patterns in acellular bovine pericardia implanted in a canine model as a vascular patch. *Journal of Biomedical Materials Research Part A*, 69A (2), pp.323–333. [Online]. Available at: doi:10.1002/jbm.a.30003 [Accessed 29 May 2024].

Chazaud, B. (2014). Macrophages: supportive cells for tissue repair and regeneration. *Immunobiology*, 219 (3), pp.172–178. [Online]. Available at: doi:10.1016/j.imbio.2013.09.001.

Chen, F., Yoo, J. J. and Atala, A. (1999). Acellular collagen matrix as a possible 'off the shelf' biomaterial for urethral repair. *Urology*, 54 (3), pp.407–410. [Online]. Available at: doi:10.1016/s0090-4295(99)00179-x.

Chen, F.-M., Zhang, M. and Wu, Z.-F. (2010). Toward delivery of multiple growth factors in tissue engineering. *Biomaterials*, 31 (24), pp.6279–6308. [Online]. Available at: doi:10.1016/j.biomaterials.2010.04.053 [Accessed 15 June 2024].

Chen, S.-C. et al. (2015). Design and evaluation of potentiometric principles for bladder volume monitoring: a preliminary study. *Sensors (Basel, Switzerland)*, 15 (6), pp.12802–12815. [Online]. Available at: doi:10.3390/s150612802.

Chowdhary, S. K. et al. (2014). Robotic augmentation ileocystoplasty with bilateral ureteric reimplantation in a young child with neuropathic bladder. *Journal of Indian Association of Pediatric Surgeons*, 19 (3), pp.162–165. [Online]. Available at: doi:10.4103/0971-9261.136473 [Accessed 15 June 2024].

Chung, Y. G. et al. (2014). Acellular Bi-Layer Silk Fibroin Scaffolds Support Tissue Regeneration in a Rabbit Model of Onlay Urethroplasty. *PLoS ONE*, 9 (3), p.e91592. [Online]. Available at: doi:10.1371/journal.pone.0091592 [Accessed 16 June 2024].

Cilento, B. G. et al. (1994). Phenotypic and cytogenetic characterization of human bladder urothelia expanded in vitro. *The Journal of Urology*, 152 (2 Pt 2), pp.665–670. [Online]. Available at: doi:10.1016/s0022-5347(17)32676-9.

Cipitria, A. et al. (2017). In-situ tissue regeneration through SDF-1α driven cell recruitment and stiffness-mediated bone regeneration in a critical-sized segmental femoral defect. *Acta Biomaterialia*, 60, pp.50–63. [Online]. Available at: doi:10.1016/j.actbio.2017.07.032.

Clementson Kockum, C., Willén, R. and Malmfors, G. (1999). Bladder augmentation with different forms of intestinal grafts: an experimental study in the pig. *BJU international*, 83 (3), pp.305–311. [Online]. Available at: doi:10.1046/j.1464-410x.1999.00895.x.

Coffin, S. T. and Gaudette, G. R. (2016). Aprotinin extends mechanical integrity time of cell-seeded fibrin sutures. *Journal of biomedical materials research. Part A*, 104 (9), pp.2271–2279. [Online]. Available at: doi:10.1002/jbm.a.35754 [Accessed 24 June 2024].

Colvert, J. R. et al. (2002). The use of small intestinal submucosa as an off-the-shelf urethral sling material for pediatric urinary incontinence. *The Journal of Urology*, 168 (4 Pt 2), pp.1872–1875; discussion 1875-1876. [Online]. Available at: doi:10.1097/01.ju.0000027285.05828.e6.

da Costa, F. D. A. et al. (2009). Thirteen years' experience with the Ross Operation. *The Journal of Heart Valve Disease*, 18 (1), pp.84–94.

Coutu, D. L. et al. (2014). Tissue Engineering of Rat Bladder Using Marrow-Derived Mesenchymal Stem Cells and Bladder Acellular Matrix. *PLoS ONE*, 9 (12), p.e111966. [Online]. Available at: doi:10.1371/journal.pone.0111966 [Accessed 16 June 2024].

Crapo, P. M., Gilbert, T. W. and Badylak, S. F. (2011). An overview of tissue and whole organ decellularization processes. *Biomaterials*, 32 (12), pp.3233–3243. [Online]. Available at: doi:10.1016/j.biomaterials.2011.01.057.

Cross, W. R. et al. (2005). A biomimetic tissue from cultured normal human urothelial cells: analysis of physiological function. *American Journal of Physiology-Renal Physiology*, 289 (2), pp.F459–F468. [Online]. Available at: doi:10.1152/ajprenal.00040.2005 [Accessed 14 June 2024].

Cruz-Diaz, O., Castellan, M. and Gosalbez, R. (2013). Use of buccal mucosa in hypospadias repair. *Current Urology Reports*, 14 (4), pp.366–372. [Online]. Available at: doi:10.1007/s11934-013-0334-9.

Dahms et al. (1998). Composition and biomechanical properties of the bladder acellular matrix graft: comparative analysis in rat, pig and human. *British Journal of Urology*, 82 (3), pp.411–419. [Online]. Available at: doi:10.1046/j.1464-410X.1998.00748.x [Accessed 15 June 2024].

Dalghi, M. G. et al. (2020). The Urothelium: Life in a Liquid Environment. *Physiological Reviews*, 100 (4), pp.1621–1705. [Online]. Available at: doi:10.1152/physrev.00041.2019 [Accessed 14 June 2024].

Daly, K. A. et al. (2012). The Host Response to Endotoxin-Contaminated Dermal Matrix. *Tissue Engineering Part A*, 18 (11–12), pp.1293–1303. [Online]. Available at: doi:10.1089/ten.tea.2011.0597 [Accessed 24 June 2024].

Dapena, L. et al. (2012). Histerocystoplasty: a novel surgical procedure in the rat. *The Journal of Surgical Research*, 175 (1), pp.157–162. [Online]. Available at: doi:10.1016/j.jss.2011.03.002.

Dapena, L. et al. (2013). Bladder autoaugmentation with protective autologous uterine flap. Experimental study in the rat. *International Journal of Surgery (London, England)*, 11 (3), pp.270–274. [Online]. Available at: doi:10.1016/j.ijsu.2013.01.012.

Davis, N. F. et al. (2010). Xenogenic extracellular matrices as potential biomaterials for interposition grafting in urological surgery. *The Journal of Urology*, 184 (6), pp.2246–2253. [Online]. Available at: doi:10.1016/j.juro.2010.07.038.

Davis, N. F. et al. (2011). Augmentation Cystoplasty and Extracellular Matrix Scaffolds: An Ex Vivo Comparative Study with Autogenous Detubularised Ileum. *PLOS ONE*, 6 (5), p.e20323. [Online]. Available at: doi:10.1371/journal.pone.0020323 [Accessed 22 May 2024].

Dewan, P. A. et al. (1994). Autoaugmentation omentocystoplasty in a sheep model. *Urology*, 43 (6), pp.888–891. [Online]. Available at: doi:10.1016/0090-4295(94)90162-7.

DiSandro, M. J. et al. (1998). Mesenchymal-epithelial interactions in bladder smooth muscle development: epithelial specificity. *The Journal of Urology*, 160 (3 Pt 2), pp.1040–1046; discussion 1079. [Online]. Available at: doi:10.1097/00005392-199809020-00022.

Dorin, R. P. et al. (2008). Tubularized urethral replacement with unseeded matrices: what is the maximum distance for normal tissue regeneration? *World Journal of Urology*, 26 (4), pp.323–326. [Online]. Available at: doi:10.1007/s00345-008-0316-6.

Draper, J. W., Stark, R. B. and Lau, M. W. (1952). Replacement of mucous membrane of urinary bladder with thick-split grafts of skin: experimental observations. *Plastic and Reconstructive Surgery (1946)*, 10 (4), pp.252–259. [Online]. Available at: doi:10.1097/00006534-195210000-00005.

Drewa, T. et al. (2008). Chitosan scaffold enhances nerve regeneration within the in vitro reconstructed bladder wall: an animal study. *Urologia Internationalis*, 81 (3), pp.330–334. [Online]. Available at: doi:10.1159/000151414.

Duckett, J. W. et al. (1995). Buccal mucosal urethral replacement. *The Journal of Urology*, 153 (5), pp.1660–1663.

Ehdaie, B. et al. (2013). Bladder perforation in augmentation cystoplasty during urodynamic investigation: a case report and review of the literature. *Journal of Pediatric Urology*, 9 (2), pp.e102-106. [Online]. Available at: doi:10.1016/j.jpurol.2012.11.013.

Elbahnasy, A. M. et al. (1998). Bladder wall substitution with synthetic and non-intestinal organic materials. *The Journal of Urology*, 159 (3), pp.628–637.

Elliott, S. P. et al. (2002). Complete laparoscopic ileal cystoplasty. *Urology*, 59 (6), pp.939–943. [Online]. Available at: doi:10.1016/s0090-4295(02)01605-9.

Engelhardt, E.-M. et al. (2010). Compressed collagen gel: a novel scaffold for human bladder cells. *Journal of Tissue Engineering and Regenerative Medicine*, 4 (2), pp.123–130. [Online]. Available at: doi:10.1002/term.222.

Engler, A. J. et al. (2006). Matrix elasticity directs stem cell lineage specification. *Cell*, 126 (4), pp.677–689. [Online]. Available at: doi:10.1016/j.cell.2006.06.044.

Evren, S. et al. (2010). Urinary Bladder Tissue Engineering Using Natural Scaffolds in a Porcine Model: Role of Toll-Like Receptors and Impact of Biomimetic Molecules. *Cells Tissues Organs*, 192 (4), pp.250–261. [Online]. Available at: doi:10.1159/000317332 [Accessed 15 June 2024].

Fairbairn, L. et al. (2011). The mononuclear phagocyte system of the pig as a model for understanding human innate immunity and disease. *Journal of Leukocyte Biology*, 89 (6), pp.855–871. [Online]. Available at: doi:10.1189/jlb.1110607.

Farhat, W. et al. (2003). Porosity of porcine bladder acellular matrix: impact of ACM thickness. *Journal of Biomedical Materials Research. Part A*, 67 (3), pp.970–974. [Online]. Available at: doi:10.1002/jbm.a.10171.

Farhat, W. A. and Yeger, H. (2008). Does mechanical stimulation have any role in urinary bladder tissue engineering? *World Journal of Urology*, 26 (4), pp.301–305. [Online]. Available at: doi:10.1007/s00345-008-0318-4.

Faure, A. et al. (2016). Two-stage graft urethroplasty for proximal and complicated hypospadias in children: A retrospective study. *Journal of Pediatric Urology*, 12 (5), p.286.e1-286.e7. [Online]. Available at: doi:10.1016/j.jpurol.2016.02.014.

Feil, G. et al. (2006). Investigations of urothelial cells seeded on commercially available small intestine submucosa. *European Urology*, 50 (6), pp.1330–1337. [Online]. Available at: doi:10.1016/j.eururo.2006.05.041.

Fishman, I. J. et al. (1987). Use of fresh placental membranes for bladder reconstruction. *The Journal of Urology*, 138 (5), pp.1291–1294. [Online]. Available at: doi:10.1016/s0022-5347(17)43586-5.

Flieger, A. et al. (2008). Primary Cultures of Human Urothelial Cells for Genotoxicity Testing. *Journal of Toxicology and Environmental Health, Part A*, 71 (13–14), pp.930–935. [Online]. Available at: doi:10.1080/15287390801988939 [Accessed 16 June 2024].

Fowler, C. J. et al. (2012). OnabotulinumtoxinA improves health-related quality of life in patients with urinary incontinence due to idiopathic overactive bladder: a 36-week, double-blind, placebo-controlled, randomized, dose-ranging trial. *European Urology*, 62 (1), pp.148–157. [Online]. Available at: doi:10.1016/j.eururo.2012.03.005.

Fraser, M. et al. (2004). A surgical model of composite cystoplasty with cultured urothelial cells: a controlled study of gross outcome and urothelial phenotype. *BJU international*, 93 (4), pp.609–616. [Online]. Available at: doi:10.1111/j.1464-410x.2003.04675.x.

Freytes, D. O. et al. (2004). Biaxial strength of multilaminated extracellular matrix scaffolds. *Biomaterials*, 25 (12), pp.2353–2361. [Online]. Available at: doi:10.1016/j.biomaterials.2003.09.015.

Freytes, D. O. et al. (2008). Hydrated versus lyophilized forms of porcine extracellular matrix derived from the urinary bladder. *Journal of Biomedical Materials Research. Part A*, 87 (4), pp.862–872. [Online]. Available at: doi:10.1002/jbm.a.31821.

Freytes, D. O. and Badylak, S. F. (2006). Sterilization of Biologic Scaffold Materials. In: *Encyclopedia of Medical Devices and Instrumentation*. John Wiley & Sons, Ltd. [Online]. Available at: doi:10.1002/0471732877.emd241 [Accessed 30 June 2024].

Frömter, E. and Diamond, J. (1972). Route of passive ion permeation in epithelia. *Nature: New Biology*, 235 (53), pp.9–13. [Online]. Available at: doi:10.1038/newbio235009a0.

Fujita, K. (1978). The use of resin-sprayed thin paper for urinary bladder regeneration. *Investigative Urology*, 15 (5), pp.355–357.

Fujiyama, C., Masaki, Z. and Sugihara, H. (1995). Reconstruction of the urinary bladder mucosa in three-dimensional collagen gel culture: fibroblast-extracellular matrix interactions on the differentiation of transitional epithelial cells. *The Journal of Urology*, 153 (6), pp.2060–2067.

Furthmayr, H. and Timpl, R. (1976). Immunochemistry of collagens and procollagens. *International Review of Connective Tissue Research*, 7, pp.61–99. [Online]. Available at: doi:10.1016/b978-0-12-363707-9.50008-3.

Furukawa, S., Nagaike, M. and Ozaki, K. (2017). Databases for technical aspects of immunohistochemistry. *Journal of Toxicologic Pathology*, 30 (1), pp.79–107. [Online]. Available at: doi:10.1293/tox.2016-0047.

Gabella, G. and Uvelius, B. (1990). Urinary bladder of rat: fine structure of normal and hypertrophic musculature. *Cell and Tissue Research*, 262 (1), pp.67–79. [Online]. Available at: doi:10.1007/BF00327747.

Gakis, G. et al. (2011). Functional detrusor myoplasty for bladder acontractility: long-term results. *The Journal of Urology*, 185 (2), pp.593–599. [Online]. Available at: doi:10.1016/j.juro.2010.09.112.

Gattazzo, F., Urciuolo, A. and Bonaldo, P. (2014). Extracellular matrix: a dynamic microenvironment for stem cell niche. *Biochimica Et Biophysica Acta*, 1840 (8), pp.2506–2519. [Online]. Available at: doi:10.1016/j.bbagen.2014.01.010.

Gaudio, C. D. et al. (2013). Evaluation of electrospun bioresorbable scaffolds for tissue-engineered urinary bladder augmentation. *Biomedical Materials*, 8 (4), p.045013. [Online]. Available at: doi:10.1088/1748-6041/8/4/045013 [Accessed 17 June 2024].

German, K. et al. (1994). An assessment of the contribution of visco-elastic factors in the aetiology of poor compliance in the human neuropathic bladder. *British Journal of Urology*, 74 (6), pp.744–748. [Online]. Available at: doi:10.1111/j.1464-410x.1994.tb07118.x.

Gilbert, T. W. et al. (2008). Collagen fiber alignment and biaxial mechanical behavior of porcine urinary bladder derived extracellular matrix. *Biomaterials*, 29 (36), pp.4775–4782. [Online]. Available at: doi:10.1016/j.biomaterials.2008.08.022.

Gilbert, T. W., Sellaro, T. L. and Badylak, S. F. (2006). Decellularization of tissues and organs. *Biomaterials*, 27 (19), pp.3675–3683. [Online]. Available at: doi:10.1016/j.biomaterials.2006.02.014.

Gilpin, A. and Yang, Y. (2017). Decellularization Strategies for Regenerative Medicine: From Processing Techniques to Applications. *BioMed Research International*, 2017, pp.1–13. [Online]. Available at: doi:10.1155/2017/9831534 [Accessed 12 March 2025].

Gloeckner, D. et al. (1999). Active and passive biaxial mechanical properties of urinary bladder wall. In: *Proceedings of the First Joint BMES/EMBS Conference. 1999 IEEE Engineering in Medicine and Biology 21st Annual Conference and the 1999 Annual Fall Meeting of the Biomedical Engineering Society (Cat. N*. 1. 1999. IEEE. pp.17-vol. [Online]. Available at: https://ieeexplore.ieee.org/abstract/document/802036/ [Accessed 21 June 2024].

Gloeckner, D. C. et al. (2002). Passive Biaxial Mechanical Properties of the Rat Bladder Wall After Spinal Cord Injury. *Journal of Urology*, 167 (5), pp.2247–2252. [Online]. Available at: doi:10.1016/S0022-5347(05)65137-3 [Accessed 21 June 2024].

Goldstein, M. B. and Dearden, L. C. (1966). Histology of omentoplasty of the urinary bladder in the rabbit. *Investigative Urology*, 3 (5), pp.460–469.

Gomez, P. et al. (2011). The effect of manipulation of silk scaffold fabrication parameters on matrix performance in a murine model of bladder augmentation. *Biomaterials*, 32 (30), pp.7562–7570. [Online]. Available at: doi:10.1016/j.biomaterials.2011.06.067 [Accessed 17 June 2024].

González-Mariscal, L. et al. (2003). Tight junction proteins. *Progress in Biophysics and Molecular Biology*, 81 (1), pp.1–44. [Online]. Available at: doi:10.1016/s0079-6107(02)00037-8.

Gosztyla, C. et al. (2020). A Comparison of Sterilization Techniques for Production of Decellularized Intestine in Mice. *Tissue Engineering. Part C, Methods*, 26 (2), pp.67–79. [Online]. Available at: doi:10.1089/ten.TEC.2019.0219.

Gray, M., Guido, S. and Kugadas, A. (2022). Editorial: The use of large animal models to improve pre-clinical translational research. *Frontiers in Veterinary Science*, 9, p.1086912. [Online]. Available at: doi:10.3389/fvets.2022.1086912.

Greaves, N. S. et al. (2013). Single-stage application of a novel decellularized dermis for treatment-resistant lower limb ulcers: Positive outcomes assessed by SIAscopy, laser perfusion, and 3D imaging, with sequential timed histological analysis. *Wound Repair and Regeneration*, 21 (6), pp.813–822. [Online]. Available at: doi:10.1111/wrr.12113 [Accessed 16 June 2024].

Greaves, N. S. et al. (2015). Acute Cutaneous Wounds Treated with Human Decellularised Dermis Show Enhanced Angiogenesis during Healing. *PLoS ONE*, 10 (1), p.e0113209. [Online]. Available at: doi:10.1371/journal.pone.0113209 [Accessed 16 June 2024].

Greenwell, T. J., Venn, S. N. and Mundy, A. R. (2001). Augmentation cystoplasty. *BJU international*, 88 (6), pp.511–525. [Online]. Available at: doi:10.1046/j.1464-4096.2001.001206.

Gundeti, M. S., Acharya, S. S. and Zagaja, G. P. (2009). The University of Chicago technique of complete intracorporeal pediatric robotic-assisted laparoscopic augmentation ileocystoplasty and Mitrofanoff appendicovesicostomy. *Journal of Robotic Surgery*, 3 (2), pp.89–93. [Online]. Available at: doi:10.1007/s11701-009-0137-7.

Gurocak, S. et al. (2007). Bladder augmentation: Review of the literature and recent advances. *Indian Journal of Urology : IJU : Journal of the Urological Society of India*, 23 (4), pp.452–457. [Online]. Available at: doi:10.4103/0970-1591.36721 [Accessed 15 June 2024].

Hafez, A. T. et al. (2003). Aerosol transfer of bladder urothelial and smooth muscle cells onto demucosalized colonic segments: a pilot study. *The Journal of Urology*, 169 (6), pp.2316–2319; discussion 2320. [Online]. Available at: doi:10.1097/01.ju.0000067485.51252.f5.

Hafez, A. T. et al. (2005). Aerosol transfer of bladder urothelial and smooth muscle cells onto demucosalized colonic segments for porcine bladder augmentation in vivo: a 6-week experimental study. *The Journal of Urology*, 174 (4 Pt 2), pp.1663–1667; discussion 1667-1668. [Online]. Available at: doi:10.1097/01.ju.0000177727.56790.98.

Hattori, K. et al. (2006). Bladder reconstruction using a collagen patch prefabricated within the omentum. *International Journal of Urology: Official Journal of the Japanese Urological Association*, 13 (5), pp.529–537. [Online]. Available at: doi:10.1111/j.1442-2042.2006.01351.x.

Heise, R. L. et al. (2009). Generating Elastin-Rich Small Intestinal Submucosa–Based Smooth Muscle Constructs Utilizing Exogenous Growth Factors and Cyclic Mechanical Stimulation. *Tissue Engineering. Part A*, 15 (12), pp.3951–3960. [Online]. Available at: doi:10.1089/ten.tea.2009.0044 [Accessed 29 June 2024].

Helliwell, J. A. et al. (2017). Development and characterisation of a low-concentration sodium dodecyl sulphate decellularised porcine dermis. *Journal of Tissue Engineering*, 8, p.2041731417724011. [Online]. Available at: doi:10.1177/2041731417724011 [Accessed 16 June 2024].

Hickman, D. L. et al. (2017). Commonly Used Animal Models. *Principles of Animal Research for Graduate and Undergraduate Students*, pp.117–175. [Online]. Available at: doi:10.1016/B978-0-12-802151-4.00007-4 [Accessed 29 June 2024].

Hicks, R. M. (1965). The fine structure of the transitional epithelium of rat ureter. *The Journal of Cell Biology*, 26 (1), pp.25–48. [Online]. Available at: doi:10.1083/jcb.26.1.25.

Hicks, R. M. (1975). The Mammalian Urinary Bladderan Accommodating Organ. *Biological Reviews*, 50 (2), pp.215–246. [Online]. Available at: doi:10.1111/j.1469-185X.1975.tb01057.x [Accessed 14 June 2024].

Hidas, G. et al. (2015). Aerosol transfer of bladder urothelial and smooth muscle cells onto demucosalized colonic segments for bladder augmentation: in vivo, long term, and functional pilot study. *Journal of Pediatric Urology*, 11 (5), p.260.e1-6. [Online]. Available at: doi:10.1016/j.jpurol.2015.02.020.

Hinz, B. (2016). The role of myofibroblasts in wound healing. *Current Research in Translational Medicine*, 64 (4), pp.171–177. [Online]. Available at: doi:10.1016/j.retram.2016.09.003.

Hodde, J. et al. (2007). Effects of sterilization on an extracellular matrix scaffold: part I. Composition and matrix architecture. *Journal of Materials Science. Materials in Medicine*, 18 (4), pp.537–543. [Online]. Available at: doi:10.1007/s10856-007-2300-x.

Hodde, J. and Hiles, M. (2002). Virus safety of a porcine-derived medical device: evaluation of a viral inactivation method. *Biotechnology and Bioengineering*, 79 (2), pp.211–216. [Online]. Available at: doi:10.1002/bit.10281.

Hogg, P. et al. (2015). Development of a terminally sterilised decellularised dermis. *Cell and Tissue Banking*, 16 (3), pp.351–359. [Online]. Available at: doi:10.1007/s10561-014-9479-0.

Horsley, H. et al. (2018). A urine-dependent human urothelial organoid offers a potential alternative to rodent models of infection. *Scientific Reports*, 8, p.1238. [Online]. Available at: doi:10.1038/s41598-018-19690-7 [Accessed 14 June 2024].

Horst, M. et al. (2014). Increased porosity of electrospun hybrid scaffolds improved bladder tissue regeneration. *Journal of Biomedical Materials Research Part A*, 102 (7), pp.2116–2124. [Online]. Available at: doi:10.1002/jbm.a.34889 [Accessed 17 June 2024].

Horst, M. et al. (2019). Tissue Engineering in Pediatric Bladder Reconstruction—The Road to Success. *Frontiers in Pediatrics*, 7, p.91. [Online]. Available at: doi:10.3389/fped.2019.00091 [Accessed 30 June 2024].

Hu, B. and Phan, S. H. (2013). Myofibroblasts. *Current Opinion in Rheumatology*, 25 (1), pp.71–77. [Online]. Available at: doi:10.1097/BOR.0b013e32835b1352.

Hu, P. et al. (2000). Ablation of Uroplakin III Gene Results in Small Urothelial Plaques, Urothelial Leakage, and Vesicoureteral Reflux. *Journal of Cell Biology*, 151 (5), pp.961–972. [Online]. Available at: doi:10.1083/jcb.151.5.961 [Accessed 14 June 2024].

Hu, P. et al. (2002). Role of membrane proteins in permeability barrier function: uroplakin ablation elevates urothelial permeability. *American Journal of Physiology-Renal Physiology*, 283 (6), pp.F1200–F1207. [Online]. Available at: doi:10.1152/ajprenal.00043.2002 [Accessed 14 June 2024].

Huang, Q. et al. (2004). Use of peracetic acid to sterilize human donor skin for production of acellular dermal matrices for clinical use. *Wound repair and regeneration : official publication of the Wound Healing Society [and] the European Tissue Repair Society*, 12, pp.276–287. [Online]. Available at: doi:10.1111/j.1067-1927.2004.012312.x.

Hubbell, J. A. (2003). Materials as morphogenetic guides in tissue engineering. *Current Opinion in Biotechnology*, 14 (5), pp.551–558. [Online]. Available at: doi:10.1016/j.copbio.2003.09.004 [Accessed 17 June 2024].

Hubrecht, R. C. and Carter, E. (2019). The 3Rs and Humane Experimental Technique: Implementing Change. *Animals : an Open Access Journal from MDPI*, 9 (10), p.754. [Online]. Available at: doi:10.3390/ani9100754 [Accessed 27 June 2024].

Hussein, K. H. et al. (2013). Sterilization using electrolyzed water highly retains the biological properties in tissue-engineered porcine liver scaffold. *The International Journal of Artificial Organs*, 36 (11), pp.781–792. [Online]. Available at: doi:10.5301/ijao.5000246.

Hustler, A. et al. (2018). Differential transcription factor expression by human epithelial cells of buccal and urothelial derivation. *Experimental Cell Research*, 369 (2), pp.284–294. [Online]. Available at: doi:10.1016/j.yexcr.2018.05.031 [Accessed 14 June 2024].

Hutschenreiter, G. et al. (1978). The free peritoneal transplant as substitute for the urinary bladder wall. *Investigative Urology*, 15 (5), pp.375–379.

Ikeguchi, E. F., Stifelman, M. D. and Hensle, T. W. (1998). Ureteral tissue expansion for bladder augmentation. *The Journal of Urology*, 159 (5), pp.1665–1668. [Online]. Available at: doi:10.1097/00005392-199805000-00086.

Itoh, S. et al. (2002). Evaluation of cross-linking procedures of collagen tubes used in peripheral nerve repair. *Biomaterials*, 23 (23), pp.4475–4481. [Online]. Available at: doi:10.1016/S0142-9612(02)00166-7 [Accessed 30 June 2024].

Jack, G. S. et al. (2009). Urinary Bladder Smooth Muscle Engineered from Adipose Stem Cells and a Three Dimensional Synthetic Composite. *Biomaterials*, 30 (19), p.3259. [Online]. Available at: doi:10.1016/j.biomaterials.2009.02.035 [Accessed 17 June 2024].

Jackson, D. W., Windler, G. E. and Simon, T. M. (1990). Intraarticular reaction associated with the use of freeze-dried, ethylene oxide-sterilized bone-patella tendon-bone allografts in the reconstruction of the anterior cruciate ligament. *The American Journal of Sports Medicine*, 18 (1), pp.1–10; discussion 10-11. [Online]. Available at: doi:10.1177/036354659001800101.

Janssen, D. A. W. et al. (2013). The distribution and function of chondroitin sulfate and other sulfated glycosaminoglycans in the human bladder and their contribution to the protective bladder barrier. *The Journal of Urology*, 189 (1), pp.336–342. [Online]. Available at: doi:10.1016/j.juro.2012.09.022.

Jayo, M. J. et al. (2008). Long-term durability, tissue regeneration and neo-organ growth during skeletal maturation with a neo-bladder augmentation construct. *Regenerative Medicine*, 3 (5), pp.671–682. [Online]. Available at: doi:10.2217/17460751.3.5.671.

Jednak, R. (2014). The Evolution of Bladder Augmentation: From Creating a Reservoir to Reconstituting an Organ. *Frontiers in Pediatrics*, 2, p.10. [Online]. Available at: doi:10.3389/fped.2014.00010 [Accessed 16 June 2024].

Jelly, O. (2010). Segmental Cystectomy with Peritoneoplasty. *Urologia Internationalis*, 25 (3), pp.236–244. [Online]. Available at: doi:10.1159/000279676 [Accessed 16 June 2024].

Jinot, J. et al. (2018). Carcinogenicity of ethylene oxide: key findings and scientific issues. *Toxicology Mechanisms and Methods*, 28 (5), pp.386–396. [Online]. Available at: doi:10.1080/15376516.2017.1414343.

Johnson, H. W. et al. (1994). Laboratory variables of bladderautoaugmentation in an animal model. *Urology*, 44 (2), pp.260–263. [Online]. Available at: doi:10.1016/S0090-4295(94)80145-2 [Accessed 15 June 2024].

Jokandan, M. S. et al. (2018). Bladder wall biomechanics: A comprehensive study on fresh porcine urinary bladder. *Journal of the Mechanical Behavior of Biomedical Materials*, 79, pp.92–103. [Online]. Available at: doi:10.1016/j.jmbbm.2017.11.034.

Jones, G. et al. (2017). Decellularization and Characterization of Porcine Superflexor Tendon: A Potential Anterior Cruciate Ligament Replacement. *Tissue Engineering. Part A*, 23 (3–4), pp.124–134. [Online]. Available at: doi:10.1089/ten.tea.2016.0114 [Accessed 16 June 2024].

Jorge-Herrero, E. et al. (1994). Inhibition of the calcification of porcine valve tissue by selective lipid removal. *Biomaterials*, 15 (10), pp.815–820. [Online]. Available at: doi:10.1016/0142-9612(94)90036-1.

Jubber, I. et al. (2023). Epidemiology of Bladder Cancer in 2023: A Systematic Review of Risk Factors. *European Urology*, 84 (2), pp.176–190. [Online]. Available at: doi:10.1016/j.eururo.2023.03.029.

Kajbafzadeh, A.-M. et al. (2014). Bladder muscular wall regeneration with autologous adipose mesenchymal stem cells on three-dimensional collagen-based tissue-engineered prepuce and biocompatible nanofibrillar scaffold. *Journal of Pediatric Urology*, 10 (6), pp.1051–1058. [Online]. Available at: doi:10.1016/j.jpurol.2014.03.010 [Accessed 17 June 2024].

Kambic, H. et al. (1992). Biodegradable pericardial implants for bladder augmentation: a 2.5-year study in dogs. *The Journal of Urology*, 148 (2 Pt 2), pp.539–543. [Online]. Available at: doi:10.1016/s0022-5347(17)36649-1.

Kanematsu, A. et al. (2003). Bladder regeneration by bladder acellular matrix combined with sustained release of exogenous growth factor. *The Journal of Urology*, 170 (4 Pt 2), pp.1633–1638. [Online]. Available at: doi:10.1097/01.ju.0000084021.51099.8a.

Kapetanovic, R. et al. (2012). Pig bone marrow-derived macrophages resemble human macrophages in their response to bacterial lipopolysaccharide. *Journal of Immunology (Baltimore, Md.: 1950)*, 188 (7), pp.3382–3394. [Online]. Available at: doi:10.4049/jimmunol.1102649.

Kara Özenler, A. et al. (2021). Development of biological meniscus scaffold: Decellularization method and recellularization with meniscal cell population derived from mesenchymal stem cells. *Journal of Biomaterials Applications*, 35, p.088532822098118. [Online]. Available at: doi:10.1177/0885328220981189.

Kaully, T. et al. (2009). Vascularization--the conduit to viable engineered tissues. *Tissue Engineering. Part B, Reviews*, 15 (2), pp.159–169. [Online]. Available at: doi:10.1089/ten.teb.2008.0193.

Kaya, C. et al. (2016). The Role of Extracellular Matrix Proteins in the Urinary Tract: A Literature Review. In: *Composition and Function of the Extracellular Matrix in the Human Body*. IntechOpen. [Online]. Available at: doi:10.5772/62807 [Accessed 21 June 2024].

Keane, T. J. et al. (2012). Consequences of ineffective decellularization of biologic scaffolds on the host response. *Biomaterials*, 33 (6), pp.1771–1781. [Online]. Available at: doi:10.1016/j.biomaterials.2011.10.054.

Keane, T. J., Saldin, L. T. and Badylak, S. F. (2016). 4 - Decellularization of mammalian tissues: Preparing extracellular matrix bioscaffolds. In: Tomlins, P. (Ed). *Characterisation and Design of Tissue Scaffolds*. Woodhead Publishing Series in Biomaterials. Woodhead Publishing. pp.75–103. [Online]. Available at: doi:10.1016/B978-1-78242-087-3.00004-3 [Accessed 23 June 2024].

Keane, T. J., Swinehart, I. T. and Badylak, S. F. (2015). Methods of tissue decellularization used for preparation of biologic scaffolds and *in vivo* relevance. *Methods*, 84, pp.25–34. [Online]. Available at: doi:10.1016/j.ymeth.2015.03.005 [Accessed 23 May 2024].

Keay, S. et al. (2000). Bladder epithelial cells from patients with interstitial cystitis produce an inhibitor of heparin-binding epidermal growth factor-like growth factor production. *The Journal of Urology*, 164 (6), pp.2112–2118.

Keay, S. et al. (2003). Decreased in vitro proliferation of bladder epithelial cells from patients with interstitial cystitis. *Urology*, 61 (6), pp.1278–1284. [Online]. Available at: doi:10.1016/s0090-4295(03)00005-0.

Kelâmi, A. et al. (1970). Experimental investigations of bladder regeneration using teflon-felt as a bladder wall substitute. *The Journal of Urology*, 104 (5), pp.693–698. [Online]. Available at: doi:10.1016/s0022-5347(17)61813-5.

Kelâmi, A. (1971). Lyophilized human dura as a bladder wall substitute: experimental and clinical results. *The Journal of Urology*, 105 (4), pp.518–522. [Online]. Available at: doi:10.1016/s0022-5347(17)61563-5.

Khan, U. and Bayat, A. (2019). Microarchitectural analysis of decellularised unscarred and scarred dermis provides insight into the organisation and ultrastructure of the human skin with implications for future dermal substitute scaffold design. *Journal of Tissue Engineering*, 10, p.2041731419843710. [Online]. Available at: doi:10.1177/2041731419843710.

Khandelwal, P., Abraham, S. N. and Apodaca, G. (2009). Cell biology and physiology of the uroepithelium. *American Journal of Physiology. Renal Physiology*, 297 (6), pp.F1477-1501. [Online]. Available at: doi:10.1152/ajprenal.00327.2009.

Khor, E. (1997). Methods for the treatment of collagenous tissues for bioprostheses. *Biomaterials*, 18 (2), pp.95–105. [Online]. Available at: doi:10.1016/s0142-9612(96)00106-8.

Khoury, J. M. et al. (1992). Complications of enterocystoplasty. *Urology*, 40 (1), pp.9–14. [Online]. Available at: doi:10.1016/0090-4295(92)90428-y.

Kikuno, N. et al. (2009). Nerve growth factor combined with vascular endothelial growth factor enhances regeneration of bladder acellular matrix graft in spinal cord injury-induced neurogenic rat bladder. *BJU international*, 103 (10), pp.1424–1428. [Online]. Available at: doi:10.1111/j.1464-410X.2008.08129.x.

Kim, B. S. et al. (1999). Cyclic mechanical strain regulates the development of engineered smooth muscle tissue. *Nature Biotechnology*, 17 (10), pp.979–983. [Online]. Available at: doi:10.1038/13671.

Kim, B. S., Baez, C. E. and Atala, A. (2000). Biomaterials for tissue engineering. *World Journal of Urology*, 18 (1), pp.2–9. [Online]. Available at: doi:10.1007/s003450050002.

Kim, B. S. and Mooney, D. J. (2000). Scaffolds for engineering smooth muscle under cyclic mechanical strain conditions. *Journal of Biomechanical Engineering*, 122 (3), pp.210–215. [Online]. Available at: doi:10.1115/1.429651.

Kim, K. M. (1976). Calcification of matrix vesicles in human aortic valve and aortic media. *Federation Proceedings*, 35 (2), pp.156–162.

Kimmel, H. and Gittleman, H. (2017). Retrospective observational analysis of the use of an architecturally unique dermal regeneration template (Derma Pure®) for the treatment of hard-to-heal wounds. *International Wound Journal*, 14 (4), pp.666–672. [Online]. Available at: doi:10.1111/iwj.12667.

Kimuli, M., Eardley, I. and Southgate, J. (2004). In vitro assessment of decellularized porcine dermis as a matrix for urinary tract reconstruction. *BJU international*, 94 (6), pp.859–866. [Online]. Available at: doi:10.1111/j.1464-410X.2004.05047.x.

Kiricuta, I. and Goldstein, A. M. B. (1972). The Repair of Extensive Vesicovaginal Fistulas with Pedicled Omentum: A Review of 27 Cases. *Journal of Urology*, 108 (5), pp.724–727. [Online]. Available at: doi:10.1016/S0022-5347(17)60851-6 [Accessed 15 June 2024].

Kispal, Z. et al. (2011). Complications after bladder augmentation or substitution in children: a prospective study of 86 patients. *BJU international*, 108 (2), pp.282–289. [Online]. Available at: doi:10.1111/j.1464-410X.2010.09862.x.

Kitta, T. et al. (2018). Benefits and limitations of animal models in partial bladder outlet obstruction for translational research. *International Journal of Urology: Official Journal of the Japanese Urological Association*, 25 (1), pp.36–44. [Online]. Available at: doi:10.1111/iju.13471.

Kitta, T. et al. (2020). Animal Model for Lower Urinary Tract Dysfunction in Parkinson's Disease. *International Journal of Molecular Sciences*, 21 (18), p.6520. [Online]. Available at: doi:10.3390/ijms21186520.

Korossis, S. et al. (2009). Regional biomechanical and histological characterisation of the passive porcine urinary bladder: Implications for augmentation and tissue engineering strategies. *Biomaterials*, 30 (2), pp.266–275. [Online]. Available at: doi:10.1016/j.biomaterials.2008.09.034 [Accessed 22 May 2024].

Korossis, S. A. et al. (2002). Tissue engineering of cardiac valve prostheses II: biomechanical characterization of decellularized porcine aortic heart valves. *The Journal of Heart Valve Disease*, 11 (4), pp.463–471.

Kotecha, R. and Toledo-Pereyra, L. H. (2012). Hysterocystoplasty: a new surgical technique for bladder reconstruction. *The Journal of Surgical Research*, 176 (2), pp.397–399. [Online]. Available at: doi:10.1016/j.jss.2011.05.011.

Kropp, B. P. et al. (1995). Experimental assessment of small intestinal submucosa as a bladder wall substitute. *Urology*, 46 (3), pp.396–400. [Online]. Available at: doi:10.1016/S0090-4295(99)80227-1.

Kropp, B. P. et al. (1996a). Characterization of small intestinal submucosa regenerated canine detrusor: assessment of reinnervation, in vitro compliance and contractility. *The Journal of Urology*, 156 (2 Pt 2), pp.599–607. [Online]. Available at: doi:10.1097/00005392-199608001-00008.

Kropp, B. P. et al. (1996b). Regenerative urinary bladder augmentation using small intestinal submucosa: urodynamic and histopathologic assessment in long-term canine bladder augmentations. *The Journal of Urology*, 155 (6), pp.2098–2104. [Online]. Available at: doi:10.1016/s0022-5347(01)66117-2.

Kropp, B. P. et al. (2004). Reliable and reproducible bladder regeneration using unseeded distal small intestinal submucosa. *The Journal of Urology*, 172 (4 Pt 2), pp.1710–1713. [Online]. Available at: doi:10.1097/01.ju.0000139952.64753.27.

Kruse, M. N., Bray, L. A. and de Groat, W. C. (1995). Influence of spinal cord injury on the morphology of bladder afferent and efferent neurons. *Journal of the Autonomic Nervous System*, 54 (3), pp.215–224. [Online]. Available at: doi:10.1016/0165-1838(95)00011-l.

Kudish, H. G. (1957). The use of polyvinyl sponge for experimental cystoplasty. *The Journal of Urology*, 78 (3), pp.232–235. [Online]. Available at: doi:10.1016/S0022-5347(17)66428-0.

Kuzin, V. V. et al. (2023). Using aerosols to decontaminate surfaces from nucleic acids. *Microbiology Independent Research Journal (MIR Journal)*, 10 (1). [Online]. Available at: doi:10.18527/2500-2236-2023-10-1-1-12 [Accessed 12 March 2025].

Kwon, T. G., Yoo, J. J. and Atala, A. (2008). Local and systemic effects of a tissue engineered neobladder in a canine cystoplasty model. *The Journal of Urology*, 179 (5), pp.2035–2041. [Online]. Available at: doi:10.1016/j.juro.2008.01.005.

Lakshmanan, Y. et al. (2005). Human embryoid body-derived stem cells in co-culture with bladder smooth muscle and urothelium. *Urology*, 65 (4), pp.821–826. [Online]. Available at: doi:10.1016/j.urology.2004.11.022 [Accessed 16 June 2024].

Lamoine, G. (1913). Creation d'une vessie nouvelle par un procede personnel apres cystectomie total pour cancer. *J d'Urol*, 4, pp.367–370. [Online]. Available at: https://cir.nii.ac.jp/crid/1571135649957651840 [Accessed 16 June 2024].

Langer, R. and Vacanti, J. P. (1993). Tissue engineering. *Science (New York, N.Y.)*, 260 (5110), pp.920–926. [Online]. Available at: doi:10.1126/science.8493529.

Langer, S. et al. (2019). Bladder augmentation in children: current problems and experimental strategies for reconstruction. *Wiener Medizinische Wochenschrift (1946)*, 169 (3), pp.61–70. [Online]. Available at: doi:10.1007/s10354-018-0645-z [Accessed 15 June 2024].

Lavelle, J. et al. (2002). Bladder permeability barrier: recovery from selective injury of surface epithelial cells. *American Journal of Physiology. Renal Physiology*, 283 (2), pp.F242-253. [Online]. Available at: doi:10.1152/ajprenal.00307.2001.

Ledet, E. H. et al. (2002). A pilot study to evaluate the effectiveness of small intestinal submucosa used to repair spinal ligaments in the goat. *The Spine Journal*, 2 (3), pp.188–196. [Online]. Available at: doi:10.1016/S1529-9430(02)00182-1 [Accessed 16 June 2024].

Lee, C. H. et al. (2010). Regeneration of the articular surface of the rabbit synovial joint by cell homing: a proof of concept study. *Lancet*, 376 (9739), pp.440–448. [Online]. Available at: doi:10.1016/S0140-6736(10)60668-X [Accessed 15 June 2024].

Lee, T. et al. (2017). Bladder perforation after augmentation cystoplasty: Determining the best management option. *Journal of Pediatric Urology*, 13 (3), p.274.e1-274.e7. [Online]. Available at: doi:10.1016/j.jpurol.2016.12.027 [Accessed 15 June 2024].

Leitner, L. et al. (2016). More Than 15 Years of Experience with Intradetrusor OnabotulinumtoxinA Injections for Treating Refractory Neurogenic Detrusor Overactivity: Lessons to Be Learned. *European Urology*, 70 (3), pp.522–528. [Online]. Available at: doi:10.1016/j.eururo.2016.03.052 [Accessed 15 June 2024].

Leong, C. H. and Ong, G. B. (1972). Gastrocystoplasty in dogs. *The Australian and New Zealand Journal of Surgery*, 41 (3), pp.272–279.

Leong, C. H. and Ong, G. B. (1975). Proceedings: gastrocystoplasty. *British Journal of Urology*, 47 (2), p.236.

Leonhäuser, D. et al. (2017). Two differentially structured collagen scaffolds for potential urinary bladder augmentation: proof of concept study in a Göttingen minipig model. *Journal of Translational Medicine*, 15 (1), p.3. [Online]. Available at: doi:10.1186/s12967-016-1112-5.

Levy, R. J. et al. (2003). Inhibition of cusp and aortic wall calcification in ethanol- and aluminum-treated bioprosthetic heart valves in sheep: background, mechanisms, and synergism. *The Journal of Heart Valve Disease*, 12 (2), pp.209–216; discussion 216.

Lewis, S. A. (2000). Everything you wanted to know about the bladder epithelium but were afraid to ask. *American Journal of Physiology. Renal Physiology*, 278 (6), pp.F867-874. [Online]. Available at: doi:10.1152/ajprenal.2000.278.6.F867.

Li, L. and Xie, T. (2005). Stem cell niche: structure and function. *Annual Review of Cell and Developmental Biology*, 21, pp.605–631. [Online]. Available at: doi:10.1146/annurev.cellbio.21.012704.131525.

Li, Z. et al. (2016). Macrophages Undergo M1-to-M2 Transition in Adipose Tissue Regeneration in a Rat Tissue Engineering Model. *Artificial Organs*, 40 (10), pp.E167–E178. [Online]. Available at: doi:10.1111/aor.12756.

Liang, R. et al. (2006). Long-term effects of porcine small intestine submucosa on the healing of medial collateral ligament: A functional tissue engineering study. *Journal of Orthopaedic Research*, 24 (4), pp.811–819. [Online]. Available at: doi:10.1002/jor.20080 [Accessed 16 June 2024].

Liatsikos, E. N. et al. (2001). URETERAL RECONSTRUCTION: SMALL INTESTINE SUBMUCOSA FOR THE MANAGEMENT OF STRICTURES AND DEFECTS OF THE UPPER THIRD OF THE URETER. *The Journal of Urology*, 165 (5), pp.1719–1723. [Online]. Available at: doi:10.1016/S0022-5347(05)66401-4 [Accessed 16 June 2024].

Lim, D.-J. (2022). Cross-Linking Agents for Electrospinning-Based Bone Tissue Engineering. *International Journal of Molecular Sciences*, 23 (10), p.5444. [Online]. Available at: doi:10.3390/ijms23105444 [Accessed 21 June 2024].

Lima, S. V. C., Araújo, L. A. P. and Vilar, F. O. (2004). Nonsecretory intestinocystoplasty: a 10-year experience. *The Journal of Urology*, 171 (6 Pt 2), pp.2636–2639; discussion 2639-2640. [Online]. Available at: doi:10.1097/01.ju.0000112782.00417.5e.

de Lima Santos, A. et al. (2020). A new decellularized tendon scaffold for rotator cuff tears – evaluation in rabbits. *BMC Musculoskeletal Disorders*, 21 (1), p.689. [Online]. Available at: doi:10.1186/s12891-020-03680-w [Accessed 24 June 2024].

Lin, H.-K. et al. (2004). Characterization of neuropathic bladder smooth muscle cells in culture. *The Journal of Urology*, 171 (3), pp.1348–1352. [Online]. Available at: doi:10.1097/01.ju.0000108800.47594.8b.

Lin, H.-K. et al. (2014). Understanding roles of porcine small intestinal submucosa in urinary bladder regeneration: identification of variable regenerative characteristics of small intestinal submucosa. *Tissue Engineering. Part B, Reviews*, 20 (1), pp.73–83. [Online]. Available at: doi:10.1089/ten.TEB.2013.0126.

Lindberg, K. and Badylak, S. F. (2001). Porcine small intestinal submucosa (SIS): a bioscaffold supporting in vitro primary human epidermal cell differentiation and synthesis of basement membrane proteins. *Burns: Journal of the International Society for Burn Injuries*, 27 (3), pp.254–266. [Online]. Available at: doi:10.1016/s0305-4179(00)00113-3.

Loai, Y. et al. (2010). Bladder tissue engineering: tissue regeneration and neovascularization of HA-VEGF-incorporated bladder acellular constructs in mouse and porcine animal models. *Journal of Biomedical Materials Research. Part A*, 94 (4), pp.1205–1215. [Online]. Available at: doi:10.1002/jbm.a.32777.

Long, C. J. et al. (2017). Intermediate-Term Followup of Proximal Hypospadias Repair Reveals High Complication Rate. *The Journal of Urology*, 197 (3 Pt 2), pp.852–858. [Online]. Available at: doi:10.1016/j.juro.2016.11.054.

Lu, S.-H. et al. (2005). Biaxial mechanical properties of muscle-derived cell seeded small intestinal submucosa for bladder wall reconstitution. *Biomaterials*, 26 (4), pp.443–449. [Online]. Available at: doi:10.1016/j.biomaterials.2004.05.006 [Accessed 16 June 2024].

Lun, S. et al. (2010). A functional extracellular matrix biomaterial derived from ovine forestomach. *Biomaterials*, 31 (16), pp.4517–4529. [Online]. Available at: doi:10.1016/j.biomaterials.2010.02.025.

Macleod, T. M. et al. (2005). Histological evaluation of Permacol as a subcutaneous implant over a 20-week period in the rat model. *British Journal of Plastic Surgery*, 58 (4), pp.518–532. [Online]. Available at: doi:10.1016/j.bjps.2004.12.012.

MacNeily, A. E. et al. (2003). Autoaugmentation by detrusor myotomy: its lack of effectiveness in the management of congenital neuropathic bladder. *The Journal of Urology*, 170 (4 Pt 2), pp.1643–1646; discussion 1646. [Online]. Available at: doi:10.1097/01.ju.0000083800.25112.22.

Manzoni, C. et al. (2001). An original technique for bladder autoaugmentation with protective abdominal rectus muscle flaps: an experimental study in rats. *The Journal of Surgical Research*, 99 (2), pp.169–174. [Online]. Available at: doi:10.1006/jsre.2001.6098.

Marçal, H. et al. (2012). A comprehensive protein expression profile of extracellular matrix biomaterial derived from porcine urinary bladder. *Regenerative Medicine*, 7 (2), pp.159–166. [Online]. Available at: doi:10.2217/rme.12.6.

Marte, A. et al. (2002). A long-term follow-up of autoaugmentation in myelodysplastic children. *BJU International*, 89 (9), pp.928–931. [Online]. Available at: doi:10.1046/j.1464-410X.2002.02781.x [Accessed 15 June 2024].

Matoka, D. J. and Cheng, E. Y. (2009). Tissue engineering in urology. *Canadian Urological Association Journal*, 3 (5), pp.403–408. [Online]. Available at: https://www.ncbi.nlm.nih.gov/pmc/articles/PMC2758503/ [Accessed 17 June 2024].

Mauney, J. R. and Adam, R. M. (2015). Dynamic Reciprocity in Cell-Scaffold Interactions. *Advanced drug delivery reviews*, 0, pp.77–85. [Online]. Available at: doi:10.1016/j.addr.2014.10.016 [Accessed 29 June 2024].

McGlohorn, J. B. et al. (2004). Evaluation of smooth muscle cell response using two types of porous polylactide scaffolds with differing pore topography. *Tissue Engineering*, 10 (3–4), pp.505–514. [Online]. Available at: doi:10.1089/107632704323061861.

McNamara, E. R. et al. (2015). Management of Proximal Hypospadias with 2-Stage Repair: 20-Year Experience. *The Journal of Urology*, 194 (4), pp.1080–1085. [Online]. Available at: doi:10.1016/j.juro.2015.04.105.

Meezan, E. et al. (1975). A simple, versatile, nondisruptive method for the isolation of morphologically and chemically pure basement membranes from several tissues. *Life Sciences*, 17 (11), pp.1721–1732. [Online]. Available at: doi:10.1016/0024-3205(75)90119-8 [Accessed 16 June 2024].

Merguerian, P. a. et al. (2000). Acellular bladder matrix allografts in the regeneration of functional bladders: evaluation of large-segment (> 24 cm2) substitution in a porcine model. *BJU International*, 85 (7), pp.894–898. [Online]. Available at: doi:10.1046/j.1464-410x.2000.00513.x [Accessed 16 June 2024].

Micallef, L. et al. (2012). The myofibroblast, multiple origins for major roles in normal and pathological tissue repair. *Fibrogenesis & Tissue Repair*, 5 (Suppl 1), p.S5. [Online]. Available at: doi:10.1186/1755-1536-5-S1-S5.

Mikos, A. G. et al. (1993). Prevascularization of porous biodegradable polymers. *Biotechnology and Bioengineering*, 42 (6), pp.716–723. [Online]. Available at: doi:10.1002/bit.260420606.

Mikulicz, J. von. (1899). Zur operation der augebornenen blasenspalte. *Zentralbl. f. Chir*, 26, pp.641–654. [Online]. Available at: https://cir.nii.ac.jp/crid/1571980075005700992 [Accessed 15 June 2024].

Mitrofanoff, P. (1980). [Trans-appendicular continent cystostomy in the management of the neurogenic bladder]. *Chirurgie Pediatrique*, 21 (4), pp.297–305.

Monaco, G. et al. (2017). Sterilization of collagen scaffolds designed for peripheral nerve regeneration: Effect on microstructure, degradation and cellular colonization. *Materials Science & Engineering. C, Materials for Biological Applications*, 71, pp.335–344. [Online]. Available at: doi:10.1016/j.msec.2016.10.030.

Mooney, D. J. et al. (1996). Novel approach to fabricate porous sponges of poly(D,L-lactic-co-glycolic acid) without the use of organic solvents. *Biomaterials*, 17 (14), pp.1417–1422. [Online]. Available at: doi:10.1016/0142-9612(96)87284-x.

Morgante, D. et al. (2021). Augmentation of the insufficient tissue bed for surgical repair of hypospadias using acellular matrix grafts: A proof of concept study. *Journal of Tissue Engineering*, 12, p.2041731421998840. [Online]. Available at: doi:10.1177/2041731421998840.

Morgante, D. and Southgate, J. (2022). Chapter 12 - Bladder tissue regeneration. In: Boccaccini, A. R., Ma, P. X. and Liverani, L. (Eds). *Tissue Engineering Using Ceramics and Polymers (Third Edition)*. Woodhead Publishing Series in Biomaterials. Woodhead Publishing. pp.459–480. [Online]. Available at: doi:10.1016/B978-0-12-820508-2.00008-8 [Accessed 15 May 2024].

Motley, R. C. et al. (1990). Augmentation cystoplasty utilizing de-epithelialized sigmoid colon: a preliminary study. *The Journal of Urology*, 143 (6), pp.1257–1260. [Online]. Available at: doi:10.1016/s0022-5347(17)40249-7.

Mukherjee, P. et al. (2022). Role of animal models in biomedical research: a review. *Laboratory Animal Research*, 38 (1), p.18. [Online]. Available at: doi:10.1186/s42826-022-00128-1 [Accessed 5 March 2025].

Murthy, P. et al. (2015). Robot-assisted Laparoscopic Augmentation Ileocystoplasty and Mitrofanoff Appendicovesicostomy in Children: Updated Interim Results. *European Urology*, 68 (6), pp.1069–1075. [Online]. Available at: doi:10.1016/j.eururo.2015.05.047.

Musahl, V. et al. (2004). The use of porcine small intestinal submucosa to enhance the healing of the medial collateral ligament--a functional tissue engineering study in rabbits. *Journal of Orthopaedic Research: Official Publication of the Orthopaedic Research Society*, 22 (1), pp.214–220. [Online]. Available at: doi:10.1016/S0736-0266(03)00163-3.

Nagata, S., Hanayama, R. and Kawane, K. (2010). Autoimmunity and the clearance of dead cells. *Cell*, 140 (5), pp.619–630. [Online]. Available at: doi:10.1016/j.cell.2010.02.014.

Nerem, R. M. and Sambanis, A. (1995). Tissue engineering: from biology to biological substitutes. *Tissue Engineering*, 1 (1), pp.3–13. [Online]. Available at: doi:10.1089/ten.1995.1.3.

Neuhof, H. (1917). Fascial transplantation into visceral defects: an experimental and clinical study. *Surg. Gynecol. Obstet.*, 25, pp.383–427. [Online]. Available at: https://cir.nii.ac.jp/crid/1574231875208013568 [Accessed 16 June 2024].

Niku, S. D. et al. (1995). Intestinal de-epithelialization and augmentation cystoplasty: an animal model. *Urology*, 46 (1), pp.36–39. [Online]. Available at: doi:10.1016/S0090-4295(99)80155-1.

Nimeh, T. and Elliott, S. (2018). Minimally Invasive Techniques for Bladder Reconstruction. *Current Urology Reports*, 19 (6), p.39. [Online]. Available at: doi:10.1007/s11934-018-0787-y.

Nomi, M. et al. (2002). Principals of neovascularization for tissue engineering. *Molecular Aspects of Medicine*, 23 (6), pp.463–483. [Online]. Available at: doi:10.1016/s0098-2997(02)00008-0.

Novick, A. C. et al. (1977). Experimental bladder substitution using biodegradable graft of natural tissue. *Urology*, 10 (2), pp.118–127. [Online]. Available at: doi:10.1016/0090-4295(77)90008-5.

Nuininga, J. E. et al. (2004). A rabbit model to tissue engineer the bladder. *Biomaterials*, 25 (9), pp.1657–1661. [Online]. Available at: doi:10.1016/s0142-9612(03)00519-2.

Oberpenning, F. et al. (1999). De novo reconstitution of a functional mammalian urinary bladder by tissue engineering. *Nature Biotechnology*, 17 (2), pp.149–155. [Online]. Available at: doi:10.1038/6146.

O'Brien, F. J. (2011). Biomaterials & scaffolds for tissue engineering. *Materials Today*, 14 (3), pp.88–95. [Online]. Available at: doi:10.1016/S1369-7021(11)70058-X [Accessed 24 June 2024].

Odegaard, J. I. and Chawla, A. (2011). Alternative macrophage activation and metabolism. *Annual Review of Pathology*, 6, pp.275–297. [Online]. Available at: doi:10.1146/annurev-pathol-011110-130138.

Oesch, I. (1988). Neourothelium in bladder augmentation. An experimental study in rats. *European Urology*, 14 (4), pp.328–329. [Online]. Available at: doi:10.1159/000472971.

Olde Damink, L. H. H. et al. (1995). Crosslinking of dermal sheep collagen using hexamethylene diisocyanate. *Journal of Materials Science: Materials in Medicine*, 6 (7), pp.429–434. [Online]. Available at: doi:10.1007/BF00120286 [Accessed 24 June 2024].

Olsburgh, J. et al. (2003). Uroplakin gene expression in normal human tissues and locally advanced bladder cancer. *The Journal of Pathology*, 199 (1), pp.41–49. [Online]. Available at: doi:10.1002/path.1252 [Accessed 14 June 2024].

Orlando, G. (2024). Transforming Organ Transplantation with Regenerative Medicine: An Interview with Giuseppe Orlando. *Regenerative Medicine*, 19 (1), pp.5–6. [Online]. Available at: doi:10.2217/rme-2023-0204 [Accessed 15 June 2024].

Pakshir, P. and Hinz, B. (2018). The big five in fibrosis: Macrophages, myofibroblasts, matrix, mechanics, and miscommunication. *Matrix Biology: Journal of the International Society for Matrix Biology*, 68–69, pp.81–93. [Online]. Available at: doi:10.1016/j.matbio.2018.01.019.

Palminteri, E. et al. (2007). Small intestinal submucosa (SIS) graft urethroplasty: short-term results. *European Urology*, 51 (6), pp.1695–1701; discussion 1701. [Online]. Available at: doi:10.1016/j.eururo.2006.12.016.

Paniagua Gutierrez, J. R. et al. (2015). Regenerative potential of low-concentration SDS-decellularized porcine aortic valved conduits in vivo. *Tissue Engineering. Part A*, 21 (1–2), pp.332–342. [Online]. Available at: doi:10.1089/ten.tea.2014.0003.

Park, S.-N. et al. (2002). Characterization of porous collagen/hyaluronic acid scaffold modified by 1-ethyl-3-(3-dimethylaminopropyl)carbodiimide cross-linking. *Biomaterials*, 23 (4), pp.1205–1212. [Online]. Available at: doi:10.1016/s0142-9612(01)00235-6 [Accessed 15 June 2024].

Parshotam Kumar, G. et al. (2010). Urinary bladder auto augmentation using INTEGRA and SURGISIS: an experimental model. *Pediatric Surgery International*, 26 (3), pp.275–280. [Online]. Available at: doi:10.1007/s00383-009-2521-9.

Parsons, B. A. et al. (2012). The validation of a functional, isolated pig bladder model for physiological experimentation. *Frontiers in Pharmacology*, 3, p.52. [Online]. Available at: doi:10.3389/fphar.2012.00052.

Patel, B. and Chakraborty, S. (2016). Biodegradable polymers: emerging excipients for the pharmaceutical and medical device industries. *International Journal of Pharmaceutical Excipients*, 4 (4). [Online]. Available at: https://jefc.scholasticahq.com/article/1010-biodegradable-polymers-emerging-excipients-for-the-pharmaceutical-and-medical-device-industries [Accessed 17 June 2024].

Pekkarinen, T. et al. (2004). Influence of ethylene oxide sterilization on the activity of native reindeer bone morphogenetic protein. *International Orthopaedics*, 28 (2), pp.97–101. [Online]. Available at: doi:10.1007/s00264-003-0524-z.

Perovic, S. V. et al. (2002). Bladder Autoaugmentation with Rectus Muscle Backing. *The Journal of Urology*, 168 (4, Supplement), pp.1877–1880. [Online]. Available at: doi:10.1016/S0022-5347(05)64434-5 [Accessed 15 June 2024].

Petrovic, V., Stankovic, J. and Stefanovic, V. (2011). Tissue Engineering of the Urinary Bladder: Current Concepts and Future Perspectives. *The Scientific World Journal*, 11 (1), p.958478. [Online]. Available at: doi:10.1100/tsw.2011.138 [Accessed 17 June 2024].

Peyton, C. C. et al. (2012). Characterization of the Early Proliferative Response of the Rodent Bladder to Subtotal Cystectomy: A Unique Model of Mammalian Organ Regeneration. *PLoS ONE*, 7 (10), p.e47414. [Online]. Available at: doi:10.1371/journal.pone.0047414 [Accessed 15 June 2024].

Piechota, H. J. et al. (1998). In vitro functional properties of the rat bladder regenerated by the bladder acellular matrix graft. *The Journal of Urology*, 159 (5), pp.1717–1724. [Online]. Available at: doi:10.1097/00005392-199805000-00100.

Piechota, H. J. et al. (1999). Bladder acellular matrix graft: in vivo functional properties of the regenerated rat bladder. *Urological Research*, 27 (3), pp.206–213. [Online]. Available at: doi:10.1007/s002400050111.

Pillai, C. K. S. and Sharma, C. P. (2010). Review paper: absorbable polymeric surgical sutures: chemistry, production, properties, biodegradability, and performance. *Journal of Biomaterials Applications*, 25 (4), pp.291–366. [Online]. Available at: doi:10.1177/0885328210384890.

Pokrywczynska, M. et al. (2013). Do mesenchymal stem cells modulate the milieu of reconstructed bladder wall? *Archivum Immunologiae Et Therapiae Experimentalis*, 61 (6), pp.483–493. [Online]. Available at: doi:10.1007/s00005-013-0249-7.

Pokrywczynska, M. et al. (2015). Application of Bladder Acellular Matrix in Urinary Bladder Regeneration: The State of the Art and Future Directions. *BioMed Research International*, 2015, p.613439. [Online]. Available at: doi:10.1155/2015/613439 [Accessed 15 June 2024].

Portilla Sanchez, R. et al. (1958). Vesical regeneration in the human after total cystectomy and implantation of a plastic mould. *British Journal of Urology*, 30 (2), pp.180–188. [Online]. Available at: doi:10.1111/j.1464-410x.1958.tb06231.x.

Probst, M. et al. (1997). Reproduction of functional smooth muscle tissue and partial bladder replacement. *British Journal of Urology*, 79 (4), pp.505–515. [Online]. Available at: doi:10.1046/j.1464-410x.1997.00103.x.

Probst, M. et al. (2000). Homologous bladder augmentation in dog with the bladder acellular matrix graft. *BJU International*, 85 (3), pp.362–371. [Online]. Available at: doi:10.1046/j.1464-410x.2000.00442.x [Accessed 16 June 2024].

Qin, H. H. and Dunn, J. C. Y. (2011). Small intestinal submucosa seeded with intestinal smooth muscle cells in a rodent jejunal interposition model. *The Journal of surgical research*, 171 (1), pp.e21–e26. [Online]. Available at: doi:10.1016/j.jss.2011.08.001 [Accessed 16 June 2024].

Ram-Liebig, G. et al. (2004). Induction of proliferation and differentiation of cultured urothelial cells on acellular biomaterials. *BJU international*, 94 (6), pp.922–927. [Online]. Available at: doi:10.1111/j.1464-410X.2004.05061.x.

Ram-Liebig, G. et al. (2006). New approaches in the modulation of bladder smooth muscle cells on viable detrusor constructs. *World Journal of Urology*, 24 (4), pp.429–437. [Online]. Available at: doi:10.1007/s00345-006-0104-0.

Reddy, P. P. et al. (2000). Regeneration of functional bladder substitutes using large segment acellular matrix allografts in a porcine model. *The Journal of Urology*, 164 (3 Pt 2), pp.936–941. [Online]. Available at: doi:10.1097/00005392-200009020-00005.

Rhodes, A. et al. (2000). Immunohistochemical demonstration of oestrogen and progesterone receptors: correlation of standards achieved on in house tumours with that achieved on external quality assessment material in over 150 laboratories from 26 countries. *Journal of Clinical Pathology*, 53 (4), pp.292–301. [Online]. Available at: doi:10.1136/jcp.53.4.292.

Rivas, D. A. et al. (1996). Comparison of bladder rupture pressure after intestinal bladder augmentation (ileocystoplasty) and myomyotomy (autoaugmentation). *Urology*, 48 (1), pp.40–46. [Online]. Available at: doi:10.1016/s0090-4295(96)00096-9.

Rizvi, A. Z. and Wong, M. H. (2005). Epithelial stem cells and their niche: there's no place like home. *Stem Cells (Dayton, Ohio)*, 23 (2), pp.150–165. [Online]. Available at: doi:10.1634/stemcells.2004-0096.

Rnjak-Kovacina, J. et al. (2015). The effect of sterilization on silk fibroin biomaterial properties. *Macromolecular Bioscience*, 15 (6), pp.861–874. [Online]. Available at: doi:10.1002/mabi.201500013.

Robinson, N. B. et al. (2019). The current state of animal models in research: A review. *International Journal of Surgery*, 72, pp.9–13. [Online]. Available at: doi:10.1016/j.ijsu.2019.10.015 [Accessed 5 March 2025].

Robotin-Johnson, M. C. et al. (1998). An experimental model of small intestinal submucosa as a growing vascular graft. *The Journal of Thoracic and Cardiovascular Surgery*, 116 (5), pp.805–811. [Online]. Available at: doi:10.1016/S0022-5223(98)00436-X [Accessed 16 June 2024].

Roelofs, L. A. J. et al. (2018). Bladder Regeneration Using Multiple Acellular Scaffolds with Growth Factors in a Bladder. *Tissue Engineering. Part A*, 24 (1–2), pp.11–20. [Online]. Available at: doi:10.1089/ten.TEA.2016.0356.

Rohman, G. et al. (2007). Influence of the physical properties of two-dimensional polyester substrates on the growth of normal human urothelial and urinary smooth muscle cells in vitro. *Biomaterials*, 28 (14), pp.2264–2274. [Online]. Available at: doi:10.1016/j.biomaterials.2007.01.032 [Accessed 15 June 2024].

Rohman, G. et al. (2009). Heparin functionalisation of porous PLGA scaffolds for controlled, biologically relevant delivery of growth factors for soft tissue engineering. *Journal of Materials Chemistry*, 19 (48), pp.9265–9273. [Online]. Available at: doi:10.1039/B911625G [Accessed 15 June 2024].

Rosario, D. J. et al. (2008). Decellularization and sterilization of porcine urinary bladder matrix for tissue engineering in the lower urinary tract. *Regenerative Medicine*, 3 (2), pp.145–156. [Online]. Available at: doi:10.2217/17460751.3.2.145 [Accessed 23 May 2024].

Rőszer, T. (2015). Understanding the Mysterious M2 Macrophage through Activation Markers and Effector Mechanisms. *Mediators of Inflammation*, 2015 (1), p.816460. [Online]. Available at: doi:10.1155/2015/816460 [Accessed 29 June 2024].

Roth, C. C. et al. (2011). Bladder regeneration in a canine model using hyaluronic acid-poly(lactic-co-glycolic-acid) nanoparticle modified porcine small intestinal submucosa. *BJU International*, 108 (1), pp.148–155. [Online]. Available at: doi:10.1111/j.1464-410X.2010.09757.x [Accessed 16 June 2024].

Roth, E. A. et al. (2004). Inkjet printing for high-throughput cell patterning. *Biomaterials*, 25 (17), pp.3707–3715. [Online]. Available at: doi:10.1016/j.biomaterials.2003.10.052.

Rowlands, A. S. et al. (2007). Polyurethane/poly(lactic-co-glycolic) acid composite scaffolds fabricated by thermally induced phase separation. *Biomaterials*, 28 (12), pp.2109–2121. [Online]. Available at: doi:10.1016/j.biomaterials.2006.12.032.

Rowley, J. A., Madlambayan, G. and Mooney, D. J. (1999). Alginate hydrogels as synthetic extracellular matrix materials. *Biomaterials*, 20 (1), pp.45–53. [Online]. Available at: doi:10.1016/S0142-9612(98)00107-0 [Accessed 15 June 2024].

Rübben, H. et al. (1983). Quantitative analysis of glycosaminoglycans in urothelium and bladder wall of calf. *Urology*, 22 (6), pp.655–657. [Online]. Available at: doi:10.1016/0090-4295(83)90321-7 [Accessed 14 June 2024].

Russell, W. M. S. and Burch, R. L. *The Principles of Humane Experimental Technique*.

Rustad, K. C. et al. (2010). Strategies for organ level tissue engineering. *Organogenesis*, 6 (3), pp.151–157. [Online]. Available at: https://www.ncbi.nlm.nih.gov/pmc/articles/PMC2946046/ [Accessed 20 May 2024].

Rutkowski, M. (1899). Zur methode der harnblasenplastik. *Zentralbl Chir*, 16 (473–478), p.19.

Salle, J. L. et al. (1990). Seromuscular enterocystoplasty in dogs. *The Journal of Urology*, 144 (2 Pt 2), pp.454–456; discussion 460. [Online]. Available at: doi:10.1016/s0022-5347(17)39487-9.

Sam, P., Nassereddin, A. and LaGrange, C. A. (2024). Anatomy, Abdomen and Pelvis: Bladder Detrusor Muscle. In: *StatPearls*. Treasure Island (FL): StatPearls Publishing. [Online]. Available at: http://www.ncbi.nlm.nih.gov/books/NBK482181/ [Accessed 14 June 2024].

Sara, B. et al. (2010). Evolution in Tissue Engineering for the Lower Urinary Tract. In: *Tissue Engineering*. IntechOpen. [Online]. Available at: https://books.google.co.uk/books?hl=en&lr=&id=aOacDwAAQBAJ&oi=fnd&pg=PA485&dq=DOI:+10.5772/8576&ots=xgd1M0IBPB&sig=DAeyOs8EuHpoO1RlJGBUshs3lnA [Accessed 30 June 2024].

Schaefer, B. M. et al. (1998). Autologous transplantation of urothelium into demucosalized gastrointestinal segments: evidence for epithelialization and differentiation of in vitro expanded and transplanted urothelial cells. *The Journal of Urology*, 159 (1), pp.284–290. [Online]. Available at: doi:10.1016/s0022-5347(01)64083-7.

Schaefer, M. et al. (2013). Bladder augmentation with small intestinal submucosa leads to unsatisfactory long-term results. *Journal of Pediatric Urology*, 9 (6 Pt A), pp.878–883. [Online]. Available at: doi:10.1016/j.jpurol.2012.12.001.

Schmidt, C. E. and Baier, J. M. (2000). Acellular vascular tissues: natural biomaterials for tissue repair and tissue engineering. *Biomaterials*, 21 (22), pp.2215–2231. [Online]. Available at: doi:10.1016/S0142-9612(00)00148-4 [Accessed 28 May 2024].

Schneeberger, E. E. and Lynch, R. D. (2004). The tight junction: a multifunctional complex. *American Journal of Physiology. Cell Physiology*, 286 (6), pp.C1213-1228. [Online]. Available at: doi:10.1152/ajpcell.00558.2003.

Schneeweiss, S. et al. (2008). Aprotinin during coronary-artery bypass grafting and risk of death. *The New England Journal of Medicine*, 358 (8), pp.771–783. [Online]. Available at: doi:10.1056/NEJMoa0707571.

Schoeller, T. et al. (2004). Capsule induction technique in a rat model for bladder wall replacement: an overview. *Biomaterials*, 25 (9), pp.1663–1673. [Online]. Available at: doi:10.1016/s0142-9612(03)00518-0.

Schwentner, C. et al. (2011). Single-stage dorsal inlay full-thickness genital skin grafts for hypospadias reoperations: extended follow up. *Journal of Pediatric Urology*, 7 (1), pp.65–71. [Online]. Available at: doi:10.1016/j.jpurol.2010.01.016.

Serrano-Aroca, Á., Vera-Donoso, C. D. and Moreno-Manzano, V. (2018). Bioengineering Approaches for Bladder Regeneration. *International Journal of Molecular Sciences*, 19 (6), p.1796. [Online]. Available at: doi:10.3390/ijms19061796.

Shakhssalim, N. et al. (2017). Bladder smooth muscle cells on electrospun poly(ε-caprolactone)/poly(l-lactic acid) scaffold promote bladder regeneration in a canine model. *Materials Science & Engineering. C, Materials for Biological Applications*, 75, pp.877–884. [Online]. Available at: doi:10.1016/j.msec.2017.02.064.

Shaw, A. D. et al. (2008). The effect of aprotinin on outcome after coronary-artery bypass grafting. *The New England Journal of Medicine*, 358 (8), pp.784–793. [Online]. Available at: doi:10.1056/NEJMoa0707768.

Sheikh, Z. et al. (2015). Macrophages, Foreign Body Giant Cells and Their Response to Implantable Biomaterials. *Materials (Basel, Switzerland)*, 8 (9), pp.5671–5701. [Online]. Available at: doi:10.3390/ma8095269.

Shekarriz, B. et al. (2000a). Surgical complications of bladder augmentation: comparison between various enterocystoplasties in 133 patients. *Urology*, 55 (1), pp.123–128. [Online]. Available at: doi:10.1016/s0090-4295(99)00443-4.

Shekarriz, B. et al. (2000b). Surgical complications of bladder augmentation: comparison between various enterocystoplasties in 133 patients. *Urology*, 55 (1), pp.123–128. [Online]. Available at: doi:10.1016/s0090-4295(99)00443-4.

Shell, D. H. et al. (2005). Comparison of Small-Intestinal Submucosa and Expanded Polytetrafluoroethylene as a Vascular Conduit in the Presence of Gram-Positive Contamination. *Annals of Surgery*, 241 (6), pp.995–1004. [Online]. Available at: doi:10.1097/01.sla.0000165186.79097.6c [Accessed 16 June 2024].

Shen, J.-D. et al. (2021). Review of Animal Models to Study Urinary Bladder Function. *Biology*, 10 (12), p.1316. [Online]. Available at: doi:10.3390/biology10121316 [Accessed 29 June 2024].

Shoemaker, W. C. (1955). Reversed seromuscular grafts in urinary tract reconstruction. *The Journal of Urology*, 74 (4), pp.453–475. [Online]. Available at: doi:10.1016/S0022-5347(17)67305-1.

Shoemaker, W. C. and Marucci, H. D. (1955). The experimental use of seromuscular grafts in bladder reconstruction; preliminary report. *The Journal of Urology*, 73 (2), pp.314–321. [Online]. Available at: doi:10.1016/S0022-5347(17)67402-0.

Sica, A. and Mantovani, A. (2012). Macrophage plasticity and polarization: in vivo veritas. *The Journal of Clinical Investigation*, 122 (3), pp.787–795. [Online]. Available at: doi:10.1172/JCI59643.

Sidney, L. E. et al. (2014). Concise review: evidence for CD34 as a common marker for diverse progenitors. *Stem Cells (Dayton, Ohio)*, 32 (6), pp.1380–1389. [Online]. Available at: doi:10.1002/stem.1661.

Sinaiko, E. (1956). Artificial bladder from segment of stomach and study of effect of urine on gastric secretion. *Surgery, Gynecology & Obstetrics*, 102 (4), pp.433–438.

Singh, A., Bivalacqua, T. J. and Sopko, N. (2018). Urinary Tissue Engineering: Challenges and Opportunities. *Sexual Medicine Reviews*, 6 (1), pp.35–44. [Online]. Available at: doi:10.1016/j.sxmr.2017.08.004.

Sirota, R. L. (2005). Error and error reduction in pathology. *Archives of Pathology & Laboratory Medicine*, 129 (10), pp.1228–1233. [Online]. Available at: doi:10.5858/2005-129-1228-EAERIP.

Sivaraman, S. et al. (2015). Tetronic®-based Composite Hydrogel scaffolds seeded with Rat-Bladder Smooth Muscle Cells for Urinary Bladder Tissue Engineering Applications. *Journal of biomaterials science. Polymer edition*, 26 (3), pp.196–210. [Online]. Available at: doi:10.1080/09205063.2014.989482 [Accessed 17 June 2024].

Skandalakis, J. (2004). *SURGICAL ANATOMY : The Embryologic and Anatomic Basis of Modern Surgery*. 1st edition. Paschalidis Medical Publications.

Slobodov, G. et al. (2004). Abnormal expression of molecular markers for bladder impermeability and differentiation in the urothelium of patients with interstitial cystitis. *The Journal of Urology*, 171 (4), pp.1554–1558. [Online]. Available at: doi:10.1097/01.ju.0000118938.09119.a5.

Smith, N. J. et al. (2015). The human urothelial tight junction: claudin 3 and the ZO-1α+ switch. *Bladder*, 2 (1), p.e9. [Online]. Available at: doi:10.14440/bladder.2015.33 [Accessed 14 June 2024].

Southgate, J. et al. (1994). Normal human urothelial cells in vitro: proliferation and induction of stratification. *Laboratory Investigation; a Journal of Technical Methods and Pathology*, 71 (4), pp.583–594.

Southgate, J., Masters, J. R. W. and Trejdosiewicz, L. K. (2002). Culture of Human Urothelium. In: *Culture of Epithelial Cells*. John Wiley & Sons, Ltd. pp.381–399. [Online]. Available at: doi:10.1002/0471221201.ch12 [Accessed 24 June 2024].

Springer, A. and Subramaniam, R. (2012a). Preliminary experience with the use of acellular collagen matrix in redo surgery for urethrocutaneous fistula. *Urology*, 80 (5), pp.1156–1160. [Online]. Available at: doi:10.1016/j.urology.2012.06.058.

Springer, A. and Subramaniam, R. (2012b). Split dorsal dartos flap transposed ventrally as a bed for preputial skin graft in primary staged hypospadias repair. *Urology*, 79 (4), pp.939–942. [Online]. Available at: doi:10.1016/j.urology.2012.01.006.

Stanasel, I. et al. (2015). Complications following Staged Hypospadias Repair Using Transposed Preputial Skin Flaps. *The Journal of Urology*, 194 (2), pp.512–516. [Online]. Available at: doi:10.1016/j.juro.2015.02.044.

Stanasel, I., Mirzazadeh, M. and Smith, J. J. (2010). Bladder tissue engineering. *The Urologic Clinics of North America*, 37 (4), pp.593–599. [Online]. Available at: doi:10.1016/j.ucl.2010.06.008.

Stankus, J. J. et al. (2008). Hybrid nanofibrous scaffolds from electrospinning of a synthetic biodegradable elastomer and urinary bladder matrix. *Journal of biomaterials science. Polymer edition*, 19 (5), pp.635–652. [Online]. Available at: doi:10.1163/156856208784089599 [Accessed 17 June 2024].

Stapleton, T. et al. (2008a). Development and Characterization of an Acellular Porcine Medial Meniscus for Use in Tissue Engineering. *Tissue engineering. Part A*, 14, pp.505–518. [Online]. Available at: doi:10.1089/tea.2007.0233.

Stapleton, T. W. et al. (2008b). Development and characterization of an acellular porcine medial meniscus for use in tissue engineering. *Tissue Engineering. Part A*, 14 (4), pp.505–518. [Online]. Available at: doi:10.1089/tea.2007.0233.

Stapleton, T. W. et al. (2011). Investigation of the Regenerative Capacity of an Acellular Porcine Medial Meniscus for Tissue Engineering Applications. *Tissue Engineering Part A*, 17 (1–2), pp.231–242. [Online]. Available at: doi:10.1089/ten.tea.2009.0807 [Accessed 16 June 2024].

Stein, J. P. and Skinner, D. G. (2006). Surgical Atlas The orthotopic T-pouch ileal neobladder. *BJU International*, 98 (2), pp.469–482. [Online]. Available at: doi:10.1111/j.1464-410X.2006.06383.x [Accessed 15 June 2024].

Stein, R., Schröder, A. and Thüroff, J. W. (2006). Surgical atlas: Primary hypospadias repair with buccal mucosa. *BJU international*, 97 (4), pp.871–889. [Online]. Available at: doi:10.1111/j.1464-410X.2006.06119.x.

Stenzl, A. et al. (2000). Reconstruction of the lower urinary tract using autologous muscle transfer and cell seeding: current status and future perspectives. *World Journal of Urology*, 18 (1), pp.44–50. [Online]. Available at: doi:10.1007/s003450050008.

Stothers, L. et al. (1994). Bladder autoaugmentation by vesicomyotomy in the pediatric neurogenic bladder. *Urology*, 44 (1), pp.110–113. [Online]. Available at: doi:10.1016/s0090-4295(94)80019-7.

Studer, U. e., Varol, C. and Danuser, H. (2004). Orthotopic ileal neobladder. *BJU International*, 93 (1), pp.183–193. [Online]. Available at: doi:10.1111/j.1464-410X.2004.04641.x [Accessed 15 June 2024].

Subramaniam, R. et al. (2011). Tissue Engineering Potential of Urothelial Cells From Diseased Bladders. *Journal of Urology*. [Online]. Available at: doi:10.1016/j.juro.2011.07.031 [Accessed 15 June 2024].

Sutherland, R. S. et al. (1996). Regeneration of bladder urothelium, smooth muscle, blood vessels and nerves into an acellular tissue matrix. *The Journal of Urology*, 156 (2 Pt 2), pp.571–577. [Online]. Available at: doi:10.1097/00005392-199608001-00002.

Tanaka, S. T. et al. (2010). Endodermal origin of bladder trigone inferred from mesenchymal-epithelial interaction. *The Journal of Urology*, 183 (1), pp.386–391. [Online]. Available at: doi:10.1016/j.juro.2009.08.107.

Tanaka, Y. et al. (2009). Differential long-term stimulation of type I versus type III collagen after infrared irradiation. *Dermatologic Surgery: Official Publication for American Society for Dermatologic Surgery [et Al.]*, 35 (7), pp.1099–1104. [Online]. Available at: doi:10.1111/j.1524-4725.2009.01194.x.

Tang, X. et al. (2023). Characterizing the inherent activity of urinary bladder matrix for adhesion, migration, and activation of fibroblasts as compared with collagen-based synthetic scaffold. *Journal of Biomaterials Applications*, 37 (8), pp.1446–1457. [Online]. Available at: doi:10.1177/08853282221130883.

Tao, M. et al. (2021). Sterilization and disinfection methods for decellularized matrix materials: Review, consideration and proposal. *Bioactive Materials*, 6 (9), pp.2927–2945. [Online]. Available at: doi:10.1016/j.bioactmat.2021.02.010.

Taylor, C. R. (1994). An exaltation of experts: concerted efforts in the standardization of immunohistochemistry. *Human Pathology*, 25 (1), pp.2–11. [Online]. Available at: doi:10.1016/0046-8177(94)90164-3.

Thangappan, R. et al. (2012). Epithelium-free bladder wall graft: epithelial ingrowth and regeneration--clinical implications for partial cystectomy. *The Journal of Urology*, 187 (4), pp.1450–1457. [Online]. Available at: doi:10.1016/j.juro.2011.12.014.

Thomas, D. F. (1997). Surgical treatment of urinary incontinence. *Archives of Disease in Childhood*, 76 (4), pp.377–380. [Online]. Available at: doi:10.1136/adc.76.4.377.

Tizzoni, G. and Foggi, A. (1888). *Die Widerhastel ling der Harnblase Centralbl f*. Chir.

Tran, L. N. and Puckett, Y. (2024). Urinary Incontinence. In: *StatPearls*. Treasure Island (FL): StatPearls Publishing. [Online]. Available at: http://www.ncbi.nlm.nih.gov/books/NBK559095/ [Accessed 21 June 2024].

Tran, T. et al. (2015). Correcting the Shrinkage Effects of Formalin Fixation and Tissue Processing for Renal Tumors: toward Standardization of Pathological Reporting of Tumor Size. *Journal of Cancer*, 6 (8), pp.759–766. [Online]. Available at: doi:10.7150/jca.12094.

Tsukita, S. and Furuse, M. (2002). Claudin-based barrier in simple and stratified cellular sheets. *Current Opinion in Cell Biology*, 14 (5), pp.531–536. [Online]. Available at: doi:10.1016/s0955-0674(02)00362-9.

Tu, D. D. et al. (2013). Bladder Tissue Regeneration Using Acellular Bi-Layer Silk Scaffolds in a Large Animal Model of Augmentation Cystoplasty. *Biomaterials*, 34 (34), p.10.1016/j.biomaterials.2013.08.001. [Online]. Available at: doi:10.1016/j.biomaterials.2013.08.001 [Accessed 17 June 2024].

Tu, L., Sun, T.-T. and Kreibich, G. (2002). Specific Heterodimer Formation Is a Prerequisite for Uroplakins to Exit from the Endoplasmic Reticulum. *Molecular Biology of the Cell*, 13 (12), pp.4221–4230. [Online]. Available at: doi:10.1091/mbc.E02-04-0211 [Accessed 14 June 2024].

Turner, A. et al. (2011). Transplantation of autologous differentiated urothelium in an experimental model of composite cystoplasty. *European Urology*, 59 (3), pp.447–454. [Online]. Available at: doi:10.1016/j.eururo.2010.12.004.

Turner, A. M. et al. (2008). Generation of a functional, differentiated porcine urothelial tissue in vitro. *European Urology*, 54 (6), pp.1423–1432. [Online]. Available at: doi:10.1016/j.eururo.2008.03.068.

Utomo, E., Groen, J. and Blok, B. F. (2014). Surgical management of functional bladder outlet obstruction in adults with neurogenic bladder dysfunction. *The Cochrane Database of Systematic Reviews*, 2014 (5), p.CD004927. [Online]. Available at: doi:10.1002/14651858.CD004927.pub4 [Accessed 15 June 2024].

Vacanti, J. P. and Langer, R. (1999). Tissue engineering: the design and fabrication of living replacement devices for surgical reconstruction and transplantation. *The Lancet*, 354, pp.S32–S34. [Online]. Available at: doi:10.1016/S0140-6736(99)90247-7 [Accessed 15 June 2024].

Vafaee, T. et al. (2018). Decellularization of human donor aortic and pulmonary valved conduits using low concentration sodium dodecyl sulfate. *Journal of Tissue Engineering and Regenerative Medicine*, 12 (2), pp.e841–e853. [Online]. Available at: doi:10.1002/term.2391 [Accessed 16 June 2024].

Valentin, J. E. et al. (2006). Extracellular matrix bioscaffolds for orthopaedic applications. A comparative histologic study. *The Journal of Bone and Joint Surgery. American Volume*, 88 (12), pp.2673–2686. [Online]. Available at: doi:10.2106/JBJS.E.01008.

Van Der Rest, M. and Garrone, R. (1991). Collagen family of proteins. *The FASEB Journal*, 5 (13), pp.2814–2823. [Online]. Available at: doi:10.1096/fasebj.5.13.1916105 [Accessed 23 May 2024].

Vardar, E. et al. (2016). IGF-1-containing multi-layered collagen-fibrin hybrid scaffolds for bladder tissue engineering. *Acta Biomaterialia*, 41, pp.75–85. [Online]. Available at: doi:10.1016/j.actbio.2016.06.010.

Varley, C. et al. (2004a). Role of PPAR? and EGFR signalling in the urothelial terminal differentiation programme. *Journal of cell science*, 117, pp.2029–2036. [Online]. Available at: doi:10.1242/jcs.01042.

Varley, C. et al. (2005). Autocrine regulation of human urothelial cell proliferation and migration during regenerative responses in vitro. *Experimental Cell Research*, 306 (1), pp.216–229. [Online]. Available at: doi:10.1016/j.yexcr.2005.02.004 [Accessed 15 June 2024].

Varley, C. L. et al. (2004b). Activation of peroxisome proliferator-activated receptor-gamma reverses squamous metaplasia and induces transitional differentiation in normal human urothelial cells. *The American Journal of Pathology*, 164 (5), pp.1789–1798. [Online]. Available at: doi:10.1016/s0002-9440(10)63737-6.

Varley, C. L. et al. (2006). PPARgamma-regulated tight junction development during human urothelial cytodifferentiation. *Journal of Cellular Physiology*, 208 (2), pp.407–417. [Online]. Available at: doi:10.1002/jcp.20676.

Vaught, J. D. et al. (1996). Detrusor regeneration in the rat using porcine small intestinal submugosal grafts: Functional innervation and receptor expression. *Journal of Urology*, 155 (1), pp.374–378. [Online]. Available at: doi:10.1016/S0022-5347(01)66663-1 [Accessed 16 June 2024].

Versteegden, L. R. M. et al. (2017). Tissue Engineering of the Urethra: A Systematic Review and Meta-analysis of Preclinical and Clinical Studies. *European Urology*, 72 (4), pp.594–606. [Online]. Available at: doi:10.1016/j.eururo.2017.03.026.

Virseda Chamorro, M. et al. (1994). [Experimental bladder augmentation with Gore-tex amine: biomechanical, biochemical and biostructural aspects]. *Archivos Espanoles De Urologia*, 47 (10), pp.958–966.

Wang, A. Y. et al. (2008). Immobilization of growth factors on collagen scaffolds mediated by polyanionic collagen mimetic peptides and its effect on endothelial cell morphogenesis. *Biomacromolecules*, 9 (10), pp.2929–2936. [Online]. Available at: doi:10.1021/bm800727z.

Wang, X., Zhang, F. and Liao, L. (2021). Current Applications and Future Directions of Bioengineering Approaches for Bladder Augmentation and Reconstruction. *Frontiers in Surgery*, 8, p.664404. [Online]. Available at: doi:10.3389/fsurg.2021.664404 [Accessed 29 June 2024].

Ward, A. et al. (2021). Translation of mechanical strain to a scalable biomanufacturing process for acellular matrix production from full thickness porcine bladders. *Biomedical Materials (Bristol, England)*, 16 (6). [Online]. Available at: doi:10.1088/1748-605X/ac2ab8.

Watanabe, T., Rivas, D. A. and Chancellor, M. B. (1996). Urodynamics of spinal cord injury. *The Urologic Clinics of North America*, 23 (3), pp.459–473. [Online]. Available at: doi:10.1016/s0094-0143(05)70325-6.

Webster, T. et al. (2013). Nanostructured polyurethane-poly-lactic- co-glycolic acid scaffolds increase bladder tissue regeneration: an in vivo study. *International Journal of Nanomedicine*, p.3285. [Online]. Available at: doi:10.2147/IJN.S44901 [Accessed 17 June 2024].

Weingarten, J. L., Cromie, W. J. and Paty, R. J. (1990). Augmentation myoperitoneocystoplasty. *The Journal of Urology*, 144 (1), pp.156–158. [Online]. Available at: doi:10.1016/s0022-5347(17)39400-4.

Wiesmann, H. P. and Lammers, L. (2009). Scaffold Structure and Fabrication. In: Meyer, U. et al. (Eds). *Fundamentals of Tissue Engineering and Regenerative Medicine*. Berlin, Heidelberg: Springer. pp.539–549. [Online]. Available at: doi:10.1007/978-3-540-77755-7_39 [Accessed 15 June 2024].

Wiestma, A. C. et al. (2016). Robotic-assisted laparoscopic bladder augmentation in the pediatric patient. *Journal of Pediatric Urology*, 12 (5), p.313.e1-313.e2. [Online]. Available at: doi:10.1016/j.jpurol.2016.06.004.

Wilshaw, S.-P. et al. (2012). Development and characterization of acellular allogeneic arterial matrices. *Tissue Engineering. Part A*, 18 (5–6), pp.471–483. [Online]. Available at: doi:10.1089/ten.tea.2011.0287.

Wu, X. R. et al. (1990). Large scale purification and immunolocalization of bovine uroplakins I, II, and III. Molecular markers of urothelial differentiation. *Journal of Biological Chemistry*, 265 (31), pp.19170–19179. [Online]. Available at: doi:10.1016/S0021-9258(17)30640-3 [Accessed 14 June 2024].

Wu, X.-R. et al. (2009). Uroplakins in urothelial biology, function, and disease. *Kidney International*, 75 (11), pp.1153–1165. [Online]. Available at: doi:10.1038/ki.2009.73.

Wynn, T. A. and Vannella, K. M. (2016). Macrophages in Tissue Repair, Regeneration, and Fibrosis. *Immunity*, 44 (3), pp.450–462. [Online]. Available at: doi:10.1016/j.immuni.2016.02.015 [Accessed 29 June 2024].

Xue, G. (2008). Sterilization, Disinfection, Antisepsis and Preservation. *People's Medical Publishing House*, pp.167–303.

Yamataka, A. et al. (2003). Living-related partial bladder transplantation for bladder augmentation in rats: an experimental study. *Journal of Pediatric Surgery*, 38 (6), pp.913–915. [Online]. Available at: doi:10.1016/s0022-3468(03)00122-2.

Yoeruek, E. et al. (2012). Decellularization of porcine corneas and repopulation with human corneal cells for tissue-engineered xenografts. *Acta Ophthalmologica*, 90 (2), pp.e125–e131. [Online]. Available at: doi:10.1111/j.1755-3768.2011.02261.x [Accessed 24 June 2024].

Yoganarasimha, S. et al. (2014). Peracetic Acid: A Practical Agent for Sterilizing Heat-Labile Polymeric Tissue-Engineering Scaffolds. *Tissue Engineering. Part C, Methods*, 20 (9), pp.714–723. [Online]. Available at: doi:10.1089/ten.tec.2013.0624 [Accessed 24 June 2024].

Yoo, J. J. et al. (1998). Bladder augmentation using allogenic bladder submucosa seeded with cells. *Urology*, 51 (2), pp.221–225. [Online]. Available at: doi:10.1016/s0090-4295(97)00644-4.

Youssif, M. et al. (2005). Effect of vascular endothelial growth factor on regeneration of bladder acellular matrix graft: Histologic and functional evaluation. *Urology*, 66 (1), pp.201–207. [Online]. Available at: doi:10.1016/j.urology.2005.01.054 [Accessed 16 June 2024].

Yu, J. et al. (1994). Uroplakins Ia and Ib, two major differentiation products of bladder epithelium, belong to a family of four transmembrane domain (4TM) proteins. *The Journal of cell biology*, 125, pp.171–182.

Zanetti, E. M. et al. (2012). Bladder tissue passive response to monotonic and cyclic loading. *Biorheology*, 49 (1), pp.49–63. [Online]. Available at: doi:10.3233/BIR-2012-0604.

Zhang, C., Brown, P. J. B. and Hu, Z. (2019). Higher functionality of bacterial plasmid DNA in water after peracetic acid disinfection compared with chlorination. *Science of The Total Environment*, 685, pp.419–427. [Online]. Available at: doi:10.1016/j.scitotenv.2019.05.074 [Accessed 12 March 2025].

Zhang, D. et al. (2023). Research Progress of Macrophages in Bone Regeneration. *Journal of Tissue Engineering and Regenerative Medicine*, 2023 (1), p.1512966. [Online]. Available at: doi:10.1155/2023/1512966 [Accessed 29 June 2024].

Zhang, Q. et al. (2010). Circulating mitochondrial DAMPs cause inflammatory responses to injury. *Nature*, 464 (7285), pp.104–107. [Online]. Available at: doi:10.1038/nature08780.

Zhang, Y. et al. (2000). Coculture of bladder urothelial and smooth muscle cells on small intestinal submucosa: potential applications for tissue engineering technology. *The Journal of Urology*, 164 (3 Pt 2), pp.928–934; discussion 934-935. [Online]. Available at: doi:10.1097/00005392-200009020-00004.

Zhang, Y. et al. (2006). Challenges in a larger bladder replacement with cell-seeded and unseeded small intestinal submucosa grafts in a subtotal cystectomy model. *BJU International*, 98 (5), pp.1100–1105. [Online]. Available at: doi:10.1111/j.1464-410X.2006.06447.x [Accessed 16 June 2024].

Zhang, Y. et al. The global landscape of bladder cancer incidence and mortality in 2020 and projections to 2040. *Journal of Global Health*, 13, p.04109. [Online]. Available at: doi:10.7189/jogh.13.04109 [Accessed 21 June 2024].

Zhao, Y. et al. (2015). Time-dependent bladder tissue regeneration using bilayer bladder acellular matrix graft-silk fibroin scaffolds in a rat bladder augmentation model. *Acta biomaterialia*, 23. [Online]. Available at: doi:10.1016/j.actbio.2015.05.032.

Zini, L. et al. (2004). [Tissue engineering in urology]. *Annales D'urologie*, 38 (6), pp.266–274. [Online]. Available at: doi:10.1016/j.anuro.2004.09.001.

Appendix I

Sources of Materials

1.Chemical/Reagent	Provider
Acetic Acid, glacial (17.4mM)	Thermo Fisher Scientific Ltd.
Aprotinin (50 ml; 10,000 KIU/ml)	Nordic
Bovine Serum Albumin	Merck
Benzonase nuclease hc, purity >99 %	Merck (250 U/ µl)
Calcium acetate 97+ % (Dried)	Thermo Fisher Scientific Ltd.
Fluorescence mounting medium	Dako
DNAse I (10,000 U/ml)	Sigma
DNeasy kit	Qiagen
Dulbecco's minimal essential medium	Sigma
EDTA disodium ethylenediaminetetraacetic acid)	Thermo Fisher Scientific Ltd.
Eosin Y	Merck Millipore
Ethanol	VWR
Haematoxylin	BDH
HBSS	Thermo Fisher Scientific
HEPES (1 M)	Sigma-Aldrich
Hydrochloric acid (6 M)	Fisher Scientific
Isopropanol	Honeywell
L-glutamine (200 mM)	Sigma

Litmus paper	
LancerClean disinfectant	Lancer UK Ltd
Magnesium chloride hexahydrate	Thermo Fisher Scientific Ltd
Molecular grade water	Sigma-Aldrich
Neutral Buffered Formalin (10 % v/v)	Biostains Ready Reagents
Paraffin wax	Raymond A Lamb Ltd
PBS tablets (Dulbecco's 'A' PBS tablets, without Ca/Mg)	Oxoid
Peracetic acid	Fluka
RNAse A (100U/ml) (83833)	Sigma
Scott's tap water	
SDS (sodium dodecyl sulphate)	Thermo Fisher Scientific Ltd
Sodium chloride (NaCl)	Thermo Fisher Scientific Ltd
Sodium hydroxide (NaOH)	Scientific Laboratory Supplies
Tris (trizma base)	Sigma-Aldrich
Virkon® Rely+On™	SLS
Xylene	Biostains Ready Reagents
2.Equipment	**Provider**
Accumax Pipette Controller	Fine Care Biosystems
Bench vice	
BioPhotometer Eppendorf	Fisher Scientific
Bunsen burner	
Camera, Olympus DP74	Olympus

Centrifuge, Harrier 15/80	Sanyo
Centrifuge, Evolution RC	Sorvall
Coplin plastic staining jars	Fisher
Dissection kit	Thackray Instruments
Eppendorf thermomixer	Eppendorf
FastPette™ V2 Pipette Controller	Labnet International, Inc
Finnpipette Pipettes (0.2–2 gil, 2–20 gil, 20–200 gil, 200–1000 gil)	Scientific Laboratory Supplies
Forceps, blue plastic Spencer Wells	Fisher Scientific Ltd
Freezer (-20 ºC, -80 ºC)	
Fridge (+4 ºC)	
Glass troughs E105	Raymond A Lamb
Heat sealer	
Heraeus Hera Safe Class II biosafety, USA cabinet	Thermo Electron Corporation
Heraeus Incubator	Jencons PLC
Histology cassettes CMB-160-030R	Thermo Fisher Scientific Ltd
Histology Mega-cassettes 38VSP59040	Leica Biosystems
Histology moulds E10.8/4161	Raymond A Lamb
Histology water bath MH8515	Barnstead Electrothermal
Hotplate Stirrer heat-stir CB162	Stuart Scientific
Hotplate E18/1	R.A. Lamb
Hot wax oven E18/31	Raymond A Lamb

HI 991001 pH Meter	Hanna Instruments Ltd
Lancer 810 LX undercounter glassware washer	Lancer UK Ltd
Magnetic flea	
Microcentaur centrifuge	MSE
Microscope Olympus BX60	Olympus
Microscope Software	Olympus CellSense
Microtome, Leica RM2135	Leica
Nanodrop ND-1000 spectrophotometer	Thermo Fisher Scientific
PIPETMAN® Pipettes (0.2–2 gil, 2–20 gil, 20–200 gil and 200–1000 gil)	Gilson, Inc
Precision Balance GR-200	A&D Instruments Ltd
Pressure Cooker Sage “Fast Slow Pro”	Sage
Purelab Option Water Purification System	ELGA
Ruler, 150 mm, stainless steel	Fisher Scientific Ltd
Ruler, 300 mm, stainless steel	Fisher Scientific Ltd
Slide holder E102	Raymond A Lamb
Spatulas	
Water bath	
Wax dispenser E66	Raymond A Lamb
Whiteley Fume hood	Whiteley
Whrli mixer CM-1 vortexer	Thermo Fisher Scientific
ZEISS Axioscan Z1	Carl Zeiss
3.Glassware/Plasticware	**Provider**

Beakers	Scientific Laboratory Supplies
Duran bottles (0.25l, 0.5l, 1 l and 2l)	Scientific Laboratory Supplies
Funnels	Scientific Laboratory Supplies
Jar, polypropylene, wide neck with lid, 1l	Thermo Scientific Nalgene
Measuring cylinders (50 mm, 100mm, 250 mm and 1000mm)	Scientific Laboratory Supplies
Petri Dish, glass (90 x 15 mm, 150 x 15 mm)	Thermo Fisher Scientific
Precisionware™ bottles, 1l	
4.Consumables	**Provider**
Autoclave tape SLS1612	Scientific Laboratory Supplies
Bijous (sterile, 5 ml)	Sterilin/SLS
Containers, sterile, yellow screw cap 120 ml	Sarstedt
Cable ties (100 mm × 2.5 mm)	ARCO Limited
Coverslips, glass, E105	Scientific Laboratory Supplies
Eppendorf, microcentrifuge tubes (2 ml)	Starlab
Flat Sterilisation Pouches	Westfield Medical Limited
Foil	
Measuring cups	Scientific Laboratory Supplies
Micro tube I, loop cap, 1.5 ml	Simport VWR International
Minisart syringe filters, 0.2 im pore size	Sartorius Stedim UK Ltd
Parafilm	
Pipettes, Pasteur	SLS

Pipette Tips, TipOne ® (10 il, 20 il, 200 il and 1000 il)	STARLAB
Serological Pipettes, sterile (5 ml, 10 ml and 25ml)	Starstedt
Sterile disposable scalpel, No. 15 and 22	Swann-Morton, SLS
Sterilin pots (250 ml)	Thermo Fisher Scientific
Superfrost slides	Scientific Laboratory Supplies
Superfrost plus slides MIC3040	Scientific Laboratory Supplies
Syringes (1ml, 2.5ml, 5ml, 10ml, 20ml and 50 ml)	Terumo UK Ltd
Universal containers (20 ml)	SLS

Appendix II

JBU SOP:

Porcine Bladders procurement, dissection and storage. Decellularisation of full-thickness flat porcine bladder sheets.

Version 2-2017

Author: Debora Morgante

The present SOP is an adaptation of the protocols developed at the Jack Birch Unit (UoY) and at the Institute of Medical and Biological Engineering (UoL).

Preparation

Prepare stock solutions as per Appendix I.

Prepare buffer solutions as per Appendix II.

Sterilise all the equipment in use for the decellularisation process by autoclaving (Appendix III).

All steps performed aseptically and at ambient temperature instead stated.

Porcine bladder procurement, transportation, preparatory dissection and storage by freezing

1. Obtain porcine bladders for experimentation from the local abbatoir (Alec Traves Ltd Abattoir. Main Street, Escrick, York, YO19 6TP. Tel: 01904728246).
2. Place the whole bladders into a leak-proof plastic bag and transport at ambient temperature to the laboratory immediately for processing.
3. Work aseptically in a class II safety cabinet, transfer each bladder into a 150 mm x 15 mm Petri dish
4. and rinse inside/outside of bladder with 10-20 ml of sterile PBS.
5. Inspect each bladder to ensure it is free from damage and suitable for use.
6. Remove excess fatty and connective tissues with sterile scissors and forceps.

7. In order to identify the ventral surface, rotate each bladder about its longitudinal (apex-to-neck) axis until symmetrical, so that one ureter is on each side of the bladder and the longitudinal connective tissue band is visible and running down the midline of the tissue: the ventral surface is now facing upwards.

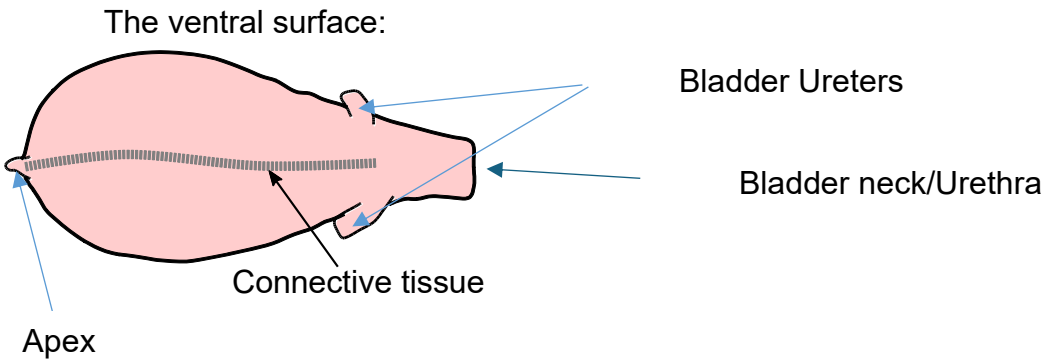

8. With the ventral surface facing upwards, dissect each bladder into a flat sheet by removing the bladder neck by cutting through both bladder layers just below the ureters (1), removing the apex by cutting approximately the same length as the previous incision through both bladder layers (2), and finally cutting longitudinally through one bladder layer along the ventral connective tissue band
(----- 3).

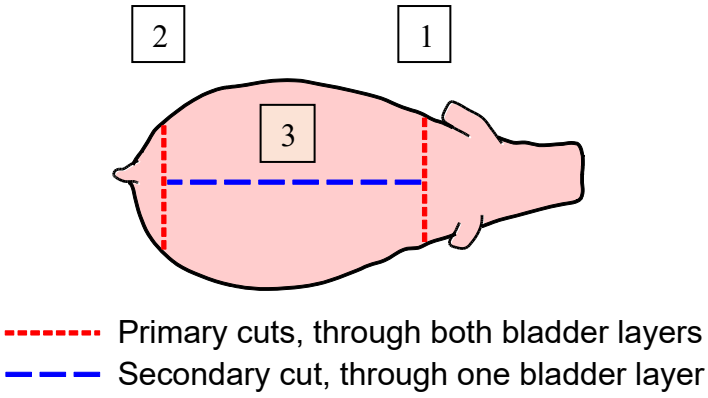

9. Open up each bladder into a flat sheet, rectangular in shape.
10. Following such preparatory dissection, remove excess moisture from the surface of each bladder by allowing it to air-dry just to the point where no moisture is visible on its surface.
11. Disinfect some gauze (or blue paper roll 20 cm x 20 cm) by adding 70% Ethanol for 10 minutes and allowing the gauze/paper to air dry.
12. Put each bladder on a gauze moistened with sterile PBS and place it in a 120 ml Sarstedt Sterile container (with yellow cap). Store at -20 ºC.

Decellularisation of full-thickness flat porcine bladder sheets

Day 1:

1. Thaw the bladder sheets at ambient temperature 4 hours before starting the decellularisation process.
2. In a class II safety cabinet, place each bladder onto the sterile cork board with the urothelium facing downwards.
3. In order to remove any residual contraction use a scalpel handle and gently push it over the bladder sheet.
4. Place a guide plate centrally onto the dorsal aspect of the rectangular bladder sheet (the longest edge is parallel to the longitudinal side of the bladder sheet).
5. Using a disposable scalpel, cut the tissue and leave a uniform 3 - 5 mm border around the guide plate.
6. With the guide and help of the indentations of the guide plate, insert the pins (total length of the needles = 55 mm) through the tissue and into the cork board.
7. Place the four corner pins first.
8. Remove the guide plate leaving the pins in situ.
9. With the help of a pair of forceps, slightly remove the pins from the cork board and move the bladder tissue up the pins.
10. Keeping the pins in the tissue, detach them from the cork board.
11. At this point it is possible to hold the tissue within the pins and gently, slowly and gradually starting stretching and moving it onto the frame.
12. By moving opposing pairs, place the corner pins first, subsequently the midpoints of the edges and finally all the other pairs of pins.

The tissue is at greatest risk of tearing when the corner pins are being moved: this can be minimised by moving some of the adjacent pins.

13. During the process, in order to avoid the tissue to become too dry, keep the sheets moisturized by gently applying drops of sterile PBS.
14. Using Spencer Wells blue plastic forceps, aseptically pick up each frame/stretched bladder sheet and place it into an autoclaved container.

(NB: 1 container 230 x 230 x 110 mm for 1 frame/bladder requiring 2.0 – 2.5 L of each buffer; 1 container 270 x 270 x 125 mm for 2 frames/bladders requiring 6.5 L of each Buffer).

15. Place the Hypotonic buffer into each container and cover with the lid.
16. Place each container (with frame and bladder) at 4 ºC for 24 hours (22-26 h).

Day 2:

In a class II safety cabinet, for each container/frame/bladder:

1. Remove the lid of the container and, using plastic forceps, aseptically move the frame onto the upturned lid.
2. Empty the old buffer from the container.
3. Using forceps, place the frame/bladder back into the empty container.
4. Place SDS buffer into the container and cover with lid.
5. Place each container (with frame and bladder) on an orbital shaker (gentle agitation) at ambient temperature for 24 hours (22-26 h).

Day 3:

In a class II safety cabinet, for each container/frame/bladder:

1. Remove the lid of the container and, using plastic forceps, aseptically move the frame onto the upturned lid.
2. Empty the old buffer from the container.
3. Using forceps, place the frame/bladder back into the empty container.
4. Place Wash buffer (no EDTA) into the container and cover with the lid.
5. Place each container (with frame and bladder) on an orbital shaker (gentle agitation) at 37 ºC for 24 hours (22-26 h).

Day 4:

In a class II safety cabinet, for each container/frame/bladder:

1. Remove the lid of the container and, using plastic forceps, aseptically move the frame onto the upturned lid.
2. Empty the old buffer from the container.
3. Using forceps, place the frame/bladder back into the empty container.
4. Place the Nuclease solution into the container and cover with the lid.
5. Place each container (with frame and bladder) on an orbital shaker (gentle agitation) at 37 ºC for 24 hours (22-26 h).

Day 5:

In a class II safety cabinet, for each container/frame/bladder:

1. Remove the lid of the container and, using plastic forceps, aseptically move the frame onto the upturned lid.
2. Empty the old buffer from the container.
3. Using forceps, place the frame/bladder back into the empty container.
4. Place the Wash buffer (with EDTA) into the container and cover with the lid.
5. Place each container (with frame and bladder) at 37 ºC for 60-74 hours.

Day 8:

In a class II safety cabinet, for each container/frame/bladder:

1. Remove the lid of the container and, using plastic forceps, aseptically move the frame onto the upturned lid.
2. Empty the old buffer from the container.
3. Using forceps, place the frame/bladder back into the empty container.
4. Place the Hypertonic buffer into the container and cover with the lid.
5. Place each container (with frame and bladder) on an orbital shaker (gentle agitation) at 37 ºC for 24 hours (22-26 h).

Day 9:

In a class II safety cabinet, for each container/frame/bladder:

1. Remove the lid of the container and, using plastic forceps, aseptically move the frame onto the upturned lid.
2. Empty the old buffer from the container.

3. Using forceps, place the frame/bladder back into the empty container.
4. Place the Wash buffer (with EDTA) into the container and cover with the lid.
5. Place each container (with frame and bladder) on an orbital shaker (gentle agitation) at 37 ºC for 24 hours (22-26 h).

Day 10:

In a class II safety cabinet, for each container/frame/bladder:

1. Remove the lid of the container and, using plastic forceps, aseptically move the frame onto the upturned lid.
2. Empty the old buffer from the container.
3. Using forceps, place the frame/bladder back into the empty container.
4. Place the Peracetic acid solution into the container and cover with the lid.
5. Place each container (with frame and bladder) on an orbital shaker (gentle agitation) at room temperature for 3.0 – 3.5 hours.
6. Following the Peracetic acid solution step, in a class II safety cabinet, remove each bladder from its container.
7. Using forceps, remove all the pins used to secure the tissue to the frame.

<u>Final dissection:</u>

1. Using sterile scissors, remove the outside border by cutting between the points where the pins were previously placed in.
2. Using sterile ruler&scalpel, from the remaining tissue, isolate the central region (8 cm x 8 cm) which corresponds with the region of tissue sufficiently stretched and decellularised.
3. Transfer each decellularised bladder sheet into a fresh Sarstedt 120 ml sterile container and fill with PBS solution.
4. Place each Sarstedt 120 ml sterile container on an orbital shaker (gentle agitation) at ambient temperature for 1 hour (50 – 70 minutes).
5. Repeat steps 3 and 4 twice more.
6. In a class II safety cabinet, for each Sarstedt 120 ml sterile container/bladder sheet, remove the lid and, using sterile forceps, aseptically transfer the bladder sheet into a fresh Sarstedt 120 ml sterile container filled with 100 ml PBS solution and cover with the lid.

7. Place each Sarstedt 120 ml sterile container (with bladder sheet) on an orbital shaker (gentle agitation) at ambient temperature for 24 hours (22 – 26 hours).

Day 11:

In a class II safety cabinet, for each Sarstedt 120 ml sterile container/bladder sheet:

1. Remove the lid of the Sarstedt 120 ml sterile container and, using sterile forceps, aseptically transfer the bladder sheet into a fresh Sarstedt 120 ml sterile container filled with 100 ml PBS solution and cover with the lid.
2. Label with a batch processing label accordingly to the following template, and store each Sarstedt 120 ml sterile container (with sterile decellularised bladder sheet) at 4 ºC:

   JBU.PB dd/mm/yy.XXx

   Where PB indicates Porcine Bladder, dd/mm/yy indicates the date of the process' completion, XX are the initials of the person who prepared the biomaterial and x is the suffix added if more than one bladder is prepared during the same session.

Appendix I

Stock Solutions:

Instructions to prepare 1 litre of each stock solution

EDTA solution (10% w/v)

- Dissolve 100 g EDTA in 900 ml deionized water using a magnetic stirrer and hotplate turned on to ~60 ℃ (if necessary, leave for several hours on the hotplate to allow the EDTA to completely dissolve)
- Make volume up to 1L using deionized water
- Autoclave the solution at 121℃ for 20 minutes
- Store at ambient temperature for up to 6 months.

SDS solution (10% w/v) – Do not autoclave

- In a fume hood, dissolve 100 g SDS in 900 ml deionized water using a magnetic stirrer
- Make up volume to 1L using deionized water
- Filter-sterilise the solution into sterile Universals (10 ml/Universal) using a filter with a pore size of 0.2 µm
- Store at ambient temperature for up to 6 months.

$MgCl_2$ solution (1 M)

- Dissolve 203.3 g magnesium chloride hexahydrate [$MgCl_2(H_2O)_6$] in 700 ml deionized water using a magnetic stirrer
- Make volume up to 1L using deionized water
- Autoclave the solution at 121℃ for 20 minutes
- Store at ambient temperature for up to 6 months.

Tris-HCL (2M, pH 7.5)

- Dissolve 242.38 g Tris in 600 ml deionized water using a magnetic stirrer and hotplate turned on to ~60 ℃ (when dissolved, allow to cool to room temperature)
- Adjust pH to 7.5 by adding hydrochloric acid (6 M)
- Make volume up to 1L using deionized water
- Autoclave the solution at 121℃ for 20 minutes
- Store at ambient temperature for up to 6 months.

Tris-HCL (2M, pH 8)

- Dissolve 242.38 g Tris in 600 ml deionized water using a magnetic stirrer and hotplate turned on to ~60 ℃ (when dissolved, allow to cool to room temperature)
- Adjust pH to 8 by adding hydrochloric acid (6 M)
- Make volume up to 1L using deionized water
- Autoclave the solution at 121℃ for 20 minutes
- Store at ambient temperature for up to 6 months.

70% Ethanol

- Fill a bottle with 300 ml of deionized water

- In a fume hood, add 700 ml Absolute Ethanol
- Store at ambient temperature for up to 6 months.

Appendix II

Decellularisation Buffers:

Instructions to prepare 1 litre of each buffer

Wash Buffer (with EDTA)

- Fill a bottle with 989 ml of deionized water
- Add required number (5 or 10) PBS tablets (suitable to make a 1L/PBS solution)
- Add 10 ml EDTA stock solution
- Autoclave the solution at 121℃ for 20 minutes
- Store at ambient temperature for up to 6 months.
- Aseptically, in a class II safety cabinet, add 1 ml Aprotinin immediately before use.

Wash Buffer (no EDTA)

- Fill a bottle with 999 ml of deionized water
- Add required number (5 or 10) PBS tablets (suitable to make a 1L/PBS solution)
- Autoclave the solution at 121℃ for 20 minutes
- Store at room temperature for up to 6 month.
- Aseptically, in a class II safety cabinet, add 1 ml Aprotinin immediately before use.

Hypotonic Buffer

- Fill a bottle with 984 ml of deionized water
- Add 5 ml Tris-HCl (2M, pH 8) stock solution
- Add 10 ml EDTA stock solution
- Autoclave the solution at 121℃ for 20 minutes
- Store at ambient temperature for up to 6 months.

- Aseptically, in a class II safety cabinet, add 1 ml Aprotinin immediately before use.

SDS Buffer

- Fill a bottle with 974 ml of deionized water
- Add 5 ml Tris-HCl (2M, pH 8) stock solution
- Add 10 ml EDTA stock solution
- Autoclave the solution at 121℃ for 20 minutes
- Store at ambient temperature for up to 6 months.
- Add 10 ml SDS stock solution
- Aseptically, in a class II safety cabinet, add 1 ml Aprotinin immediately before use.

Nuclease Solution

- Fill a bottle with 965 ml of deionized water
- Add 25 ml Tris-HCl (pH 7.5) stock solution
- Add 10 ml $MgCl_2$ stock solution
- Autoclave the solution at 121℃ for 20 minutes
- Store at ambient temperature for up to 6 months.
- Aseptically, in a class II safety cabinet, add 4 µl of Benzonase (250 U/µl) before use (use solution within 10 minutes of preparation).

Hypertonic Buffer

- Fill a bottle with 800 ml of deionized water
- Dissolve 87.66 g NaCl using a magnetic stirrer
- Dissolve 6.057 g Tris using a magnetic stirrer
- Adjust pH to 7.5 by adding hydrochloric acid (6 M)
- Make volume up to 1 L using deionized water
- Autoclave the solution at 121℃ for 20 minutes
- Store at ambient temperature for up to 6 months.

Peracetic Acid solution (0.1% v/v)

- Fill a bottle with 800 ml of ELGA water

- Add required number (5 or 10) PBS tablets (suitable to make a 1L/PBS solution)
- In a fume cupboard, add 2.8 ml Peracetic Acid (36-40%)

  [NB: COSSH form]

- Adjust pH to 7.2 by adding NaOH (6 M)
- Make volume up to 1 L using deionized water
- Use within 1 hour of preparation.

PBS Solution

- Fill a bottle with 1000 ml of deionized water
- Add required number (5 or 10) PBS tablets (suitable to make a 1L/PBS solution)
- Autoclave the solution at 121℃ for 20 minutes
- Store at ambient temperature for up to 6 months.

Table 1: Chemicals/Reagents

Chemical/Reagent	Cat. No.	Supplier
Aprotinin (10,000 KIU/ml)	AP/R	Nordic Pharma
EDTA (disodium ethylenediaminetetraacetic acid)	D/0700/53	Fisher Scientific Ltd
SDS (sodium dodecyl sulphate)	L4390-100G	Sigma
Magnesium chloride hexahydrate	M2393-100G	Sigma
UltraPure Tris Hydrochloride	15506-017	Invitrogen – Thermo Fisher Scientific

PBS (phosphate buffered saline) tablets Or Dulbecco's 'A' PBS tablets, without Ca/Mg	P4417-50TAB BR0014	Sigma (5 tablets/L) Oxoid (10 tablets/L)
Benzonase Nuclease (>99% purity)	71206-3	Novagen-Merck
NaCl (sodium chloride)	S/3160/53	Fisher Scientific Ltd
Peracetic acid (36-40%)	433241-500ml	Honeywell (Sigma-Aldrich)
Sodium hydroxide - pellets	S/4920/53	Fisher Scientific Ltd
Ethanol Absolute	20821.330	VWR Chemicals

Appendix III

List of equipment:

- Leak-proof plastic bags
- Sterile Petri Dishes (150 mm dia x 15 mm H)
- Class II safety cabinet
- Fume hood
- Sterile scissors
- Sterile forceps
- Sterile scalpels/rulers
- Sterile gauzes (10 cm x 10 cm)
- Blue paper roll
- Sarstedt 120 ml sterile containers with screw cap
- Minus 20 ºC freezer
- 4 ºC fridge
- Cork board
- Guide plate
- Pins (total length of the needles = 55 mm)

- Sterile Spencer Wells blue plastic forceps (needed in pairs)
- Frame (flat-bed rig)
- Plastic sterile container and lid (230 x 230 x 110 mm)
- Plastic sterile container and lid (270 x 270 x 125 mm)
- Orbital shaker
- Orbital shaker at 37 ºC
- Sterile gloves
- Disposable laboratory gloves
- White Lab coats
- Green Lab gawns
- 2 L Glass Lab Bottles with screw cap
- 1 L Glass Lab Bottles with screw cap
- Autoclave
- Autoclave tape
- Lab sealing tape (Parafilm)
- Sterile 20 ml syringe
- Syringe filter (pore size 0.2 µm)
- Sterile Universal tubes with screw cap
- Magnetic stirrer
- Hotplate stirrer
- pH meter

Appendix III

NELSON LABORATORIES

Sponsor:
Gill Riches
TRx Orthopaedic Limited
Unit 1 & 2, Astley Lane Industrial Estate
Astley Wy, Swillington
Leeds, LS26 8XT
UNITED KINGDOM

MEM Elution Final Report

Test Article: Decellularised porcine bladder samples
1) 1.1
2) 2.1
3) 3.1
4) 4.1
5) 5.1
6) 6.1
Purchase Order: POHTRLT11010
Study Number: 962927-S01
Study Received Date: 05 May 2017
Testing Facility: Nelson Laboratories, LLC, a Business Unit of Sterigenics International
6280 S. Redwood Rd.
Salt Lake City, UT 84123 U.S.A.
Test Procedure(s): Standard Test Protocol (STP) Number: 801-STP0032 Rev 09
Protocol Detail Sheet (PDS) Number: 201501917 Rev 01

Summary: The Minimal Essential Media (MEM) Elution test was designed to determine the cytotoxicity of extractable substances. An extract of the test article was added to cell monolayers and incubated. The cell monolayers were examined and scored based on the degree of cellular destruction. All test method acceptance criteria were met. Testing was performed in compliance with US FDA good manufacturing practice (GMP) regulations 21 CFR Parts 210, 211 and 820. The test procedure(s) listed above were followed without deviation.

Results:
Test Article:

Identification	Results Pass/Fail	Scores				Extraction Ratio	Amount Tested / Extraction Solvent Amount
		#1	#2	#3	Average		
1	**Pass**	0	0	0	0	0.1 g/mL	4.0 g / 40 mL
2	**Pass**	0	0	0	0	0.1 g/mL	8.2 g / 82 mL
3	**Pass**	0	0	0	0	0.1 g/mL	4.2 g / 42 mL
4	**Pass**	0	0	0	0	0.1 g/mL	2.9 g / 29 mL
5	**Pass**	0	0	0	0	0.1 g/mL	4.3 g / 43 mL
6	**Pass**	0	0	0	0	0.1 g/mL	3.2 g / 32 mL

ANAB ACCREDITED TESTING LABORATORY

Study Director — McKenna Wild, B.S.

12 May 2017
Study Completion Date

962927-S01

Appendix IV

Appendix V

Translation of mechanical strain to a scalable biomanufacturing process for acellular matrix production from full thickness porcine bladders

To cite this article: Ashley Ward *et al* 2021 *Biomed. Mater.* 16 065023

Appendix VI

Original Article

Journal of Tissue Engineering
Volume 12: 1–12

DOI: 10.1177/20417314211998840
journals.sagepub.com/home/tej
SAGE

Augmentation of the insufficient tissue bed for surgical repair of hypospadias using acellular matrix grafts: A proof of concept study

Debora Morgante[1,2,3*], Anna Radford[1,2,3*], Syed K Abbas[4], Eileen Ingham[5], Ramnath Subramaniam[3*] and Jennifer Southgate[1*]

Abstract

Acellular matrices produced by tissue decellularisation are reported to have tissue integrative properties. We examined the potential for incorporating acellular matrix grafts during procedures where there is an inadequate natural tissue bed to support an enduring surgical repair. Hypospadias is a common congenital defect requiring surgery, but associated with long-term complications due to deficiencies in the quality and quantity of the host tissue bed at the repair site. Biomaterials were implanted as single on-lay grafts in a peri-urethral position in male pigs. Two acellular tissue matrices were compared: full-thickness porcine acellular bladder matrix (PABM) and commercially-sourced cross-linked acellular matrix from porcine dermis (Permacol™). Anatomical and immunohistological outcomes were assessed 3 months post-surgery. There were no complications and surgical sites underwent full cosmetic repair. PABM grafts were fully incorporated, whilst Permacol™ grafts remained palpable. Immunohistochemical analysis indicated a non-inflammatory, remodelling-type response to both biomaterials. PABM implants showed extensive stromal cell infiltration and neovascularisation, with a significantly higher density of cells ($p < 0.001$) than Permacol™, which showed poor cellularisation and partial encapsulation. This study supports the anti-inflammatory and tissue-integrative nature of non-crosslinked acellular matrices and provides proof-of-principle for incorporating acellular matrices during surgical procedures, such as in primary complex hypospadias repair.

Keywords

Acellular matrix, biomaterial, surgery, hypospadias repair, tissue integration

Received: 07 November 2020; accepted: 10 February 2021

Introduction

Decellularised tissue matrices offer a promising natural biomaterial in surgical situations where there is either an inherent lack of a tissue bed for repair, or where the healthy tissue bed is compromised by trauma or fibrotic scarring. One such need is encountered in surgical repair for hypospadias. With reported frequencies of 0.3 to 7.0 per 1000 live births, hypospadias is one of the most common genitourinary birth defects, requiring revision in as many as 1 in 300 boys (reviewed[1,2]). Hypospadias is associated with the development of a foreshortened urethra resulting in an aberrantly-positioned external orifice (meatus) on the ventral aspect of the penis. Surgical repair is the mainstay treatment for the majority of infants with hypospadias, but

[1]Jack Birch Unit for Molecular Carcinogenesis, Department of Biology and York Biomedical Research Institute, University of York, Heslington, York, UK
[2]Hull York Medical School, Heslington, York, UK
[3]Paediatric Urology, Leeds Teaching Hospitals NHS Trust, Leeds General Infirmary, Leeds, UK
[4]Central Biomedical Services, University of Leeds, Leeds, UK
[5]School of Biomedical Sciences, Institute of Medical and Biological Engineering, University of Leeds, Leeds, UK

*DM and AR contributed equally and, RS and JS contributed equally to this work.

Corresponding author:
Jennifer Southgate, Jack Birch Unit for Molecular Carcinogenesis, Department of Biology and York Biomedical Research Institute, University of York, Heslington, York YO10 5DD, UK.
Email: j.southgate@york.ac.uk

ARRIVE guidelines 2.0. https://arriveguidelines.org/

	Essential 10	
1a	The groups being compared	We developed a porcine experimental model of urethroplasty to study the effect of incorporating an onlay free graft of acellular matrix at the repair site. We compared two acellular matrices: 1) PABM (Porcine Acellular Bladder Matrix a non-crosslinked, full thickness matrix) and 2) Permacol™ (a commercial porcine dermis-derived acellular matrix that is licensed for human use and has previously been used as an off-label product in a small clinical series undergoing hypospadias repair).
1b	The experimental unit	Single animal
2a	Experimental units allocated to each group and total number in each experiment; total number of animals used	Twelve large white hybrid (LWH) pigs were used in the experimental study with a total of six animals implanted with PABM and six with Permacol.
2b	How sample size was decided	A maximum of 6 pigs could be housed at any one time
3a	Inclusion or exclusion criteria and data points during the analysis	Only male pigs were used - both sexes of animal were not used because the study was targeted for a condition that does not occur in females. All animals included in the study remained healthy and none were excluded at any stage of the study
3b	Any animals not included in the analysis and why.	NA
3c	Report exact value of n in each group	12 animals total in 2 groups of n=6 each.
4a	Randomisation of animals to control and treatment groups	Six animals were implanted with PABM and six with Permacol™. The animals were divided into two groups of six with three pigs having PABM and the other Permacol™ implanted into the peri-urethral tissues. The surgery for first and second groups took place ~five months apart. 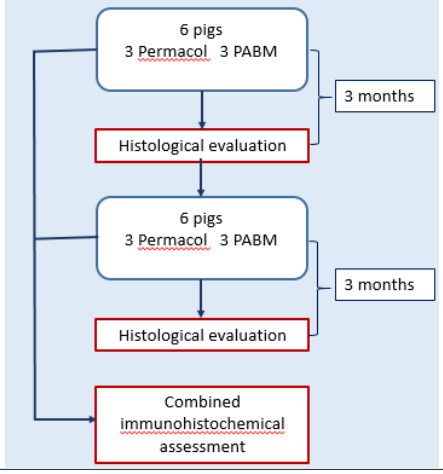

Appendix VII

Scientific production

Publications

Debora Morgante, Jennifer Southgate. Chapter 12 - Bladder tissue regeneration. Editor(s): Aldo R. Boccaccini, Peter X. Ma, Liliana Liverani. In Woodhead Publishing Series in Biomaterials. Tissue Engineering Using Ceramics and Polymers (Third Edition). Woodhead Publishing, 2022, Pages 459-480. ISBN 9780128205082. doi.org/10.1016/B978-0-12-820508-2.00008-8.

Morgante D, Radford A, Abbas SK, Ingham E, Subramaniam R, Southgate J. Augmentation of the insufficient tissue bed for surgical repair of hypospadias using acellular matrix grafts: A proof of concept study. Journal of Tissue Engineering. 2021;12. doi:10.1177/2041731421998840.

Ashley Ward, Debora Morgante, John Fisher, Eileen Ingham, Jennifer Southgate. Translation of mechanical strain to a scalable biomanufacturing process for acellular matrix production from full thickness porcine bladders. 2021 Biomed. Mater. 16 065023. doi 10.1088/1748-605X/ac2ab8.

Participation in congresses

22 - 25 June 2016. 27th ESPU Congress, Harrogate, UK.

Oral presentation. Morgante D.: Early experience of a surgeon in a lab.

23 June 2017. Regener8 Annual Conference, Leeds, UK

Poster Presentation. Morgante D., Southgate J., Subramaniam R.: Porcine Acellular Bladder Matrix: from the bench to the market.

11 – 14 April 2018. 29th ESPU Congress, Helsinki, Finland.

ePoster and Presentation. Morgante D., Abbas S.K., Hinley J., Ingham E., Southgate J., Subramaniam R.: Urinary bladder auto-augmentation: homologous use of a decellularised biomaterial.

4 - 7 September 2018. 5th World TERMIS Congress, Kyoto, Japan.

Oral Presentation. Morgante D., Hinley J. Abbas S.K., Ingham E., Subramaniam R., Southgate J.: Homologous use of a decellularised biomaterial in a urinary bladder auto-augmentation large animal model.

17th December 2018. 20th BiTEG Annual Meeting, Sheffield, UK.

Oral presentation. Morgante D., Hinley J. Abbas S.K., Ingham E., Subramaniam R., Southgate J.: Homologous application of porcine acellular bladder matrix (PABM) in urinary bladder auto-augmentation.

13 - 14 November 2019. iMech, Institution of Mechanical Engineers, London, UK

Abstract co-author. Morgante, D., Radford A., Ward A., Subramaniam R., Fisher J., Ingham E., Southgate J.: "Natural Homologous Biomaterials for Reconstructive Bioengineering of the Lower Urinary Tract".

10 - 13 June 2020, Vienna, Austria. 21st EUPSA Annual Congress joint with IPEG and ESPES.

Abstract accepted for oral presentation. Morgante, D., Radford A., Abbas S.K., Ingham E., Subramaniam R., Southgate J. Qualitative and quantitative outcomes of acellular matrix grafts used to augment the peri-urethral tissue bed in a porcine surgical model. (Congress cancelled because of the COVID-19 pandemic).

17th December 2020. 22nd Annual Meeting of the Biomaterials and Tissue Engineering Group (BiTEG), Leeds, UK (virtual due to COVID-19 pandemic).

Oral presentation. Morgante, D., Radford A., Abbas S.K., Ingham E., Subramaniam R., Southgate J: On-lay grafts of acellular matrix to augment the peri-urethral tissue bed for hypospadias repair. Awarded with the Prize for "best podium oral research and presentation".

6 - 8 May 2021. 11th Biological Scaffolds for Regenerative Medicine (BSRM) Symposium, University of Pittsburgh / Silverado Resort in Napa, CA, USA.

Abstract accepted for oral presentation. Morgante, D., Abbas S.K., Ingham E., Subramaniam R., Southgate J: Application of a homologous tissue-integrative acellular biomaterial for urinary bladder auto-augmentation (participation cancelled due to the COVID-19 pandemic).

7-9th July 2021. 67th BAPS Annual Congress (virtual due to COVID-19 pandemic).

Oral presentation. Morgante D., Hinley J. Abbas S.K., Ingham E., Subramaniam R., Southgate J.: Realising the promise of auto-augmentation with a homologous tissue-integrative biomaterial.

15-19th November 2021. 6th World Congress of the Tissue Engineering and Regenerative Medicine International Society (TERMIS), Maastricht, The Netherlands (virtual due to COVID-19 pandemic).

Oral presentation. Morgante, D., Radford A., Abbas S.K., Ingham E., Subramaniam R., Southgate J.: Acellular matrix grafts to augment the peri-urethral tissue bed for hypospadias repair.

List of abbreviations

ACM	Acellular matrix
AF	Anti-fade
AR	Antigen retrieval
αSMA	Alpha smooth muscle actin
AUM	Asymmetric unit membrane
BAM	Bladder acellular matrix
BC	Basal cells (of the urothelium
BSA	Bovine serum albumin
CD163	Cluster of Differentiation 163
CISC	Clean intermittent self-catheterisation
CK20.8	Cytokeratin 20 (clone K20.8)
CZI	Carl Zeiss image
DAB	3, 3'-Diaminobenzidine
DAPI	4',6-diamidino-2-phenoylindole
DMEM	Dulbecco's minimal essential medium
DMSO	Dimethyl sulfoxide
DNA	Deoxyribonucleic acid
DPBS	Dulbecco's phosphate-buffered saline
dsDNA	Double-stranded deoxyribonucleic acid
ECM	Extracellular matrix
EDTA	Ethylene-diamine tetra-acetic acid

FDA	Food and Drug Administration
FFPE	Formalin fixed paraffin wax embedded
FGF	Fibroblast growth factor
FU	Follow-up
GAG	Glycosaminoglycan
GMP	Good manufacturing practice
HBSS	Hanks' balanced salt solution
HCl	Hydrochloric acid
H&E	Haematoxylin and eosin
IC	Intermediate cells (of the urothelium)
IGF	Insulin-like growth factor
IHC	Immunohistochemistry
JBUMC	Jack Birch Unit for molecular carcinogenesis
JAM	Junctional adhesion molecule
Ki67	Kiel 67
Myo11hc	Myosin 11 heavy chain
NaCl	Sodium chloride
NaOH	Sodium hydroxide
NBF	Neutral buffered formalin
NFP	Neurofilament protein
PAA	Peracetic acid
PABM	Porcine acellular bladder matrix

PBS	Phosphate-buffered saline
PCL	Poly(ε-caprolactone)
PEG	Poly(ethylene glycol)
PGA	Polyglycolic acid
PLA	Polylactic acid
PLGA	Poly(lactic-co-glycolic acid)
PoC	Proof of concept
PoF	Proof of feasibility
PPARγ	Peroxisome proliferator-activated receptor γ
PVA	Polyvinyl alcohol
RM	Regenerative Medicine
RNA	Ribonucleic acid
ROI	Region of interest
Rpm	revolutions per minute
SDS	Sodium dodecyl sulphate
SF	Silk fibroin
SIS	Small intestine submucosa
SMCs	Smooth muscle cells
SM22α	Smooth muscle 22 alpha
SOP	Standard of practice
TE	Tissue Engineering
TERM	Tissue Engineering and Regenerative Medicine

TJ	Tight junctions
Tris	Trizma® Base
TRX	Tissue Regenix Group plc
UP	Urothelium-plaque
UP3a	Uroplakin 3a
UTI	Urinary tract infection
UV	Ultraviolet
ZO	Zonular occludens